OLARTEMOURE
OLARTE MOURE & ASOCIADOS LTDA.

Carlos R. Olarte
Juan G. Moure

Alexander Agudelo
Carlos A. Parra
Juan F. Acosta
Andrés Rincón
Mónica Guevara
Andrés Alvarado
María C. Calderón
Mauricio Ávila
Gina Cáceres
Isabella Herrera
Zaava Ravid
Alejandro Moure
Miguel F. Porras
Camila Vásquez
Catalina Amaya
Laura M. Escobar
Lorena Andrade
Sergio Arboleda
Catalina Jiménez
Daniela González
Maritza Sierra
Gina A. Ánas
Guillermo Parra
Erika Jhiset Suárez
Liliana Galindo

Medellín
María C. Múnera
Eddie Manotas
Adrián Santamaría
Camilo A. Bernal
Daniela Lopera

Barranquilla
Gina De Echeona
José J. Dangond

Señores
SUPERINTENDENCIA DE INDUSTRIA Y COMERCIO
DIRECCIÓN DE NUEVAS CREACIONES
E. S. D.

SUPERINTENDENCIA DE INDUSTRIA Y COMERCIO
No. 13-019546- -00018-0000
Fecha: 2015-11-06 17:16:47 Dep: 2020 DIR NUEVASCR
Tra: 11 PATENTEIYII Eve: 378 FASENACIONALI
Act: 412 REPOSPRESRECU Folios: 154 - 153

Re: Expediente Nº. 13-019.546
Solicitud de Patente de Invención titulada: "MÉTODO PARA INACTIVAR VIRUS DE LA VARICELA ZOSTER (VVZ) INACTIVADO"
Solicitante: MERCK SHARP & DOHME CORP.
Nuestra Ref.: P2013/000022

RECURSO DE REPOSICIÓN

CARLOS R. OLARTE, mayor de edad y vecino de Bogotá, D.C., identificado como aparece al pie de mi firma, en mi condición de apoderado de la sociedad solicitante, y dentro del término legal previsto por el artículo 76 del Código de Procedimiento Administrativo y de lo Contencioso Administrativo, me permito interponer RECURSO DE REPOSICIÓN en contra de la Resolución No. 64616, notificada por edicto desfijado el 22 de octubre de 2015.

1. ANTECEDENTES

1.1 La solicitud de patente ventilada en este expediente fue presentada el 01 de febrero de 2013, con un Capítulo Reivindicatorio original de 26 reivindicaciones.

1.2 La Superintendencia de Industria y Comercio (SIC) emitió el primer examen de fondo notificado por fijación en la lista No. 09 del 04 de marzo de 2014, correspondiente al Oficio No. 2799, objetando la claridad, la novedad de la presente invención, y además que la materia reclamada no es una invención.

2

1.3 En respuesta al primer y único examen de fondo, el 11 de julio de 2014 presenté un Capítulo Reivindicatorio Modificado con 18 reivindicaciones, y proporcioné argumentos en favor de la claridad, la novedad y que la materia reclamada si es una invención.

1.4 La Superintendencia de Industria y Comercio (SIC) emitió el segundo examen de fondo notificado por fijación en la lista No. 001 del 06 de enero de 2015, correspondiente al Oficio No. 15825, objetando el Capítulo Descriptivo, y la claridad y el nivel inventivo de la presente invención.

1.5 En respuesta al primer y único examen de fondo, el 15 de mayo de 2015 presenté un Capítulo Reivindicatorio Modificado con 12 reivindicaciones, y proporcioné argumentos en favor del Capítulo Descriptivo y en favor de la claridad y el nivel inventivo de la materia limitada.

1.6 La SIC por medio de la Resolución No. 64616, notificada por edicto desfijado el 22 de octubre de 2015, niega las Reivindicaciones 1 a 12 por supuesta falta de claridad y el nivel inventivo.

2. OBJETO DEL RECURSO

Que se revoque la Resolución recurrida, y en su lugar se conceda el privilegio de patente de invención para las reivindicaciones contenidas en el **Capítulo Reivindicatorio Modificado adjunto** al presente Recurso de Reposición, o en su defecto aquellas reivindicaciones que el Despacho considere cumplen con los requisitos de patentabilidad.

3. FUNDAMENTO DEL RECURSO

Con referencia a los argumentos presentados por la SIC para desvirtuar la patentabilidad de las Reivindicaciones 1 a 12 en la Resolución aquí recurrida, respetuosamente difiero del análisis expuesto y procedo a refutar cada uno de dichos argumentos, exponiendo las motivaciones técnicas que desvirtúan la posición de ese Despacho.

3.1 a- La SIC insiste en que el Capítulo Reivindicatorio Modificado presentado junto con mi respuesta al segundo examen de fondo carece de claridad porque definen un método en términos de la infectividad alcanzada por el virus VVZ o porque se induce una respuesta inmune

contra VVZ lo que corresponde a un resultado a alcanzar que no permite establecer el alcance de la materia reivindicada.

b- En primer lugar, con el ánimo de brindar mayor claridad a la presente solicitud, me permito adjuntar un **Capítulo Reivindicatorio Modificado**, que reemplaza en su totalidad al Capitulo Reivindicatorio Modificado presentado el 15 de mayo de 2015 en respuesta al segundo examen de fondo, en el cual, siguiendo las recomendaciones de la Examinadora, se eliminaron las expresiones "*en donde la infectividad del VVZ inactivado es <0,040 unidades formadoras de placas (UFP)/mL*" y "*en donde el VVZ inactivado induce una respuesta inmune contra VVZ.*", las cuales estaban dirigidas a resultados a alcanzar. De esta manera, respetuosamente considero que el Capítulo Reivindicatorio Modificado adjunto cumple a cabalidad con los requerimientos del Articulo 30 de la Decisión 486, por lo que su claridad debe ser reconocida.

Valga anotar que las modificaciones efectuadas al Capítulo Reivindicatorio cumplen a cabalidad con lo estipulado en el Artículo 34 de la Decisión 486, ya que éstas de ninguna manera implican una ampliación de la protección correspondiente a la divulgación contenida en la solicitud inicial. Por el contrario, dichas modificaciones corresponden a una limitación de la materia reclamada.

3.2 a- La SIC señala que se requirió allegar el certificado de depósito del material biológico de acuerdo con lo previsto en el artículo 29 de la Decisión 486, por cuanto la solicitud se refiere a un virus inactivado de la varicela zóster de la cepa Oka, la cual no puede describirse de manera que pueda ser comprendido y ejecutado por una persona capacitada en la materia técnica. Dicho requerimiento no fue atendido por parte de la solicitante.

b- i) En respuesta a lo anterior, respetuosamente considero que la Examinadora no ha entendido completamente el objeto de la invención. Tal como lo señalé en respuesta al segundo examen de fondo, la presente invención reclama un método de preparación de un VVZ inactivado el cual es aplicable a **cualquier virus VVZ**. Es decir, la presente invención no busca protección sobre una cepa Oka particular, por el contrario, busca protección para un método novedoso e inventivo de inactivación de cualquier VVZ usando radiación gamma, por lo que requerir el certificado del depósito de dicha cepa resulta técnica y legalmente incorrecto sin mencionar que innecesario.

Adicionalmente, el solicitante desea llamar la atención sobre el hecho de que el depósito al cual se hace referencia en la solicitud **no es un depósito que haya sido hecho por Merck**. Por el contrario, dicho número de depósito de la ATCC fue incorporado en el Capítulo Descriptivo

simplemente para indicarle a la persona medianamente versada en la materia, a modo de ejemplo, una de las muchas fuentes de la cepa Oka de VZV. En este sentido, como Merck no hizo el depósito, evidentemente no tiene el acceso al certificado de depósito y por lo tanto, dado que la invención no recae exclusivamente sobre dicha cepa, el certificado resulta innecesario. La Examinadora no puede confundir la simple mención en el Capítulo Descriptivo de determinada cepa a modo ilustrativo con el hecho de que la invención necesariamente recae sobre ella y por lo tanto sea obligatorio presentar un certificado que no aplica para el presente caso.

Adicionalmente, el Artículo 29 de la Decisión 486 establece que "*Cuando la invención se refiera a un producto o a un procedimiento relativo a un material biológico y la invención no pueda describirse de manera que pueda ser comprendida y ejecutada por una persona capacitada en la materia técnica, la descripción deberá complementarse con un depósito de dicho material*". Así las cosas, la Decisión 486 obliga al solicitante a presentar un certificado de deposito **si y solo si** la invención no puede ser comprendida y ejecutada por la persona versada en la materia. En este caso, tal como lo demostré con los anexos presentados en respuesta al segundo examen de fondo, que aparentemente fueron completamente ignorados por el Despacho y que por lo tanto vuelvo a adjuntar (ANEXOS 1, 2, 3, 4 y 5), se evidencia completamente que la cepa Oka **es ampliamente conocida en el estado del arte** y puede obtenerse de cualquier otra fuente diferente a la mencionada en el Capítulo Descriptivo, de tal forma que cualquier persona medianamente versada en la materia, con la simple mención de ella, puede comprender y reproducir la invención sin necesidad de tener un certificado de deposito. Además, valga la pena mencionar que dicha cepa es tan ampliamente conocida, que cualquier persona medianamente versada en la materia sabe que dichas cepas Oka se pueden obtener muy fácilmente con técnicas y métodos comunes en el arte, tal como se demuestra en los Anexos 1, 2, 3, 4 y 5.

Por lo tanto, dado que: i) la invención no busca protección sobre la cepa Oka específicamente mencionada en el Capítulo Descriptivo; ii) dicha cepa Oka no fue desarrollada por Merck; iii) dicha cepa es conocida por cualquier persona medianamente versada en la materia; iv) dicha cepa Oka puede obtenerse fácilmente de otras fuentes conocidas y comunes y, v) dicha cepa es ampliamente conocida por cualquier persona medianamente versada en la materia; respetuosamente considero que **ningún certificado de deposito debe ser presentado** y por el contrario, considero que la invención no va en contra de las disposiciones del Artículo 29 de la Decisión 486.

ii) De otra parte, me permito aclarar al Despacho, nuevamente, sobre el hecho que un inventor está en su derecho de reclamar protección para la totalidad de un concepto inventivo desarrollado, **sin importar la amplitud de éste**, siempre y cuando se conserve el principio de unidad de invención y no haya arte previo que afecte su patentabilidad. Es decir, un

Capítulo Reivindicatorio puede ser tan amplio como se requiera para así poder enmarcar la totalidad del concepto inventivo desarrollado y todas sus posibles modalidades, más no solamente las modalidades preferidas o específicamente ejemplificadas en dicha solicitud.

Así, el concepto inventivo desarrollado en la presente solicitud corresponde a un método de preparación de un virus de varicela zóster (VVZ) inactivado que comprende: irradiar con radiación gamma una muestra que comprende un VVZ, usando de 10 a 25 kGy de radiación gamma, en donde la radiación gamma se proporciona a la muestra mediante la exposición de la muestra a rayos de 60Co. De esta manera, es claro que dicho concepto inventivo desarrollado aplica completamente para cualquier virus de varicela zóster. Por lo tanto, limitar únicamente a la cepa Oka es injusto, y por el contrario, tan importante es la protección a la totalidad del concepto inventivo desarrollado y a las diferentes modalidades que lo comprenden, que en caso de que existiese un producto competidor en el mercado, dicho producto evitaría una infracción de patente mediante la modificación de características no esenciales, tales como variar entre cepas del VVZ, en caso de limitar excesivamente la invención a la cepa Oka. Asimismo, la compañía productora del competidor no se vería en la necesidad de solicitar autorización del inventor para comercializar dicho producto, desdibujando el propósito del sistema de patentes.

Es decir, la novedad y el nivel inventivo del concepto inventivo dependen únicamente de la novedad y nivel inventivo del método reclamado, aplicado a cualquier cepa de VVZ. De hecho, obligar al solicitante a incluir características no esenciales en dichas reivindicaciones solamente limitaría el alcance de protección al que tiene derecho, pues productos infractores posteriores podrían salirse fácilmente de las limitaciones no esenciales incluidas, como por ejemplo, variar de una cepa de VVZ a otra. El Despacho debe comprender que el concepto inventivo no recae exclusivamente a una cepa en particular, sino a la aplicación de cierto tipo de radiación gamma a cualquier virus de varicela zoster. Es por esto que el solicitante no solicita protección del método para cualquier virus existente, sino que lo limita exclusivamente al virus de varicela zoster, puesto que con la inactivación de este virus en particular es que se presentan los efectos sorprendentes e inesperados en relación con la disminución en la inefectividad y además inducción de una respuesta inmune contra VVZ.

En conclusión, considero respetuosamente que el Capítulo Reivindicatorio Modificado adjunto cumple con los requisitos de claridad y concisión establecidos en la Decisión 486, y a la luz del Manual Andino de Patentes (MAP) y la Guía para Examen de Solicitudes de Patente de Invención y Modelo de Utilidad de la SIC, permitiéndole a la persona medianamente versada en la materia comprender inequívocamente el alcance de la materia reclamada.

3.3 a- El Despacho insiste en que la patente US6214354 (D1) y el documento "*Virus inactivation studies using ion beams, electron and gamma irradiation*"[1] (D2), afectan el nivel inventivo de la presente invención.

La SIC presenta la siguiente tabla comparativa:

Tabla 1

Características esenciales	D1	D2
Método de preparación de un virus de varicela zóster (VVZ) inactivado que comprende:	Inactivación de virus de váricela zóster de la cepa Oka.	
Irradiar con radiación gamma una muestra que comprende VVZ usando de 10 a 25kGy de radiación gamma mediante la exposición de la muestra a rayos de ^{60}Co.	Exposición del virus VZV a radiación gamma .(Col. 9 línea 60)	Inactivación del virus de váricela zóster por radiación gamma a diferentes dosis de radiación gamma (20-30 kGy) (Fig. 1) de ^{60}Co (Pág. 250).

El Despacho señala que el documento D1 es considerado el estado de la técnica cercano a la invención definida en la Reivindicación 1 porque divulga la inactivación del virus de váricela zóster de la cepa Oka a partir de la exposición del virus VZV a radiación gamma (Col. 9 línea 60). El documento también divulga una composición vacunal que contiene el virus atenuado (Col. 6 ln 15-62) (Ej. 2).

D2 divulga la inactivación del virus de la varicela zóster expuesto a diferentes dosis de radiación gamma (20-30 kGy) (Fig. 1) de 60Co (Pág. 250).

La diferencia entre la solicitud y la divulgada en el documento D1 consiste en que la solicitud divulga que el virus se irradia con radiación gamma usando de 10 a 25 kGy mediante la exposición de la muestra a rayos de 60 Co.

En las figuras 1 y 2 se describe que la exposición de la muestra viral a radiación gamma de entre 5 a 25 kGy mostró una pérdida de ½ unidad logarítmica, sin llegar al 100% de la pérdida de infectividad, por tanto no se evidencia un efecto técnico sorprendente asociado a un método para inactivar un virus de la varicela zóster.

[1] Eduardo E. Smolko, Nuclear Instruments and Methods in Physics Research Section B: Beam interactions with Materials & Atoms, 2005, vol. 236, issues 1-4, páginas 249-253.

El problema técnico objetivo que pretende resolver esta invención se puede formular así: Cómo proporcionar un método alternativo para inactivar un virus de varicela zóster.

Sin embargo, virus de varicela zóster inactivado a partir de la exposición a radiación gamma, ya está divulgado en D2 que se refiere a diferentes dosis de rayos gamma de 60Co (20-30 kGy) con un 100% de inactivación total (Fig. 1). Ahora bien, teniendo en cuenta que D1 da a conocer que el virus de varicela zoster puede ser inactivado por técnicas como la radiación gamma, empleando cantidades conocidas de tiempo e intensidad siempre y cuando la integridad del virus no se vea comprometida (Ejemplo 2, Col 4) y D2 se refiere a diferentes dosis de rayos gamma de 60Co (20-30 kGy) con un 100% de inactivación total existe una motivación para irradiar a diferentes dosis de rayos gamma de 60Co (20-30 kGy) una muestra de virus de varicela zóster de D2 en un método para inactivar un virus de varicela zóster de D1. En consecuencia, una persona medianamente versada en la materia, incluiría diferentes dosis de rayos gamma de Co del documento D2 en el método sugerido en el documento, esperando con certeza, un método para preparar un virus de varicela zóster inactivado, por tanto la reivindicación 1 carece de nivel inventivo.

Puesto que las Reivindicaciones dependientes 2 a 3 no proporcionan características esenciales adicionales se considera que tampoco cumplen con el requisito de nivel inventivo. Las Reivindicaciones 4 a 12 que se refieren al virus inactivado producido mediante el método de la Reivindicación 1 tampoco tienen nivel inventivo teniendo en cuenta que son obtenidos por el método que ya se demostró que no cumple con los requisitos de patentabilidad, y por qué adicionalmente no se proporcionan las características estructurales del mismo de manera que no es posible distinguir dicho virus reclamado y la correspondiente vacuna que los contiene de los divulgados previamente en los documentos D1 (Reivindicación 1) y D2 (introducción Pág. 249).

b- En referencia mi argumento, según el cual el documento D1 es insuficiente en cuanto a las enseñanzas relacionadas con virus de VVZ inactivado por radiación gamma, aunque mencione la radiación gamma no reclama un rango de radiación de 10 a 25kGy, la SIC aclara que lo que la solicitud reclama es un método para inactivar un virus VVZ, para lo cual el D1 divulga la inactivación del virus de váricela zóster de la cepa Oka a partir de la exposición del virus VZV a radiación gamma (Col. 9 línea 60) y D2 se refiere a diferentes dosis de rayos gamma de 60Co (20-30 kGy) con un 100% de inactivación total.

De otra parte, en respuesta a mi argumento según el cual D2 tan solo muestra resultados de inactivación para cada uno de los virus citados, en donde se logra un 0.0001% de actividad de los virus alrededor de una radiación gamma de 20kGy y la presente invención proporciona un virus activo alrededor de 0.000015% de virus activo, lo cual corresponde a 10 veces más virus

inactivados que lo descrito en D2, la SIC aclara en primer lugar, que la presente solicitud solamente enseña en las figuras 1 y 2 que la exposición de la muestra viral a radiación gamma de entre 5 a 25 kGy mostró una pérdida de tan solo la mitad de una unidad logarítmica, sin llegar al 100% de la perdida de infectividad, de igual manera el documento D2 enseña la inactivación del virus de la varicela zóster expuesto a diferentes dosis de radiación gamma (20-30 kGy) (Fig. 1) de 60Co (Pág. 250), y por tanto el método reclamado carece de altura inventiva.

3.4 a- En primer lugar, me permito aclarar nuevamente que la presente invención reclama particularmente un método de preparación de un virus de varicela zóster (VVZ) inactivado que comprende: irradiar con radiación gamma una muestra que comprende un VVZ, usando de 10 a 25 kGy de radiación gamma, en donde la radiación gamma se proporciona a la muestra mediante la exposición de la muestra a rayos de 60Co.

b- En este mismo orden de ideas, me permito realizar el análisis de nivel inventivo de acuerdo con la Guía de la SIC[2] en donde se señala que "*Durante el examen de nivel inventivo debe hacerse un juicio de valor y un análisis objetivo de las divulgaciones previas del estado de la técnica, no influenciados por el conocimiento que ya se tiene de la Invención que se está evaluando. Por tanto, con el fin de minimizar la subjetividad y evitar que se realice un análisis en retrospectiva ("hindsight" ó "a posteriori"), el examen debe relacionar la invención con la solución de un problema técnico, mediante el Método "problema-solución"* (subrayado fuera de texto).

A. Identificar el estado de la técnica cercano a la invención reivindicada.

Para el presente caso, D1 es considerado como el arte previo más cercano, tal como lo reconoce el Despacho.

B. Determinar la diferencia entre la invención y el estado de la técnica más cercano.

De acuerdo con los lineamientos establecidos por la SIC, me permito presentar el siguiente cuadro comparativo entre las características esenciales de la presente invención y las enseñanzas del documento del arte previo citado:

[2] Guía para Examen de Solicitudes de Patente de Invención y Modelo de Utilidad de la SIC , 2014, sección 2.13.5, páginas 131-134

Características esenciales	D1
Un método de preparación	**No menciona**
un virus de varicela zóster (VVZ) inactivado que comprende	Cepa Oka
irradiar con radiación gamma una muestra que comprende un VVZ,	**Inactivar el virus con calor** (Enseñanza primordial y predominante en D1. Mencionada a lo largo de todo el contenido de D1) Exponer el VVZ a radiación gamma (mencionada una vez en D1)
usando de 10 a 25 kGy de radiación gamma	**No menciona**
en donde la radiación gamma se proporciona a la muestra mediante la exposición de la muestra a rayos de ^{60}Co	**No menciona**

Con base en la tabla anterior, se puede concluir que D1 no sugiere un **método de preparación** tal como se reclama en la presente invención. La SIC comete un error al intentar hacer parecer que D1 si enseña un método, cuando en realidad las divulgaciones de D1 están orientadas a métodos de tratamiento, que de manera dispersa y bastante general enseñan, a modo de ejemplo, que la radiación gamma junto con muchas otras técnicas, pueden ser utilizadas para inactivar un virus. Evidentemente el arte previo fue escogido utilizando el beneficio de la retrospectiva, y simplemente se basó en buscar palabras claves de la invención en los motores de búsqueda.

Por consiguiente, existen al menos **tres** elementos esenciales de la presente invención que no son motivados ni tampoco sugeridos por D1. En este punto el Despacho no puede confundir la mención de ciertas características esenciales de la invención en los documentos del arte previo, con el hecho de que dicha mención conduzca necesariamente a la invención. El Despacho está pasando completamente por alto la **motivación** que dicho documento le brinda a la persona medianamente versada en la materia. Si bien, D1 menciona la radiación gamma sobre cepas Oka de VVZ (de manera muy general), el documento, en su totalidad, pretende enseñarle al lector sobre un método de tratamiento para prevenir la neuralgia post-herpes aprovechando la estimulación antigénica y enfocándose exclusivamente en vacunas con VVZ completo, vivo y atenuado. De nuevo, la radiación gamma es mencionada con fines netamente ilustrativos, y jamás fue intención de D1 mencionarlo como una característica esencial o fundamental de sus enseñanzas al lector.

Tal y como lo ilustra el Ejemplo 2 de D1, esta referencia muestra la preparación de una vacuna de virus varicela zóster inactivado solamente por calor (véanse las columnas 6 y 7) y solamente menciona la posibilidad de preparar una vacuna de VVZ inactivado mediante la irradiación con

rayos gamma, con una única referencia general en la columna 4 a radiación gamma "en cantidades conocidas de tiempo e intensidad", sin detalle adicional particular alguno. D1 sólo sugiere que la inactivación se llevará a cabo "para cantidades conocidas de tiempo e intensidad" para lograr la inactivada VZV (véase la columna 4 de D1). Los solicitantes consideran que esta divulgación limitada no enseña que 10-25 kGy de radiación gamma se pueden utilizar para inactivar una muestra VZV, resultando en una VZV con una infectividad residual de <0,04, que es capaz de inducir una respuesta inmune contra VZV que difiere de la respuesta inmune provocada por una muestra de control no inactivado por 25% o menos.

Por lo tanto, la única enseñanza concreta de D1 corresponde al Ejemplo 2, en relación el tratamiento de virus VVZ para **inactivarlo con calor,** alcanzando una infectividad de 2,4 unidades formadoras de placas/mL, lo cual es bastante diferente de lo que se reclama específicamente en la presente solicitud.

En otras palabras, D1 es insuficiente en cuanto a enseñanzas relacionadas con virus de VVZ inactivado por radiación gamma. Aunque D1 mencione la radiación gamma, es evidente que dicho documento no proporciona datos o información relevantes. Por el contrario, D1 solamente proporciona información esencial para producir vacunas mediante la inactivación por calor, dejando la producción de vacunas por radiación como una simple especulación. En conclusión D1 no sugiere las condiciones de radiación que específicamente aplica la presente invención, en donde se reclama un rango de radiación gamma de 10 a 25kGy.

C. Definir el efecto técnico causado y atribuible al elemento diferencial.

i) Las diferencias entre el método reclamado y D1 es la característica esencial de utilizar 10-25 kGy de radiación gamma para inactivar el virus VZ, lo cual reduce la infectividad de una preparación viral VZ a niveles indetectables (es decir <0.040 de PFU/ml), y a su vez, conserva significativamente la antigenicidad, la inmunogenicidad y las características estructurales de un control no inactivado. Un método para producir un VZV inactivado con tales características no se enseña o sugiere en D1. Los solicitantes han demostrado que la inactivación de las vacunas de VZV mediante la exposición de una muestra a los rayos 60Co no sólo podría lograr inesperadamente **bajos niveles de infectividad** con solamente 10 a 25 kGy de radiación gamma, sino también producir una vacuna que induce una respuesta inmune que no fue significativamente diferente de la producida por una vacuna viva atenuada VZV, medida por un ensayo de ELISPOT de IFN VZV (véase el Ejemplo 5) y un VZV Ag ELISA (véase el Ejemplo 7). El logro de tales niveles bajos de infectividad residual con irradiación gamma, al tiempo que se conserva la inmunogenicidad que aún es suficiente para el uso de la vacuna fue totalmente inesperado a la luz de D1, que ni siquiera habla de métodos de producción. Además, es claro

para cualquier persona medianamente versada en la materia que el uso de altos niveles de radiación, si bien van a desactivar cualquier estructura viral, es potencialmente perjudicial puesto que no se va a conservar la viabilidad biológica del virus, de tal forma que lo haría completamente inútil para producir una vacuna. De esta manera, el hecho que la presente invención logre desarrollar un proceso en el cual, se logre la desactivación del virus y además se logre conversar su viabilidad inmunogénica es un efecto completamente sorprendente e inesperado, que demuestran el nivel inventivo de la invención.

De esta manera, si una persona medianamente versada en la materia midiera la infectividad de (1) un control no inactivado, o (2) un VZV inactivado con calor (como lo sugiere D1), encontraría que dichas infectividades serían mucho más altas que la infectividad de un VZV inactivado con 10-25 kGy de radiación gamma, como se discute a lo largo del Capítulo Descriptivo. Ninguno de estos, (1) o (2), produciría un VZV que sea útil como una vacuna en una población de pacientes inmunocomprometidos. Del mismo modo, y como ya lo mencioné, el uso de niveles más altos de radiación gamma produciría daños a la estructura del virus y no sería óptimo para uso en vacunas. Véase el ejemplo 6, último párrafo, que establece: "Los resultados de Cryo EM indican efectos de partículas potenciales a dosis de irradiación de alta gama, con una reducción en la densidad de electrones (que quizás refleja la degradación del ADN viral) ..." Por lo tanto, el método reivindicado produce sorprendentemente un VZV inactivada que es útil como vacuna en pacientes inmunocomprometidos, lo cual no esta sugerido ni mucho menos motivado en D1.

De esta manera, vale la pena resaltar que fue inesperado que un VZV se pueda inactivar a un nivel de infectividad residual tan bajo al tiempo que conserva una respuesta inmune que difiere de la de un control en un 25% o menos. Véase, por ejemplo, el ANEXO 6 (Budowsky et al), que establece:

> *"Debido a la acción de agentes de inactivación conduce a daños directos o indirectos de los antígenos virales, los viriones en las vacunas muertas por lo general contienen un conjunto incompleto de antígenos activos, y por lo tanto su inmunogenicidad puede ser menor que la del virus nativo. Usando la misma dosis de vacuna de virus muertos como vacuna viva, la disminución en el número de copias activas de cualquier antígeno conduce a una disminución en la eficiencia inmunogénica con respecto a este antígeno." (Página 275)*

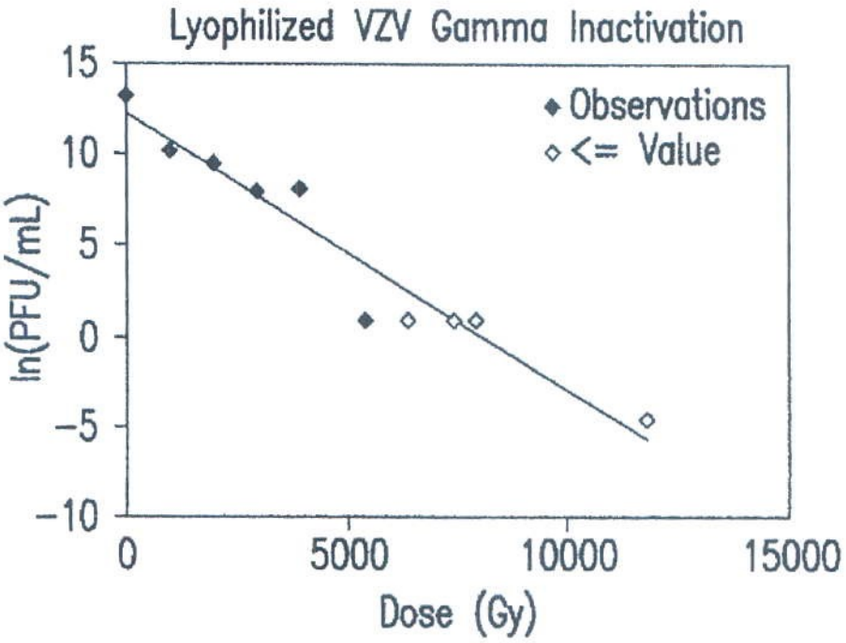
Véase también, el ANEXO 7 (Rosen et al), que indica que, en el caso de virus del herpes simple, la capacidad de formación de placas se mantuvo intacta cuando el virus se irradió con 60Co a dosis de hasta 40 kGy (resumen). Rosen llegó a la conclusión de su estudio que "*los resultados*

... *sugieren que se necesita fragmentación casi completa de ADN viral para destruir su infectividad por completo.*" (Página 803, primer párrafo).

Del mismo modo, un VZV producido por los métodos reivindicados también es estructuralmente diferente de una VZV inactivado producido por la inactivación por calor, el cual no puede alcanzar niveles de infectividad residual tan bajos como los producidos por 10-25 kGy. Véase, por ejemplo en el ANEXO 8 (Wigginton et al), que muestra de que los virus inactivado por calor no sufren grandes daños en el genoma (página 12072, columna 2, primer párrafo completo), declarando: "*el daño en el genoma era insignificante después del tratamiento térmico.*") Este hallazgo está en contraste directo a los efectos dañinos que los rayos gamma se sabe que tienen sobre el ADN y las proteínas, tal como se sustentan en los ANEXOS 9 y 10, (Kempner et al y Miller et al).

Con base en los resultados y conclusiones particulares de los inventores, como se demostró anteriormente, es evidente que las vacunas de la presente invención son efectivas y son completamente impredecibles a partir de las enseñanzas del arte previo. Particularmente, y como mencionaré con detalle más adelante, estos resultados demuestran que, contrario a las enseñanzas del arte, previo, el desarrollo de una vacuna con un virus inactivado por radiación gamma, sin afectar el genómica del virus, y por tanto sus propiedades inmunogénicas.

ii) De otra parte, considero respetuosamente que la SIC malinterpreta los datos que se muestran en la Figura 1 de esta solicitud, en donde se muestra la cinética de inactivación de VVZ liofilizado, sometido a irradiación g (log UFP/ml v. dosis de radiación, véase el Ejemplo 4). Se irradiaron viales de VVZ con diferentes niveles de rayos ^{60}Co, usando un irradiador ^{60}Co Gammacell®. Las UFP residuales/ml de cada vial por dosis de radiación (Gy) se determinaron usando el ensayo en placas de varicela en células MRC-5. Los puntos de datos observados se muestran como rombos negros ("observaciones") y los datos máximos medibles por el ensayo, con valores mayores de 5kGy, los valores se muestran por rombos grises ("<= Valor"), para los que no se observaron placas. Es decir, se muestran resultados para radiación de 0 a 5 kGy, en donde la inefectividad está marcada con rombos negros y las plaquetas no observadas son reportadas como "<=" (dicho valor indica que el titulo pudo haber tenido 1 plaqueta detectada en el volumen medido) como se puede observar a continuación:



En la solicitud también se ensayó un volumen de material grande de 100mL, el cual fue medido en la Figura 1 (Ejemplo 4, pág. 18). Los 100mL de volumen de material fueron irradiados con 12 kGy y no se detectó inefectividad residual. En este caso, el mínimo de inefectividad detectable pudo ser 1 PFU en 100mL o 0.01 PFU/mL. El valor medido indica que la inefectividad del materia irradiado a 12 kGy es entonces <=0.01 PFU/mL. En la escala ln(PFU/mL) eje-y de la Figura 1, esto correspondería -4.6.

El argumento de la SIC afirmando que la muestra del virus pierde la mitad de una unidad logarítmica a 5-25 kGy de radiación gamma sin lograr un 100% de desactivación, es incorrecto. Para las pruebas del volumen en la Figura 1, se obtuvo la desactivación completa (por ejemplo, cero plaquetas fueron detectadas en ensayos con varicela), con la cantidad de radiación probada mayor de 5kGy. Los diamante blancos en la gráfica indican el límite de detección del ensayo. Aunque no se muestran resultados a 25 kGy en la Figura 1, el ln(PFU/mL) puede extrapolarse basado en la linealidad de la curva, que sería bastante bajo. Esto resulta completamente inesperado, ya que el rango de radiación reclamado resulta en tales niveles menores de inefectividad residual, mientras se mantienen el requerimiento de inmunogenicidad, antigénicidad y características estructurales requeridas para la vacuna propuesta.

En este sentido, me permito llamar la atención sobre el Artículo 18 de la Decisión 486, el cual establece que "*Se considerará que una invención tiene nivel inventivo, si para una persona del oficio normalmente versada en la materia técnica correspondiente, esa invención no hubiese resultado obvia ni se hubiese derivado de manera evidente del estado de la técnica*".

A la luz de lo anterior, lo único que solicita la Decisión 486 para reconocer el nivel inventivo es que el invento no se derive de manera obvia a partir del arte previo. Así, a pesar de la presente invención logra valores de infectividad adecuados para el desarrollo de una vacuna, es arbitrario que el Despacho únicamente reconozca una perdida de infectividad del **100%** como los únicos efectos técnicos válidos en este tipo de invención y más cuando no existe requerimiento legal alguno que lo exija. Por lo tanto, es oportuno señalar que **cualquier** tipo de efecto **técnico** que presente la invención **debe** ser reconocido, evaluado y, si dicho efecto no es evidente a la luz del arte previo, debe ser aceptado para reconocer el nivel inventivo de la invención.

Así, gracias a las diferencias encontradas entre la presente invención y el arte previo citado por el Despacho, y teniendo en cuenta que cualquier efecto técnico que no sea obvio a la luz del arte previo **es completamente válido en materia de patentes**, es oportuno recalcar nuevamente que el método reclamado en la presente solicitud resulta tener efectos sorprendentes e inesperados a la luz del arte previo más cercano, y mas cuando el arte previo sugiere inactivación por calor en vez de la radiación gamma aquí reclamada. Demostrando lo anterior que las consideraciones anteriormente presentadas no fueron tenidas en cuenta por el Despacho en su análisis, por lo cual no pudo apreciar el efecto técnico real que se logra mediante la materialización de la presente invención.

Ahora bien, vale la pena recalcar nuevamente que esta etapa del método problema-solución se centra en la definición del efecto técnico atribuible al (los) elemento(s) esenciales y diferenciadores de la invención, mas no en la determinación de si existe un efecto técnico necesariamente ventajoso. El Despacho no puede confundir efecto técnico con efecto superior; incluso, en esta etapa no hay lugar a determinar si dicho efecto es ventajoso o no, ya que por definición, el objetivo de una invención es proporcionar una solución a un problema técnico, el cual incluso podría ser desventajoso o comercialmente inviable, sin que esto afecte los requisitos de patentabilidad. Es un error que el Despacho considere que todas las solicitudes de patente siempre deben presentan un efecto ventajoso. Lo único que debe determinar es si la invención es derivable de manera obvia a partir del arte previo.

Aquí valga la pena señalar que el Solicitante está en el derecho de consignar la información que considere relevante y necesaria en relación con el concepto inventivo desarrollado, ya que el único requisito es que dicha información le permita a cualquier persona medianamente versada en la materia reproducir la invención. En el presente caso, la Examinadora compara abiertamente los resultados de D2 con los de la presente invención (sin mencionar que estaban siendo mal interpretados por la Examinadora). En cualquier caso, es un error que el Despacho pretenda que todas las patentes presenten la misma información, con los mismos datos, los mismos ensayos, solo porque pertenecen a un campo técnico similar, y sobre todo, exigir que la invención tenga obligatoriamente datos comparativos exclusivamente con el arte previo citado en

Colombia. El Solicitante no está en la obligación de consignar datos comparativos dentro de la patente, y anticiparse a las posibles objeciones de patentabilidad de una oficina de patentes en particular.

En el presente caso, existe un efecto técnico, el cual es completamente atribuible a las diferencias encontradas entre la presente invención y el estado de la técnica más cercano. Así las cosas, no sólo existe un efecto técnico que soluciona un problema técnico, sino que dicho efecto además resulta ser sorprendente e inesperado, puesto que el estado de la técnica más cercano ni siquiera menciona cómo desarrollar el proceso de la presente invención.

Así las cosas, dado el esfuerzo involucrado en el desarrollo de estas mejoras, y dado que éstas proporcionan ventajas comerciales competitivas, y se derivan directamente de la investigación y creatividad humanas, el sistema de patentes *debe* garantizar su protección. La SIC no puede basarse en apreciaciones subjetivas para privar al inventor de la protección merecida para su desarrollo novedoso y no sugerido por el estado de la técnica.

D. Deducir el problema técnico a solucionar.

Con base en lo anteriormente mencionado respecto al arte previo, el problema técnico de la presente invención está planteado de manera bastante general por el Despacho y además ignorando completamente los efectos de la invención. De esta manera, el problema técnico a solucionar es: ¿Cómo modificar el método de inactivación por calor de VVZ de D1 que no altere el genoma del virus y que no altere la capacidad inmunogénica del virus?

E. Evaluar si la invención reivindicada, partiendo del estado de la técnica cercano y del problema técnico objetivo, habría sido obvia para la persona medianamente versada en la materia.

Evidentemente, el arte previo citado por el Despacho no brinda las enseñanzas suficientes para que la persona medianamente versada en la materia desarrolle la presente invención sin ambigüedad alguna. Tal y como lo he mencionado a lo largo del presente Recurso de Reposición y en mi respuesta al segundo examen de fondo, D1 ni D2 sugieren todas las características esenciales del proceso reclamado, y por el contrario, se encuentran alejados de la materia aquí reclamada.

D2 sugiere un método para la inactivación de virus, particularmente enseñando pruebas con radiación gamma en Virus de Fiebre Aftosa (VFA), virus Rauscher de leucemia (RLV) y virus del herpes simple (VHS). Evidentemente, D2 no contiene enseñanza alguna sobre la aplicación y utilidad de la inactivación de **VVZ** usando radiación gamma.

D2 tan solo muestra resultados de inactivación en la Figura 1 para cada uno de los virus citados, en donde se logra un 0.0001% de actividad de los virus alrededor de una radiación gamma de 20kGy. Sin embargo, la presente invención proporciona un virus activo alrededor de 0.000015% de virus activo, lo cual corresponde al menos a **10 veces** más virus inactivados que lo descrito en D2. Claramente, D2 no conduce a la persona medianamente versada en la materia a usar la radiación gamma específica sobre VZV para llegar a la presente invención, pues ni siguiera se refiere al mismo tipo de virus, ni brinda enseñanzas sobre los resultados obtenidos.

En conclusión, D2 se refiere a virus inactivos pero no al virus de varicela zóster, y además sin sugerir un protocolo de inactivación específico. D2 sólo describe diferentes estructuras de virus que no llevan a la persona medianamente versada en la materia a llegar al objeto aquí reclamado. Es más, D2 enseña que la inactivación de diferentes virus no es alcanzable con un protocolo ge inactivación general (que pueda predecirse, funcionaría para todos (ver Figuras 1 u 2 de D2).

De otra parte, D2 no proporciona ningún dato biológico en su publicación en relación con muestras de virus que fueron irradiados con radiación gamma. D2 solamente muestra la inactivación de un virus a la mitad del volumen. Es imposible entender a partir de D2 que la inactivación de VVZ usando una alta cantidad de radiación sea útil para inactivar completamente la muestra, pues el daño que puede causarse a las muestras (ADN y proteínas) puede resultar en virus incapaces de inducir una respuesta inmune efectiva. Así, inactivar un virus corresponde sólo a la mitad del trabajo.

En adición a lo anterior, nuevamente me permito señalar que para que la combinación de documentos sea válida, ésta debe proporcionar argumentos sólidos sobre el éxito de llegar a la invención reclamada. Es decir, se deben encontrar argumentos sólidos que lleven a creer de forma técnica que dicha combinación de documentos llevaría de manera inequívoca a la materia reclamada. En el presente caso, la diferente combinación de los documentos no lleva de manera inequívoca a la presente solicitud, y por el contrario, la persona medianamente versada en la materia estaría motivada a inactivar los virus de D2 utilizando la inactivación por calor de D1.

La combinación de las 2 anterioridades citadas por la SIC no habría guiado de ninguna manera a la persona medianamente versada en la materia a desarrollar de manera obvia el proceso de la presente invención. Tal análisis debe basarse únicamente en si existen sugerencias y motivación explícitas y suficientes en el arte previo para lograr desarrollar de manera obvia la invención, la cual, como se demostró anteriormente, no existen.

No es aceptable a quien examina una patente desvirtuar el nivel inventivo de la misma por simplemente desglosar sus elementos separadamente y luego buscar referencias en el estado del arte que los incluyan, como si de armar un rompecabezas con piezas aisladas, o una colcha de retazos, se tratara. En este caso particular, y contrario al análisis del Despacho, como es evidente del análisis del arte previo realizado anteriormente, la única forma en que una persona medianamente versada en la podría llegar al proceso de la presente invención siguiendo los argumentos del Despacho, sería al realizar un análisis en retrospectiva una vez conoce la invención aquí reclamada, que de igual manera tampoco llevaría a las características esenciales del proceso y mucho menos a los resultados obtenidos dado que todos los documentos citados por la SIC no contienen un hilo conductor que las una o ligue de una forma coherente que guiara directa y necesariamente al proceso aquí reclamado.

El estudio de solicitudes de patente que conduzca a ese tipo de conclusiones anticipadas corresponde abiertamente a un análisis conocido en el ámbito de patentes como "***análisis hindsight***". Para entender el análisis equivocado que realiza la SIC, podemos citar el Manual Andino de Patentes, que indica claramente: *"...la búsqueda de anterioridades se efectúa a posteriori, tomando como punto de partida la misma invención,...La SIC debe realizar el esfuerzo intelectual de colocarse en la situación que ha tenido que afrontar el técnico con conocimientos medios en la materia en un momento en que la invención no era conocida, es decir antes de la invención*"[3] (mi subrayado). Por ende, no es apropiado anticiparse a los resultados presentados por la invención, ya que así, siempre resultará "*obvio*" todo objeto de una solicitud de patente, pues inevitablemente está parecerá derivada de la teoría en que se basa su desarrollo, sin dar mayor importancia al trabajo, intelecto y creatividad involucrados en la invención para llegar a la solución del problema planteado en la solicitud.

De aceptar el estándar de nivel inventivo de la SIC, donde supuestamente el desarrollo del proceso aquí reclamado es obvia, equivaldría a desdibujar el objetivo principal del sistema de patentes, que es precisamente fomentar la investigación y desarrollo de mejoras incrementales. Nada se inventa de la nada. En este sentido, el Tribunal Andino de Justicia (TAJ) ha determinado que la divulgación del arte previo utilizada para desvirtuar la patentabilidad de una invención, debe ser lo suficientemente detallada para que una persona medianamente versada en la materia pueda usar dicha información para reproducir y explotar la invención sin acudir a experimentación adicional alguna[4]. Evidentemente, la SIC simplemente buscó algunas palabras clave en D1 relacionadas con el virus y la radiación gamma de la presente invención y la combinó con las escasas enseñanzas de D2 en relación con otros virus y radiación, sin explicar de manera coherente, motivada y detallada los argumentos en contra del nivel inventivo.

[3] Manual Andino de Patentes. (2004). Sección 10.2.1 (disponible en http://www.comunidadandina.org/public/patentes.pdf).
[4] Proceso 06-IP-89 (http://intranet.comunidadandina.org/Documentos/Procesos/209-IP-2005.doc); y Proceso 36-IP-2004 (http://www.notinet.com.co/serverfiles/servicios/archivos/30jul04/ca36-04.htm)

Por lo tanto, me permito señalar que el hecho de que las características esenciales del proceso reivindicado no pueda predecirse a partir de las enseñanzas del arte previo concuerda completamente con los principios fundamentales del nivel inventivo como lo establece el Manual Andino de Patentes (MAP), el cual establece que para que pueda negarse la existencia de nivel inventivo, es necesario no solamente que la combinación de las enseñanzas pueda hacerse, sino también que exista una sugerencia o razón tal, que lleve al técnico con conocimientos medios a combinar las enseñanzas de los documentos.[5] Además, el MAP también establece que las invenciones en el campo de la química tienen nivel inventivo cuando la materia reclamada tiene características **estructurales inesperadas** (no derivable por la persona medianamente versada en la materia) o cuando presentan un **efecto técnico inesperado o mejorado impredecible del arte previo**[6]. Por lo tanto y en vista de que D1 no sugiere el proceso aquí reclamado y mucho menos que dicho proceso tenga la capacidad de inactivar el virus y además mantener las propiedades inmunogénicas sin destruir el genoma del virus luego de la radiación gamma, la persona medianamente versada en la materia en la materia no podría haber llegado a ella de manera obvia y evidente a la luz de las enseñanzas de D1.

Así, resulta notable que en el momento de la realización de la resolución negatoria, el Despacho no se rigió por lo estipulado en la Guía de la SIC en cuanto la evaluación de nivel inventivo, ya que este debe basarse únicamente en si existen **sugerencias explícitas** y suficientes en el arte previo para lograr desarrollar de manera obvia el proceso aquí reclamado, la cual, como se demostró anteriormente, no existen. Por el contrario, el análisis que realiza la SIC es subjetivo, y simplemente pretende negar la existencia del nivel inventivo con razones técnicas equivocadas, tal como quedó demostrado en el presente recurso de reposición. En este orden de ideas, es evidente que el Despacho olvida que la Guía de la SIC dice que "*Una vez formulada una nueva idea, a menudo se puede demostrar teóricamente el modo en el que se podría llegar a ella, a partir de algo conocido, a través de una serie de etapas aparentemente fáciles. El examinador de patentes debe evitar el uso de un análisis ex post facto de este tipo.*"[7].

Además, la Guía de la SIC establece claramente que "si el estado de la técnica provee las enseñanzas para derivar la solución, revisar si el conjunto de enseñanzas del estado de la técnica **lo llevarían de forma inmediata a la solución propuesta por la solicitud**. Si se requiere de pasos adicionales o de corroboración o de superar obstáculos revelados por las propias

[5]Manual Andino de Patentes. (2004). Sección 10.2.1 Ejemplo 1. (http://www.comunidadandina.org/public/patentes.pdf).
[6] Ibidem. Sección 10.8.1.
[7] Guía para Examen de Solicitudes de Patente de Invención y Modelo de Utilidad de la SIC , 2014, sección 2.13.6.3, página 137 (disponible en http://api.sic.gov.co/Documentos/Guia_Examen_Patentes.pdf)

enseñanzas entonces el estado de la técnica no revela la solución al problema"[8] (subrayado y negrilla fuera de texto). Evidentemente, la dicha persona medianamente versada en la materia necesitaría investigación y experimentación adicional con el fin de establecer el método reclamado y los virus VVZ obtenidos.

En conclusión, a la luz de la clara evidencia en favor del nivel inventivo de la presente invención suministrada anteriormente, la persona medianamente versada en la materia no habría encontrado sugerencia o motivación alguna que la condujera directamente a desarrollar el proceso aquí reclamado, por lo que la presente invención reviste nivel inventivo sobre D1 y D2.

3.5. Finalmente, y con un propósito meramente informativo y sabiendo de antemano que en materia de patentes imperan los principios de territorialidad, autonomía e independencia, siendo cada país autónomo e independiente al momento de conceder o denegar un privilegio de patente en virtud de sus propios análisis, exámenes de patentabilidad y normatividad aplicable, me permito anotar que a la fecha ha sido otorgado el privilegio de patente para el concepto inventivo comprendido en la presente solicitud en Australia, Nueva Zelanda, Sur África y próximamente en China.

Si bien es cierto que las concesiones de patentes en oficinas de otros países no son vinculantes en el sentido que obliguen a la SIC a tomar una decisión en el mismo sentido, es a la vez cierto que los criterios de patentabilidad en los que deben fundamentarse el análisis de solicitudes de patente, en particular en cuanto a la novedad se refiere, **son análogos globalmente**, y concesiones en otras jurisdicciones sugieren el cumplimiento de dichos requisitos, ya que claramente, los criterios de evaluación y estudio aplicados para determinar la novedad y nivel inventivo resultan equivalentes a los que la Superintendencia debe emplear, establecidos de manera semejante por las legislaciones de patentes a lo largo del mundo entero.

4. Para terminar, de conformidad con lo establecido en el artículo 80 del Código de Procedimiento Administrativo y de lo Contencioso Administrativo, solicito respetuosamente que todos y cada uno de los puntos planteados en el presente recurso sean resueltos de manera individual, completa y motivada, respecto de las razones de hecho, derecho y/o conveniencia que lleven a esa Superintendencia a adoptar la decisión que estime frente a la solicitud aquí formulada.

[8] Superintendencia de Industria y Comercio, Guía para Examen de solicitudes de Patente de Invención y Modelo de Utilidad, 2014, sección 2.6.5.4, p. 76.

5. NOTIFICACIÓN

Recibiré notificaciones en mis oficinas ubicadas en la Carrera 5 No. 34-03, de Bogotá.

Atentamente,

CARLOS R. OLARTE
C.C. No. 79.782.747 de Bogotá
T.P. 74.295

Anexos:

- Capítulo Reivindicatorio Modificado;
- Recibo de pago por modificación voluntaria
- Recibo de pago por 2 reivindicaciones adicionales;
- ANEXO 1: "Comparison of the complete DNA sequences of the Oka varicella vaccine and its parental virus";
- ANEXO 2: "Complete DNA sequences of two Oka strain VZV genomes", J Virol 2008;
- ANEXO 3: "Correction to Comparison of the Complete DNA sequences of the Oka varicalla vaccine and its parental virus", J Virol, 2003;
- ANEXO 4: "Population diversity in batches of the varicella Oka vaccine", Kanda et al. Vaccine, 2011;
- ANEXO 5: "Molecular Analysis of the Oka Vaccine Strain of Varicella-Zoster Virus", Yamanishi et al., 2008.
- ANEXO 6: "Problems and Prospects for Preparation of Killed Antiviral Vaccines," Advances in Virus Research 39:255-291.
- ANEXO 7: Rosen et al
- ANEXO 8 Wigginton et al
- ANEXO 9, Kempner et al
- ANEXO 10 Miller et al

CAPÍTULO REIVINDICATORIO MODIFICADO

(Recurso de Reposición)

1. Un método de preparación de un virus de varicela zóster (VVZ) inactivado que comprende:

irradiar con radiación gamma una muestra que comprende un VVZ, usando de 10 a 25 kGy de radiación gamma,

en donde la radiación gamma se proporciona a la muestra mediante la exposición de la muestra a rayos de ^{60}Co.

2. El método de la Reivindicación 1, en donde la muestra de VVZ es una cepa Oka o una cepa derivada de la cepa Oka.

3. El método de la Reivindicación 1, en el que la muestra se liofiliza antes de irradiarse.

4. Un virus VVZ inactivado producido por el método de cualquiera de las Reivindicaciones 1 a 3.

5. Una vacuna de VVZ inactivado que comprende una cantidad terapéuticamente efectiva del VVZ inactivado de la Reivindicación 4 y un vehículo farmacéuticamente aceptable.

6. La vacuna de VVZ inactivado de la Reivindicación 5, en donde la vacuna es una formulación líquida a granel.

7. La vacuna de VVZ inactivado de cualquiera de las Reivindicaciones 5 o 6, en donde la infectividad del VVZ inactivado es $\leq$0,010 unidades formadoras de placas (UFP)/mL.

8. La vacuna de VVZ inactivado de cualquiera de las Reivindicaciones 5 o 6, en donde la infectividad del VVZ inactivado es $\leq$0,002 unidades formadoras de placas (UFP)/mL.

9. La vacuna de VVZ inactivado de las Reivindicaciones 7 u 8, en donde la respuesta inmune inducida por la el VVZ inactivado no es significativamente diferente de la respuesta inmune inducida por una muestra de control que comprende la misma cantidad del VVZ que no se ha inactivado.

10. La vacuna de VVZ inactivado de las Reivindicaciones 7 u 8, en donde la infectividad del VVZ se determina por un ensayo en placas de varicela.

22

11. La vacuna de VVZ inactivado de las Reivindicaciones 7 u 8, en donde la respuesta inmune se mide con un ensayo de ELISA.

12. La vacuna de VVZ inactivado de las Reivindicaciones 7 u 8, en donde la respuesta inmune se mide con un ensayo IFNγ ELISPOT.

****

Anexo 1 23

JOURNAL OF VIROLOGY, Nov. 2002, p. 11447–11459 Vol. 76, No. 22
0022-538X/02/$04.00+0 DOI: 10.1128/JVI.76.22.11447–11459.2002
Copyright © 2002, American Society for Microbiology. All Rights Reserved.

Comparison of the Complete DNA Sequences of the Oka Varicella Vaccine and Its Parental Virus

Yasuyuki Gomi,[1] Hiroki Sunamachi,[1] Yasuko Mori,[2] Kazuhiro Nagaike,[1,2] Michiaki Takahashi,[3] and Koichi Yamanishi[2]*

Kanonji Institute, The Research Foundation for Microbial Diseases of Osaka University, Kanonji, Kagawa,[1] and The Research Foundation for Microbial Diseases of Osaka University[3] and Department of Microbiology, Osaka University Medical School,[2] Suita, Osaka, Japan

Received 25 March 2002/Accepted 14 August 2002

The DNA sequences of the Oka varicella vaccine virus (V-Oka) and its parental virus (P-Oka) were completed. Comparison of the sequences revealed 42 base substitutions, which led to 20 amino acid conversions and length differences in tandem repeat regions (R1, R3, and R4) and in an origin of DNA replication. Amino acid substitutions existed in open reading frames (ORFs) 6, 9A, 10, 21, 31, 39, 50, 52, 55, 59, 62, and 64. Of these, 15 base substitutions, leading to eight amino acid substitutions, were in the gene 62 region alone. Further DNA sequence analysis showed that these substitutions were specific for V-Oka and were not present in nine clinical isolates. The immediate-early gene 62 product (IE62) of P-Oka had stronger transactivational activity than the mutant IE62 contained in V-Oka in 293 and CV-1 cells. An infectious center assay of a plaque-purified clone (S7-01) from the V-Oka with 8 amino acid substitutions in ORF 62 showed smaller plaque formation and less-efficient virus-spreading activity than did P-Oka in human embryonic lung cells. Another clone (S-13) with only five substitutions in ORF 62 spread slightly faster than S7-01 but not as effectively as P-Oka. Moreover, transient luciferase assay in 293 cells showed that transactivational activities of IE62s of S7-01 and S7-13 were lower than that of P-Oka. Based on these results, it appears that amino acid substitutions in ORF 62 are responsible for virus growth and spreading from infected to uninfected cells. Furthermore, the Oka vaccine virus was completely distinguishable from P-Oka and 54 clinical isolates by seven restriction-enzyme fragment length polymorphisms that detected differences in the DNA sequence.

Varicella-zoster virus (VZV) is a human herpesvirus that causes chickenpox (varicella) and shingles (herpes zoster). A live attenuated varicella vaccine, the Oka strain was originally developed by Takahashi et al. in Japan (56) and is routinely used in children in Japan and other countries, including the United States. Clinical symptoms caused by this live vaccine are very rare in healthy children. Although the Oka vaccine virus (V-Oka) is an avirulent virus, its parental virus (P-Oka), isolated from a patient with typical varicella, is thought to be virulent in vivo. It has not been clarified which gene(s) is involved in the pathogenicity of VZV infection. Thus, comparison of the complete genomes of V-Oka and P-Oka should reveal correlations between DNA sequence and virulence.

The complete DNA sequence of the VZV Dumas strain was first determined by Davison and Scott (9). The genome is a linear double-stranded DNA of ca. 125,000 bp and consists of unique long regions (ULs) flanked by terminal repeat long (TRL) and internal repeat long (IRL) inverted repeat regions, and a unique short (US) region flanked by internal repeat short (IRS) and terminal repeat short (TRS) inverted repeat regions. The genome contains ca. 70 open reading frames (ORFs), three of which exist in both IRS and TRS regions; genes 62 through 64 correspond to genes 69 through 71.

We previously determined the sequences of several genes from V-Oka and P-Oka and found differences between them (15, 16). As many as 15 base substitutions, representing 8 amino acid differences, were found in gene 62, located within the IRS region (or in gene 71 located within the TRS region) and its flanking regions, although no mutations were found in genes encoding other transactivators, such as genes 4, 10, 61, and 63. In addition to our report, another author reported that the DNA sequences of the P-Oka virus and a cosmid clone from the vaccine virus were different in gene 62 (2). The immediate-early gene 62 product (IE62) is an immediate-early (IE) protein consisting of 1,310 amino acids and is functionally conserved with herpes simplex virus type 1 (HSV-1) ICP4 (13). High levels of IE62 are associated with viral tegument (24) and a recombinant HSV-1 with both copies of ICP4 replaced by VZV IE62 has been constructed (11). IE62 can transactivate all three putative kinetic classes of VZV gene promoters—i.e., the IE, early, and late gene promoters (5, 10, 15, 16, 22, 38, 47, 52)—and can transrepress its own promoter (5, 12, 49). Production of infectious VZV generated by the transfection of purified viral DNA is strongly increased by the addition of an IE62-expressing plasmid, and it has been hypothesized that virion-associated IE62 may play a crucial role in stimulating the IE events upon infection (44). In our previous study, the transcriptional activity of the P-Oka IE62 was higher than that of V-Oka IE62, which possessed all eight amino acid substitutions, on all classes of VZV gene promoters, leading us to hypothesize that IE62 might play an important role in the VZV replicative cycle and, moreover, in the attenuation of VZV (15, 16). However, it is possible that other substitution(s) are responsible for the pathogenicity of VZV, since the DNA sequence comparisons between the Oka viruses have only been

* Corresponding author. Mailing address: Department of Microbiology, Osaka University Medical School, 2-2 Yamada-oka, Suita, Osaka 565-0871, Japan. Phone: 81-6-6879-3321. Fax: 81-6-6879-3329. E-mail: yamanisi@micro.med.osaka-u.ac.jp.

done for several genes, but not for the complete genome. To resolve this issue, the complete DNA sequence of both viruses was needed.

We determined here the complete genome sequences of the Oka viruses and found remarkable differences in some of the VZV genes. The present study provides the first step toward investigating the genes involved in VZV attenuation. Furthermore, new methods for distinguishing V-Oka from clinical isolates, including P-Oka, were established, based on the newly identified substitutions. These methods can be used for typing VZV strains and for quality control of the Oka varicella vaccine.

MATERIALS AND METHODS

Cells and viruses. P-Oka was isolated in Japan from a patient with varicella and was propagated only in human embryonic lung (HEL) cells. A live, attenuated varicella vaccine (BIKEN, lot V-65), manufactured by the Research Foundation for Microbial Diseases of Osaka University, was used as V-Oka. Virus strains used as clinical isolates in the present study were isolated in Japan from patients with varicella (Kawaguchi, Inoue, RT-283, RT-342, and OZ-4) or zoster (Z-4, Z-5, Z-8, or RT-345) who had never been vaccinated. Strain RT-342 was isolated from the vesicles of a patient 10 days after vaccination, and strain RT-345 was isolated from the vesicles of a patient with shingles 19 months after vaccination. Clinical samples were isolated by the inoculation of HEL cells with vesicular fluids from patients and were propagated by three to five passages in HEL cells or MRC-5 cells.

PCR. Genomic DNA was extracted from the infected cells as described previously (42). Approximately 500 primers (25 bp in length) were designed by referring to the nucleotide sequence of the Dumas strain (9). Almost all regions covering each genome were amplified as 43 overlapping pieces by PCR. The reaction mixtures for PCR contained 2.5 U of Ex *Taq* (Takara Shuzo Co., Kyoto, Japan), 200 μM concentrations of each deoxynucleoside triphosphate, 0.3 mM concentrations of each primer, and an extremely low amount of template DNA in 50 μl of Ex *Taq* buffer. Thirty cycles of amplification were performed, in which each cycle consisted of a denaturation step at 94°C for 1 min, an annealing step at 55°C for 1.5 min, and an extension step at 72°C for an appropriate period (1 min/kbp) in a thermal cycler (Takara Shuzo). For only the regions containing the R3 reiteration region and gene 62, the PCR conditions were as described above except that the denaturation time and the annealing time were each changed to 30 s. For an origin of replication region only, the amplified DNA fragments were obtained by shuttle PCR by using 2.5 U of LA *Taq* polymerase (Takara Shuzo), 200 μM concentrations of each deoxynucleoside triphosphate, 0.3 μM concentrations of each primer (32 bp in length), and an extremely low amount of template DNA in 50 μl of LA *Taq* buffer. Shuttle PCR conditions were follows: an incubation at 98°C for 2 min for the hot start and 30 cycles of 98°C for 30 s and 68°C for 2.5 min. All amplified products were purified by using a QIA PCR purification kit (Qiagen) to remove the primers.

Cloning of PCR products. Determinations of the DNA sequences at both ends of the genomes, the flanking regions between the internal repeat long and IRS regions, and the R3 repeat were difficult to obtain by direct sequencing of the PCR products as described below, implying that various clones containing different sequences existed. Thus, PCR products containing the regions were individually inserted into a pCR2.1 vector and then transformed into competent *Escherichia coli* TOP10 5′ cells by the TA cloning method (Invitrogen). The plasmid DNAs were purified from cultured cells by using the QIA Prep Spin Kit (Qiagen).

Sequencing. Direct sequencing of purified PCR products and plasmids was performed by using the BigDye-terminator cycle sequencing kit and a Genetic Analyzer 310 (both from Perkin-Elmer/Applied Biosystems, Chiba, Japan). The viral sequences were compiled by using the DNASIS computer programs (Hitachi Computer Engineering, Tokyo, Japan).

Plasmids. Two effector plasmids were constructed for a transient luciferase assay to analyze the transcriptional activity of ORF 10 protein containing an amino acid substitution, which was caused by a partial base substitution within the *Hin*dIII site. A DNA fragment containing ORF 10 from V-Oka was amplified by PCR under the conditions described above. The amplified product was inserted into the pCR2.1 vector by the TA cloning method and then checked for the direction of the inserted fragment and whether the *Hin*dIII site was present or not. Plasmids pCG10(−) and pCG10(+) were constructed by inserting the *Kpn*I-*Xho*I fragment from clones obtained by TA cloning into pCDNA3.1 (Invitrogen) containing the cytomegalovirus IE promoter. The *Hin*dIII site existed in pCG10(−), which bore the ORF 10 from P-Oka, but not in pCG10(+), which contained the ORF 10 present in V-Oka.

Five kinds of effector plasmids expressing IE62s were constructed. pPar-G62 and pVac-G62, which had eight amino acids that were different from each other, were selected from the clones and used for our previous study (15). After pPar-G62 and pVac-G62 were digested by *Nco*I and *Pst*I (Takara Shuzo), pPV-G62*Nco* and pVP-G62*Nco* were constructed by connecting the small fragment from the digested pPar-G62 and pVac-G62 and the large fragment from the digested pVac-G62 and pPar-G62, respectively. pVmut4 was also selected from the clones from V-Oka; this clone had four amino acid differences in ORF 62 compared to pPar-G62. The reporter plasmid pPol-Luc contained ca. 750 bases upstream from the initiation codon of gene 29. This was constructed by transferring the *Nhe*I-*Bgl*II fragment from plasmid pPol-CAT as described previously (15) to the region upstream of the firefly luciferase gene in pGL3-Basic (Promega).

Transfection. To analyze the transactivational activity of the ORF 10 proteins, CV1 cells, which were cultured in 35-mm plastic dishes at 10^5 cells/dish, were transfected by lipofection with SuperFect (Qiagen). Each reaction mixture for transfection consisted of 0.5 μg of the reporter plasmid, various amounts (0 to 2 μg) of either effector plasmid pCG10(+) or pCG10(−), and 0.25 μg of β-galactosidase-expressing plasmid pCH110 (Amersham Pharmacia) for normalizing the transfection efficiency between different dishes. The total amount of plasmid DNA in each transfection experiment was kept constant at 2.75 μg by adding the vector pCDNA3.1.

To analyze the transactivational activity of the different IE62s, 293 cells and guinea pig embryonic (GPE) cells (derived from the fourth week of pregnant guinea pigs), which were cultured in 35-mm plastic dishes at 10^5 cells/dish, were transfected with the SuperFect and Lipofectamine Plus reagents (Gibco-BRL), respectively. Each reaction mixture for transfection consisted of 0.25 mg of the reporter plasmid, the same amount of one of five effector plasmids that express IE62s, and 2 mg of the vector pUC19. All experiments were repeated at least three times independently.

Luciferase and β-galactosidase assays. At 24 h after transfection, the cells were washed twice with phosphate-buffered saline. The cells were then lysed by the addition of 100 μl of reporter lysis buffer (Promega), followed by mixing for 15 min at room temperature. The lysate was collected in a new microcentrifuge tube, and the cell debris was removed by centrifugation at 12,000 rpm for 2 min. The luciferase activity of 10 μl of supernatant was determined by using a Berthold luminometer, model LB9507 (Berthold Japan, Tokyo, Japan), after the addition of 50 μl of substrate buffer (Promega). To normalize this transient assay for ORF 10 proteins to the transfection efficiency, the β-galactosidase activity of 10 μl of supernatant was also determined by using the luminometer, after the addition of 100 μl of the reaction buffer of the luminescent β-galactosidase detection kit II (Clontech) and incubation of the mixture at room temperature for 1 h. In another transient assay for various IE62s, the luciferase activity in each lysate was standardized to the protein concentration determined with the Bio-Rad protein reagent, because all of the internal plasmids used to normalize the transfection efficiency were stimulated by the IE62s.

Comparison of plaque sizes and infectious center assay. HEL cells were infected with cell-free V-Oka, and virus clones were plaque purified twice. Two clones, S7-01 and S7-13, were obtained after DNA sequencing for use in further experiments. These clones were then propagated in HEL cells, and cell-free viruses were harvested by sonication as described previously (15). HEL or GPE cells were infected with the cell-free cloned viruses, P-Oka, and V-Oka, and their plaque sizes were compared after fixation and staining with methylene blue. An infectious center assay was also performed to examine the spreading of the viruses. HEL or GPE cells in 35-mm dishes were infected with cell-free viruses (ca. 50 PFU/plate). At 0 to 5 days postinfection, they were washed with phosphate-buffered saline (37°C) and treated with trypsin. The trypsin-treated cells were diluted and transferred onto monolayers of HEL cells in 35-mm dishes, and the numbers of infected cells were assessed by counting the plaques 7 days after the inoculation.

Restriction fragment length polymorphism (RFLP) analysis. Six parts of the genome were amplified by PCR with six sets of primer pairs as shown in Table 1. The conditions for the PCR were as described above. Portions (3 μl) of the amplified products with three primer pairs—01-N12 and 01-R13, 50-N15 and 50-R17, or 60-N11 and 60-R12—were digested with 4 U of the restriction endonucleases *Alu*I (Takara Shuzo), *Bst*XI (Takara Shuzo), or *Bsr*I (New England Biolabs), respectively. The same volumes of the products obtained by using primer pair 60-N06 and 60-R06 and primer pair 60-N26 and 60-R28 were digested independently with 4 U of the enzymes *Sfa*NI (New England Biolabs)-

TABLE 1. Primers used in the RFLP analysis in this study[a]

Name	Sequence	Position (nucleotide range)
01-N12	5′-ATTGTATGCATGCGATTGCTATCGC-3′	5372–5396
01-R13	5′-GGTCTTCCACTTTAAAGGGGTTTGC-3′	6134–6110
50-N15	5′-CGATCACGTCGCTCACATCCAACCC-3′	93685–93709
50-R17	5′-ATGGCAGAAGAAACACGTATTGCCG-3′	94457–94433
60-N06	5′-GAGGACAACAGCTCCACCTTGACCG-3′	105277–105301
60-R06	5′-GAGTAATGTGGCCGCCCGGTTTTGG-3′	105613–105589
60-N26	5′-CCAAAACCGGGCGGCCACATTACTC-3′	105589–105613
60-R28	5′-ATTACTGTCGACCCGAGACCTGGCC-3′	106380–106356
60-N11	5′-AAGGGCTTCCGTCGGGCATCATGAG-3′	107729–107753
60-R12	5′-TCGGGTAAAAAGCCGGGCGATGAGC-3′	108497–108473

[a] These primers were designed by referring to the nucleotide sequence of the Dumas strain. Nucleotide positions refer to those in the sequence of the Dumas strain.

*Acc*II (Takara Shuzo) and *Sac*II (New England Biolabs)-*Sma*I (New England Biolabs), respectively. Samples were digested for 1 h at 25°C for *Sma*I; 37°C for *Alu*I, *Sfa*NI, and *Sac*II; 45°C for *Bst*XI; 60°C for *Acc*II; and 65°C for *Bsr*I. The digested products were analyzed by electrophoresis in a 4% agarose gel (NuSieve 3:1; FMC BioProducts Co., Rockland, Maine) with ethidium bromide staining and then visualized with short-wave UV illumination of the gel.

RESULTS

Comparison of the complete DNA sequences of V-Oka and P-Oka. (i) Substitutions of bases and amino acids. The entire VZV DNA sequences of V-Oka and P-Oka were determined mainly by the direct sequencing of PCR products. Thus, the determined sequences reflect the VZV DNA population in infected cells; that is, if mutated viruses also exist within a sample, more than two kinds of nucleotides would be recognized at one base position by this method. The genome sizes of both the Oka viruses were ca. 125 kbp, and >95% of the sequences were determined by this method on both the sense and antisense strands of the DNAs. When the complete DNA sequences of the Oka viruses were compared, only 42 bases were found to be different (Fig. 1A and Table 2), not including the substitutions in the TRS region, which are duplications of the IRS region. Two base substitutions were found in genes 10 and 14 for the first time in the present study, although we had missed them in our earlier study (15, 16). Base substitutions at 20 nucleotide positions in V-Oka caused amino acid conversions, and the base substitutions at 17 nucleotide positions were silent mutations. The remaining five base substitutions were found to be in noncoding regions. Thirty-one base substitutions in V-Oka were mixtures of two kinds of base at each of these positions (Table 2). Every base substitution was a G-versus-A or a C-versus-T conversion except for a G-versus-T conversion only at position 39227 in gene 22. Fifteen amino acid substitutions in V-Oka were partial, resulting in mixtures of two kinds of amino acids at each of these positions. Surprisingly, more than one-third (15 of 42) of the substitutions were found in gene 62 (or gene 71) and its flanking regions, and about half of the amino-acid substitutions (8 of 20) were within ORF 62. Thus, the gene 62 region was obviously the most variable region in the V-Oka virus. The major transactivating domains of IE62 are divided into five regions (regions 1 to 5) based on sequence homology in comparison with HSV-1 ICP4 (9, 35). Regions 4 and 5 contained one and three amino acid substitutions each, respectively.

There were 12 amino acid substitutions between the Oka viruses in the entire genome outside of gene 62. These existed in genes 6, 9A, 10, 21, 31, 39, 50, 52, 55, 59, and 64 (Fig. 1A and Table 2). The HSV-1 helicase-primase complex consists of three proteins encoded by UL52, UL8, and UL5 (8); their homologs in VZV are ORFs 6, 52, and 55, respectively. Interestingly, four amino acid substitutions were found in these proteins. One amino acid substitution was located near the carboxyl terminus of gene 6, which was Ser in P-Oka and Gly in V-Oka. Another substitution occurred in gene 52. In this case, the amino acid residue in P-Oka was Ile, which was incompletely altered to Val in V-Oka; V-Oka contained two kinds of base at a single position, resulting in two kinds of ORF 52 protein. The remaining two amino acid substitutions were located in ORF 55. An Ala at position 97748 and a Cys at position 97796 in P-Oka were partially substituted by Thr and Arg in V-Oka, respectively.

There was only one amino acid substitution among the seven known VZV surface glycoproteins gK, gC, gB, gH, gL, gI, and gE, encoded in genes 5, 14, 31, 37, 60, 67, and 68, respectively. gB contained an amino acid substitution in which an Ile in P-Oka was substituted by Val in about half of the virus population of V-Oka. Another substitution was found in ORF 50, which is homologous to the gene encoding the HSV-1 glycoprotein gM, but it has not been established whether gM exists and is functional in VZV. Gene 9A is homologous to HSV-1 UL49.5, which encodes a hydrophobic protein with only 91 amino acids (4). The gene product in VZV, the ORF 9A protein, is present in the membrane fraction of infected MeWo cells, although it is absent in the cytosolic fraction, and cells infected with a recombinant virus that is unable to express the ORF 9A protein produce smaller plaques than cells infected with the parental virus (50). A partial amino acid substitution was located at the end of the carboxyl terminus of ORF 9A protein. It is possible that this substitution affects the stability of the protein. ORF 10 protein is a tegument protein (24) that regulates positively to the IE62 gene promoter, and V-Oka contained both Ala and Val at a single position (i.e., 12779) in the middle of the protein. In the gene 21 protein, whose function is unknown, Thr in P-Oka was incompletely substituted by Ile in V-Oka as a result of a base substitution at position 31732. Amino acid substitutions also existed in genes 39 and 64. The HSV-1 homologue to the gene 39 product is the UL20 product, which is known to be a membrane protein, and the homologue to gene 64 is the US10 product, which is known to be a tegument protein, but the function of either of these products in VZV is not clear. Finally, an amino acid substitution was found in the gene 59-encoded uracil-DNA glycosylase, which is a DNA repair enzyme responsible for the removal of uracil residues misincorporated into DNA.

The DNA sequence differences of the Oka viruses were then compared with the Dumas strain. The G+C content was 46.1% for both V-Oka and P-Oka; this value is very close to that of the Dumas strain (46.0%). When the complete DNA sequences of V-Oka and P-Oka were compared with the Dumas strain, 213 and 171 base substitutions leading to 75 and 55 amino acid conversions, respectively (Fig. 1B), were found. All 176 substitutions between the Dumas virus and P-Oka are

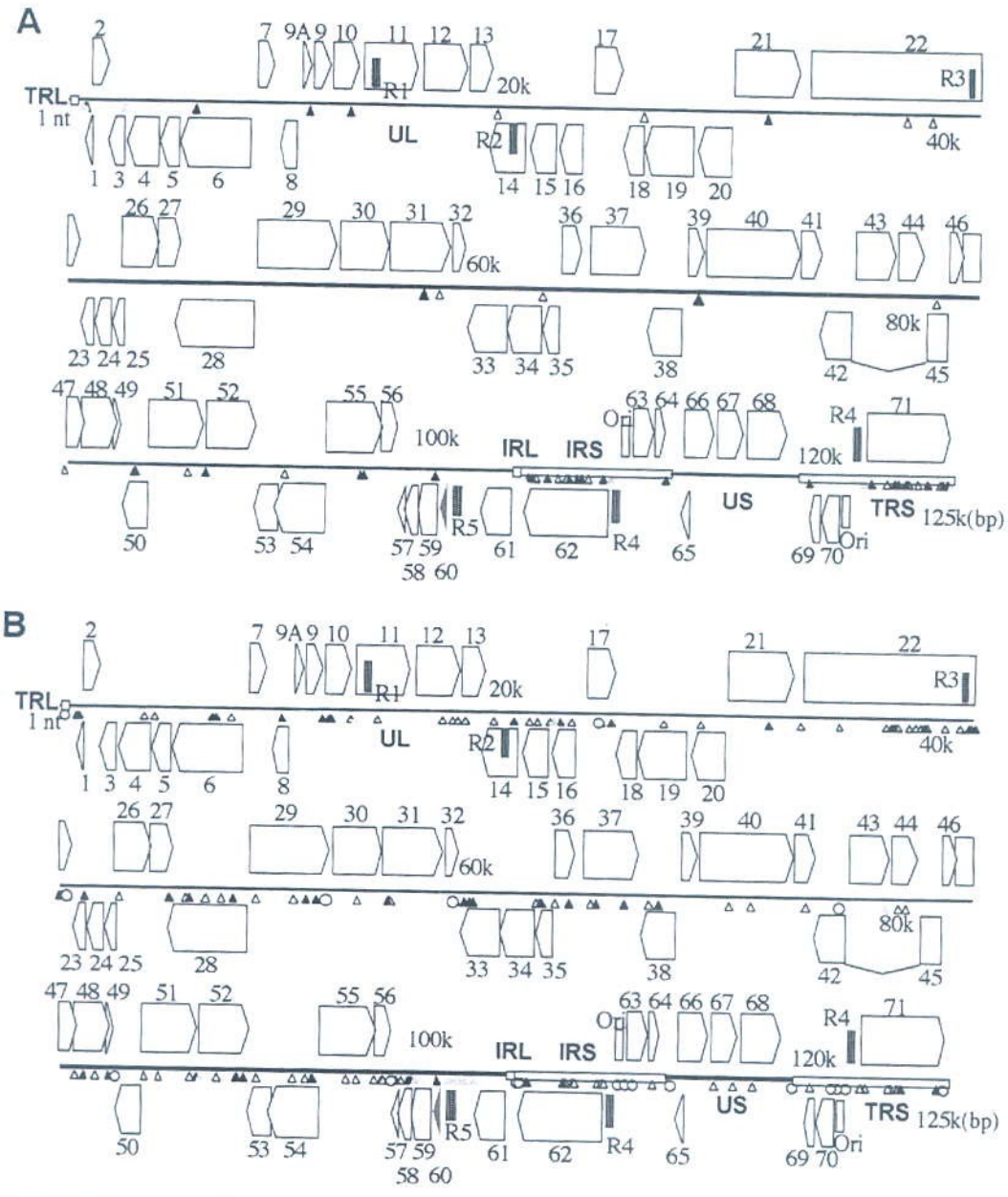


FIG. 1. Comparisons of complete DNA sequences. The genome is presented in sections; horizontal lines indicate unique regions, and open boxes indicate inverted repeat regions. ORFs 1 to 71 are illustrated as pentagons. ORFs 62 through 64 are duplications of ORFs 69 through 71. Solid, shaded, and open symbols show the base substitutions causing amino acid conversions, base substitutions in noncoding regions, and silent mutations, respectively. (A) Forty-two base substitutions between P-Oka and V-Oka. (B) One hundred seventy-six base substitutions between the Dumas virus and P-Oka. All 176 substitutions between the Dumas virus and P-Oka are contained within 218 substitutions between the Dumas virus and V-Oka; the 218 substitutions between the Dumas virus and V-Oka were the total of 176 plus 42 substitutions.

contained within 218 substitutions between the Dumas virus and V-Oka; 218 substitutions between the Dumas virus and V-Oka were the total of 176 plus 42 substitutions. In the entire DNA sequences, excluding the repeat regions, the mutation rates of P-Oka and V-Oka were 0.16 and 0.19% compared with the Dumas strain, respectively. Thus, P-Oka is genetically slightly closer to the Dumas strain than is V-Oka. Several regions in gene 22 and genes 55 through 61 were variable between the Dumas strain and P-Oka (Fig. 1B). The gene 62 region was an additional variable region when the Dumas strain was compared with V-Oka; 24 base substitutions existed in gene 62 and its flanking regions between V-Oka and the Dumas strain. At the amino acid level, the mutation rate in all of the ORFs between the Dumas strain and P-Oka was 0.16%, whereas that between the Dumas strain and V-Oka was 0.21%. V-Oka ORF62 possessed the greatest mutation rate (0.84%) among all of the ORFs compared with the Dumas strain.

(ii) Deletions and insertions in V-Oka. V-Oka had several deletions and insertions compared to P-Oka in certain regions, including the tandem repeat regions and an origin of DNA

TABLE 2. Base and amino acid substitutions found by comparing the complete DNA sequences of V-Oka and P-Oka[a]

Position[b]	Gene	Amino acid substitution(s)	
		V-Oka	P-Oka
560	5′ noncoding	C (NCR)	T (NCR)
703	1	T/C (Gln)	T (Gln)
763	1	T/C (Pro)	T (Pro)
2515	3/4	T/C (NCR)	T (NCR)
5745 (945)	6	G (Pro)	A (Ser)
10900 (91)	9A	T/C (Trp/Arg)	T (Trp)
12779 (207)	10	T/C (Ala/Val)	T (Ala)
19431	14	T/C (OCH/AMB)	T (OCH)
26125	18	G (Asn)	A (Asn)
31732 (325)	21	T/C (Thr/Ile)	C (Thr)
38036	22	T/C (Thr)	T (Thr)
39227	22	T/G (Pro)	T (Pro)
58595 (530)	31	A/G (Ile/Val)	A (Ile)
59287	31	A/G (Pro)	A (Pro)
64067	35	A/G (Ala)	A (Ala)
71252 (207)	39	T/C (Met/Thr)	T (Met)
82225	45	A/G (Pro)	A (Pro)
84091	47	A/G (Glu)	G (Glu)
87280	50	A/G (Cys)	A (Cys)
87306 (193)	50	T/C (Ser/Gly)	T (Ser)
89734	51	A/G (Thr)	A (Thr)
90535 (15)	52	A/G (Ile/Val)	A (Ile)
94167	54	C (Leu)	T (Leu)
97748 (585)	55	G/A (Ala/Thr)	G (Ala)
97796 (601)	55	T/C (Cys/Arg)	T (Cys)
101089 (44)	59	A/G (Leu/Pro)	A (Leu)
105169	61/62	A/G (NCR)	A (NCR)
105310 (1275)	62	A/G (Leu/Ser)	A (Leu)
105356 (1260)	62	C (Val)	T (Ile)
105544 (1197)	62	G (Ala)	A (Val)
105705	62	C (Ala)	T (Ala)
106262 (958)	62	C (Gly)	T (Arg)
106710	62	A/G (Ala)	A (Ala)
107136	62	C (Ala)	T (Ala)
107252 (628)	62	C (Gly)	T (Ser)
107599 (512)	62	A/G (Val/Ala)	A (Val)
107797 (446)	62	A/G (Leu/Pro)	A (Leu)
108111	62	C (Pro)	T (Pro)
108838 (99)	62	A/G (Met/Thr)	A (Met)
109137	62/63	A/G (NCR)	A (NCR)
109200	62/63	A/G (NCR)	A (NCR)
111650 (29)	64	A/G (Gln/Arg)	A (Gln)

[a] Mutations in the repeat region are not shown here (see Fig. 2). The number at the base position refers to the sequence analysis of the Dumas virus. Base substitutions leading to amino acid conversions are indicated by filled cells. P-Oka has a base identical to that in the Dumas virus at every position. NCR, noncoding region; OCH, ocher; AMB, amber.

[b] Numbers in parentheses refer to the amino acid number within a particular ORF.

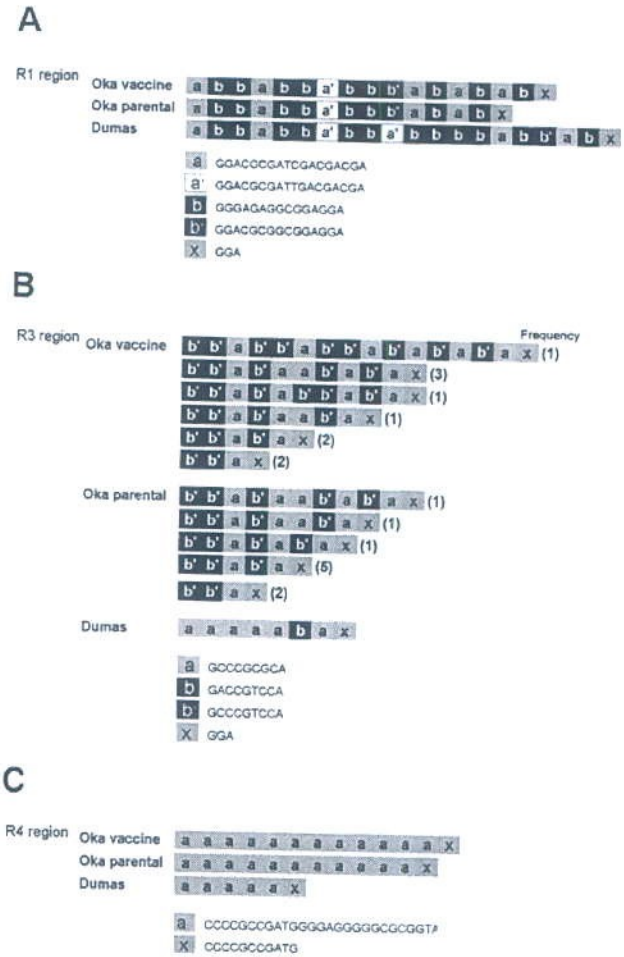


FIG. 2. Comparisons of repeat regions. V-Oka has different structures in R1 (A), R4 (B), and R3 (C) compared to P-Oka. Both V-Oka and P-Oka contain multiple clones that have different patterns and combinations of repeat elements in R3.

replication. Five repeat regions—R1, R2, R3, R4, and R5—lie in genes 11, 14, and 22, and in the flanking regions between genes 62 and 63 (and genes 70 and 71), and genes 60 and 61, respectively. There were length differences in regions R1, R3, and R4. In particular, differences in the length of the R1 region have been used to distinguish different VZV strains (18, 62). R1 is composed of four kinds of allele, i.e., a, a′, b, and b′, which are 15 or 18 bp in length and partial copies of them, x, which are 3 bp in length. V-Oka had 17 reiteration elements in the R1 region, whereas P-Oka had 15 elements (Fig. 2A). The R3 region consists of three kinds of allele, a, b, and b′, which are 9 bp in length, and partial copies of them, x, which are 3 bp. The DNA sequences of the R3 regions from both Oka viruses could not be completely determined by the direct sequencing of the PCR products. The sequences could be determined to just before the fourth element, b′b′a, with sense primers, and the last three elements, b′ax, with antisense primers. These results indicated that the R3 regions contained mixtures of multiple sequences from the fourth element to just before the last three elements. Thus, the R3 region appeared to be unstable, and each virus was represented by more than two clones containing different numbers and combination patterns in this region. Sequencing analysis of fragments containing the R3 region of each virus revealed that the numbers and types of combination patterns varied (Fig. 2B). All of the clones from the viruses had more than four elements. The maximum number of reiteration elements that we detected from V-Oka was 16, whereas that from P-Oka was 11. However, Davison and Scott reported that the R3 region might contain over 100 copies of the 9-bp element (9). Although we amplified the fragment containing the R3 region under various PCR conditions, we did not obtain any fragment containing this many elements. No frameshifts occurred in spite of the differences in the R1 and R3 regions located within the ORFs because the



FIG. 3. Comparisons of DNA sequences in the origin region. An almost palindromic sequence (underline) is located in the middle of this region. P-Oka and V-Oka have deletions, $(TA)_4$ and $(TA)_7$, in the palindromic sequence, respectively. The other deletion site is in the (GA) repeat just after the palindromic sequence.

base numbers of elements were multiples of 3. R4 is located in both the IRS and TRS regions and consists of a single element, a, which is 27 bp in length, and a partial copy of it, x, which is 11 bp in length. V-Oka had 9 repeat elements in the R4 region, whereas P-Oka had 10 elements (Fig. 2c).

Finally, the VZV genome contains origin regions of replication in both the IRS and the TRS regions, and each origin region is ca. 270 bp in length (Fig. 3). P-Oka contained 269 bp in this region and was 8 bp longer than V-Oka. The Dumas strain has an almost perfect palindrome of 45 bp in the middle of the origin region (Fig. 3, underline) (9, 54), and both Oka viruses had additional sequence following the palindrome. P-Oka had part of the palindromic sequence $(TA)_{12}$ and just following $(GA)_{10}$, whereas V-Oka had a different sequence $(TA)_9$ and $(GA)_9$. The genome size of V-Oka was slightly longer than that of P-Oka due to these insertions and deletions. The whole genomes of V-Oka and P-Oka consisted of 125,076 and 125,069 bp, respectively.

Transactivational activity of ORF 10 protein containing an amino acid substitution. ORF 10 protein, which is a homolog of HSV-1 VP16, is a virion-associated transactivator (24). It is reported that the ORF 10 protein can stimulate the IE62 gene promoter but has no regulatory effect on the gene 4 promoter (43). A base substitution that existed within the *Hin*dIII site in ORF 10 caused an amino acid conversion in which an Ala in the middle of the ORF 10 protein in P-Oka was altered to a mixture of Ala and Val in V-Oka. When the PCR product containing the site from V-Oka was digested by *Hin*dIII, approximately half of the product was cleaved similar to P-Oka. To compare the transcriptional activity of the ORF 10 protein from clones with the amino-acid substitution, a transient luciferase assay was performed. The effector plasmids pCG10(+) and pCG10(−) had Ala and Val at the substituted positions, respectively. ORF 10 proteins from the V-Oka and P-Oka viruses could both transactivate the gene 62 promoter in CV1 cells in a dose-dependent fashion. The transactivational activity of pCG10(−) on the gene 62 promoter was slightly higher than that of pCG10(+), but this difference was not significant.

Plaque sizes and infectious center assay of cloned viruses. V-Oka was a mixture of different clones (15, 16). To obtain clones of V-Oka, plaque purification was carried out and 13 clones were obtained. Because we found 20 base replacements that led to amino acid differences between V-Oka and P-Oka as described above, these clones were sequenced. In gene 62, one of the clones, S7-01, had all eight amino acid substitutions compared to P-Oka. In contrast, another clone, S7-13, had the minimum number of substitutions compared to P-Oka, with only five amino acid differences, and the remaining three amino acids conserved with P-Oka (Table 3). Thus, these two clones were chosen to determine whether the mutations in gene 62 were correlated with viral growth. A comparison of the plaque sizes of S7-01, S7-13, V-Oka, and P-Oka showed that P-Oka gave rise to the largest plaques (Fig. 4). V-Oka and S7-13 showed relatively larger plaques than S7-01. In particu-

TABLE 3. Amino acid substitutions in clones S7-01 and S7-13 relative to V-Oka and P-Oka

Position	Gene	Amino acid substitution(s)		S7-01	S7-13
		Oka parental	Oka vaccine		
5745	6	A (Ser)	G (Pro)	G (Pro)	G (Pro)
10900	9A	T (Trp)	T/C (Trp/Arg)	T (Trp)	C (Arg)
12779	10	T (Ala)	T/C (Ala/Val)	C (Val)	C (Val)
31732	21	C (Thr)	C/T (Thr/Ile)	T (Ile)	C (Thr)
58595	31	A (Ile)	A/G (Ile/Val)	G (Val)	A (Ile)
71252	39	T (Met)	T/C (Met/Thr)	C (Thr)	C (Thr)
87306	50	T (Ser)	T/C (Ser/Gly)	T (Ser)	T (Ser)
90535	52	A (Ile)	A/G (Ile/Val)	A (Ile)	G (Val)
97748	55	G (Ala)	G/A (Ala/Thr)	G (Ala)	A (Thr)
97796	55	T (Cys)	T/C (Cys/Arg)	C (Arg)	T (Cys)
101089	59	A (Leu)	A/G (Leu/Pro)	A (Leu)	A (Leu)
105310	62	A (Leu)	A/G (Leu/Ser)	G (Ser)	G (Ser)
105356	62	T (Ile)	C (Val)	C (Val)	C (Val)
105544	62	A (Val)	G (Ala)	G (Ala)	G (Ala)
106262	62	A (Arg)	C (Gly)	C (Gly)	C (Gly)
107252	62	T (Ser)	C (Gly)	C (Gly)	C (Gly)
107599	62	A (Val)	A/G (Val/Ala)	G (Ala)	A (Val)
107797	62	A (Leu)	A/G (Leu/Pro)	G (Pro)	A (Leu)
108838	62	A (Met)	A/G (Met/Thr)	G (Thr)	A (Met)
111650	64	A (Gln)	A/G (Gln/Arg)	G (Arg)	A (Gln)

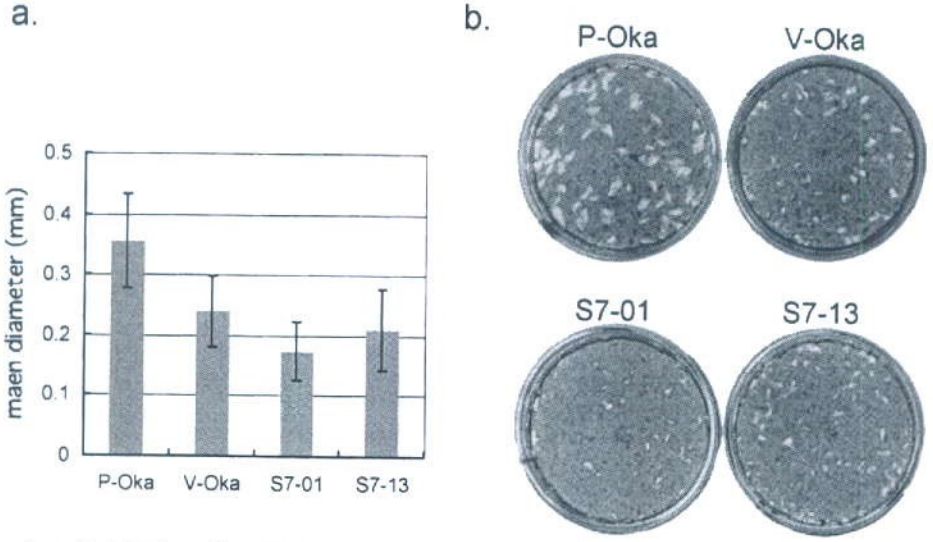


FIG. 4. (a) Plaque sizes after infection with cell-free P-Oka, V-Oka, S7-01, and S7-13. (b) HEL cells were infected with each cell-free virus and cultured for 10 days. The cells were stained with methylene blue.

lar, S7-01 showed significantly smaller plaques compared with P-Oka ($P < 0.01$); the mean diameter of the plaques resulting from S7-01 infection (1.73 mm) was about half the size of those resulting from P-Oka (3.55 mm). V-Oka and S7-13 had smaller plaque diameters (2.40 and 2.10 mm, respectively) than did P-Oka. In addition, the cytopathic effect (CPE) of P-Oka appeared 2 days after infection, whereas the CPE of the other viruses appeared in 3 to 4 days. Thus, an infectious center assay was performed to examine the difference in cell-to-cell spreading of progeny viruses. HEL cells were infected with P-Oka, V-Oka, S7-01, or S7-13, and the numbers of infected cells from 0 to 5 days were titrated. In this assay, P-Oka exhibited an obviously faster spread than the other viruses in HEL cells. After 5 days, the numbers of cells infected by P-Oka were 2.1-, 4.2-, and 2.6-fold higher than the numbers infected by V-Oka, S7-01, and S7-13, respectively (Fig. 5a). These results suggested that the virus growth was slightly different among the V-Oka clones and that P-Oka grew best among these Oka viruses in HEL cells. On the other hand, in GPE cells, the plaque sizes of the viruses derived from Oka vaccine were not significantly different from those of its parental viruses (data not shown). Moreover, both Oka viruses showed similar propagation in cell-to-cell spreading by infectious center assay in GPE cells (Fig. 5b).

Transactivational activities of mutant IE62s. We next analyzed whether the transactivational activities of the IE62s of these clones differed from the parental activity. pLuc-Pol, containing the cloned VZV DNA polymerase gene promoter upstream of the luciferase ORF, was used as the reporter plasmid for transient luciferase assays, because the transactivation of

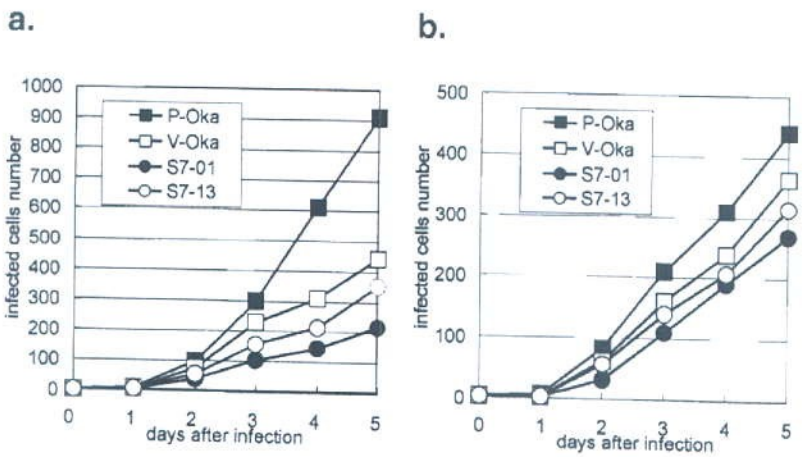


FIG. 5. Infectious center assay of P-Oka, V-Oka, S7-01, and S7-13. HEL cells (a) and GPE cells (b) in 35-mm dishes were infected independently with similar titers of these four kinds of cell-free viruses, and then the cells were washed and treated with trypsin from 1 to 5 days postinfection. The trypsin-treated cells were diluted and transferred onto monolayers of uninfected HEL cells in 35-mm dishes, and the numbers of infected cells were assessed by counting the number of VZV plaques appearing after 7 days. The number of infected cells was normalized to the initial viral titer per dish; the fold increase indicates the number of infected cells spread from one initial infected cell at day 0.

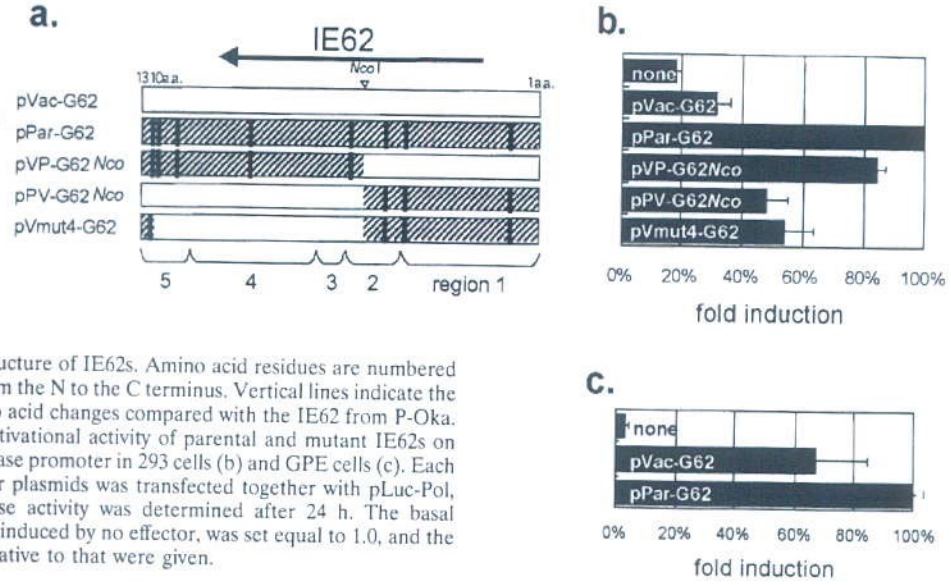


FIG. 6. (a) Structure of IE62s. Amino acid residues are numbered from 1 to 1310 from the N to the C terminus. Vertical lines indicate the positions of amino acid changes compared with the IE62 from P-Oka. (b and c) Transactivational activity of parental and mutant IE62s on the DNA polymerase promoter in 293 cells (b) and GPE cells (c). Each of the five effector plasmids was transfected together with pLuc-Pol, and each luciferase activity was determined after 24 h. The basal luciferase activity, induced by no effector, was set equal to 1.0, and the other activities relative to that were given.

this promoter by IE62 is well known. Five kinds of effector plasmids expressing IE62s were constructed (Fig. 6a). Two of them, pPar-G62 derived from P-Oka and pVac-G62 derived from V-Oka, were used in our previous study (15, 16). One clone containing an IE62 gene was selected from V-Oka and used as pVac-G62 because this clone had all eight amino acid mutations compared to pPar-G62. In addition, another clone was selected from V-Oka, called pVmut4-G62, which had the minimum four mutations; all of the other clones contained in V-Oka had these four mutations and one to four of the other mutations. pPV-G62*Nco* and pVP-G62*Nco* were chimeric IE62-expressing plasmids, which were bounded by an *Nco*I site. pPV-G62*Nco* expressed the amino terminus of parental IE62 and the carboxyl terminus of pVac-G62. pVP-G62*Nco* was constructed to contrast with pPV-G62*Nco* and expressed the amino terminus of pVac-G62 and the carboxyl terminus of pPar-G62. The IE62 genes of P-Oka, S7-01, and S7-13 corresponded with those of pPar-G62, pVac-G62, and pPV-G62*Nco*, respectively. V-Oka contained from four (like pVmut4-G62) to eight (like pVac-G62) amino acid mutations. The relative luciferase activity was set equal to 100% in cells, where the reporter plasmid pLuc-Pol was cotransfected with pPar-G62. The basal activity of the DNA polymerase promoter was 18% of the activity of parental IE62 (Fig. 6b). pVac-G62 and pVmut4-G62 showed 32 and 54% activities. Therefore, the mutant IE62s contained in the clones of V-Oka were likely to have lower activity than the parental IE62. The chimeric IE62 expressed by pVP-G62*Nco* transfection possessed an activity that was still high (84%), whereas the other chimera expressed by pPV-G62*Nco* showed 48% activity, suggesting that the first five amino acid mutations from the carboxyl terminus, rather than the other three mutations, were more important for transactivating the promoter. The mutation closest to the carboxyl terminus changed IE62's activity moderately but significantly. pPar-G62 and pVac-G62 exhibited the highest and lowest activities among the forms we analyzed, respectively, and pPV-G62*Nco* led to more effective luciferase expression than pVac-G62 but was not as effective as pPar-G62. These transient assay results roughly showed trends that were consistent with both the mean plaque sizes and the square roots of the number of infected cells determined in the infectious center assay. These findings support the possibility that viral growth and spreading may be regulated by the transactivational activity of IE62.

Transient luciferase assay with GPE cells were also performed to analyze the transactivational activities of the Oka vaccine IE62 and its parental IE62 in these cells. The assay showed that pVac-G62, the most heavily substituted, had 67% of the activity of pPar-G62 (Fig. 6c), suggesting that the transactivational activity of the IE62 of V-Oka was relatively higher in GEF cells compared to that found in other cells as described above.

Differentiation of the DNA sequence in gene 62 among clinical isolates. Comparison of the DNA sequences of the Oka viruses showed that gene 62 was the most variable region in the VZV genes, as described above. Furthermore, V-Oka consisted of at least eight different virus clones (15). Thus, we determined the nucleotide sequences of gene 62 from clinical isolates and compared the sequences among different VZV strains (Fig. 7b). Four clinical isolates (RT-283, OZ-4, Inoue, and Kawaguchi) were derived from patients with varicella. The first two strains were recently isolated but the latter two were isolated more than 30 years ago. Three isolates (Z-4, Z-5, and Z-8) were obtained from patients with zoster. Only the RT-342 and RT-345 strains were obtained from vaccinated patients, as described in Materials and Methods. Seven bases (at positions 105356, 105544, 105705, 106262, 107136, 107252, and 108111) were conserved in the clinical isolates and were only different in V-Oka, and four of these led to amino acid substitutions that were specific for V-Oka. Some of the clones contained in V-Oka showed different bases at eight positions (i.e., 105169, 105310, 106710, 107599, 107797, 108838, 109137, and 109200) that were not seen in the clinical isolates, and four of them led to partial amino acid substitutions. In summary, all of the clinical isolates differed from V-Oka in 15 bases that were found to be different between V-Oka and P-Oka. Only one base substitution (at position 105451) causing an amino acid

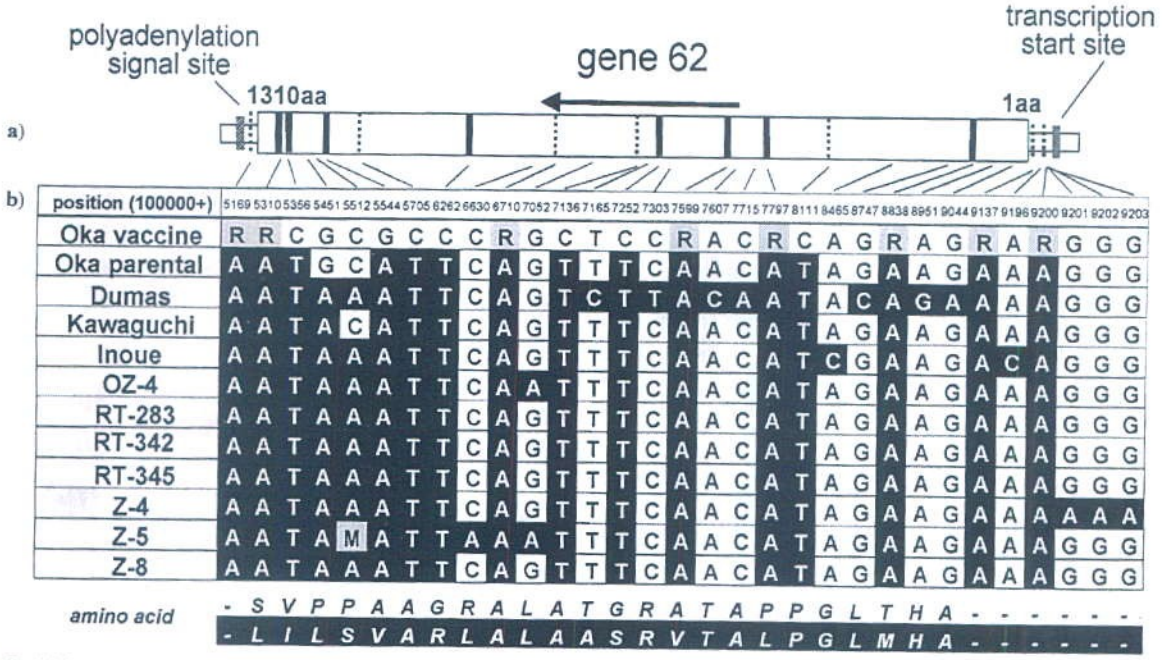


FIG. 7. (a) Structure of gene 62. Amino acid residues are numbered from 1 to 1310 from the N to the C terminus. Fifteen vertical lines indicate the positions of base changes between Oka vaccine and its parental virus. Bold or broken lines show base mutations with or without amino acid conversions, respectively. (b) Sequence analysis of gene 62 from the V-Oka vaccine, Oka parental, Dumas strains, and nine clonal isolates. Filled cells indicate base differences compared with V-Oka. All nine viruses have identical bases at these 15 positions, but V-Oka has different bases. R, mixture of G and A; M, mixture of A and C

conversion was specific for the Oka viruses. Interestingly, an identical sequence was seen in RT-283, RT-342, and RT-345. These strains were isolated from patients in the same clinic; thus, it was likely that the same virus strain was circulating there.

Genetic differentiation of the Oka vaccine virus from other viruses by RFLP analysis. Comparison of the complete DNA sequences of the Oka viruses revealed 11 bases that were completely substituted by other bases. These bases (at positions 560, 5745, 26125, 94167, 105356, 105544, 105705, 106262, 107136, 107252, and 108111) were located within sites recognized by the restriction enzymes *Nla*III, *Alu*I, *Mae*II, *Bst*XI, *Sfa*NI, *Acc*II, *Sac*II, *Sma*I, *Bss*HII, *Nae*I, and *Bsr*I, respectively. A method for distinguishing V-Oka from other viruses, including P-Oka, was established in our previous study, which demonstrated that the cleavage sites for *Bss*HII and *Nae*I were useful for identifying V-Oka (15). Here we sought to establish new methods for distinguishing the viruses by using the eight other restriction enzyme sites, and V-Oka was successfully identified by using all of these enzymes except for *Nla*III and *Mae*II. First, the base substitution at position 5745 in gene 6, which encodes a putative subunit of the helicase-primase complex of V-Oka, resulted in the loss of a restriction site that is recognized by *Alu*I (Fig. 8a). Immediately adjacent to this position, another site recognized by this enzyme was present in every virus and was predicted to be cleaved. The PCR product containing these sites in gene 6 of V-Oka was cleaved at only one site with the enzyme, resulting in two fragments, whereas that of P-Oka was cleaved at two sites by the enzyme, resulting in three fragments. The RFLP study was further performed with 54 clinical isolates. The results of this PCR-RFLP analysis demonstrated that the clinical isolates tested did not show a pattern identical to that of V-Oka. Similar results were obtained in six other experiments. P-Oka and all 54 clinical isolates contained cleavage sites for *Sfa*NI and *Bsr*I, whereas only V-Oka lost those sites. In contrast, four other sites, which were recognized by *Bst*XI, *Acc*II, *Sac*II, and *Sma*I, were specific only for V-Oka (Fig. 8b to g) but not for the clinical isolates. Moreover, V-Oka could be distinguished from five clinical isolates such as RT-342 and RT-348, which were from vaccinated patients with clinical symptoms, by using some of these restriction enzyme sites in gene 62 (data not shown). Therefore, these findings suggested that these clinical symptoms were caused by wild-type viruses and not by V-Oka.

DISCUSSION

We found here that the VZV DNA sequences were quite highly conserved (>99.8%) among the Dumas strain, P-Oka, and V-Oka. In particular, there was only a 0.034% sequence difference between the two Oka viruses. However, clinical reactions after vaccination with the Oka varicella vaccine are very rare in healthy children. It was reported that V-Oka grows better than wild-type viruses, including the Oka parental virus, in GPE cells (34) and that the immune response in guinea pigs could be induced by V-Oka but not by wild-type strains (61). These results indicate that a sequence difference of ca. 0.034% of can make a biological difference in such properties as the pathogenicity and growth of VZV. In this and previous studies, gene 62 has emerged as having the potential to be involved in the attenuation of the Oka virus, based on the following remarkable features of V-Oka. First, gene 62 shows the highest

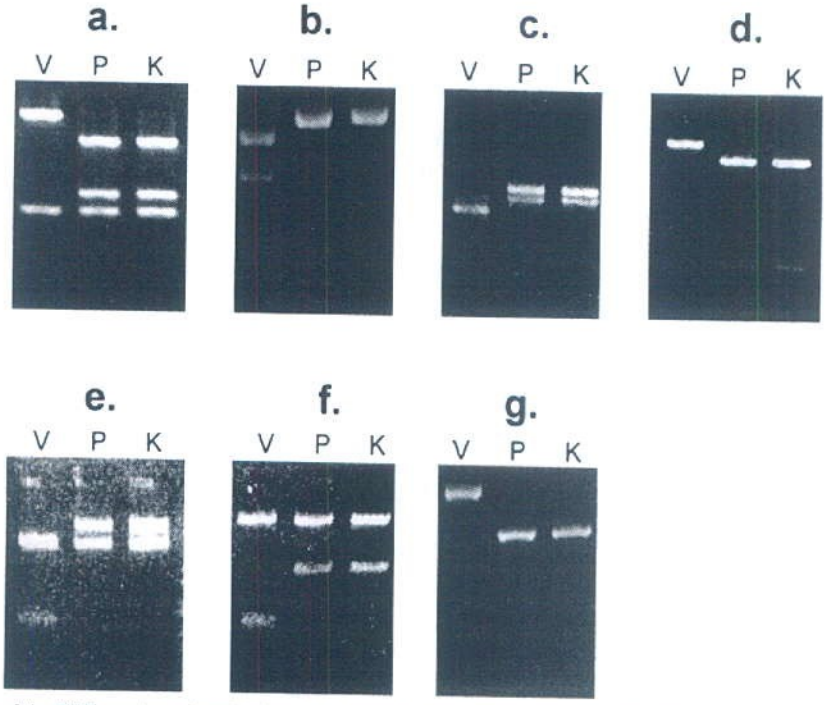


FIG. 8. RFLP analysis of the PCR products from V-Oka, P-Oka, and 54 wild-type viruses. V-Oka (V) can be distinguished not only from P-Oka (P) but also from all wild-type viruses. The Kawaguchi strain (K) was used to represent the wild-type viruses by using *Alu*I (a), *Bst*XI (b), *Acc*II (c), *Sfa*NI (d), *Sac*II (e), *Sma*I (f), and *Bsr*I (g).

divergence in both base and amino acid sequences when V-Oka is compared to P-Oka. In particular, comparison of the Oka viruses revealed that gene 62 and its duplicate gene (gene 71), which cover only 7% of the whole genome, contained more than one-third of the base substitutions, although the other three IE genes (genes 4, 61, and 63) had no substitutions. Second, comparisons of gene 62 from nine clinical isolates showed that all 15 base substitutions leading to eight amino acid conversions were specific for V-Oka. Third, the sequence analysis of a fragment including the gene 62 region from nine clones revealed that V-Oka is a mixture of at least eight different viruses that had a variety of mutations (15). Fourth, our previous studies had demonstrated that the vaccine IE62, which contained all eight amino acid substitutions, had less transactivational activity than parental IE62 in activating all three kinetic classes of VZV promoters in CV1 cells (15, 16). Fifth, S7-01 virus, which had mutations in all eight amino acids in IE62, showed slower virus spreading in HEL cells. Thus, the substitutions that have accumulated in gene 62 are most likely to be important for the differences in the replication and the attenuation of VZV. Because V-Oka had been passaged in guinea pig cells and also in human fibroblast cells at a low temperature (56), mutant viruses must have been selected and grown under selective pressure. The reason why so many amino acid substitutions were accumulated in gene 62 of V-Oka is still unclear, but it is possible that the mutant IE62s contained in V-Oka may have a competitive advantage over parental IE62 in interacting with some cellular transcription factors in guinea pig cells. The five amino acid substitutions closest to the carboxyl terminus in IE62 directly reduced its transactivational activity, and these locate in regions 4 and 5. Region 2 contains the DNA-binding domain (5), which is located between amino acids 472 and 646 (59, 60) and is essential for the protein's regulatory functions (58). A substitution of Lys residue 548, which lies within a highly conserved quartet of residues, WLQN, in region 2 drastically reduces the DNA-binding activity (58). Although the DNA-binding region of V-Oka had three amino acid mutations, no substitutions were found in the WLQN region. There were also no amino acid substitutions in other domains of IE62 that are important for its transcriptional activity, such as the proline-rich domain between regions 4 and 5 (5), the nuclear localization signal (5, 26), the potent activation domain in the N terminus (48), the kinase catalytic domain, and the ATP-binding domain (23). Thus, further studies are needed to determine the mechanism by which the expression of VZV genes is affected by the amino acid substitutions in IE62.

We detected insertions and a deletion in three repeat regions—R1, R3, and R4—that could potentially lead to different biological behaviors in V-Oka. R1 and R3 lie in ORF 11 and ORF 22, respectively, but both of these reiteration elements are multiples of 3 bp, so there were no frameshifts. The function of the ORF 11 protein is unclear, although it is homologous to HSV-1 UL47, a nucleotidylylated tegument phosphoprotein reported to modulate the activity of VP16 (6, 63, 64). It is difficult to differentiate V-Oka from wild-type viruses in Japan by analyzing R1 because a predominant R1 structure is contained in both the wild-type viruses and V-Oka (62). The R1 sequence in V-Oka determined by us is also identical to that in some viruses from patients with acute retinal necrosis syndrome (1). Thus, the deletion in the R1 region is not likely to be important for viral pathogenesis. R3 is unstable, as de-

scribed above, and lies within the longest ORF in VZV, ORF 22. The ORF 22 product is homologous to the UL36 virion tegument phosphoprotein (36, 37). It is not clear whether the variable R3 exerts a function in ORF 22, because little is known about this gene. R4 lies in a noncoding region situated ca. 550 bp upstream from the transcription start site, ca. 620 bp upstream from the initiator codon, of gene 62. It is possible that the deletion of R4 in V-Oka affects the expression level of IE62 despite its far distance from the transcription start site. In contrast, Perera et al. (46) reported that IE62 could autoactivate a truncated IE62 promoter that contained only 45 bp upstream of the transcription start site and suggested that IE62 self-activation might be mediated by a TATA sequence-dependent mechanism. Thus, at least the autoactivating activity of IE62 is independent of R4. Finally, a comparison of the Oka viruses showed that V-Oka had a deletion of $(TA)_3$ and GA in the origin regions in IRS and TRS. Plasmid replication experiments showed that the yields of deletion mutants that lost $(TA)_6$, and $(TA)_{10}$ in the corresponding region from the Dumas virus were 45 and 18%, respectively (54). Thus, the deletion in V-Oka may cause a reduced replication of VZV. Further studies are required to clarify the correlation between these candidates, including IE62, and pathogenicity. Recombinant virus could be prepared from viral DNA clones as previously reported (7, 32). Viral pathogenesis and proteins that are important for virus replication could be analyzed by using two systems: the SCID-hu mouse implanted with human fetal tissue (39, 40) and human mononuclear cells in umbilical cord blood infected with VZV (53). Studies are in progress to examine the pathogenesis of the IE62 mutant virus. The sequence differences presented here and the application of these techniques may provide new insights into mechanisms for the molecular pathogenesis of VZV infection.

Interestingly, differences in virus spreading to HEL cells were found among P-Oka, V-Oka, S7-01, and S7-13. P-Oka is known to be as virulent in vivo as other wild-type viruses. Naturally infected children who develop varicella have viremia that is detectable by virus isolation, whereas no viruses are isolated from healthy children immunized by the vaccine (3). Despite the different infection routes in these situations, the findings suggest that the vaccine virus cannot propagate in vivo to the same level as wild-type viruses. The behavior of V-Oka and its constituents both in vitro and in vivo differ from that of P-Oka and the wild-type viruses. Our data showed that viral pathogenicity was affected in association with 20 amino acid substitutions and slow spreading was associated with 15 of them, in ORFs 6, 10, 21, 31, 39, 55, 62, and 64, in the S7-01 virus. IE62 may be the most attractive candidate for causing the different biological properties of the vaccine. S7-01 had 14 amino acid substitutions, including all 8 amino acid substitutions in IE62. The IE62 of S7-01 is identical to a mutant IE62 that exhibited less transcriptional activity than the IE62 of P-Oka in CV1 cells in our previous study (15, 16), and similar results were obtained with the human 293 cell line (data not shown). It is possible that the lower activity of the mutant IE62 may be involved in the ineffective spreading or, moreover, the avirulence of the vaccine. On the other hand, S7-01 did not have mutations in genes 9A, 50, 52, 55, or 59. P-Oka not only is known to be virulent in vivo but also was more efficient in spreading in vitro than was S7-01 in the present study. Thus, the amino acid mutations in these gene products, which were the ORF 9A protein, two helicase-primase components, gM, and uracil-DNA glycosylase, did not seem to be important for efficient spreading. On the other hand, S7-13 exhibited moderately better growth than did S7-1, based on in the analysis of plaque sizes and spreading. Seven amino acids, in genes 21, 31, 55, 62, and 64, of S7-13 were found to be identical with P-Oka but not with S7-01. Three of these amino acids were in IE62, and when we expressed this mutant IE62 from pPV-G62*Nco*, it was shown to have <50% of the activity of parental IE62. These data indicate that the difference in viral spreading was likely to have been determined by the three mutations in IE62 rather than the four mutations in other gene products, ORF21 protein, gB glycoprotein, helicase-primase component, or ORF64 protein. Studies with recombinant VZVs will be needed to confirm the amino acid substitution(s) responsible for the differences in spreading activity.

Several candidates other than IE62 are potentially responsible for the biological differences in different forms of the virus. First, ORF 10 protein transactivates the IE62 gene promoter, although it does not transactivate the IE ORF 4 and ORF 61 promoters (43, 44). In the present study, both the parent and mutant ORF 10 proteins stimulated the IE62 promoter, and the amino acid substitution in ORF 10 failed to affect its transactivation activity. Thus, the mutant ORF 10 protein is unlikely to cause attenuation by repressing the expression level of IE62. Second, there were four amino acid substitutions in ORFs 6, 52, and 55, which are homologous to HSV-1 UL52, UL8, and UL5, respectively. ORFs 52 and 55 encode two kinds of protein each, as a result of partial amino acid substitutions, whereas ORF 6 is a single clone, as shown by RFLP analysis, indicating that eight (i.e., 2^3) isomeric complexes may exist by combining these three proteins. It is possible that different helicase-primase activities might exist among different isomeric complexes. Third, a base substitution led to an amino acid conversion in the uracil-DNA glycosylase. If this amino acid substitution were responsible for making the base substitutions in gene 62 in V-Oka, then uracil residues should misincorporate randomly in all of the genes, and substitutions should accumulate in dispensable genes rather than in essential genes. Nonetheless, more than one-third of the substitutions accumulated in gene 62, the homologue of HSV-1 ICP-4, which is essential in vitro (31). Therefore, the amino acid substitution in uracil-DNA glycosylase is not involved in promoting mutations during replication.

VZV glycoproteins are known to induce a strong humoral response both in natural infection and in vaccination with the Oka varicella vaccine. VZV produces at least seven glycoproteins, as described above. The expression level of gC, the gene 14 product, was dependent on the strain of VZV, and the gC level of V-Oka was much lower than that of wild-type viruses (25, 30). SCID-hu mouse experiments showed that a decrease in gC played a critical role in attenuation (39). However, we found no differences in its ORF or flanking regions except for a silent substitution in a termination codon of the gC gene: an ocher (TAA) incompletely altered to an amber (TAG). In our earlier study we found no evidence that the decrease in gC in V-Oka was caused by amino acid substitutions in IE62 because the gC promoter was unresponsive to IE62. The transactivational activity of IE62 is negatively regulated at later stages of

the infectious cycle by its phosphorylation by the ORF66 protein kinase, which inhibits its nuclear import (23, 26). Therefore, vaccine IE62 is not directly involved with the decrease in gC by transactivating the gene to a lesser extent. We found amino acid substitution in only gB of V-Oka; i.e., an Ile in the gB of P-Oka was Ile plus Val in V-Oka. gB is the second most abundant and immunogenic glycoprotein in VZV. It appears to play a role in the attachment and penetration of particles, along with gH and gC, and can elicit a monoclonal antibody that neutralizes viral infectivity in vitro. VZV gB is associated with cell-to-cell infection, as is HSV-1 gB (41, 45). gB was also shown to have great fusogenic properties in the presence of gE (33). Nonetheless, it is thought that the amino acid substitution in gB is not crucial for the antigenicity of the vaccine because about half of the clones in V-Oka contain identical sequences to P-Oka in this gene; moreover, Ile and Val have similar properties, and this substitution would be unlikely to change the protein's properties in the remaining half of the clones. These findings indicate that the cell-mediated and humoral immunities led by the glycoproteins of V-Oka are identical to those of P-Oka without adapting to the heterogeneous host, guinea pig cells. V-Oka is likely to have few functional differences in viral attachment and penetration from P-Oka. Although it was reported that V-Oka shows a higher adsorption rate than P-Oka in GPE cells as determined by the infectious center assay (34), the higher adsorption of V-Oka appeared to be caused by the virus's capacity to replicate in guinea pig cells but not by the substitution in gB.

Some cases of chickenpox or shingles in immunocompromised individuals after vaccination have been reported. In rare cases, even healthy vaccine recipients develop rashes within a few weeks after vaccination. However, it has not been clear whether these cases were caused by the vaccine virus or by a wild-type virus. In addition, some reports concerning transmission of the vaccine virus have been reported (21, 29, 51). Therefore, it is epidemiologically important to differentiate the Oka vaccine virus from circulating wild-type viruses. At present, the Oka viruses, which include V-Oka and P-Oka, are identified by using restriction endonuclease digestion of extracted purified viral DNA (14, 19), analysis of repeat regions (17, 55), and RFLP assays after PCR (17, 20, 27, 28, 55, 57). We also have reported an identifying method that combines the single-strand conformational polymorphism of repeat region 2 (R2) with *Pst*I cleavage of the *Pst*I-site-less region (42). Although the Oka viruses can be distinguished from other clinical isolates by these methods, it is difficult to distinguish V-Oka from P-Oka. Therefore, we attempted to identify only V-Oka by another method that uses the simplified RFLP analysis by *Nae*I and *Bss*HII (15, 16). This method was established based on the first known sequence differences we found in gene 62, and V-Oka could be distinguished not only from clinical isolates but also from P-Oka. Therefore, comparisons of the gene 62 sequence may enable the epidemiological typing of VZV strains. Thus, the comparison of the DNAs is important for quality control of varicella vaccine, molecular epidemiology and, in particular, the development and improvement of new vaccines.

The mechanism of attenuation is still unclear because the mutations were found not only in gene 62 but also in other genes. Therefore, further study to analyze more in detail by using recombinant viruses and suitable animals are needed to resolve the mechanism of attenuation of VZV.

REFERENCES

1. **Abe, T., M. Sato, and M. Tamai.** 2000. Variable R1 region in varicella zoster virus in fulminant type of acute retinal necrosis syndrome. Br. J. Ophthalmol. **84:**193–198.
2. **Argaw, T., J. I. Cohen, M. Klutch, K. Lekstrom, T. Yoshikawa, Y. Asano, and P. R. Krause.** 2000. Nucleotide sequences that distinguish Oka vaccine from parental Oka and other varicella-zoster virus isolates. J. Infect. Dis. **181:** 1153–1157.
3. **Asano, Y., N. Itakura, Y. Hiroishi, S. Hirose, T. Ozaki, K. Kuno, T. Nagai, T. Yazaki, K. Yamanishi, and M. Takahashi.** 1985. Viral replication and immunologic responses in children naturally infected with varicella-zoster virus and in varicella vaccine recipients. J. Infect. Dis. **152:**863–868.
4. **Barker, D. E., and B. Roizman.** 1992. The unique sequence of the herpes simplex virus 1 L component contains an additional translated open reading frame designated UL49.5. J. Virol. **66:**562–566.
5. **Baudoux, L., P. Defechereux, S. Schoonbroodt, M. P. Merville, B. Rentier, and J. Piette.** 1995. Mutational analysis of varicella-zoster virus major immediate-early protein IE62. Nucleic Acids Res. **23:**1341–1349.
6. **Blaho, J. A., C. Mitchell, and B. Roizman.** 1994. An amino acid sequence shared by the herpes simplex virus 1 alpha regulatory proteins 0, 4, 22, and 27 predicts the nucleotidylylation of the UL21, UL31, UL47, and UL49 gene products. J. Biol. Chem. **269:**17401–17410.
7. **Cohen, J. I., and K. E. Seidel.** 1993. Generation of varicella-zoster virus (VZV) and viral mutants from cosmid DNAs: VZV thymidylate synthetase is not essential for replication in vitro. Proc. Natl. Acad. Sci. USA **90:**7376–7380.
8. **Crute, J. J., T. Tsurumi, L. A. Zhu, S. K. Weller, P. D. Olivo, M. D. Challberg, E. S. Mocarski, and I. R. Lehman.** 1989. Herpes simplex virus 1 helicase-primase: a complex of three herpes-encoded gene products. Proc. Natl. Acad. Sci. USA **86:**2186–2189.
9. **Davison, A. J., and J. E. Scott.** 1986. The complete DNA sequence of varicella-zoster virus. J. Gen. Virol. **67:**1759–1816.
10. **Defechereux, P., L. Melen, L. Baudoux, M. P. Merville-Louis, B. Rentier, and J. Piette.** 1993. Characterization of the regulatory functions of varicella-zoster virus open reading frame 4 gene product. J. Infect. Dis. **168:**1330–1331.
11. **Disney, G. H., and R. D. Everett.** 1990. A herpes simplex virus type 1 recombinant with both copies of the Vmw175 coding sequences replaced by the homologous varicella-zoster virus open reading frame. J. Gen. Virol. **71:**2681–2689.
12. **Disney, G. H., T. A. McKee, C. M. Preston, and R. D. Everett.** 1990. The product of varicella-zoster virus gene 62 autoregulates its own promoter. J. Gen. Virol. **71:**2999–3003.
13. **Felser, J. M., P. R. Kinchington, G. Inchauspe, S. E. Straus, and J. M. Ostrove.** 1988. Cell lines containing varicella-zoster virus open reading frame 62 and expressing the "IE" 175 protein complement ICP4 mutants of herpes simplex virus type 1. J. Gen. Virol. **69:**2585–2593.
14. **Gelb, L. D., D. E. Dohner, A. A. Gershon, S. P. Steinberg, J. L. Waner, M. Takahashi, P. H. Dennehy, and A. E. Brown.** 1987. Molecular epidemiology of live, attenuated varicella virus vaccine in children with leukemia and in normal adults. J. Infect. Dis. **155:**633–640.
15. **Gomi, Y., T. Imagawa, M. Takahashi, and K. Yamanishi.** 2000. Oka varicella vaccine is distinguishable from its parental virus in DNA sequence of open reading frame 62 and its transactivation activity. J. Med. Virol. **61:**497–503.
16. **Gomi, Y., T. Imagawa, M. Takahashi, and K. Yamanishi.** 2001. Comparison of DNA sequence and transactivation activity of open reading frame 62 of Oka varicella vaccine and its parental viruses. Arch. Virol. Suppl. **17:**49–56.
17. **Hawrami, K., and J. Breuer.** 1997. Analysis of United Kingdom wild-type strains of varicella-zoster virus: differentiation from the Oka vaccine strain. J. Med. Virol. **53:**60–62.
18. **Hawrami, K., D. Harper, and J. Breuer.** 1996. Typing of varicella-zoster virus by amplification of DNA polymorphisms. J. Virol. Methods **57:**169–174.
19. **Hayakawa, Y., T. Yamamoto, K. Yamanishi, and M. Takahashi.** 1986. Analysis of varicella-zoster virus DNAs of clinical isolates by endonuclease *Hpa*I. J. Gen. Virol. **67:**1817–1829.
20. **Hondo, R., and Y. Yogo.** 1989. Strain variation of R5 direct repeats in the right-hand portion of the long unique segment of varicella-zoster virus DNA. Jpn. J. Exp. Med. **59:**233–237.
21. **Hughes, P., P. LaRussa, J. M. Pearce, M. Lepow, S. Steinberg, and A. Gershon.** 1994. Transmission of varicella-zoster virus from a vaccinee with leukemia, demonstrated by polymerase chain reaction. J. Pediatr. **124:**932–935.
22. **Inchauspe, G., and J. M. Ostrove.** 1990. Differential regulation by varicella-zoster virus (VZV) and herpes simplex virus type-1 *trans*-activating genes. Adv. Virus Res. **38:**45–98.
23. **Kinchington, P. R., K. Fite, and S. E. Turse.** 2000. Nuclear accumulation of IE62, the varicella-zoster virus (VZV) major transcriptional regulatory pro-

tein, is inhibited by phosphorylation mediated by the VZV open reading frame 66 protein kinase. J. Virol. **74**:2265–2277.
24. **Kinchington, P. R., J. K. Hougland, A. M. Arvin, W. T. Ruyechan, and J. Hay.** 1992. The varicella-zoster virus immediate-early protein IE62 is a major component of virus particles. J. Virol. **66**:359–366.
25. **Kinchington, P. R., P. Ling, M. Pensiero, A. Gershon, J. Hay, and W. T. Ruyechan.** 1990. A possible role for glycoprotein gpV in the pathogenesis of varicella-zoster virus. Adv. Exp. Med. Biol. **278**:83–91.
26. **Kinchington, P. R., and S. E. Turse.** 1998. Regulated nuclear localization of the varicella-zoster virus major regulatory protein, IE62. J. Infect. Dis. **178**(Suppl. 1):S16–S21.
27. **LaRussa, P., O. Lungu, I. Hardy, A. Gershon, S. P. Steinberg, and S. Silverstein.** 1992. Restriction fragment length polymorphism of polymerase chain reaction products from vaccine and wild-type varicella-zoster virus isolates. J. Virol. **66**:1016–1020.
28. **LaRussa, P., S. Steinberg, A. Arvin, D. Dwyer, M. Burgess, M. Menegus, K. Rekrut, K. Yamanishi, and A. Gershon.** 1999. Polymerase chain reaction and restriction fragment length polymorphism analysis of varicella-zoster virus isolates from the United States and other parts of the world. J. Infect. Dis. **178**(Suppl. 1):S64–S66.
29. **LaRussa, P., S. Steinberg, F. Meurice, and A. Gershon.** 1997. Transmission of vaccine strain varicella-zoster virus from a healthy adult with vaccine-associated rash to susceptible household contacts. J. Infect. Dis. **176**:1072–1075.
30. **Ling, P., P. R. Kinchington, W. T. Ruyechan, and J. Hay.** 1991. A detailed analysis of transcripts mapping to varicella-zoster virus gene 14 (glycoprotein V). Virol. **184**:625–635.
31. **Longnecker, R., and B. Roizman.** 1986. Generation of an inverting herpes simplex virus 1 mutant lacking the L-S junction a sequences, an origin of DNA synthesis, and several genes, including those specifying glycoprotein E and the alpha 47 gene. J. Virol. **58**:583–591.
32. **Mallory, S., M. Sommer, and A. M. Arvin.** 1997. Mutational analysis of the role of glycoprotein I in varicella-zoster virus replication and its effects on glycoprotein E conformation and trafficking. J. Virol. **71**:8279–8288.
33. **Maresova, L., T. J. Pasieka, and C. Grose.** 2001. Varicella-zoster virus gB and gE coexpression, but not gB or gE alone, leads to abundant fusion and syncytium formation equivalent to those from gH and gL coexpression. J. Virol. **75**:9483–9492.
34. **Matsunaga, Y., K. Yamanishi, and M. Takahashi.** 1982. Experimental infection and immune response of guinea pigs with varicella-zoster virus. Infect. Immun. **37**:407–412.
35. **McGeoch, D. J., A. Dolan, S. Donald, and D. H. Brauer.** 1986. Complete DNA sequence of the short repeat region in the genome of herpes simplex virus type 1. Nucleic Acids Res. **14**:1727–1745.
36. **McNabb, D. S., and R. J. Courtney.** 1992. Analysis of the UL36 open reading frame encoding the large tegument protein (ICP1/2) of herpes simplex virus type 1. J. Virol. **66**:7581–7584.
37. **McNabb, D. S., and R. J. Courtney.** 1992. Characterization of the large tegument protein (ICP1/2) of herpes simplex virus type 1. Virology **190**:221–232.
38. **Meier, J. L., X. Luo, M. Sawadogo, and S. E. Straus.** 1994. The cellular transcription factor USF cooperates with varicella-zoster virus immediate-early protein 62 to symmetrically activate a bidirectional viral promoter. Mol. Cell. Biol. **14**:6896–6906.
39. **Moffat, J. F., L. Zerboni, P. R. Kinchington, C. Grose, H. Kaneshima, and A. M. Arvin.** 1998. Attenuation of the vaccine Oka strain of varicella-zoster virus and role of glycoprotein C in alphaherpesvirus virulence demonstrated in the SCID-hu mouse. J. Virol. **72**:1542–1551.
40. **Moffat, J. F., L. Zerboni, M. H. Sommer, T. C. Heineman, J. I. Cohen, H. Kaneshima, and A. M. Arvin.** 1998. The ORF47 and ORF66 putative protein kinases of varicella-zoster virus determine tropism for human T cells and skin in the SCID-hu mouse. Proc. Natl. Acad. Sci. USA **95**:11969–11974.
41. **Montalvo, E., and C. Grose.** 1987. Assembly and processing of the disulfide-linked varicella-zoster virus glycoprotein gpII(140). J. Virol. **61**:2877–2884.
42. **Mori, C., R. Takahara, T. Toriyama, T. Nagai, M. Takahashi, and K. Yamanishi.** 1998. Identification of the Oka strain of the live attenuated varicella vaccine from other clinical isolates by molecular epidemiologic analysis. J. Infect. Dis. **178**:35–38.
43. **Moriuchi, H., M. Moriuchi, S. E. Straus, and J. I. Cohen.** 1993. Varicella-zoster virus open reading frame 10 protein, the herpes simplex virus VP16 homolog, transactivates herpesvirus immediate-early gene promoters. J. Virol. **67**:2739–2746.
44. **Moriuchi, M., H. Moriuchi, S. E. Straus, and J. I. Cohen.** 1994. Varicella-zoster virus (VZV) virion-associated transactivator open reading frame 62 protein enhances the infectivity of VZV DNA. Virology **200**:297–300.
45. **Navarro, D., P. Paz, and L. Pereira.** 1992. Domains of herpes simplex virus I glycoprotein B that function in virus penetration, cell-to-cell spread, and cell fusion. Virology **186**:99–112.
46. **Perera, L. P.** 2000. The TATA motif specifies the differential activation of minimal promoters by varicella-zoster virus immediate-early regulatory protein IE62. J. Biol. Chem. **275**:487–496.
47. **Perera, L. P., J. D. Mosca, W. T. Ruyechan, and J. Hay.** 1992. Regulation of varicella-zoster virus gene expression in human T lymphocytes. J. Virol. **66**:5298–5304.
48. **Perera, L. P., J. D. Mosca, W. T. Ruyechan, G. S. Hayward, S. E. Straus, and J. Hay.** 1993. A major transactivator of varicella-zoster virus, the immediate-early protein IE62, contains a potent N-terminal activation domain. J. Virol. **67**:4474–4483.
49. **Perera, L. P., J. D. Mosca, M. Sadeghi-Zadeh, W. T. Ruyechan, and J. Hay.** 1992. The varicella-zoster virus immediate early protein, IE62, can positively regulate its cognate promoter. Virology **191**:346–354.
50. **Ross, J., M. Williams, and J. I. Cohen.** 1997. Disruption of the varicella-zoster virus dUTPase and the adjacent ORF9A gene results in impaired growth and reduced syncytia formation in vitro. Virology **234**:186–195.
51. **Salzman, M. B., R. G. Sharrar, S. Steinberg, and P. LaRussa.** 1997. Transmission of varicella-vaccine virus from a healthy 12-month-old child to his pregnant mother. J. Pediatr. **131**:151–154.
52. **Schoonbroodt, S., J. Piette, L. Baudoux, P. Defechereux, B. Rentier, and M. P. Merville.** 1996. Enhancement of varicella-zoster virus infection in cell lines expressing ORF4- or ORF62-encoded proteins. J. Med. Virol. **49**:264–273.
53. **Soong, W., J. C. Schultz, A. C. Patera, M. H. Sommer, and J. I. Cohen.** 2000. Infection of human T lymphocytes with varicella-zoster virus: an analysis with viral mutants and clinical isolates. J. Virol. **74**:1864–1870.
54. **Stow, N. D., and A. J. Davison.** 1986. Identification of a varicella-zoster virus origin of DNA replication and its activation by herpes simplex virus type 1 gene products. J. Gen. Virol. **67**:1613–1623.
55. **Takada, M., T. Suzutani, I. Yoshida, M. Matoba, and M. Azuma.** 1995. Identification of varicella-zoster virus strains by PCR analysis of three repeat elements and a *Pst*I-site-less region. J. Clin. Microbiol. **33**:658–660.
56. **Takahashi, M., T. Otsuka, Y. Okuno, Y. Asano, and T. Yazaki.** 1974. Live vaccine used to prevent the spread of varicella in children in hospital. Lancet **ii**:1288–1290.
57. **Takayama, M., N. Takayama, N. Inoue, and Y. Kameoka.** 1997. Application of long PCR method of identification of variations in nucleotide sequences among varicella-zoster virus isolates. J. Clin. Microbiol. **34**:2869–2874.
58. **Tyler, J. K., K. E. Allen, and R. D. Everett.** 1994. Mutation of a single lysine residue severely impairs the DNA recognition and regulatory functions of the VZV gene 62 transactivator protein. Nucleic Acids Res. **22**:270–278.
59. **Tyler, J. K., and R. D. Everett.** 1994. The DNA binding domain of the varicella-zoster virus gene 62 protein interacts with multiple sequences which are similar to the binding site of the related protein of herpes simplex virus type 1. Nucleic Acids Res. **22**:711–721.
60. **Wu, C. L., and K. W. Wilcox.** 1991. The conserved DNA-binding domains encoded by the herpes simplex virus type 1 ICP4, pseudorabies virus IE180, and varicella-zoster virus ORF62 genes recognize similar sites in the corresponding promoters. J. Virol. **65**:1149–1159.
61. **Yamanishi, K., Y. Matsunaga, T. Otsuka, and M. Takahashi.** 1980. Immune response of guinea pigs to varicella vaccine strain (OKA) and wild strains. Biken J. **23**:53–55.
62. **Yoshida, M., T. Tamura, and M. Hiruma.** 2000. Analysis of strain variation of R1 repeated structure in varicella-zoster virus DNA by polymerase chain reaction. J. Med. Virol. **58**:76–78.
63. **Zhang, Y., and J. L. McKnight.** 1993. Herpes simplex virus type 1 UL46 and UL47 deletion mutants lack VP11 and VP12 or VP13 and VP14, respectively, and exhibit altered viral thymidine kinase expression. J. Virol. **67**:1482–1492.
64. **Zhang, Y., D. A. Sirko, and J. L. McKnight.** 1991. Role of herpes simplex virus type 1 UL46 and UL47 in αTIF-mediated transcriptional induction: characterization of three viral deletion mutants. J. Virol. **65**:829–841.

Anexo 2 36

JOURNAL OF VIROLOGY, Nov. 2008, p. 11023–11044
0022-538X/08/$08.00+0 doi:10.1128/JVI.00777-08
Copyright © 2008, American Society for Microbiology. All Rights Reserved.
Vol. 82, No. 22

Complete DNA Sequences of Two Oka Strain Varicella-Zoster Virus Genomes▽

Sueli L. Tillieux,[1] Wendy S. Halsey,[2] Elizabeth S. Thomas,[2] John J. Voycik,[2]‡ Ganesh M. Sathe,[2] and Ventzislav Vassilev[1]*

GlaxoSmithKline Biologicals, Research and Development, Viral Vaccines, B-1330 Rixensart, Belgium,[1] and GlaxoSmithKline, Discovery Technology Group, 1250 South Collegeville Road, Collegeville, Pennsylvania 19426[2]

Received 10 April 2008/Accepted 3 September 2008

Varicella-zoster virus (VZV) is a herpesvirus and is the causative agent of chicken pox (varicella) and shingles (herpes zoster). Active immunization against varicella became possible with the development of live attenuated varicella vaccine. The Oka vaccine strain was isolated in Japan from a child who had typical varicella, and it was then attenuated by serial passages in cell culture. Several manufacturers have obtained this attenuated Oka strain and, following additional passages, have developed their own vaccine strains. Notably, the vaccines Varilrix and Varivax are produced by GlaxoSmithKline Biologicals and Merck & Co., Inc., respectively. Both vaccines have been well studied in terms of safety and immunogenicity. In this study, we report the complete nucleotide sequence of the Varilrix (Oka-V_{GSK}) and Varivax (Oka-V_{Merck}) vaccine strain genomes. Their genomes are composed of 124,821 and 124,815 bp, respectively. Full genome annotations covering the features of Oka-derived vaccine genomes have been established for the first time. Sequence analysis indicates 36 nucleotide differences between the two vaccine strains throughout the entire genome, among which only 14 are involved in unique amino acid substitutions. These results demonstrate that, although Oka-V_{GSK} and Oka-V_{Merck} vaccine strains are not identical, they are very similar, which supports the clinical data showing that both vaccines are well tolerated and elicit strong immune responses against varicella.

Varicella-zoster virus (VZV) is a human alphaherpesvirus that causes chicken pox (varicella) and shingles (herpes zoster) (75). VZV has a linear, double-stranded DNA genome of approximately 125 kb that encodes at least 71 proteins (12). Primary infection with VZV results in varicella, which is a widespread, highly contagious disease. Varicella is commonly regarded as a mild childhood illness, but it may lead to serious complications, such as secondary bacterial infection, pneumonia, encephalitis, congenital infection, and death (76).

Like other herpesviruses, VZV has the capacity to persist in the body after the primary acute infection as a latent infection in sensory nerve ganglia. This lifelong latent infection commonly reactivates to cause herpes zoster, typically in elderly or immunocompromised patients (65).

In 1974, Takahashi et al. reported the development of a live-attenuated varicella vaccine through serial passages of wild-type virus in cell culture (67). The parental virus, Oka-P, was isolated in primary human embryo lung cell culture from vesicle fluid from a 3-year-old boy with typical varicella. The virus was attenuated by 10 passages in HEL and 12 passages in guinea pig embryo cells, plaque-purified, and passaged five times further in human diploid cells (WI38) to prepare a strain suitable for use as a vaccine (Oka-V) (Fig. 1) (67).

The Oka-V strain was first supplied in 1976 under license from the Biken Institute in Japan. Several manufacturers (SmithKline RIT, Merck Sharp & Dohme, and Pasteur Mérieux) subsequently used the Oka-V strain in the development of proprietary vaccines. A product license was obtained for Varilrix (frozen formulation) in 1984 by SmithKline RIT for use in groups at high risk for severe varicella and their healthy close contacts. SmithKline RIT—now GlaxoSmithKline (GSK) Biologicals—subsequently developed a refrigerator-stable formulation of this varicella vaccine. Varilrix is indicated in many countries for use in healthy and immunocompromised subjects from 9 months of age. GSK Biologicals' varicella vaccine production is based on the seed lot system (6, 14) using classical cell culture methods (Fig. 1). A manufacturer's working cell bank of human diploid cells, MRC-5, was prepared and tested according to World Health Organization requirements.

The Biken vaccine was licensed in Japan and Korea, in 1986 and 1988, respectively, for use in healthy subjects, and a license for Varivax with the same indication was granted in the United States in 1995 (1). In 1993, the vaccine manufactured by Pasteur Mérieux was licensed in France for use in potentially immunocompromised subjects.

Although the varicella vaccine is licensed in many countries, it is not routinely used because complications associated with varicella disease are often underestimated. Universal mass vaccination against varicella is implemented only in few countries; however, it is under consideration in many others (38, 40, 54, 72). The incidence of varicella disease and the rate of varicella-related hospitalizations in the United States have declined by about 80% since implementation of universal mass vaccination against varicella (using Varivax) in 1996 (8, 16, 81). A similar

* Corresponding author. Mailing address: Viral Vaccines Research and Development, GlaxoSmithKline Biologicals, Rue de l'Institut, 89 (P31-005), B-1330 Rixensart, Belgium. Phone: 32-2-656-6422. Fax: 32-2-656-8113. E-mail: ventzislav.vassilev@gskbio.com.

‡ Present address: PerkinElmer Life and Analytical Sciences, 710 Bridgeport Ave, Shelton, CT 06484-4794.

▽ Published ahead of print on 10 September 2008.

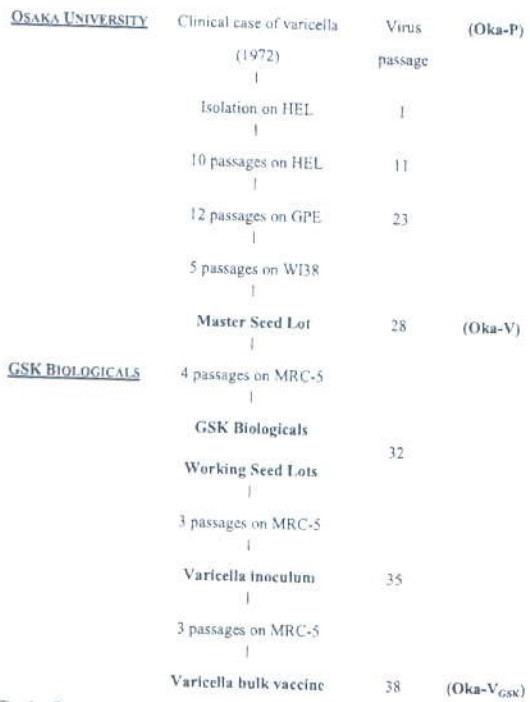


FIG. 1. Passage history of the live attenuated Oka varicella vaccine. HEL, human embryonic lung cells; GPE, guinea pig embryo cells; WI38 and MRC-5, human diploid cells.

decrease was observed in Uruguay since the introduction of varicella vaccination (using Varilrix) into the routine childhood immunization program in 1999, with the greatest reduction in children aged 1 to 4 years (51). Most pre- and postlicense studies showed that vaccination with one dose of varicella-containing vaccine provides 70% to 90% protection from chicken pox and over 95% protection against the most severe forms of the disease for a 7- to 10-year period after vaccination (2, 17, 33, 33a, 34, 40, 61). However, vaccine-induced immunity wanes over time (9), leading countries such as the United States to recommend a two-dose schedule for varicella vaccination (40). This strategy aims to overcome primary vaccine failures and to improve long-term protection, thereby reducing the risk of breakthrough varicella (4). Combined vaccine products containing the VZV Oka strain have been developed as well. For instance, GSK Biologicals and Merck & Co., Inc., developed combined tetravalent measles-mumps-rubella-varicella vaccines (Priorix-Tetra and ProQuad, respectively), providing the benefits of measles-mumps-rubella and varicella vaccination in a single injection (19, 30, 35, 48, 71, 72, 79).

Different sets of serological readouts have been used to characterize the adaptive humoral immune response after varicella vaccination or infection (4, 13, 26, 31, 34, 58, 73, 74). Comparative analysis has raised the possibility that differences in the genetic code between the vaccine strains could be responsible for disparity in vaccine-induced humoral responses (36).

Oka-V, and presumably its derivative vaccine strains, was not cloned during the development and the preparation of vaccine (67). Sequencing of the complete genome of the original Oka-V vaccine preparation revealed that it contained multiple variants that could be separated in cell culture (20, 22).

The aim of the present study was to analyze the complete consensus nucleotide sequences of Oka-V strain viruses contained in Varilrix (GSK Biologicals; Oka-V_{GSK}) and Varivax (Merck & Co., Inc.; Oka-V_{Merck}) and to compare them to the published sequences of Oka-V and Oka-P (22). The full-length genomic sequences were also compared to published partial sequencing information on Oka-V_{GSK} and Oka-V_{Merck} (3, 32, 60, 63).

MATERIALS AND METHODS

Nucleic acid extraction. Total DNA was extracted from a single vial of recent production lots of Varilrix (lot VAV10118, produced in April 2002; GSK Biologicals, Rixensart, Belgium) and Varivax (lot 0895 M, purchased in 2003; Merck & Co., Inc., Whitehouse Station, NJ) vaccines using a High Pure viral nucleic acid kit from Roche (Basel, Switzerland). In brief, 100 μl of sample was lysed in a lysing-binding buffer in the presence of proteinase K. The lysis mixture was then applied to a glass fiber filter, which binds the nucleic acids in the presence of the lysis and binding buffer containing chaotropic salts. Bound nucleic acids were eluted in 50 μl of nuclease-free water by centrifugation and stored at −70°C.

PCR. Around 540 primers were designed using Primer D software (GSK in-house software) and the nucleotide sequence of the Dumas strain (GenBank accession no. X04370) (12). Overlapping primers were designed approximately 500 bases apart to cover the entire genomic sequence of VZV. Sequences of primers used for amplification and sequencing are available upon request. The reaction mixtures for PCR contained 15 μl of HotStarTaq Plus Master Mix solution (Qiagen, Valencia, CA), 0.3 μM of each primer, and 5 ng of template DNA. A Tetrad thermal cycler (MJ Research, Waltham, MA) was used for all amplifications. An initial hot-start PCR step of 96°C for 15 min was followed by 35 cycles of amplification (95°C for 20 s, 55°C for 30 s, and 72°C for 45 s) and a final elongation step at 72°C for 3 min. All amplified products were then purified using QIAquick PCR purification kit (Qiagen). Direct sequencing of both DNA strands was performed on the generated amplicons.

Sequencing. Direct sequencing of purified PCR products and plasmid DNA was performed with BigDye Terminator cycle sequencing kit and a 3730XL genetic analyzer (both from Applied Biosystems, Foster City, CA). The viral sequences were compiled and analyzed with Sequencher software (Gene Codes Corp, Ann Arbor, MI). The following GenBank sequences were used for comparison: for the European (The Netherlands) reference strain (Dumas), X04370 (12); for Oka-P, AB097933 (22); and for Oka-V, AB097932 (22), AF206304 (3), AY016450 (15), and the sequencing information provided by Schmidt et al. (60). Unless otherwise stated, all described nucleotide sequence positions in this paper correspond to the genome of Dumas strain, X04370 (12).

Cloning of PCR products. When direct sequencing did not generate information of sufficient quality or when particular single nucleotide polymorphisms (SNPs) could not be reliably confirmed, additional subcloning was performed, followed by sequencing of numerous generated clones to confirm the consensus sequence of the region. Direct sequencing of the PCR products derived from regions with highly complex secondary structure (flanking regions between internal repeat long and internal repeat short regions, and the R3 repeat region) was complemented by subcloning of amplicons and sequencing of plasmid clones. PCR products containing these regions were individually inserted into a pCR2.1 vector (Invitrogen, Carlsbad, CA) and then transformed into competent *Escherichia coli* by the TOPO TA cloning method (Invitrogen). The plasmid DNAs were purified from cultured bacteria with a QIAprep spin kit (Qiagen). DNA sequences of the cloned inserts were determined using vector-specific sequencing primers.

Sequencing of ends of the viral genomes. The direct sequencing data for viral genome ends were complemented by sequencing of overlapping amplicons generated after circularization using T4 DNA ligase (Roche). The PCR mixtures contained 500 μM of each deoxynucleoside triphosphate, 10 pmol of each primer, and 2.5 U high-fidelity Platinum *Taq* polymerase (Invitrogen). PCR products were inserted into a pCR4-TOPO vector and transformed into competent *E. coli* TOP10 bacteria by the TOPO TA cloning method (Invitrogen). The plasmid DNAs were purified with a QIAprep spin kit (Qiagen). The consensus sequence of the cloned amplicons was confirmed by sequencing and alignment of multiple *E. coli* plasmid clones.

Nucleotide sequence accession numbers. The complete nucleotide consensus sequences of the Oka-V_{GSK} (Varilrix) and Oka-V_{Merck} (Varivax) strains are

TABLE 1. Complete Oka-V_{GSK} genome annotation

Start	Stop	Feature[a]	ORF	Function or comment
88	89	Miscellaneous		TRL/UL boundary
914	587	Gene	1	
592	587	Poly(A) signal		
914	588	CDS	1	
1133	1861	Gene	2	
1133	1849	CDS	2	
1856	1861	Poly(A) signal		
2446	1889	Gene	3	
1894	1889	Poly(A) signal		
2446	1907	CDS	3	
4140	2781	Gene	4	
2781	2776	Poly(A) signal		
4140	2782	CDS	4	Transactivator, tegument protein
5273	4251	Gene	5	
5273	4251	CDS	5	gK
8576	5325	Gene	6	
8606	9398	Gene	7	
9393	9398	Poly(A) signal		
8606	9385	CDS	7	
10666	9425	Gene	8	
9430	9425	Poly(A) signal		
10666	9476	CDS	8	Deoxyuridine triphosphatase
10641	10904	CDS	9A[b]	gN
11008	11963	Gene	9	
11958	11963	Poly(A) signal		
11008	11916	CDS	9	Syncytium formation, virion protein
12159	13420	Gene	10	
13415	13420	Poly(A) signal		
12159	13391	CDS	10	Transactivator, tegument protein
13589	16076	Gene	11	
13936	14196	Repeat region		Reiteration R1
16071	16076	Poly(A) signal		
13589	16003	CDS	11	
16168	18153	Gene	12	
18695	19350	Gene	13	
19345	19350	Poly(A) signal		
18395	19300	CDS	13	
21067	19296	Gene	14	
19301	19296	Poly(A) signal		
20526	20851	Repeat region		Reiteration R2
21067	19385	CDS	14	
22432	21198	Gene	15	
21203	21198	Poly(A) signal		
22432	21212	CDS	15	
23748	22522	Gene	16	
24103	25468	Gene	17	
25463	25468	Poly(A) signal		
24103	25467	CDS	17	
26444	25501	Gene	18	
25506	25501	Poly(A) signal		
26444	25524	CDS	18	Ribonucleotide reductase, small subunit
28796	26469	Gene	19	Ribonucleotide reductase, big subunit
30426	28956	Gene	20	
28961	28956	Poly(A) signal		
30426	28975	CDS	20	
30710	33856	Gene	21	
33851	33856	Poly(A) signal		
30710	33826	CDS	21	Nucleocapsid
34034	42341	Gene	22	
41405	41470	Repeat region		Reiteration R3
42336	42341	Poly(A) signal		
34034	42325	CDS	22	
43090	42378	Gene	23	
42383	42378	Poly(A) signal		
43090	42383	CDS	23	
43973	43163	Gene	24	
43168	43163	Poly(A) signal		
43973	43164	CDS	24	
44570	44083	Gene	25	
44088	44083	Poly(A) signal		
44570	44100	CDS	25	
44458	46125	Gene	26	
46079	47195	Gene	27	
47190	47195	Poly(A) signal		
46079	47080	CDS	27	
50588	46983	Gene	28	
46988	46983	Poly(A) signal		
50588	47004	CDS	28	DNA polymerase
50809	54460	Gene	29	
54455	54460	Poly(A) signal		
50809	54408	CDS	29	ssDNA binding protein
54587	56899	Gene	30	
56944	59584	Gene	31	
59579	59584	Poly(A) signal		
56944	59550	CDS	31	gB, fusogen
59703	60150	Gene	32	
60145	60150	Poly(A) signal		
59703	60134	CDS	32	Substrate for ORF 47 kinase
62074	60245	Gene	33	
60250	60245	Poly(A) signal		
62074	60257	CDS	33	Protease
63846	62107	Gene	34	
64689	63913	CDS	35	
64300	64306	promoter		TATA element
64321	64325	5′end of dPyKmRNA		
64743	65800	Gene	36	
65795	65800	Poly(A) signal		
64743	65768	CDS	36	Thymidine kinase
65817	65821	3′end of dPyKmRNA		
66010	68552	Gene	37	
68747	68552	Poly(A) signal		
66010	68535	CDS	37	gH
70229	68583	Gene	38	
68588	68583	Poly(A) signal		
70229	68604	CDS	38	
70569	71305	Gene	39	
71300	71305	Poly(A) signal		
70569	71291	CDS	39	
71476	75699	Gene	40	
75694	75699	Poly(A) signal		
71476	75666	CDS	40	Major nucleocapsid protein
75783	76748	Gene	41	
76743	76748	Poly(A) signal		
75783	76733	CDS	41	
77974	76791	Gene	42	
76786	76791	Poly(A) signal		ORF 45+ORF 42
77974	76787	CDS	42	
78105	80136	Gene	43	
80131	80136	Poly(A) signal		
78105	80135	CDS	43	
80295	81449	Gene	44	
81444	81449	Poly(A) signal		
80295	81386	CDS	44	
82529	81474	CDS	45	
82654	83253	CDS	46	
83103	84635	CDS	47	Protein kinase, tegument protein
84602	86257	CDS	48	
86161	86429	Gene	49	
86424	86429	Poly(A) signal		
86161	86406	CDS	49	
87807	86466	Gene	50	
86471	86466	Poly(A) signal		
87807	86500	CDS	50	
87806	90313	CDS	51	Origin binding protein
90418	92771	Gene	52	
92766	92771	Poly(A) signal		
90418	92733	CDS	52	
93775	92775	Gene	53	
92780	92775	Poly(A) signal		
93775	92780	CDS	53	
95909	93600	CDS	54	
95921	98566	CDS	55	
98493	99280	Gene	56	
99275	99280	Poly(A) signal		
98493	99224	CDS	56	
99548	99309	Gene	57	
99314	99309	Poly(A) signal		
99548	99333	CDS	57	Cytoplasmic protein
100194	99529	CDS	58	
101141	100224	CDS	59	Uracil-DNA glycosylase
101574	101092	CDS	60	gL, chaperone for gH
104410	102926	Gene	61	
102931	102926	Poly(A) signal		
104410	103007	CDS	61	Transactivator, transrepressor
104849	104850	Miscellaneous		UL/IRL boundary
104938	104939	Miscellaneous		IRL/IRS boundary
109061	105065	Gene	62	
105071	105065	Poly(A) signal		
109061	105129	CDS	62	Transactivator, tegument protein
109693	109718	Repeat region		Reiteration 4
110017	110278	Origin of replication		Origin of replication
110507	111359	Gene	63	
111352	111357	Poly(A) signal		
110507	111343	CDS	63	Tegument protein
111491	112072	Gene	64	
112067	112072	Poly(A) signal		
111491	112033	CDS	64	
112571	112107	Gene	65	
112112	112107	Poly(A) signal		
112571	112263	CDS	65	Virion protein
112263	112264	Miscellaneous		IRS/US boundary
112968	114172	Gene	66	
114167	114172	Poly(A) signal		
112968	114149	CDS	66	Protein kinase
114427	115523	Gene	67	
115518	115523	Poly(A) signal		
114427	115491	CDS	67	gI
115739	117652	Gene	68	
117647	117652	Poly(A) signal		
115739	117610	CDS	68	gE
117498	117499	Miscellaneous		US/TRS boundary
118266	117690	Gene	69	
117495	117490	Poly(A) signal		
118266	117724	CDS	69	
119250	118400	Gene	70	
118405	118400	Poly(A) signal		
119250	118414	CDS	70	Tegument protein
119479	119742	Origin of replication		Origin of replication
119921	120066	Repeat region		Reiteration R4
120698	124694	Gene	71	
124689	124694	Poly(A) signal		
120698	124630	CDS	71	Transactivator, tegument protein

[a] CDS, coding sequence; dPyKmRNA, deoxypyrimidine kinase mRNA.
[b] ORF was annotated according to the work of Gomi et al. (20)

TABLE 2. Complete Oka-V_{Merck} genome annotation

Start	Stop	Feature[a]	ORF	Function or comment
88	89	Miscellaneous		TRL/UL boundary
914	587	Gene	1	
592	587	Poly(A) signal		
914	588	CDS	1	
1133	1861	Gene	2	
1133	1849	CDS	2	
1856	1861	Poly(A) signal		
2446	1889	Gene	3	
1894	1889	Poly(A) signal		
2446	1907	CDS	3	
4140	2781	Gene	4	
2781	2776	Poly(A) signal		
4140	2782	CDS	4	Transactivator, tegument protein
5273	4251	Gene	5	
5273	4251	CDS	5	gK
8576	5325	Gene	6	
8606	9398	Gene	7	
9393	9398	Poly(A) signal		
8606	9385	CDS	7	
10666	9425	Gene	8	
9430	9425	Poly(A) signal		
10666	9476	CDS	8	Deoxyuridine triphosphatase
10641	10904	CDS	9A[b]	gN
11008	11963	Gene	9	
11958	11963	Poly(A) signal		
11008	11916	CDS	9	Syncytium formation, virion protein
12159	13420	Gene	10	
13415	13420	Poly(A) signal		
12159	13391	CDS	10	Transactivator, tegument protein
13589	16076	Gene	11	
13936	14196	Repeat region		Reiteration R1
16071	16076	Poly(A) signal		
13589	16003	CDS	11	
16168	18153	Gene	12	
18695	19350	Gene	13	
19345	19350	Poly(A) signal		
18395	19300	CDS	13	
21067	19296	Gene	14	
19301	19296	Poly(A) signal		
20526	20851	Repeat region		Reiteration R2
21067	19385	CDS	14	
22432	21198	Gene	15	
21203	21198	Poly(A) signal		
22432	21212	CDS	15	
23748	22522	Gene	16	
24103	25468	Gene	17	
25463	25468	Poly(A) signal		
24103	25467	CDS	17	
26444	25501	Gene	18	
25506	25501	Poly(A) signal		
26444	25524	CDS	18	Ribonucleotide reductase, small subunit
28796	26469	Gene	19	Ribonucleotide reductase, big subunit
30426	28956	Gene	20	
28961	28956	Poly(A) signal		
30426	28975	CDS	20	
30710	33856	Gene	21	
33851	33856	Poly(A) signal		
30710	33826	CDS	21	Nucleocapsid
34034	42341	Gene	22	
41405	41470	Repeat region		Reiteration R3
42336	42341	Poly(A) signal		
34034	42325	CDS	22	
43088	42376	Gene	23	
42381	42376	Poly(A) signal		
43088	42381	CDS	23	
43971	43161	Gene	24	
43166	43161	Poly(A) signal		
43971	43162	CDS	24	
44568	44081	Gene	25	
44086	44081	Poly(A) signal		
44568	44098	CDS	25	
44456	46123	Gene	26	
46077	47193	Gene	27	
47188	47193	Poly(A) signal		
46077	47078	CDS	27	
50586	46981	Gene	28	
46986	46981	Poly(A) signal		
50586	47002	CDS	28	DNA polymerase
50807	54458	Gene	29	
54453	54458	Poly(A) signal		
50807	54406	CDS	29	Single-stranded-DNA binding protein
54585	56897	Gene	30	
56942	59582	Gene	31	
59577	59582	Poly(A) signal		
56942	59548	CDS	31	gB, fusogen
59701	60148	Gene	32	
60143	60148	Poly(A) signal		
59701	60132	CDS	32	Substrate for ORF 47 kinase
62071	60242	Gene	33	
60247	60242	Poly(A) signal		
62071	60254	CDS	33	Protease
63843	62104	Gene	34	
64686	63910	CDS	35	
64297	64303	Promoter		TATA element
64321	64325	5′ end of dPyKmRNA		
64740	65797	Gene	36	
65793	65797	Poly(A) signal		
64741	65765	CDS	36	Thymidine kinase
65814	65818	3′end of dPyKmRNA		
66007	68549	Gene	37	
68744	68549	Poly(A) signal		
66007	68532	CDS	37	gH
70226	68580	Gene	38	
68585	68580	Poly(A) signal		
70226	68601	CDS	38	
70566	71302	Gene	39	
71297	71302	Poly(A) signal		
70566	71288	CDS	39	
71473	75696	Gene	40	
75691	75696	Poly(A) signal		
71473	75663	CDS	40	Major nucleocapsid protein
75780	76745	Gene	41	
76740	76745	Poly(A) signal		
75780	76730	CDS	41	
77971	76788	Gene	42	
76783	76788	Poly(A) signal		ORF 45+ORF 42
77971	76784	CDS	42	
78102	80133	Gene	43	
80128	80133	Poly(A) signal		
78102	80132	CDS	43	
80292	81446	Gene	44	
81441	81446	Poly(A) signal		
80292	81383	CDS	44	
82526	81471	CDS	45	
82651	83250	CDS	46	
83100	84632	CDS	47	Protein kinase, tegument protein
84599	86254	CDS	48	
86158	86426	Gene	49	
86421	86426	Poly(A) signal		
86158	86403	CDS	49	
87804	86463	Gene	50	
86468	86463	Poly(A) signal		
87804	86497	CDS	50	
87803	90310	CDS	51	Origin binding protein
90415	92768	Gene	52	
92763	92768	Poly(A) signal		
90415	92730	CDS	52	
93772	92772	Gene	53	
92777	92772	Poly(A) signal		
93772	92777	CDS	53	
95906	93597	CDS	54	
95918	98563	CDS	55	
98490	99277	Gene	56	
99272	99277	Poly(A) signal		
98490	99221	CDS	56	
99545	99306	Gene	57	
99311	99306	Poly(A) signal		
99545	99330	CDS	57	Cytoplasmic protein
100191	99526	CDS	58	
101138	100221	CDS	59	Uracil-DNA glycosylase
101571	101089	CDS	60	gL_n chaperone for gH
104407	102923	Gene	61	
102928	102923	Poly(A) signal		
104407	103004	CDS	61	Transactivator, transrepressor
104846	104847	Miscellaneous		UL/IRL boundary
104935	104936	Miscellaneous		IRL/IRS boundary
109058	105062	Gene	62	
105068	105062	Poly(A) signal		
109058	105126	CDS	62	Transactivator, tegument protein
109690	109715	Repeat region		Reiteration 4
110014	110277	Origin of replication		Origin of replication
110506	111356	Gene	63	
111351	111356	Poly(A) signal		
110506	111342	CDS	63	Tegument protein
111490	112067	Gene	64	
112062	112067	Poly(A) signal		
111490	112032	CDS	64	
112566	112102	Gene	65	
112107	112102	Poly(A) signal		
112566	112258	CDS	65	Virion protein
112258	112259	Miscellaneous		IRS/US boundary
112963	114167	Gene	66	
114162	114167	Poly(A) signal		
112963	114144	CDS	66	Protein kinase
114422	115518	Gene	67	
115513	115518	Poly(A) signal		
114422	115486	CDS	67	gI
115734	117647	Gene	68	
117642	117647	Poly(A) signal		
115734	117605	CDS	68	gE
117490	117491	Miscellaneous		US/TRS boundary
118260	117682	Gene	69	
117687	117682	Poly(A) signal		
118260	117718	CDS	69	
119244	118394	Gene	70	
118399	118394	Poly(A) signal		
119244	118408	CDS	70	Tegument protein
119473	119736	Origin of replication		Origin of replication
119915	120060	Repeat region		Reiteration R4
120692	124688	Gene	71	
124683	124688	Poly(A) signal		
120692	124624	CDS	71	Transactivator, tegument protein

[a] CDS, coding sequence; dPyKmRNA, deoxypyrimidine kinase mRNA.
[b] ORF was annotated according to the work of Gomi et al. (20).

available in GenBank under the accession numbers DQ008354 and DQ008355, respectively.

RESULTS

Oka-V_{GSK} and Oka-V_{Merck} genome organization. The full-length consensus sequence of Oka-V_{GSK} and Oka-V_{Merck} vaccine strains was essentially determined by bidirectional sequencing of overlapping PCR-amplified fragments. Occasionally, when the amplified region contained SNPs that could not be conclusively resolved, the amplified fragments were subcloned and a consensus sequence was derived from multiple plasmid clones. The obtained sequences were assembled and the complete genomes of the vaccines were annotated using the VZV sequence of the Dumas strain published by Davison and Scott as a template (12). The full annotations for Oka-V_{GSK} and Oka-V_{Merck} are presented in Tables 1 and 2, respectively.

The complete genomes of Oka-V_{GSK} and Oka-V_{Merck} strains are comprised of 124,821 and 124,815 bp, respectively. Like the wild-type Dumas strain and the parental Japanese Oka-V strain, the Oka-V_{GSK} and Oka-V_{Merck} genomes consist of a unique long region flanked by terminal repeat long and internal repeat long inverted repeat regions, as well as a unique short region flanked by internal repeat short (IRS) and terminal repeat short (TRS) inverted repeat regions. An origin of replication was found in both the IRS and TRS regions. Four unique reiteration regions (R1 to R4) were found along the genome, with R4 duplicated in the IRS and TRS regions.

All the open reading frames (ORFs) described for the Dumas VZV strain (12) and the Oka vaccine parental strain (22) were found in the two Oka-derived vaccine strains (Tables 1 and 2). The 72 ORFs predicted to encode proteins were evenly distributed on both DNA strands. Three genes were located within the repeat sequences and were therefore duplicated within the VZV genome, so that ORFs 69 to 71 in the IRS region correspond to ORFs 62 to 64 in the TRS region.

Comparison of Oka strain genomes to the Dumas strain genome. The obtained sequences of Oka-V_{GSK} and Oka-V_{Merck} were aligned with the full-length VZV genomes of Oka-P, Oka-V, and Dumas strains. All sequence differences between the four Oka strains and the Dumas strain are given in Table 3. A total of 326 nucleotide positions displaying differences relative to the genome of Dumas strain (X04370 [12]) were identified. Among these, 228 were common to the four Oka strains, and the remaining 98 were specific to one, two, or three of the Oka strains. Several deletions or insertions were found, but most mutations were substitutions of one nucleotide, i.e., SNPs. Frequently, the original nucleotide was nonetheless preserved, resulting in a mixture of two nucleotides present at the same position (Table 3). Because, to our knowledge, the vaccine strains were never cloned, this is consistent with the existence of multiple viral species that evolved during the attenuation process. Multiple SNPs were found to still contain the original Oka-P-specific nucleotide. This supports the cooperative effect of the overall pattern of nucleotide substitutions in the expression of the attenuation phenotype and, to a lesser extent, the contribution of individual SNPs.

The 98 differences between the Oka-V_{GSK} (124,821 bp), Oka-V_{Merck} (124,815 bp), Oka-P (125,125 bp), and Oka-V (125,078 bp) genomes were found in 25 ORFs (ORFs 1, 2, 6, 9A, 10, 11, 14, 18, 21, 22, 31, 35, 39, 45, 47, 48, 50, 51, 52, 54, 55, 62, 64, and 71), the R1 and R3 repeat regions (in ORFs 11 and 22, respectively), and one origin of replication (Table 3).

The total number of differences between the four Oka strains was determined (Table 4). Of the 98 differences identified, 69 were found between Oka-P and Oka-V, 51 between Oka-V and Oka-V_{GSK}, and 68 between Oka-V and Oka-V_{Merck}. Consequently, Oka-V_{Merck} contains 17 more differences that discriminate it from Oka-V compared with Oka-V_{GSK}.

Although the highest convergence was found for Oka-V_{GSK} and Oka-V_{Merck}, they still had 36 nucleotide differences (Table 4). For 12 of these positions, Oka-V_{Merck} had nucleotides matching the Oka-P strain, whereas the Oka-V_{GSK} strain had only a single position (119683) where the sequence was Oka-P-like. Overall, for the positions in which Oka-V_{GSK} differed from Oka-V_{Merck}, the Oka-V_{GSK} sequence was closer to Oka-V, whereas the Oka-V_{Merck} sequence was closer to Oka-P.

Sixty-nine nucleotide changes between the Oka-V and the Oka-P strains were identified (Table 5). Among these 69 differences, 56 positions in Oka-P were identical to the reference Dumas strain, whereas only 11 positions in Oka-V were identical to the Dumas strain. Identical nucleotides for many of these positions were also present in Oka-V_{GSK} and Oka-V_{Merck}.

To better characterize the observed differences, the substitution spectra were analyzed (Fig. 2). The large majority of mutations were SNPs and only partial, with two different nucleotides at the same position. Compared to Oka-P, transitions (i.e., mutations resulting in substitution of a purine for a purine [A↔ G] or a pyrimidine for a pyrimidine [C↔ T]) were more frequently (64% to 69%) observed for the Oka-V_{GSK} and Oka-V_{Merck} strains than transversions (i.e., mutations resulting in substitution of a purine for a pyrimidine and vice versa; 13% to 17%). Transversions were more common than insertions or deletions (≤10%). The majority of the identified mutations were silent mutations, either because they were located in intergenic regions or because of the degenerated genetic code. A significant proportion of mutations in intragenic regions (~45%) caused single amino acid substitutions in both the Oka-V_{GSK} and Oka-V_{Merck} strains (Fig. 2). No stop or frameshift mutations were identified. All deletions and insertions either were located in intergenic regions or, when located within coding regions, were multiples of three bases.

Comparison of Oka-V_{GSK} and Oka-V_{Merck} genomes. Sequence differences observed between the Oka-V_{GSK} and Oka-V_{Merck} strains are described in Table 6. Only 36 differences were found throughout the complete genomes (i.e., ~125 kb), three of which were repeated in ORF 62 and its duplicate, ORF 71. These 33 nucleotide unique position changes resulted in 14 amino acid changes, 1 each in ORFs 6, 9A, 10, 31, 39, and 52 and 2 each in ORFs 14, 55, and 62/71 and the R3 repeat region.

Among these 36 position differences between Oka-V_{GSK} and Oka-V_{Merck}, Oka-V_{GSK} had 23 nucleotide sequences identical to Oka-V but only 3 identical to Oka-P. In contrast, Oka-V_{Merck} had 18 positions identical to Oka-P but only 6 identical to Oka-V (Table 6 and Fig. 3).

TABLE 3. Comparison of complete genomic sequences of Dumas and Oka strains of VZV[a]

Feature relative to WT (Dumas)	Position (WT)	Feature in:				Position in:	
		Oka-P	Oka-V	Oka-V_{GSK}	Oka-V_{Merck}	Oka-V_{GSK}	Oka-V_{Merck}
A→G	1	X	X	X	X	1	1
G→C	3	X	X	X	X	3	3
Deletion of C (from WT)	109	X	X	X	X	109	109
G→C	178	-	-	X	X	177	177
A→G	236	X	X	X	X	235	235
C→T	262	X	X	X	X	261	261
T→C	560	-	X	X	X	559	559
G→A (ORF 1), N, silent	685	X	X	X	X	684	684
T→T/C (ORF 1), Q, silent	703	-	X	C	C	702	702
T→T/C (ORF 1), P, silent	763	-	X	C	C	762	762
T→C (ORF 1), T→A	789	X	X	X	X	788	788
T→C (ORF 1), Q→R	790	X	X	X	X	789	789
T→C (ORF 1), Q→R	791	X	X	X	X	790	790
C→G (ORF 2), G, silent	1838	-	X	-	-	1837	1837
T→T/C	2515	-	X	C	-	2514	2514
A→G (ORF 4), T, silent	3764	X	X	X	X	3763	3763
C→T (ORF 5), K, silent	4258	X	X	X	X	4257	4257
A→G (ORF 6), S→P	5745	-	X	X	A/G	5744	5744
G→T (ORF 6), H→Q	6853	X	X	X	X	6852	6852
C→A (ORF 6), G→V	7091	X	X	X	X	7090	7090
C→T (ORF 6), P, silent	7753	X	X	X	X	7752	7752
T→C	9460	X	X	X	X	9459	9459
G→A (ORF 8), P→S	10079	X	X	X	X	10078	10078
T→C/T (ORF 9A), W→R	10900	-	X	X	-	10899	10899
T→G (ORF 9), S, silent	11890	X	X	X	X	11889	11889
A→G (ORF 9), T→A	11906	X	X	X	X	11905	11905
C→A (ORF 10), P→H	12188	X	X	X	X	12187	12187
T→C (ORF 10), F→S	12284	X	X	X	X	12283	12283
T→C (ORF 10), F→S	12285	X	X	X	X	12284	12284
C→C/T (ORF 10), A→V	12779	-	X	X	-	12778	12778
T→G (ORF 10), G, silent	13173	X	X	X	X	13172	13172
G→A	13407	X	X	X	X	13406	13406
Deletion (ORF 11, R1), ATTGACGACGAGG GAGAGGCGGAGGA GGGAGAGGCGGA GGAGGGAGAGGC GGAGGAGGGA GAG, IDDEGEAEEG EAEEGEAEEGE	14088	X	X	X	X	14086	14086
Deletion (ORF 11, R1), GCGGAGGAGGAC GCG, AEEDA	14199–213	X	X	X	X	14134–48	14134–48
Insertion (ORF 11, R1), CGCGATCGACGAC GAGGGAGAGGCG GAGGAGGA	14242	X	-	X	X	14164–96	14164–96
T→C	14390	X	X	X	X	14344	14344
C→T (ORF 12), V, silent	17404	X	X	X	X	17358	17358
C→T (ORF 12), L, silent	17834	X	X	X	X	17788	17788
C→T (ORF 12), T, silent	18082	X	X	X	X	18036	18036
G→A (ORF 13), K, silent	18467	X	X	X	X	18421	18421
T→T/C (ORF 14), stop	19431	-	X	-	-	19385	19385
A→G (ORF 14), I, silent	19719	X	X	X	X	19673	19673
T→A (ORF 14), Y→F	20656	X	X	X	X	20610	20610
T→C (ORF 14), T→A	20684	X	X	X	X	20638	20638
C→C/T (ORF 14), K, silent	20703	-	-	X	-	20657	20657
A→T (ORF 14), E→V	20711	X	X	-	-	20665	20665
C→A (ORF 14), C→A	20745	X	X	-	-	20699	20699
T→A (ORF 14), T→S	20753	X	X	X	X	20707	20707

Continued on following page

TABLE 3—*Continued*

Feature relative to WT (Dumas)	Position (WT)	Feature in:				Position in:	
		Oka-P	Oka-V	Oka-V_{GSK}	Oka-V_{Merck}	Oka-V_{GSK}	Oka-V_{Merck}
C→A (ORF 14), K→N	20787	X	X	C/A	-	20741	20741
C→A (ORF 14), K→N	20829	X	X	C/A	C/A	20783	20783
T→A/T (ORF 14), T→S	20837	-	-	X	X	20791	20791
C→A (ORF 14), K→N	20871	-	-	C/A	C/A	20825	20825
A→T (ORF 14), S→T	20879	-	-	A/T		20833	20833
C→A (ORF 14), K→N	20913	-	-	A/C	A/C	20867	20867
T→A (ORF 14), T→S	21005	X	X	X	X	20959	20959
G→A (ORF 15), L, silent	21371	X	X	X	X	21325	21325
G→T (ORF 15), R, silent	21734	X	X	X	X	21688	21688
G→A (ORF 15), S, silent	22311	X	X	X	X	22265	22265
A→G	22504	X	X	X	X	22458	22458
A→G (ORF 16), M→T	22794	X	X	X	X	22748	22748
A→G (ORF 16), F, silent	23294	X	X	X	X	23248	23248
Deletion (ORF 17), dCAT (delS)	24516	X	X	X	X	24469	24469
A→G (ORF 17), T→A	24578	X	X	X	X	24529	24529
C→T (ORF 17), T→M	24654	X	X	X	X	24605	24605
G→A (ORF 17), V→I	25067	X	X	X	X	25018	25018
A→G (ORF 18), N, silent	26125	-	X	X	A/G	26076	26076
A→G (ORF 19), H, silent	27523	X	X	X	X	27474	27474
T→G (ORF 20), G, silent	29201	X	X	X	X	29152	29152
C→T/C (ORF 21), T→I	31732	-	X	-	-	31683	31683
A→G (ORF 21), T→A	32274	X	X	X	X	32225	32225
T→C (ORF 21), H, silent	33722	X	X	X	X	33673	33673
T→C (ORF 21), D, silent	33725	X	X	X	X	33676	33676
T→C (ORF 21), N, silent	33728	X	X	X	X	33679	33679
T→C (ORF 22), V, silent	35543	X	X	X	X	35494	35494
A→G (ORF 22), L, silent	37649	X	X	X	X	37600	37600
A→G (ORF 22), I→V	37902	X	X	X	X	37853	37853
T→C (ORF 22), T, silent	38036	-	-	C/T	C/T	37987	37987
T→C (ORF 22), Y→H	38055	X	X	X	X	38006	38006
A→C (ORF 22), P, silent	38081	X	X	X	X	38032	38032
G→A (ORF 22), E, silent	38177	X	X	X	X	38128	38128
G→T (ORF 22), T, silent	38714	X	X	X	X	38665	38665
C→T (ORF 22), A, silent	38717	X	X	X	X	38668	38668
A→G (ORF 22), R, silent	39023	X	X	X	X	38974	38974
T→T/G (ORF 22), P, silent	39227	-	X	X	-	39178	39178
G→A (ORF 22), Q, silent	39263	X	X	X	X	39214	39214
G→A (ORF 22), R→H	39394	X	X	X	X	39345	39345
A→G (ORF 22), V, silent	39530	X	X	X	X	39481	39481
A→G (ORF 22), Q, silent	40388	X	X	X	X	40339	40339
T→C (ORF 22), P, silent	41057	X	X	X	X	41008	41008
G→A	41452	X	X	X	X	41403	41403
C→T (R3 repeat), A→V	41458	X	X	X	X	41409	41409
G→C (R3 repeat), A→V	41459	X	X	X	X	41410	41410
C→T (R3 repeat), A→V	41476	X	-	X	X	41427	41427
Deletion, GCGCAGCCC	41475–83	-	X	-	-	41426–34	41426–34
G→C (R3 repeat), A→V	41476	X	-	X	X	41427	41427
Deletion, GCGCAGCCC GCGCAGACCGTCC AGCCCGCGCAG CCC, AQPAQTVQ PAQP	41484–519	X	X	-	-	41435–70	41435–70

Continued on following page

TABLE 3—*Continued*

Feature relative to WT (Dumas)	Position (WT)	Feature in:				Position in:	
		Oka-P	Oka-V	Oka-V_{GSK}	Oka-V_{Merck}	Oka-V_{GSK}	Oka-V_{Merck}
C→T (R3 repeat), A→V	41485	-	-	X	-	41436	41436
C→C/T (R3 repeat), A→V	41494	-	-	X	-	41445	41445
A→C (R3 repeat), T→P	41499	-	-	X	X	41450	41450
C→T (ORF 22), T, silent	41618	X	X	X	X	41569	41569
G→A (ORF 22), S→N	41764	X	X	X	X	41715	41715
C→G (ORF 22), Q→E	42069	X	X	X	X	42020	42020
C→T (ORF 22), R, silent	42176	X	X	X	X	42127	42127
A→C (ORF 22), A, silent	42242	X	X	X	X	42193	42193
	42403	Del AAA	Del AA	Ins A	Del A	42355	42353
T→G (ORF 23), S, silent	42476	X	X	X	X	42428	42426
T→C (ORF 24), I→V	43262	X	X	X	X	43214	43212
C→T (ORF 26), C, silent	44835	X	X	X	X	44787	44785
A→G (ORF 28), C→R	47162	X	X	X	X	47114	47112
C→T (ORF 28), L, silent	47940	X	X	X	X	47892	47890
T→C (ORF 28), S→G	48050	X	X	X	X	48002	48000
G→A (ORF 28), T, silent	48825	X	X	X	X	48777	48775
G→A (ORF 28), L, silent	49535	X	X	X	X	49487	49485
C→A (ORF 28), G→C	50081	X	X	X	X	50033	50031
C→T (ORF 29), S, silent	51168	X	X	X	X	51120	51118
A→G (ORF 29), Q, silent	52917	X	X	X	X	52869	52867
A→C (ORF 29), I→L	53482	X	X	X	X	53434	53432
G→A (ORF 29), A→T	53938	X	X	X	X	53890	53888
Deletion (ORF 29), ACA TTTCAGGGTCAA, NISGS	54359–73	X	X	X	X	54310	54308
Deletion, T	54562	X	X	X	X	54498	54496
T→C	54564	X	X	X	X	54500	54498
A→G (ORF 30), P, silent	55820	X	X	X	X	55756	55754
A→C (ORF 31), T→P	57224	X	X	X	X	57160	57158
A→C (ORF 31), A, silent	57301	X	X	X	X	57237	57235
G→T (ORF 31), A, silent	57397	X	X	X	X	57333	57331
A→G (ORF 31), I→V	58595	-	A/G	A/G	X	58531	58529
A→A/G (ORF 31), P, silent	59287	-	X	X	X	59223	59221
Insertion, G	59760	X	X	X	X	59697	59695
Deletion	60278	Del5A	Del5A	Del A	Del AA	60214	60211
A→C	60279	X	X	X	X	60215	60212
C→A (ORF 33), A, silent	60405	X	X	X	X	60341	60338
T→G (ORF 33), Y→S	60781	X	X	X	X	60717	60714
G→A (ORF 33), P→L	61018	X	X	X	X	60954	60951
G→A (ORF 33), P→L	61019	X	X	X	X	60955	60952
T→C (ORF 33), N→G	61201	X	X	X	X	61137	61134
T→C (ORF 33), N→G	61202	X	X	X	X	61138	61135
A→G (ORF 35), A, silent	64067	-	X	X	A/G	64003	64000
A→G (ORF 35), C, silent	64136	X	X	X	X	64072	64069
T→C (ORF 35), P, silent	64259	X	X	X	X	64195	64192
T→C (ORF 35), M→V	64375	X	X	X	X	64311	64308
C→T (ORF 36), A, silent	64989	X	X	X	X	64925	64922
C→T (ORF 36), S→L	65669	X	X	X	X	65605	65602
G→T (ORF 37), L, silent	66646	X	X	X	X	66582	66579
C→T (ORF 37), P→L	66879	X	X	X	X	66815	66812
G→A (ORF 37), R→K	68172	X	X	X	X	68108	68105
A→G (ORF 38), T, silent	69349	X	X	X	X	69285	69282
T→C (ORF 38), S→G	69756	X	X	X	X	69692	69689

Continued on following page

TABLE 3—*Continued*

Feature relative to WT (Dumas)	Position (WT)	Feature in:				Position in:	
		Oka-P	Oka-V	Oka-V_{GSK}	Oka-V_{Merck}	Oka-V_{GSK}	Oka-V_{Merck}
T→C (ORF 39), M→T	71252	-	X	X	C/T	71188	71185
C→T (ORF 40), V, silent	72997	X	X	X	X	72933	72930
T→C (ORF 40), T, silent	73993	X	X	X	X	73929	73926
C→T (ORF 41), V, silent	76530	X	X	X	X	76466	76463
Deletion, T	78144	X	X	X	X	78079	78076
G→T	80244	X	X	X	X	80179	80176
A→G (ORF 44), N→D	80840	X	X	X	X	80775	80772
C→T (ORF 44), A, silent	81187	X	X	X	X	81122	81119
A→A/G (ORF 45), P, silent	82225	-	X	-	-	82160	82157
G→A/G (ORF 47), E, silent	84091	-	X	-	-	84026	84023
A→G (ORF 47), T, silent	84616	X	X	X	X	84551	84548
G→A (ORF 48), R→H	84983	X	X	X	X	84918	84915
C→T (ORF 48), D, silent	85563	X	X	X	X	85498	85495
A→A/G (ORF 48), T→A	85594	-	-	X	X	85529	85526
C→A (ORF 48), Q→K	86170	X	X	X	X	86105	86102
Deletion, CCTGAT AAAC	86484–93	X	X	X	X	86418	86415
T→G	86556	X	X	X	X	86481	86478
A→A/G (ORF 50), C, silent	87280	-	X	-	-	87205	87202
T→C/T (ORF 50), S→G	87306	-	X	-	-	87231	87228
C→T (ORF 50), S, silent	87841	X	X	X	X	87766	87763
G→T (ORF 51), S, silent	88477	X	X	X	X	88402	88399
A→G (ORF 51), T, silent	89734	-	X	X	-	89659	89656
T→C (ORF 51), T, silent	89905	X	X	X	X	89830	89827
G→T (ORF 51), Q→H	90202	X	X	X	X	90127	90124
T→C (ORF 51), S, silent	90217	X	X	X	X	90142	90139
G→A	90392	X	X	X	X	90317	90314
A→A/G (ORF 52), I→V	90535	-	X	X	-	90460	90457
C→T (ORF 52), G, silent	91191	X	X	X	X	91116	91113
A→G (ORF 52), T→A	92026	X	X	X	X	91951	91948
A→G (ORF 52), T→A	92092	X	X	X	X	92017	92014
A→G (ORF 52), H→R	92375	X	X	X	X	92300	92297
T→C (ORF 53), V, silent	92999	X	X	X	X	92924	92921
T→C (ORF 54), L, silent	94167	-	X	X	T/C	94092	94089
A→G (ORF 54), V, silent	94632	X	X	X	X	94557	94554
A→T (ORF 54), T, silent	94641	X	X	X	X	94566	94563
T→C (ORF 54), G, silent	95241	X	X	X	X	95166	95163
G→A (ORF 54), L, silent	95546	X	X	X	X	95471	95468
T→G (ORF 54), E→D	95601	X	X	X	X	95526	95523
T→C (ORF 55), L, silent	97141	X	X	X	X	97066	97063
T→T/C (ORF 55), V→A	97479	-	-	-	X	97404	97401
C→T (ORF 55), I, silent	97591	X	X	X	X	97516	97513
G→A/G (ORF 55), A→T	97748	-	X	X	X	97673	97670
T→C/T (ORF 55), C→R	97796	-	X	X	-	97721	97718
T→C (ORF 55), G, silent	98437	X	X	X	X	98362	98359
T→C (ORF 56), V, silent	98765	X	X	X	X	98690	98687
A→C (ORF 56), T, silent	98807	X	X	X	X	98732	98729
Deletion (ORF 56), TTC, S	99227–29	X	X	X	X	99148	99145
T→G (ORF 57), H→P	99421	X	X	X	X	99343	99340
A→G (ORF 58), Y, silent	99709	X	X	X	X	99631	99628
C→T (ORF 58), V→I	99981	X	X	X	X	99903	99900
T→A (ORF 58), K→N	100114	X	X	X	X	100036	100033
T→G (ORF 58), N→T	100151	X	X	X	X	100073	100070
A→G	100283	X	X	X	X	100205	100202
A→A/G (ORF 59), L→P	101089	X	X	X	X	101011	101008
C→T (ORF 60), A→T	101331	X	X	X	X	101253	101250

Continued on following page

TABLE 3—*Continued*

Feature relative to WT (Dumas)	Position (WT)	Feature in:				Position in:	
		Oka-P	Oka-V	Oka-V_{GSK}	Oka-V_{Merck}	Oka-V_{GSK}	Oka-V_{Merck}
Insertion (ORF 60), ATC	101623	X	X	X	X	101543–101545	101540–101542
T→C	101886	X	X	X	X	101811	101808
C→T	101991	X	X	X	X	101916	101913
G→A	102192	X	X	X	X	102117	102114
A→G	102203	X	X	X	X	102128	102125
Insertion, TCAAGCTTT AAAAACGTACCCCA AACTTAAAACGCTC AAATTGCCTTTTGG AGGCCTGCCCAACG GCCATTATCCCTTG GATCTAAGATTGAT TTGCGGTAACGTTT GCCAA	102219	X	X	-	-	102144	102141
C→A	102309	X	X	X	X	102234	102231
A→C	102351	X	X	X	X	102276	102273
A→G	102458	X	X	X	X	102383	102380
T→G	102601	X	X	X	X	102526	102523
T→C	103043	X	X	X	X	102968	102965
A→G	104898	X	X	X	X	104823	104820
C→G	105010	X	X	X	X	104935	104932
T→C	105012	X	X	X	X	104937	104934
T→C	105015	X	X	X	X	104940	104937
T→C	105017	X	X	X	X	104942	104939
Insertion, C	105020	X	-	X	X	104946	104943
Deletion, G	105054	X	X	X	X	104979	104976
Deletion, G	105071	X	X	X	X	104995	104992
Insertion, ACAA	105145	X	X	X	X	105075	105072
A→A/G	105169	-	X	X	X	105097	105094
A→A/G (ORF 62), L→S	105310	-	X	X	X	105238	105235
A→G (ORF 62), G, silent	105312	X	X	X	X	105240	105237
T→C (ORF 62), I→V	105356	-	X	X	T/C	105284	105281
A→G (ORF 62), L→P	105451	X	X	X	X	105379	105376
A→C (ORF 62), S→A	105512	X	X	X	X	105440	105437
A→G (ORF 62), V→A	105544	-	X	X	X	105472	105469
T→C (ORF 62), A, silent	105705	-	X	X	X	105633	105630
T→C (ORF 62), R→G	106262	-	X	X	X	106190	106187
T→C (ORF 62), A, silent	107136	-	X	X	T/C	107064	107061
C→T (ORF 62), A→T	107165	X	X	X	X	107093	107090
T→C (ORF 62), S→G	107252	-	X	X	X	107180	107177
T→C (ORF 62), R, silent	107307	X	X	X	X	107235	107232
A→A/G (ORF 62), V→A	107599	-	X	X	-	107527	107524
C→A (ORF 62), T, silent	107607	X	X	X	X	107535	107532
T→C (ORF 62), A, silent	107715	X	X	X	X	107643	107640
T→C (ORF 62), P, silent	108111	-	X	X	X	108039	108036
A→G (ORF 62), L, silent	108747	X	X	X	X	108675	108672
A→A/G (ORF 62), M→T	108838	-	X	X	X	108766	108763
G→A (ORF 62), H, silent	108951	X	X	X	X	108879	108876
C→G (ORF 62), A, silent	109044	X	X	X	X	108972	108969
A→A/G	109137	-	X	X	X	109065	109062
A→A/G	109200	-	X	X	-	109128	109125
T→C/T	109546	-	-	X	-	109474	109471
G→T	109654	X	X	X	X	109582	109579
Insertion, CAT	109696	X	X	X	X	109625–109627	109622–109624
Insertion, GGGAGGGG GCGCGGTACCCCGC CGATGGGGAGGGG GCGCGGTACCCCGC CGATGGGGAGGGG GCGCGGTACCCCGC CGATGGGGAGGGG GCGCGGTACCCCGC CGATG	109907	X	X	-	-	109838	109835
Insertion, GGGAGGGG GCGCGGTACCCCGC CGATG	109907	X	-	-	-	109838	109835

Continued on following page

46

TABLE 3—*Continued*

Feature relative to WT (Dumas)	Position (WT)	Feature in:				Position in:	
		Oka-P	Oka-V	Oka-V_{GSK}	Oka-V_{Merck}	Oka-V_{GSK}	Oka-V_{Merck}
G→A	110003	X	X	X	X	109934	109931
Deletion, G	110058	X	X	X	X	109988	109985
G→A (Ori), -, silent	110112	X	X	X	X	109934	109931
Deletion, AT	110212	-	X	X	-	110142	110140–110141
T→G	110214	-	-	-	X		110141
Insertion, ATATAG	110214	X	-	-	-	110142	110141
T→G (Ori)	110216	X	X	X	X	110144	110143
T→G (Ori)	110218	X	X	X	X	110146	110145
T→G (Ori)	110220	X	X	X	X	110148	110147
T→G (Ori)	110222	X	X	X	X	110150	110149
T→G (Ori)	110224	X	X	X	X	110152	110151
T→G (Ori)	110226	X	X	X	X	110154	110153
A→G (Ori)	110232	X	X	X	X	110160	110159
A→G (Ori)	110235	X	X	X	X	110163	110162
Deletion, GC	110378–110379	X	X	X	X	110305	110304
A→G (ORF 63), T, silent	111312	X	X	X	X	110238	110237
A→G (ORF 64), Q→R	111650	-	X	A/G	A/G	111576	111575
T→C (ORF 64), Y→H	112093	X	X	X	X	112019	112018
Deletion/insertion	112128	Del A	Del A	Ins 5a	Ins A	112064–112068	112063
G→A	112198	X	X	X	X	112129	112124
A→G (ORF 66), S, silent	114140	X	X	X	X	114071	114066
G→A (ORF 67), P, silent	115041	X	X	X	X	114072	114967
C→T (ORF 68), T→I	115926	X	X	X	X	115857	115852
C→T	117699	X	X	X	X	117630	117625
Deletion/insertion	117769	Del T	Del T	Ins 5T	Ins T	117701–117705	117696
A→G (ORF 69), Y→H	117804	X	X	X	X	117740	117731
T→C (ORF 69), Q→R	118247	-	X	T/C	T/C	118183	118174
T→C (ORF 70), T, silent	118585	X	X	X	X	118521	118512
Deletion, GC	119518–119519	X	X	X	X	119453	119444
Insertion, CTCTCT	119654	X	X	-	-	119588	119579
T→C (Ori)	119656	X	X	-	-	119590	119581
T→C (Ori)	119665	X	X	X	X	119599	119590
A→C (Ori)	119671	X	X	X	X	119605	119596
A→C (Ori)	119673	X	X	X	X	119607	119598
A→C (Ori)	119675	X	X	X	X	119609	119600
A→C (Ori)	119677	X	-	X	X	119611	119602
Deletion, ATATATAT	119677–119684	-	X	-		119611–119618	119602–119609
A→C (Ori)	119679	X	-	X	X	119613	119604
A→C (Ori)	119681	X	-	X	X	119615	119606
A→C (Ori)	119683	X	-	X	A/C	119617	119608
C→T (Ori)	119785	X	X	X	X	119719	119710
Deletion, C	119847	X	X	X	X	119780	119771
C→T,	119894	X	X	X	X	119827	119818
Insertion, TACCGCGCC CCCTCCCCATCGGC GGGGTACCGCGCCC CCTCCCCATCGGCG GGGTACCGCGCCCC CTCCCCATCGGCGG GGTACCGCGCCCCC TCCCCATCGGCGGG GTACCGCGCCCCCT CCCCATCGGCGGGG	120135	X	X	-	-	120068	120059
Insertion, TACCGCGCC CCCTCCCCATCGGC GGGG	120135	X	-	-		120068	120060
Insertion, GAT	120202	X	X	X	X	120136–120138	120127–120129
C→A	120243	X	X	X	X	120179	120170
A→A/G	120351	-	-	X	-	120287	120278
T→T/C	120697	-	X	X	-	120633	120624
T→T/C	120760	-	X	X	X	120696	120687
G→C (ORF 71), A, silent	120853	X	X	X	X	120789	120780
C→T (ORF 71), H, silent	120946	X	X	X	X	120882	120873
T→C/T (ORF 71), M→T	121059	-	X	X	X	120995	120986
T→C (ORF 71), L, silent	121150	X	X	X	X	121086	121077
A→G (ORF 71), P, silent	121786	-	X	X	X	121722	121713

Continued on following page

TABLE 3—*Continued*

Feature relative to WT (Dumas)	Position (WT)	Feature in:				Position in:	
		Oka-P	Oka-V	Oka-V_{GSK}	Oka-V_{Merck}	Oka-V_{GSK}	Oka-V_{Merck}
A→G (ORF 71), A, silent	122182	X	X	X	X	122118	122109
G→T (ORF 71), T, silent	122290	X	X	X	X	122226	122217
T→C/T (ORF 71), V→A	122298	-	X	X	-	122234	122225
A→G (ORF 71), R, silent	122590	X	X	X	X	122526	122517
A→G (ORF 71), S→G	122645	-	X	X	X	122581	122572
G→A (ORF 71), A→T	122732	X	X	X	X	122668	122659
A→G (ORF 71), A, silent	122761	-	X	X	A/G	122697	122688
A→G (ORF 71), R→G	123635	-	X	X	X	123571	123563
A→G (ORF 71), A, silent	124192	-	X	X	X	124128	124119
T→C (ORF 71), V→A	124353	-	X	X	X	124289	124280
T→G (ORF 71), S→A	124385	X	X	X	X	124321	124312
T→C (ORF 71), L→P	124446	X	X	X	X	124382	124373
A→G (ORF 71), I→V	124541	-	X	X	A/G	124477	124468
T→C (ORF 71), G, silent	124585	X	X	X	X	124521	124512
T→C (ORF 71), L→S	124587	-	T/C	T/C	T/C	124523	124514
T→T/C	124728	-	X	X	X	124664	124655
Insertion, TGTT	124750	X	X	X	X	124687–124690	124678–124681
Deletion, C	124834	X	X	X	X	124773	124764
Deletion, C	124851	X	X	X	X	124789	124780
A→G	124880	NA	NA	X	X	124818	124809
A→G	124882	NA	NA	X	X	124820	124811

[a] A partial analysis of 20 of these nucleotide differences was published previously (70). Nucleotide positions within ORFs are indicated, as well as the encoded amino acids. Ori, origin of replication; WT, wild type. X, difference relative to Dumas strain; -, identical nucleotide relative to Dumas strain; NA, not applicable; Del, deletion; Ins, insertion. Where applicable, the resulting codon switch is specified.

DISCUSSION

In this study, we compared the complete genomes of the varicella vaccine strains Oka-V_{GSK} and Oka-V_{Merck}, both derived from the original attenuated Oka-V strain (67). Phylogenetic analyses of these sequences along with 16 other complete VZV genomes were recently reported (50, 69), providing new insight into strain variability (69) and evidence of recombination between major circulating VZV clades (50).

Although VZV is a monotypic virus with a very low rate of interstrain sequence variations (0.061%) compared to other members of the *Herpesviridae* family of viruses (between 0.32% and 3.0% [47]), the sequence analysis of the Oka vaccine strains is not straightforward due to the presence of heterogeneous genomes with distinct sequences (21). Therefore, consensus sequencing provides only an indication of the most prevalent bases for each position. In the present study, we determined the full-length sequences of both Oka-V_{GSK} and Oka-V_{Merck} largely by bidirectional sequencing of overlapping PCR fragments, but when direct sequencing did not generate results of sufficient quality, fragments were subcloned and the consensus sequence was derived from numerous plasmid clones. All sequences obtained were confirmed on both DNA strands. This approach gave a high-quality assessment of the whole genomes of Oka-V_{GSK} and Oka-V_{Merck}, and this is, to our knowledge, the first published comparative analysis of the complete genomes of these two strains.

TABLE 4. Numbers of genomic sequence differences between the four Oka strains

Strain	No. of differences from:		
	Oka-V	Oka-V_{GSK}	Oka-V_{Merck}
Oka-P	69 (Table 5)	79	64
Oka-V		51	68
Oka-V_{GSK}			36 (Table 6)

Comparison with partial sequencing information published on these strains and the other Oka strains, Oka-P and Oka-V, is shown in Table 7 (3, 22, 32, 59, 60, 63, 69). Argaw et al. sequenced approximately 34 kb from the 3′ ends of Oka-V, Oka-P, and Oka-V_{Merck} strains, and Schmidt et al. sequenced approximately 26 kb of the Oka-V_{GSK} strain (3, 60). Two sequence differences were found for Oka-V_{Merck} in ORF 59 (position 101089; A versus A/G) and ORF 62 (position 105310; G versus A/G) (3). Six differences were observed between the present results and those previously published for Oka-V_{GSK}, and 13 differences were observed for Oka-V_{Merck} (60). Finally, comparison between the present study and a previous one (32) revealed quantitative (number of sequence differences between Oka-V_{GSK} and Oka-V_{Merck} strains) and qualitative (ORFs involved) discrepancies.

Our analysis of Oka-V_{GSK} and Oka-V_{Merck} sequences revealed that they have very few nucleotide differences. When we compared their complete genomic sequences (i.e., ~125 kb), we found that only 36 positions were different between Oka-V_{GSK} and Oka-V_{Merck}. These differences lead to 14 unique amino acid substitutions, which suggests that although these two vaccine strains are not identical, they are very similar. The differences resulting in amino acid substitutions were found in 10 different ORFs and in the R3 repeat region, while silent

TABLE 5. Comparison of complete genomic sequences of Oka-P and Oka-V strains of VZV[a]

Feature relative to WT (Dumas)	Position (WT)	Feature in:				Position in:	
		Oka-P	Oka-V	Oka-V_{GSK}	Oka-V_{Merck}	Oka-V_{GSK}	Oka-V_{Merck}
T→C	560	-	X	X	X	559	559
T→T/C (ORF 1), Q, silent	703	-	X	C	C	702	702
T→T/C (ORF 1), P, silent	763	-	X	C	C	762	762
C→G (ORF 2), G, silent	1838	-	X	-	-	1837	1837
T→T/C	2515	-	X	C	-	2514	2514
A→G (ORF 6), S→P	5745	-	X	X	A/G	5744	5744
T→C/T (ORF 9A), W→R	10900	-	X	X	-	10899	10899
C→C/T (ORF 10), A→V	12779	-	X	X	-	12778	12778
Insertion (ORF 11, R1), CGCGATCGA CGACGAGGGAGAGGCGGAGG AGGA	14242	X		X	X	14164–14196	14164–14196
T→T/C (ORF 14), stop	19431	-	X	-	-	19385	19385
A→G (ORF 18), N, silent	26125	-	X	X	A/G	26076	26076
C→T/C (ORF 21), T→I	31732	-	X	-	-	31683	31683
T→T/G (ORF 22), P, silent	39227	-	X	X	-	39178	39178
C→T (R3 repeat), A→V	41476	X		X	X	41427	41427
Deletion, GCGCAGCCC	41475–83	-	X	-	-	41426–41434	41426–41434
G→C (R3 repeat), A→V	41476	X		X	X	41427	41427
Deletion/insertion	42403	Del AAA	Del AA	Ins A	Del A	42355	42353
A→G (ORF 31), I→V	58595	-	A/G	A/G	X	58531	58529
A→A/G (ORF 31), P, silent	59287	-	X	X	X	59223	59221
A→G (ORF 35), A, silent	64067	-	X	X	A/G	64003	64000
T→C (ORF 39), M→T	71252	-	X	X	C/T	71188	71185
A→A/G (ORF 45), P, silent	82225	-	X	-	-	82160	82157
G→A/G (ORF 47), E, silent	84091	-	X	-	-	84026	84023
A→A/G (ORF 50), C, silent	87280	-	X	-	-	87205	87202
T→C/T (ORF 50), S→G	87306	-	X	-	-	87231	87228
A→G (ORF 51), T, silent	89734	-	X	X	-	89659	89656
A→A/G (ORF 52), I→V	90535	-	X	X	-	90460	90457
T→C (ORF 54), L, silent	94167	-	X	X	T/C	94092	94089
G→A/G (ORF 55), A→T	97748	-	X	X	X	97673	97670
T→C/T (ORF 55), C→R	97796	-	X	X	-	97721	97718
Insertion, C	105020	X		X	X	104946	104943
A→A/G	105169	-	X	X	X	105097	105094
A→A/G (ORF 62), L→S	105310	-	X	X	X	105238	105235
T→C (ORF 62), I→V	105356	-	X	X	T/C	105284	105281
A→G (ORF 62), V→A	105544	-	X	X	X	105472	105469
T→C (ORF 62), A, silent	105705	-	X	X	X	105633	105630
T→C (ORF 62), R→G	106262	-	X	X	X	106190	106187
T→C (ORF 62), A, silent	107136	-	X	X	T/C	107064	107061
T→C (ORF 62), S→G	107252	-	X	X	X	107180	107177
A→A/G (ORF 62), V→A	107599	-	X	X	-	107527	107524
T→C (ORF 62), P, silent	108111	-	X	X	X	108039	108036
A→A/G (ORF 62), M→T	108838	-	X	X	X	108766	108763
A→A/G	109137	-	X	X	X	109065	109062
A→A/G	109200	-	X	X		109128	109125
Insertion, GGGAGGGGGCGCGGTAC CCCGCCGATG	109907	X	-	-	-	109838	109835
Deletion, AT	110212	-	X	X	-	110142	110140–110141
Insertion, ATATAG	110214	X	-	-	-	110142	110141
A→G (ORF 64), Q→R	111650	-	X	A/G	A/G	111576	111575
T→C (ORF 69), Q→R	118247	-	X	T/C	T/C	118183	118174
A→C (Ori)	119677	X	-	X	X	119611	119602
Deletion, ATATATAT	119677–119684	-	X	-	-	119611–119618	119602–119609
A→C (Ori)	119679	X	-	X	X	119613	119604
A→C (Ori)	119681	X	-	X	X	119615	119606
A→C (Ori)	119683	X	-	X	A/C	119617	119608
Insertion, TACCGCGCCCCCTCCCCA TCGGCGGGG	120135	X	-	-	-	120068	120060
T→T/C	120697	-	X	X		120633	120624
T→T/C	120760	-	X	X	X	120696	120687
T→C/T (ORF 71), M→T	121059	-	X	X	X	120995	120986
A→G (ORF 71), P, silent	121786	-	X	X	X	121722	121713
T→C/T (ORF 71), V→A	122298	-	X	X		122234	122225
A→G (ORF 71), S→G	122645	-	X	X	X	122581	122572
A→G (ORF 71), A, silent	122761	-	X	X	A/G	122697	122688
A→G (ORF 71), R→G	123635	-	X	X	X	123571	123563
A→G (ORF 71), A, silent	124192	-	X	X	X	124128	124119
T→C (ORF 71), V→A	124353	-	X	X	X	124289	124280
A→G (ORF 71), I→V	124541	-	X	X	A/G	124477	124468
T→C (ORF 71), L→S	124587	-	T/C	T/C	T/C	124523	124514
T→T/C	124728	-	X	X	X	124664	124655

[a] Ori, origin of replication; WT, wild type. X, difference relative to Dumas strain; -, identical nucleotide relative to Dumas strain; Del, deletion; Ins, insertion. Where applicable, the resulting codon switch is specified. Boldface highlights homologies between genomic sequences of Oka-V and genomic sequences of Oka-V_{GSK} and/or Oka-V_{Merck}.

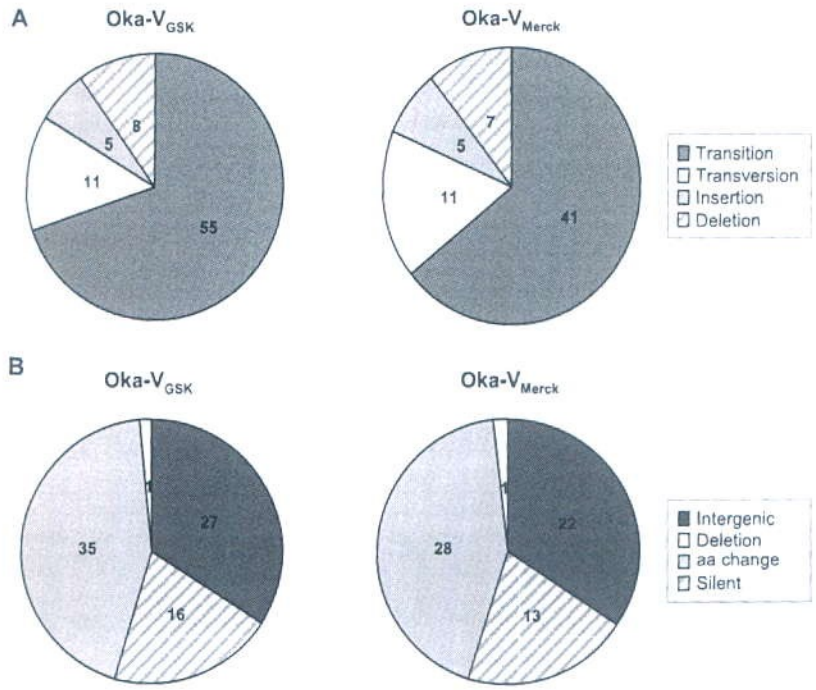


FIG. 2. Type (A) and function (B) of the mutations between Oka-P and the Oka-V_{GSK} and Oka-V_{Merck} vaccine strains of VZV. The numbers indicate the number of events identified for each category of mutations. aa, amino acid.

nucleotide substitutions were found in 8 different ORFs, and 1 noncoding substitution was found in the origin of replication.

Transactivation. ORF 62 encodes immediate early protein 62 (IE62), also known as a transcription regulator, which is the major component of the virion tegument and an important transactivating protein for all classes of VZV promoters (28, 49, 56). It is located in the short repeat sequences and has therefore a duplicate gene, ORF 71. These two duplicated genes cover 7% of the whole VZV genome. Recent studies suggested that ORF 62 could play a central role in the attenuated phenotype of the Oka vaccine strains (3, 20–22). Defined amino acid substitutions in ORF 62 that are associated with individual virus variants purified from the vaccine mixture have been linked to enhanced virus growth and spread in monolayer cell culture (22).

The present analysis of vaccine strains confirmed that a high number of mutations could be detected within ORF 62 (20–22). As previously discussed, these SNPs in ORF 62/71 may be important for attenuation of VZV (50, 69). The current analysis identified a nucleotide transition (position 105356 in ORF 62, corresponding to 124541 in ORF 71) that altered an Ile of the IE62 protein to a Val only partially in Oka-V_{Merck} and completely in Oka-V_{GSK} and Oka-V. Because Oka-P encodes only Ile at this position, it is likely that the Oka-V_{Merck} passaging history has selected for minor Oka-P-related species that might be present in the Oka-V vaccine. The second substitution (position 107599 in ORF 62 and 122298 in ORF 71) partially changed a Val to Ala in Oka-V_{GSK} and Oka-V; for Oka-V_{Merck}, this position is identical to the one found in Oka-P and encodes Val only. In both cases, the amino acids involved are small hydrophobic residues. Gomi et al. demonstrated that five amino acid substitutions, including the 105356 mutation, in the carboxyl terminus of IE62 directly reduced transactivational activity (22). Experiments with recombinant VZV will be required to determine how these mutations in ORF 62 modulate VZV gene expression and which amino acid substitutions are responsible for the differences in viral spreading.

The product of ORF 10, the virion-associated transactivator, is a tegument protein that regulates the IE62 promoter (28, 46). A nucleotide substitution (C→C/T) at position 12779 results in a conversion of an Ala in the Dumas, Oka-P, and Oka-V_{Merck} strains to a mixture of Ala and Val in the Oka-V and Oka-V_{GSK} strains. Similarly, minor subspecies from Oka-V that were originally present in Oka-P may have been selected in Oka-V_{Merck}. This position, which corresponds to a location in the middle of the protein, in Oka-V and Oka-V_{GSK} encodes two small hydrophobic amino acids (Val and Ala) that could have similar functions. Indeed, no statistically significant differences in transactivational activity of the ORF 10 gene product could be detected between the wild type and the mutant form, suggesting that this alternative form of ORF 10 has a minimal effect on viral attenuation through modulation of the expression level of IE62 (22). Furthermore, in vitro studies have shown that ORF 10 product was dispensable for VZV replication in vitro (10).

The helicase-primase complex. The helicase-primase complex consists of three proteins encoded by ORF 6 (primase) and ORFs 52 and 55 (helicase). Interestingly, we found four amino acid substitutions in these proteins, three of which were described previously (22).

The first amino acid substitution was located near the C terminus of ORF 6 (position 5745, A→G), which was a Ser in Dumas and Oka-P, a Pro in Oka-V and Oka-V_{GSK}, and a

TABLE 6. Comparison of complete genomic sequences of Oka-V_{GSK} and Oka-V_{Merck} vaccine strains of VZV[a]

Feature relative to WT (Dumas)	Position (WT)	Feature in:				Position in:	
		Oka-P	Oka-V	Oka-V_{GSK}	Oka-V_{Merck}	Oka-V_{GSK}	Oka-V_{Merck}
T→T/C	2515	-	X	C	-	2514	2514
A→G (ORF 6), S→P	5745	-	X	X	A/G	5744	5744
T→C/T (ORF 9A), W→R	10900	-	X	X	-	10899	10899
C→C/T (ORF 10), A→V	12779	-	X	X	-	12778	12778
C→C/T (ORF 14), K, silent	20703	-	-	X	-	20657	20657
C→A (ORF 14), K→N	20787	X	X	C/A	-	20741	20741
A→T (ORF 14), S→T	20879	-	-	A/T	-	20833	20833
A→G (ORF 18), N, silent	26125	-	X	X	A/G	26076	26076
T→T/G (ORF 22), P, silent	39227	-	X	X	-	39178	39178
C→T (R3 repeat), A→V	41485	-	-	X	-	41436	41436
C→C/T (R3 repeat), A→V	41494	-	-	X	-	41445	41445
Deletion/insertion	42403	Del AAA	Del AA	Ins A	Del A	42355	42353
A→G (ORF 31), I→V	58595	-	A/G	A/G	X	58531	58529
Deletion	60278	Del 5A	Del 5A	Del A	Del AA	60214	60211
A→G (ORF 35), A, silent	64067	-	X	X	A/G	64003	64000
T→C (ORF 39), M→T	71252	-	X	X	C/T	71188	71185
A→G (ORF 51), T, silent	89734	-	X	X	-	89659	89656
A→A/G (ORF 52), I→V	90535	-	X	X	-	90460	90457
T→C (ORF 54), L, silent	94167	-	X	X	T/C	94092	94089
T→T/C (ORF 55), V→A	97479	-	-	-	X	97404	97401
T→C/T (ORF 55), C→R	97796	-	X	X	-	97721	97718
T→C (ORF 62), I→V	105356	-	X	X	T/C	105284	105281
T→C (ORF 62), A, silent	107136	-	X	X	T/C	107064	107061
A→A/G (ORF 62), V→A	107599	-	X	X	-	107527	107524
A→A/G	109200	-	X	X	-	109128	109125
T→C/T	109546	-	-	X	-	109474	109471
Deletion, AT	110212	-	X	X	-	110142	110140–110141
T→G	110214	-	-	-	X	-	110141
Deletion/insertion	112128	Del A	Del A	Ins 5a	Ins A	112064–112068	112063
Deletion/insertion	117769	Del T	Del T	Ins 5T	Ins T	117701–117705	117696
A→C (Ori)	119683	X	-	X	A/C	119617	119608
A→A/G	120351	-	-	X	-	120287	120278
T→T/C	120697	-	X	X	-	120633	120624
T→C/T (ORF 71), V→A	122298	-	X	X	-	122234	122225
A→G (ORF 71), A, silent	122761	-	X	X	A/G	122697	122688
A→G (ORF 71), I→V	124541	-	X	X	A/G	124477	124468

[a] WT, wild type. X, difference relative to Dumas strain; -, identical nucleotide relative to Dumas strain; Ori, origin of replication; Del, deletion; Ins, insertion. When applicable, the resulting codon switch is specified. Boldface highlights homologies between genomic sequences of Oka-V and genomic sequences of Oka-V_{GSK} and/or Oka-V_{Merck}.

mixture of both in Oka-V_{Merck}. Pro is a rigid residue that could induce substantial changes in the protein conformation. This nucleotide substitution was also comprised in an AluI restriction site. Interestingly, Quinlivan et al. found no differences between Oka-V_{GSK} and Oka-V_{Merck} by AluI restriction analysis: both Oka-V_{GSK} and Oka-V_{Merck} were A/G (±AluI), whereas Oka-V was G (+AluI) (52).

The second substitution occurred in ORF 52 (position 90535, A→A/G). In this case, the amino acid residue in Oka-P and Oka-V_{Merck} was Ile, which was partially changed to Val in Oka-V and Oka-V_{GSK}.

The last two substitutions were located in ORF 55. Val at position 97479 was partially replaced by Ala in Oka-V_{Merck}, and Cys at position 97796 was partially replaced by Arg in Oka-V and Oka-V_{GSK}.

Gomi et al. demonstrated that pathogenicity and spreading of VZV were affected by mutations in ORFs 6, 10, and 62, whereas ORFs 52 and 55 did not seem to be important for efficient VZV spreading (22). Because these substitutions were only partial, they could result in the coexistence of different helicase-primase activities resulting from different isomeric complexes, as shown by restriction fragment length polymorphism analysis (22). For most of these positions Oka-V_{GSK} was similar to Oka-V, whereas Oka-V_{Merck} was similar to Oka-P.

Envelope glycoproteins. VZV produces at least seven glycoproteins, gK, gC, gB, gH, gL, gI, and gE, which are the products of ORFs 5, 14, 31, 37, 60, 67, and 68, respectively (11). Two putative additional glycoproteins were recently described, gN (ORF 9A) and gM (ORF 50) (55, 77). It is known that VZV glycoproteins induce a strong humoral immune response following either natural infection or vaccination with the Oka strain. The SNPs in the nine VZV glycoproteins were reviewed in a recent comparative analysis (64). Some of them are specific to the vaccine strains and thus could be involved in VZV attenuation.

The product of ORF 68, gE, is the most abundant glycoprotein expressed during infection. A single amino acid substitution in this protein was shown to induce the accelerated replication phenotype of the VZV-MSP mutant strain (57). Recently, Grose at al. reported the sequences of two VZV isolates harboring a D150N mutation within ORF 68 (25). That study identified only one mutation, common to all four Oka

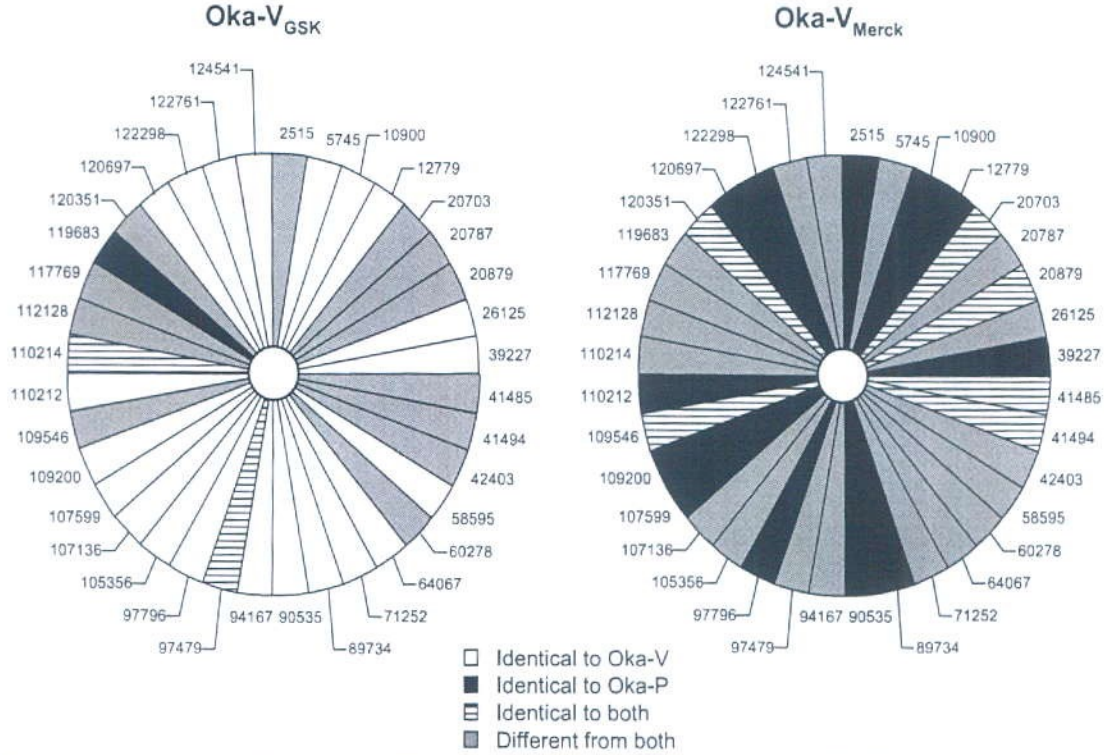


FIG. 3. Sequence comparisons of Oka-V$_{GSK}$ and Oka-V$_{Merck}$ with Oka-P and Oka-V strains of VZV. The 36 nucleotide positions that are different in Oka-V$_{GSK}$ and Oka-V$_{Merck}$ vaccines were compared to the sequence of the original vaccine strain Oka-V and its parental virus, Oka-P.

strains (position 115926, C→T), which induced the replacement of a Thr by Ile.

The product of ORF 31, gB, is the second most abundant and immunogenic envelope glycoprotein of VZV after gE. Along with gH and gC, it seems to play a role in the attachment and penetration of viral particles. It was also shown to have important fusogenic properties in the presence of gE and to be associated with cell-to-cell infection (39, 45). An A→G transition at position 58595 induced a conversion of Ile to Val in Oka-V$_{Merck}$ and a mixture of Ile and Val in both Oka-V$_{GSK}$ and Oka-V. Both amino acids are small and hydrophobic, suggesting that this substitution would probably not affect the properties of this glycoprotein.

ORF 14 exhibited one silent replacement and two amino acid substitutions in its product, gC. At position 20787, a coexistence of C and A induced the partial replacement of a Lys by Asn in Oka-V$_{GSK}$, whereas the original C residue was completely replaced by A in Oka-V$_{Merck}$, entirely replacing Lys with Asn. Both residues are hydrophilic; however, Lys is basic and Asn is polar, with an uncharged side chain. Because Asn was not detected in either Oka-P or Oka-V, it is likely that this amino acid substitution evolved as a result of additional vaccine passages and might reflect additional cell culture adaptation. The second modification (position 20879, A→T) was found only in the Oka-V$_{GSK}$ strain. It partially changed a Ser to Thr. Both residues are hydrophilic and polar with an uncharged side chain. Grinfeld et al. showed that products of ORF 14 and ORF 67 were dispensable for the establishment of latency in a rat model (24). However, experiments with SCID-hu mice showed that gC is important for viral tropism in skin cells and that a decrease in gC plays a critical role in attenuation (44). It was also previously shown that expression of gC is dependent on the strain of VZV, with the gC level of Oka-V being much lower than that of wild-type viruses (29, 37).

A nucleotide substitution at position 71252 induced the replacement of a Met by a Thr in the product of ORF 39, one of the two multiply inserted membrane proteins of VZV. This change was complete in Oka-V$_{GSK}$ and Oka-V but only partial in Oka-V$_{Merck}$. Although both amino acids are neutral, Thr is polar and Met is hydrophobic. This difference may have some effect on the properties of the protein, although these are unclear at present (23).

We also found a mutation in the gN envelope glycoprotein. This glycoprotein is the product of ORF 9A, a newly identified gene positioned closely upstream of the ORF 9 initiation codon (55). Glycoprotein gN is an 87-amino-acid protein whose amino-terminal extremity overlaps with the first nine amino acids of the ORF 8 product, coded on the complementary strand. The observed T-to-T/C shift at position 10900 involves a Trp-to-Arg switch in the very last amino acid of the protein in Oka-V and Oka-V$_{GSK}$. This change leads to replacement of a hydrophobic amino acid with a large aromatic side chain at the carboxyl terminus of the protein by a hydrophilic basic amino acid, which could alter the membrane topology of the protein or its stability.

R3 repeat region. The R3 reiteration region is located in ORF 22, the longest ORF in VZV. The product of ORF 22 is

TABLE 7. Comparison of Oka-V_{GSK} and Oka-V_{Merck} genomic sequences with previously published Oka genomic sequences[a,s]

Reference	Position	ORF	Previously reported feature					Feature in present study	
			Dumas	Oka-P	Oka-V	Oka-V_{GSK}	Oka-V_{Merck}	Oka-V_{GSK}	Oka-V_{Merck}
3	84983	48	G	A	A		A	A	A
	85563	48	C	T	T		T	T	T
	86484		cctgataaac		-			cctgataaac	cctgataaac
	86556		T		G			G	G
	87841	50	C		T			T	T
	88477	51	G		T			T	T
	89734	51	A		G			G	A
	89905	51	T		C			C	C
	90202	51	G		T			T	T
	90217	51	T		C			C	C
	90392		G		A			A	A
	91191	52	C		T			T	T
	92092	52	A		G			G	G
	92375	52	A		G			G	G
	92999	52	T		C			C	C
	94167	54	T		C			C	T/C
	94632	54	T		G			G	G
	94641	54	A		T			T	T
	95241	54	T	C	C		C	C	C
	95546	54	G		A			A	A
	97141	55	T		C			C	C
	97470[b]	55	G		C			G	G
	97591	55	C		T			T	T
	97748	55	G		A			A/G	A/G
	97834[c]	55	C		T			C	C
	98437	55	T		C			C	C
	98765	56	T		C			C	C
	98807	56	A		C			C	C
	99227	56	TTC	-	-			TTC	TTC
	99709	58	A	G	G		G	G	G
	99981	58	C	T	T		T	T	T
	100114	58	T	A	A		A	A	A
	100151	58	T	G	G		G	G	G
	100283		A		G			G	G
	101089	59	A	A	G		A	A/G	A/G
	101331	60	C	T	T		T	T	T
	101623	60	-	+ATC	+ATC			+ATC	+ATC
	101886		T		C			C	C
	101991		C		T			T	T
	102192		G		A			A	A
	102203		A		G			G	G
	102219				+112 bp				
	102309		C		A			A	A
	102351		A		C			C	C
	102458		A		G			G	G
	102601		T		G			G	G
	103043		T		C			C	C
	104898		A		G			G	G
	105010		cctcctct	cctcctct	gcccttaccce		cctcctct	cctcctct	cctcctct
	105054		G		Del G			Del G	Del G
	105063[d]		G		Del G			Del G	Del G
	105145			+AACA	+AACA			+AACA	+ACAA
	105310	62	A	A	G		G	A/G	A/G
	105312	62	A	G	G		G	G	G
	105356	62	T	T	C		C	C	C
	105451	62	A		G			G	G
	105512	62	A		C			C	C
	105544	62	A		G			G	G
	105705	62	T		C			C	C
	106262	62	T	T	C		C	C	C
	107136	62	T		C			C	C
	107165	62	C		T			T	T
	107252	62	T		C			C	C
	107307	62	T		C			C	C
	107607	62	C		A			A	A
	107715	62	T		C			C	C

Continued on following page

TABLE 7—*Continued*

Reference	Position	ORF	Previously reported feature					Feature in present study	
			Dumas	Oka-P	Oka-V	Oka-V_{GSK}	Oka-V_{Merck}	Oka-V_{GSK}	Oka-V_{Merck}
	108111	62	T		C			C	C
	108747	62	A		G			G	G
	108951	62	G		A			A	A
	109044	62	C		G			G	G
	109694[e]				+ATC			+CAT	+CAT
	109762				+27 bp			C	C
	110196				Del TA			No del	No del
	110216		$(ga)_9gg$		$(ta)_6(gc)_2aaga$		$(ta)_{16}gag(ga)_4$		$(ta)_{10}(ga)_9aaa(ga)_4$
	110378				Del GC			Del GC	Del GC
	111312	63	A		G			G	G
	111650	64	A	A	G		A/G	A/G	A/G
	112093	64	T	C	C		C	C	C
	112130[f]		-	-	$+A_8$		$+A_8$	$+A_{12}$	$+A_9$
	112198		G	A	A		A	A	A
	114140	66	A		G			G	G
	115041	67	G		A			A	A
	115926	68	C		T			T	T
60	1		A	G	G	G	A	G	G
	3		G	C	C	C	G	C	C
	178		G	G	G	C	C	C	C
	560		T	T	C	C	C	C	C
	703[g]	1	T	T	T	C	C	C	C
	82225[d]	45	A	A	A	G	A	A	A
	86363	49	A	A	A	T	A	A	A
	87677	50	A	A	A	G	A	A	A
	89734	51	A	A	G	A	A	G	A
	90115[i]	51	A	A	stop	A	A	A	A
	105054		G	-	-	-	G	Del G	Del G
	105071		G	G	-	-	G	Del G	Del G
	105145	Poly(A)	-	AACA	AACA	AACA	-	ACAA	ACAA
	105169		A	A	A/G	A/G	A	A/G	A/G
	105310	62	A	A	A/G	G	A	A/G	A/G
	105356	62	T	T	C	C	T	C	T/C
	105544	62	A	A	G	G	G	G	G
	124353	71	T	T	C	C	C	C	C
	124541	71	A	A	G	G	G	G	A/G
	124587	71	T	T	C/T	C	T	C	C/T
	124728		T	T	C/T	C/T	T	C/T	C/T
	124750	pA-71	-	TGTT	TGTT	TGTT	TGTT	TGTT	TGTT
	124834		C	-	-	-	C	Del C	Del C
	124851		C	-	-	-	C	Del C	Del C
22	560			T	C			C	C
	703	1		T	T/C			C	C
	763	1		T	T/C			C	C
	2515			T	T/C			C	T
	5745	6		A	G			G	A/G
	10900	9A		T	T/C			T/C	T
	12779[j]	10		T	T/C			T/C	C
	19431	14		T	T/C			T	T
	26125	18		A	G			G	A/G
	31732	21		C	T/C			C	C
	38036[k]	22		T	T/C			T/C	T/C
	39227	22		T	T/G			T/G	T
	58595	31		A	A/G			A/G	G
	59287	31		A	A/G			A/G	A/G
	64067[l]	35		A	A/G			G	A/G
	71252[m]	39		T	T/C			C	T/C
	82225	45		A	A/G			A	A
	84091	47		G	A/G			G	G
	87280	50		A	A/G			A	A
	87306	50		T	T/C			T	T
	89734[n]	51		A	A/G			G	A
	90535	52		A	A/G			A/G	A

Continued on following page

TABLE 7—*Continued*

Reference	Position	ORF	Previously reported feature					Feature in present study	
			Dumas	Oka-P	Oka-V	Oka-V_{GSK}	Oka-V_{Merck}	Oka-V_{GSK}	Oka-V_{Merck}
	94167	54		T	C			C	T/C
	97748	55		G	A/G			A/G	A/G
	97796	55		T	T/C			T/C	T
	101089[o]	59		A	A/G			A/G	A/G
	105169			A	A/G			A/G	A/G
	105310	62		A	A/G			A/G	A/G
	105356	62		T	C			C	T/C
	105544	62		A	G			G	G
	105705	62		T	C			C	C
	106262	62		T	C			C	C
	106710[p]	62		A	A/G			A	A
	107136	62		T	C			C	T/C
	107252	62		T	C			C	C
	107599	62		A	A/G			A/G	A
	107797[q]	62		A	A/G			A	A
	108111	62		T	C			C	C
	108838	62		A	A/G			A/G	A/G
	109137			A	A/G			A/G	A/G
	109200			A	A/G			A/G	A
	111650[r]	64		A	A/G			A/G	A/G

[a] Boldface highlights differences (3, 60) and homologies (22) between results from published studies and results from the present study. Lowercase indicates insertion; -, missing nucleotide position.
[b] Indicated as G in the Oka-V GenBank submission AB097932.
[c] Indicated as C in the Oka-V GenBank submission AB097932.
[d] In the present alignment, this position is 105071.
[e] In the present alignment, this position is 109696.
[f] In the present alignment, this position is 112128.
[g] Indicated as Y in the Oka-V GenBank submission AB097932.
[h] Indicated as R in the Oka-V GenBank submission AB097932.
[i] Indicated as A in the Oka-V GenBank submission AB097932.
[j] Indicated as C in the Oka-P GenBank submission AB097933.
[k] Indicated as T in the Oka-V GenBank submission AB097932.
[l] Indicated as G in the Oka-V GenBank submission AB097932.
[m] Indicated as C in the Oka-V GenBank submission AB097932.
[n] Indicated as G in the Oka-V GenBank submission AB097932.
[o] Indicated as R in the Oka-P GenBank submission AB097933.
[p] Indicated as A in the Oka-V GenBank submission AB097932.
[q] Indicated as A in the Oka-V GenBank submission AB097932.
[r] Indicated as A in the Oka-V GenBank submission AB097932.

homologous to the UL36 virion tegument phosphoprotein of herpes simplex virus type 1 (41, 42). R3 is a highly variable region consisting of repeated elements that can vary in number and combination (12, 22), but the impact of this region on the function of ORF 22 phosphoprotein remains mostly unknown because the function of the phosphoprotein itself is poorly understood.

Despite the high variability of the R3 region, no frameshift mutations were detected in ORF 22, because the repeated elements are present as multiples of 3 bp. Nevertheless, two mutations (positions 41485 and 41494, C→T) in the Oka-V_{GSK} strain were identified, both of which convert Ala into Val, another amino acid with similar properties that probably does not affect the function of the ORF 22 protein.

Attenuation and reactivation. Comparison of the four Oka strain sequences of VZV indicated that Oka-V_{GSK} is genetically closer to Oka-V than Oka-V_{Merck} is but that Oka-V_{Merck} is closer to Oka-P than Oka-V_{GSK} is (reference 50 and the present study). In agreement with these findings, Sauerbrei et al. demonstrated that Oka-V_{Merck} is genetically closer to Oka-P than Oka-V_{GSK} is (59). Nevertheless, it is well established that both vaccine strains are attenuated but remain strongly immunogenic (43, 73). Recently, Quinlivan et al. suggested an association of particular SNPs in the VZV genome with frequency of vaccine-induced rash (53). Four SNP positions were suggested to contain nucleotides specific to Oka-P in most of the viruses isolated from vaccine rashes. The first one is a silent nucleotide change within ORF 51 (A→G at position 89734). The nucleotide at this position is A in Oka-V_{Merck} and Oka-P but G in Oka-V_{GSK} and Oka-V. The second SNP, at position 105169, contains mixed A/G nucleotides for Oka-V_{Merck}, Oka-V_{GSK}, and Oka-V, whereas the parental Oka-P contains only A. The third SNP, at position 105356, is located within ORF 62. The change from T to C is responsible for an amino acid switch (Ile→Val) for both Oka-V_{GSK} and Oka-V. At the same position, the parental Oka-P contains T (Ile), and Oka-V_{Merck} contains a mixture of T and C (Ile/Val). The last position (nucleotide 107797) was not identified as a SNP in our sequencing data, which agrees with a previous study (22).

Although the genetic basis of Oka-V attenuation has not been determined, Oka-V and Oka-P genomes have nucleotide differences predicted to change amino acids in every class of viral proteins (3, 21). VZV attenuation is a multifactorial phe-

nomenon whose mechanism remains unclear (80), but it is conceivable that mutations of the vaccine genome, in particular, mutations resulting in amino acid modifications, could affect virulence or latency of the vaccine strain. Recently, Peters and coworkers sequenced 11 VZV genomes from different clades, bringing the current number of available full-length VZV sequences to 18 (50, 69). To assess variations that can occur during serial passage in cell culture, these studies included the four Oka strains (Oka-P and the three Oka vaccine strains) and a VZV strain sequenced at passages 5, 22, and 72. As discussed by Tyler et al. (69), the SNPs in ORF 62/71 found in the three Oka vaccine strains and in the VZV strain at high passage level (S628G, R958G, and I1260V in IE62) could be involved in the attenuation of VZV. In addition, it was suggested that other mutations could play a role, particularly those in regions containing ORFs 30 to 55 (69, 78, 80). However, we found that numerous SNPs contain the original Oka-P nucleotide, supporting the idea that the attenuated phenotype is the result of a cooperative effect between several SNPs rather than the result of selected mutations. Therefore, our analysis of SNP importance is aligned with the conclusions of Tyler et al. regarding VZV attenuation (69).

VZV remains latent in sensory-nerve ganglia and can reactivate later, causing herpes zoster. It was suggested that herpes zoster is less common after vaccination, because initial access of Oka-V to neural cells is reduced by limited skin replication or because Oka-V reactivation and secondary viral infection of skin are less efficient, rather than because of an intrinsic attenuation of Oka-V neurotropism (5). Indeed, even though the Oka-V strain of VZV can cause herpes zoster, it seems to reactivate less often than the wild-type VZV even in immunocompromised children (18, 27, 68), and increased incidences of reactivation after vaccination have not been demonstrated in either clinical studies or postmarketing surveillance (33a, 43, 62, 66, 70, 73). In addition, the Oka vaccines have been shown to elicit a strong and protective immune response against varicella (7, 43, 73).

Conclusion. Overall, this study shows that, throughout the entire VZV genome, only 36 nucleotide positions differ between the Oka-V_{GSK} and Oka-V_{Merck} vaccine strains. Analysis of the complete genome of VZV also shows that, genetically, Oka-V_{GSK} is closer to Oka-V and that Oka-V_{Merck} is closer to Oka-P. Although Oka-V_{GSK} and Oka-V_{Merck} exhibit differences, there is a high degree of conservation between these strains at both the nucleotide and amino acid levels. This result supports the clinical data showing that both vaccines are well tolerated and elicit strong immune responses against varicella.

ACKNOWLEDGMENTS

We are grateful to Catherine Arnaudeau-Bégard, Julie Harriague, and Anne Hepburn for their constructive discussions and editorial assistance in the preparation of the manuscript. Technical support from various sequencing staff members is acknowledged.

REFERENCES

1. **American Academy of Pediatrics Committee on Infectious Diseases.** 1995. Recommendations for the use of live attenuated varicella vaccine. Pediatrics **95:**791–796.
2. **Arbeter, A. M., S. E. Starr, and S. A. Plotkin.** 1986. Varicella vaccine studies in healthy children and adults. Pediatrics **78:**748–756.
3. **Argaw, T., J. I. Cohen, M. Klutch, K. Lekstrom, T. Yoshikawa, Y. Asano, and P. R. Krause.** 2000. Nucleotide sequences that distinguish Oka vaccine from parental Oka and other varicella-zoster virus isolates. J. Infect. Dis. **181:** 1153–1157.
4. **Arvin, A., and A. Gershon.** 2006. Control of varicella: why is a two-dose schedule necessary? Pediatr. Infect. Dis. J. **25:**475–476.
5. **Arvin, A. M.** 2001. Varicella vaccine: genesis, efficacy, and attenuation. Virology **284:**153–158.
6. **Arvin, A. M.** 2002. Varilrix (GlaxoSmithKline). Curr. Opin. Investig. Drugs **3:**996–999.
7. **Asano, Y.** 1996. Varicella vaccine: the Japanese experience. J. Infect. Dis. **174**(Suppl. 3)**:**S310–S313.
8. **Centers for Disease Control and Prevention.** 1996. Prevention of varicella: recommendations of the Advisory Committee on Immunization Practices (ACIP). MMWR Recommend. Rep. **45:**1–36.
9. **Chaves, S. S., P. Gargiullo, J. X. Zhang, R. Civen, D. Guris, L. Mascola, and J. F. Seward.** 2007. Loss of vaccine-induced immunity to varicella over time. N. Engl. J. Med. **356:**1121–1129.
10. **Cohen, J. I., and K. Seidel.** 1994. Varicella-zoster virus (VZV) open reading frame 10 protein, the homolog of the essential herpes simplex virus protein VP16, is dispensable for VZV replication in vitro. J. Virol. **68:**7850–7858.
11. **Cole, N. L., and C. Grose.** 2003. Membrane fusion mediated by herpesvirus glycoproteins: the paradigm of varicella-zoster virus. Rev. Med. Virol. **13:** 207–222.
12. **Davison, A. J., and J. E. Scott.** 1986. The complete DNA sequence of varicella-zoster virus. J. Gen. Virol. **67:**1759–1816.
13. **de Ory, F., J. M. Echevarría, G. Kafatos, C. Anastassopoulou, N. Andrews, J. Backhouse, G. Berbers, B. Bruckova, D. I. Cohen, H. de Melker, I. Davidkin, G. Gabutti, L. M. Hesketh, K. Johansen, S. Jokinen, L. Jones, A. Linde, E. Miller, J. Mossong, A. Nardone, M. C. Rota, A. Sauerbrei, F. Schneider, Z. Smetana, A. Tischer, A. Tsakris, and R. Vranckx.** 2006. European seroepidemiology network 2: standardisation of assays for seroepidemiology of varicella zoster virus. J. Clin. Virol. **36:**111–118.
14. **D'Hondt, E., E. Berge, G. Colinet, M. Duchene, and J. Peetermans.** 1985. Production and quality control of the Oka-strain live varicella vaccine. Postgrad Med. J. **61:**53–56.
15. **Faga, B., W. Maury, D. A. Bruckner, and C. Grose.** 2001. Identification and mapping of single nucleotide polymorphisms in the varicella-zoster virus genome. Virology **280:**1–6.
16. **Galil, K., B. Lee, T. Strine, C. Carraher, A. L. Baughman, M. Eaton, J. Montero, and J. Seward.** 2002. Outbreak of varicella at a day-care center despite vaccination. N. Engl. J. Med. **347:**1909–1915.
17. **Gershon, A. A.** 2001. The current status of live attenuated varicella vaccine. Arch. Virol. Suppl. **2001:**1–6.
18. **Gershon, A. A., P. LaRussa, I. Hardy, S. Steinberg, and S. Silverstein.** 1992. Varicella vaccine: the American experience. J. Infect. Dis. **166**(Suppl. 1)**:** S63–S68.
19. **Goh, P., F. S. Lim, H. H. Han, and P. Willems.** 2007. Safety and immunogenicity of early vaccination with two doses of tetravalent measles-mumps-rubella-varicella (MMRV) vaccine in healthy children from 9 months of age. Infection **35:**326–333.
20. **Gomi, Y., T. Imagawa, M. Takahashi, and K. Yamanishi.** 2001. Comparison of DNA sequence and transactivation activity of open reading frame 62 of Oka varicella vaccine and its parental viruses. Arch. Virol. Suppl. **2001:**49–56.
21. **Gomi, Y., T. Imagawa, M. Takahashi, and K. Yamanishi.** 2000. Oka varicella vaccine is distinguishable from its parental virus in DNA sequence of open reading frame 62 and its transactivation activity. J. Med. Virol. **61:**497–503.
22. **Gomi, Y., H. Sunamachi, Y. Mori, K. Nagaike, M. Takahashi, and K. Yamanishi.** 2002. Comparison of the complete DNA sequences of the Oka varicella vaccine and its parental virus. J. Virol. **76:**11447–11459.
23. **Govero, J., S. Hall, and T. C. Heineman.** 2007. Intracellular localization of varicella-zoster virus ORF39 protein and its functional relationship to glycoprotein K. Virology **358:**291–302.
24. **Grinfeld, E., C. Sadzot-Delvaux, and P. G. Kennedy.** 2004. Varicella-zoster virus proteins encoded by open reading frames 14 and 67 are both dispensable for the establishment of latency in a rat model. Virology **323:**85–90.
25. **Grose, C., S. Tyler, G. Peters, J. Hiebert, G. M. Stephens, W. T. Ruyechan, W. Jackson, J. Storlie, and G. A. Tipples.** 2004. Complete DNA sequence analyses of the first two varicella-zoster virus glycoprotein E (D150N) mutant viruses found in North America: evolution of genotypes with an accelerated cell spread phenotype. J. Virol. **78:**6799–6807.
26. **Hammond, O., Y. Wang, T. Green, J. Antonello, R. Kuhn, C. Motley, P. Stump, B. Rich, N. Chirmule, and R. D. Marchese.** 2006. The optimization and validation of the glycoprotein ELISA assay for quantitative varicella-zoster virus (VZV) antibody detection. J. Med. Virol. **78:**1679–1687.
27. **Hardy, I., A. A. Gershon, S. P. Steinberg, P. LaRussa, et al.** 1991. The incidence of zoster after immunization with live attenuated varicella vaccine. A study in children with leukemia. N. Engl. J. Med. **325:**1545–1550.
28. **Kinchington, P., J. Hougland, A. Arvin, W. Ruyechan, and J. Hay.** 1992. The varicella-zoster virus immediate-early protein IE62 is a major component of virus particles. J. Virol. **66:**359–366.
29. **Kinchington, P. R., P. Ling, M. Pensiero, A. Gershon, J. Hay, and W. T.**

Ruyechan. 1990. A possible role for glycoprotein gpV in the pathogenesis of varicella-zoster virus. Adv. Exp. Med. Biol. **278:**83–91.

30. **Knuf, M., P. Habermehl, F. Zepp, W. Mannhardt, M. Kuttnig, P. Muttonen, A. Prieler, H. Maurer, H. Bisanz, N. Tornieporth, D. Descamps, and P. Willems.** 2006. Immunogenicity and safety of two doses of tetravalent measles-mumps-rubella-varicella vaccine in healthy children. Pediatr. Infect. Dis. J. **25:**12–18.
31. **Krah, D. L., I. Cho, T. Schofield, and R. W. Ellis.** 1997. Comparison of gpELISA and neutralizing antibody responses to Oka/Merck live varicella vaccine (Varivax) in children and adults. Vaccine **15:**61–64.
32. **Kraiouchkine, N., A. R. Shaw, P. M. Keller, and D. J. Distefano.** 2003. Comparison of the complete genome sequences of Varicella Zoster Virus Oka/Merck (Varivax) and Oka/GSK (Varilrix), abstr. G-1652, p. 295. Abstr. 43rd Annu. Intersci. Conf. Antimicrob. Agents Chemother. Chicago, IL, 14 to 17 September 2003.
33. **Krause, P. R., and D. M. Klinman.** 1995. Efficacy, immunogenicity, safety, and use of live attenuated chickenpox vaccine. J. Pediatr. **127:**518–525.

33a. **Kreth, H. W., B. W. Lee, P. Kosuwon, J. Salazar, N. Gloriani-Barzaga, H. L. Bock, F. Meurice.** 16 years of global experience with the first refrigerator-stable varicella vaccine (*Varilrix*™). BioDrugs, in press.

34. **Kuter, B., H. Matthews, H. Shinefield, S. Black, P. Dennehy, B. Watson, K. Reisinger, L. L. Kim, L. Lupinacci, J. Hartzel, and I. Chan.** 2004. Ten year follow-up of healthy children who received one or two injections of varicella vaccine. Pediatr. Infect. Dis. J. **23:**132–137.
35. **Kuter, B. J., M. L. Brown, J. Hartzel, W. R. Williams, K. A. Eves, S. Black, H. Shinefield, K. S. Reisinger, C. D. Marchant, B. J. Sullivan, M. Thear, S. Klopfer, J. Xu, J. O. Gress, and F. Schodel.** 2006. Safety and immunogenicity of a combination measles, mumps, rubella and varicella vaccine (ProQuad). Hum. Vaccines **2:**205–214.
36. **Lau, Y. L., S. J. Vessey, I. S. Chan, T. L. Lee, L. M. Huang, C. Y. Lee, T. Y. Lin, B. W. Lee, K. Kwan, S. M. Kasim, C. Y. Chan, K. M. Kaplan, D. J. Distefano, A. L. Harmon, A. Golie, J. Hartzel, J. Xu, S. Li, H. Matthews, J. C. Sadoff, and A. Shaw.** 2002. A comparison of safety, tolerability and immunogenicity of Oka/Merck varicella vaccine and VARILRIX in healthy children. Vaccine **20:**2942–2949.
37. **Ling, P., P. R. Kinchington, W. T. Ruyechan, and J. Hay.** 1991. A detailed analysis of transcripts mapping to varicella zoster virus gene 14 (glycoprotein V). Virology **184:**625–635.
38. **Macartney, K. K., P. Beutels, P. McIntyre, and M. A. Burgess.** 2005. Varicella vaccination in Australia. J. Paediatr. Child Health **41:**544–552.
39. **Maresova, L., T. J. Pasieka, and C. Grose.** 2001. Varicella-zoster Virus gB and gE coexpression, but not gB or gE alone, leads to abundant fusion and syncytium formation equivalent to those from gH and gL coexpression. J. Virol. **75:**9483–9492.
40. **Marin, M., D. Guris, S. S. Chaves, S. Schmid, and J. F. Seward.** 2007. Prevention of varicella: recommendations of the Advisory Committee on Immunization Practices (ACIP). MMWR Recommend. Rep. **56:**1–40.
41. **McNabb, D. S., and R. J. Courtney.** 1992. Analysis of the UL36 open reading frame encoding the large tegument protein (ICP1/2) of herpes simplex virus type 1. J. Virol. **66:**7581–7584.
42. **McNabb, D. S., and R. J. Courtney.** 1992. Characterization of the large tegument protein (ICP1/2) of herpes simplex virus type 1. Virology **190:**221–232.
43. **Meurice, F., J. L. De Bouver, D. Vandevoorde, S. Woods, and H. Bogaerts.** 1996. Immunogenicity and safety of a live attenuated varicella vaccine (Oka/SB Bio) in healthy children. J. Infect. Dis. **174**(Suppl. 3)**:**S324–S329.
44. **Moffat, J. F., L. Zerboni, P. R. Kinchington, C. Grose, H. Kaneshima, and A. M. Arvin.** 1998. Attenuation of the vaccine Oka strain of varicella-zoster virus and role of glycoprotein C in alphaherpesvirus virulence demonstrated in the SCID-hu mouse. J. Virol. **72:**965–974.
45. **Montalvo, E. A., and C. Grose.** 1987. Assembly and processing of the disulfide-linked varicella-zoster virus glycoprotein gpII(140). J. Virol. **61:**2877–2884.
46. **Moriuchi, H., M. Moriuchi, and J. I. Cohen.** 1995. Proteins and cis-acting elements associated with transactivation of the varicella-zoster virus (VZV) immediate-early gene 62 promoter by VZV open reading frame 10 protein. J. Virol. **69:**4693–4701.
47. **Muir, W., K. Hawrami, J. Clarke, and J. Breuer.** 2001. Investigation of varicella-zoster virus variation by heteroduplex mobility assay, p. 17–25. *In* C. C. Gershon and A. A. Arvin (ed.), Immunity to and prevention of herpes zoster. Springer-Verlag, Vienna, Austria.
48. **Nolan, T., P. McIntyre, D. Roberton, and D. Descamps.** 2002. Reactogenicity and immunogenicity of a live attenuated tetravalent measles-mumps-rubella-varicella (MMRV) vaccine. Vaccine **21:**281–289.
49. **Perera, L. P., J. D. Mosca, W. T. Ruyechan, G. S. Hayward, S. E. Straus, and J. Hay.** 1993. A major transactivator of varicella-zoster virus, the immediate-early protein IE62, contains a potent N-terminal activation domain. J. Virol. **67:**4474–4483.
50. **Peters, G. A., S. D. Tyler, C. Grose, A. Severini, M. J. Gray, C. Upton, and G. A. Tipples.** 2006. A full-genome phylogenetic analysis of varicella-zoster virus reveals a novel origin of replication-based genotyping scheme and evidence of recombination between major circulating clades. J. Virol. **80:** 9850–9860.
51. **Quian, J., R. Rüttimann, C. Romero, P. Dall'Orso, A. Cerisola, T. Breuer, M. Greenberg, and T. Verstraeten.** 2008. Impact of universal varicella vaccination on 1-year-olds in Uruguay: 1997-2005. Arch. Dis. Child. **93:**845–850.
52. **Quinlivan, M., A. A. Gershon, S. P. Steinberg, and J. Breuer.** 2005. An evaluation of single nucleotide polymorphisms used to differentiate vaccine and wild type strains of varicella-zoster virus. J. Med. Virol. **75:**174–180.
53. **Quinlivan, M. L., A. A. Gershon, M. M. Al Bassam, S. P. Steinberg, P. LaRussa, R. A. Nichols, and J. Breuer.** 2007. Natural selection for rash-forming genotypes of the varicella-zoster vaccine virus detected within immunized human hosts. Proc. Natl. Acad. Sci. USA **104:**208–212.
54. **Robert Koch Institut.** 2001. Empfehlungen der Ständigen Impfkommission (STIKO). Epidemiol. Bull. **29:**219–223.
55. **Ross, J., M. Williams, and J. I. Cohen.** 1997. Disruption of the varicella-zoster virus dUTPase and the adjacent ORF9A gene results in impaired growth and reduced syncytia formation in vitro. Virology **234:**186–195.
56. **Sadzot-Delvaux, C., and B. Rentier.** 2001. The role of varicella zoster virus immediate-early proteins in latency and their potential use as components of vaccines. Arch. Virol. Suppl. **17:**81–89.
57. **Santos, R. A., C. C. Hatfield, N. L. Cole, J. A. Padilla, J. F. Moffat, A. M. Arvin, W. T. Ruyechan, J. Hay, and C. Grose.** 2000. Varicella-zoster virus gE escape mutant VZV-MSP exhibits an accelerated cell-to-cell spread phenotype in both infected cell cultures and SCID-hu mice. Virology **275:**306–317.
58. **Sauerbrei, A., I. Farber, A. Brandstadt, M. Schacke, and P. Wutzler.** 2004. Immunofluorescence test for sensitive detection of varicella-zoster virus-specific IgG: an alternative to fluorescent antibody to membrane antigen test. J. Virol. Methods **119:**25–30.
59. **Sauerbrei, A., E. Rubtcova, P. Wutzler, D. S. Schmid, and V. N. Loparev.** 2004. Genetic profile of an Oka varicella vaccine virus variant isolated from an infant with zoster. J. Clin. Microbiol. **42:**5604–5608.
60. **Schmidt, M., M. Kress, S. Heinemann, and H. Fickenscher.** 2003. Varicella-zoster virus isolates, but not the vaccine strain OKA, induce sensitivity to alpha-1 and beta-1 adrenergic stimulation of sensory neurons in culture. J. Med. Virol. **70:**S82–S89.
61. **Seward, J. F., B. M. Watson, C. L. Peterson, L. Mascola, J. W. Pelosi, J. X. Zhang, T. J. Maupin, G. S. Goldman, L. J. Tabony, K. G. Brodovicz, A. O. Jumaan, and M. Wharton.** 2002. Varicella disease after introduction of varicella vaccine in the United States, 1995-2000. JAMA **287:**606–611.
62. **Sharrar, R. G., P. LaRussa, S. A. Galea, S. P. Steinberg, A. R. Sweet, R. M. Keatley, M. E. Wells, W. P. Stephenson, and A. A. Gershon.** 2000. The postmarketing safety profile of varicella vaccine. Vaccine **19:**916–923.
63. **Shaw, A. R., N. Kraiouchkine, J. Condra, D. Graham, X. Liu, and D. DiStefano.** 2001. Genetic differences between OKA varicella vaccines, abstr. 69. 19th Annu. Meet. Eur. Soc. Paediatr. Infect. Dis.
64. **Storlie, J., L. Maresova, W. Jackson, and C. Grose.** 2008. Comparative analyses of the 9 glycoprotein genes found in wild-type and vaccine strains of varicella-zoster virus. J. Infect. Dis. **197**(Suppl. 2)**:**S49–S53.
65. **Straus, S. E., W. Reinhold, H. A. Smith, W. T. Ruyechan, D. K. Henderson, R. M. Blaese, and J. Hay.** 1984. Endonuclease analysis of viral DNA from varicella and subsequent zoster infections in the same patient. N. Engl. J. Med. **311:**1362–1364.
66. **Takahashi, M.** 2001. 25 years' experience with the Biken Oka strain varicella vaccine: a clinical overview. Paediatr. Drugs **3:**285–292.
67. **Takahashi, M., T. Otsuka, Y. Okuno, Y. Asano, and T. Yazaki.** 1974. Live vaccine used to prevent the spread of varicella in children in hospital. Lancet **ii:**1288–1290.
68. **Takayama, N., M. Takayama, and J. Takita.** 2000. Herpes zoster in healthy children immunized with varicella vaccine. Pediatr. Infect. Dis. J. **19:**169–170.
69. **Tyler, S. D., G. A. Peters, C. Grose, A. Severini, M. J. Gray, C. Upton, and G. A. Tipples.** 2007. Genomic cartography of varicella-zoster virus: a complete genome-based analysis of strain variability with implications for attenuation and phenotypic differences. Virology **359:**447–458.
70. **Vassilev, V.** 2005. Stable and consistent genetic profile of Oka varicella vaccine virus is not linked with appearance of infrequent breakthrough cases postvaccination. J. Clin. Microbiol. **43:**5415–5416.
71. **Vesikari, T., M. Baer, and P. Willems.** 2007. Immunogenicity and safety of a second dose of measles-mumps-rubella-varicella vaccine in healthy children aged 5 to 6 years. Pediatr. Infect. Dis. J. **26:**153–158.
72. **Vesikari, T., C. Sadzot-Delvaux, B. Rentier, and A. Gershon.** 2007. Increasing coverage and efficiency of measles, mumps, and rubella vaccine and introducing universal varicella vaccination in Europe: a role for the combined vaccine. Pediatr. Infect. Dis. J. **26:**632–638.
73. **White, C. J., B. J. Kuter, C. S. Hildebrand, K. L. Isganitis, H. Matthews, W. J. Miller, P. J. Provost, R. W. Ellis, R. J. Gerety, and G. B. Calandra.** 1991. Varicella vaccine (VARIVAX) in healthy children and adolescents: results from clinical trials, 1987 to 1989. Pediatrics **87:**604–610.
74. **Williams, V., A. Gershon, and P. A. Brunell.** 1974. Serologic response to varicella-zoster membrane antigens measured by direct immunofluorescence. J. Infect. Dis. **130:**669–672.

75. **Wood, M. J.** 2000. History of varicella zoster virus. Herpes **7**:60–65.
76. **World Health Organization.** 1998. Varicella vaccines. WHO position paper. Wkly. Epidemiol. Rec. **73**:241–248.
77. **Yamagishi, Y., T. Sadaoka, H. Yoshii, P. Somboonthum, T. Imazawa, K. Nagaike, K. Ozono, K. Yamanishi, and Y. Mori.** 2008. Varicella-zoster virus glycoprotein M homolog is glycosylated, is expressed on the viral envelope, and functions in virus cell-to-cell spread. J. Virol. **82**:795–804.
78. **Yamanishi, K.** 2008. Molecular analysis of the Oka vaccine strain of varicella-zoster virus. J. Infect. Dis. **197**(Suppl. 2):S45–S48.
79. **Zepp, F., U. Behre, K. Kindler, K. H. Laakmann, H. Pankow-Culot, W. Mannhardt-Laakmann, F. Beckers, D. Descamps, and P. Willems.** 2007. Immunogenicity and safety of a tetravalent measles-mumps-rubella-varicella vaccine co-administered with a booster dose of a combined diphtheria-tetanus-acellular pertussis-hepatitis B-inactivated poliovirus-Haemophilus influenzae type b conjugate vaccine in healthy children aged 12-23 months. Eur. J. Pediatr. **166**:857–864.
80. **Zerboni, L., S. Hinchliffe, M. H. Sommer, H. Ito, J. Besser, S. Stamatis, J. Cheng, D. Distefano, N. Kraiouchkine, A. Shaw, and A. M. Arvin.** 2005. Analysis of varicella zoster virus attenuation by evaluation of chimeric parent Oka/vaccine Oka recombinant viruses in skin xenografts in the SCIDhu mouse model. Virology **332**:337–346.
81. **Zhou, F., R. Harpaz, A. O. Jumaan, C. A. Winston, and A. Shefer.** 2005. Impact of varicella vaccination on health care utilization. JAMA **294**:797–802.

Anexo 3 58

JOURNAL OF VIROLOGY, Mar. 2003, p. 3351
0022-538X/03/$08.00+0 DOI: 10.1128/JVI.77.5.3351.2003

Vol. 77, No. 5

AUTHOR'S CORRECTION

Comparison of the Complete DNA Sequences of the Oka Varicella Vaccine and Its Parental Virus

Yasuyuki Gomi, Hiroki Sunamachi, Yasuko Mori, Kazuhiro Nagaike, Michiaki Takahashi, and Koichi Yamanishi

Kanonji Institute, The Research Foundation for Microbial Diseases of Osaka University, Kanonji, Kagawa, and The Research Foundation for Microbial Diseases of Osaka University and Department of Microbiology, Osaka University Medical School, Suita, Osaka, Japan

Volume 76, no. 22, p. 11447–11459, 2002. Page 11449: The last paragraph of Materials and Methods should appear as shown below.

Nucleotide sequence accession number. The complete sequences of VZV Oka parental and vaccine have been deposited in the DDBJ Data Library under accession no. AB097932 and AB097933, respectively.

Anexo 4

59

Vaccine 29 (2011) 3293–3298

Contents lists available at ScienceDirect

Vaccine

journal homepage: www.elsevier.com/locate/vaccine

Population diversity in batches of the varicella Oka vaccine

R.K. Kanda [a,*], M.L. Quinlivan [a], A.A. Gershon [c], R.A. Nichols [b], J. Breuer [a]

[a] Department of Infection, The Windeyer Institute, University College London, 46 Cleveland Street, London WC1T 4JF, England, UK
[b] School of Biological and Chemical Sciences, Queen Mary University of London, London E1 4NS, UK
[c] Columbia University Medical Center, Department of Pediatrics, 630 West 168th Street, PH4-468, New York, NY 10032, United States

ARTICLE INFO

Article history:
Received 28 September 2010
Received in revised form 27 January 2011
Accepted 7 February 2011
Available online 22 February 2011

Keywords:
Varicella-zoster virus
Oka vaccine
Pyrosequencing
Comparative sequence alignment
Batch
Variation
Genetic diversity

ABSTRACT

The Oka vaccine is a live attenuated vaccine for the prevention of varicella. Although the vaccine differs from the progenitor virus by over 40 mutations, only three of these are fixed, the rest being a mixture of the wildtype and the vaccine allele. To examine the extent of this variability between two of the three commercially available vaccine preparations, we analysed the vaccine/wildtype allele frequencies present at fifteen vaccine loci in five preparations each from two different manufacturers of the vOka vaccine. Our results suggest that differences in manufacturing processes between the two companies have resulted in significant variation in the frequencies of the vaccine/wildtype alleles in their vaccines. Yet despite these differences, the allele frequencies in the vaccines from the two companies are strongly correlated. We discuss the significance of these findings and the role of evolutionary processes that influence the production of this live attenuated vaccine.

© 2011 Elsevier Ltd. All rights reserved.

1. Introduction

The live attenuated Oka vaccine is licensed for the prevention of varicella in children in the USA, Japan, Korea, Germany, Greece, Australia and Canada and for targeted immunisation of seronegative health care workers in several countries, including the UK. Over 15 years of experience has demonstrated that VZV vaccines are safe and well tolerated [1–4]. Universal vaccination in the USA has massively decreased the incidence of varicella in both vaccinated individuals and, by herd immunity, unvaccinated individuals, with significant reduction of associated hospitalization and mortality (reviewed in [5]). The commonest adverse event is a mild rash occurring following vaccination, which occurs in around 5% of children and a higher proportion of adults. Life threatening vOka (vaccine Oka) infection has only been described in subjects with undiagnosed cell mediated immunodeficiencies.

The original Oka vaccine strain was derived by serial passage of a wildtype Japanese VZV isolate, pOka (parental Oka) which had been obtained from a child with chickenpox [6]. Three main preparations derived from the original vaccine seed stock are licensed for use, the Biken vaccine, Varivax (Merck) and Varilrix (GSK). In addition, combined vOka with live attenuated measles, mumps and rubella, is marketed by both Merck and GSK. Comparative Sanger sequencing of the Biken strain vOka and pOka, the wildtype progenitor, genomes identified 42 loci at which vaccine substations have occurred, 20 of which are non-synonymous [7]. In addition, length polymorphisms in the known variable repeat R1, R3 and R4 repeat regions and the viral origin of replication OriS were observed and five loci identified that were fixed for the vaccine polymorphism, the rest being polymorphic for vaccine and wildtype single nucleotide polymorphisms (SNPs). Sequencing of 10 clones of the Biken vaccine ORF62 confirmed the Biken vaccine to contain a mixture of related but distinct haplotypes [8]. Subsequently, both the Merck and GSK vOka vaccine preparations were also found to be heterogeneous [9–11].

Only three loci in the ORF 62 gene, which codes for the major immediate transactivating protein, are fixed for the vaccine SNP in all three vaccine preparations, the remainder being either wildtype or mixtures of vaccine and wildtype SNPs [7,11–13]. Overall the GSK vaccine has been found to carry more loci which are fixed for vaccine mutations and fewer which are wildtype than either the Merck or Biken vaccines [11]. Merck and Biken vaccines also differ from one another, with the former having at least one SNP that was not previously identified [9]. However, unlike the Merck vaccine [10,13], there has been no analysis of vaccine allele frequencies in the GSK vaccine. Differences between Merck and GSK vaccines could have arisen due to differences in the downstream manufacturing process by each company (Fig. 1). For example,

* Corresponding author. Present address: Department of Life Sciences, Imperial College London, Silwood Park, Buckhurst Rd, Ascot, Berkshire SL5 7PY, UK.
Tel.: +44 0207 594 1780; fax: +44 020 7594 2339.
E-mail address: r.kanda@imperial.ac.uk (R.K. Kanda).

0264-410X/$ – see front matter © 2011 Elsevier Ltd. All rights reserved.
doi:10.1016/j.vaccine.2011.02.021

60

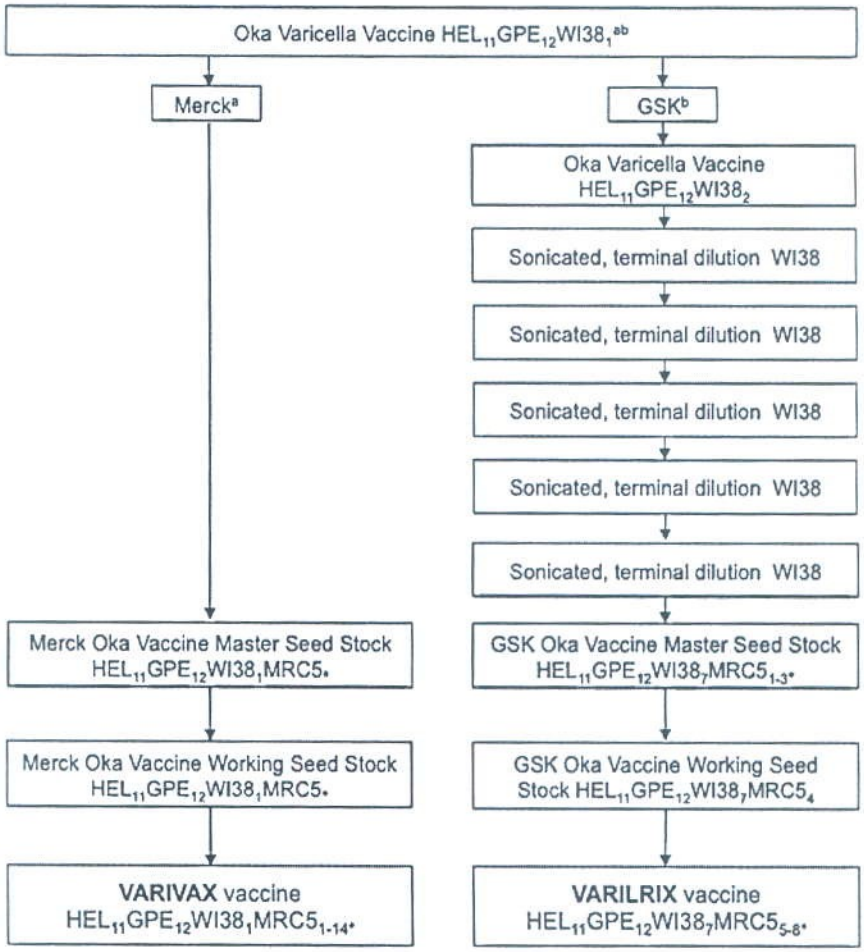


Fig. 1. Overview of varicella vaccine production. HEL, human embryonic lung cell cultures; GPE, embryonic guinea pig cell cultures; WI38, human diploid cell cultures; MRC5, human diploid cell cultures. Subscript numbers indicate passage levels. [a]Information obtained from Merck Product information IPC-VRV3-1-032008. [b]Information obtained from D'Hondt et al. [14]. *Unknown number of passage levels in MRC5 cells. Where passage levels are given next to a "•", these have been inferred from [a] and [b]. World Health Organisation guidelines indicate a limit for Oka-strain varicella vaccine at passage level 38, hence final levels of passage in MRC5 cells can be estimated [14].

the GSK vaccine was subjected to five rounds of terminal dilution in an attempt to generate a genetically uniform vaccine strain [14]. Somewhat surprisingly this process did not appear to generate new vaccine mutations [11]. Limited analysis of different batches of vOka vaccines suggests little variation, [13], however, this has not been extensively characterised. To further examine variability between companies and among batches/lots, we analysed vaccine/wildtype allele frequencies present at 15 vaccine loci in five preparations each of the Merck and GSK Oka vaccines, which are currently available for vaccine programmes in Europe and the USA.

2. Methodology

2.1. Vaccine batches and SNPs

Five lots each of GSK and Merck vaccines derived in each case from three batches were available for analysis (Table 1). Fifteen loci at which vaccine substitutions have been identified were selected for analysis. Nine of these were located in ORF62, which contains over 30% of all the vaccine SNPs identified—several of these SNPs (105169, 105705, 105724, 107136 and 107797) have been identified as being of potential biological importance for vaccine attenuation and as immune targets [13,15]. Two of these were previously identified as fixed vaccine SNPs. The remainder were chosen as they have previously been found to be variable and therefore informative [10,13] and to consistently be present in ORFs across the VZV genome.

2.2. Nucleic acid extractions

Total DNA was extracted using a QIAamp® DNA Mini Kit (Qiagen LTD., UK) according to the manufacturers instructions. The lot numbers, their date of issue and the number of loci analysed in each are shown in Table 1. Prior to extraction, lyophilised vaccine preparations were resuspended in the 500 μl of accompanying buffer. DNA from each preparation was extracted from 2× 200 μl and 1× 100 μl (mixed with 100 μl of PBS) aliquots. The 3× 200 μl aliquots of eluted DNA were merged to form a 600 μl DNA pool, which was used for subsequent experiments. A negative control was used during the extraction process by replacing sample material with 200 μl of water.

2.3. PCR reactions

All PCRs were performed in a GeneAmp 2700 thermocycler (Perkin Elmer, UK), initiated by hot start activation at 95 °C for 10 min and ended with a step of 72 °C for 10 min before being incubated at 4 °C. For direct sequencing, reactions included 35 cycles of amplification (95 °C, 1 min; primer annealing temperature (supplementary Table 1), 1 min, 72 °C, 1 min). For pyrosequencing, reactions included 45 cycles of amplification (95 °C, 15 s; primer

annealing temperature (supplementary Table 2), 30 s, 72 °C, 15 s). PCR reactions included 5 μl of template DNA, 5 μl of PCR buffer II (Perkin Elmer, UK), 1.5 mM $MgCl_2$ (Perkin Elmer, UK), 200 μM of each deoxynucleotide triphosphate (Advanced Biotechnologies, UK), 12 pmol of each primer and 1 unit of AmpliTaq Gold DNA polymerase (Perkin Elmer, UK). Final reaction volumes were adjusted to 50 μl using DNAse/RNAse free water (Sigma, UK). For PCR reactions with each primer set, two negative controls were employed. The first consisted of PCR reaction mix, in which template DNA was replaced with water. The second consisted of PCR reaction mix, in which template DNA was replaced with the water used as a negative control during the DNA extraction process. PCR with each set of CSA and pyrosequencing primers also included a reaction containing DNA homogenous for the wildtype allele. For pyrosequencing primers a second reaction containing DNA homogenous for the vaccine allele was also included.

2.4. Determining allele frequencies

In the past we have used two methods for determining allele frequencies, comparative sequence analysis (CSA) and pyrosequencing, using primers directed against 35 of 42 vaccine SNPs identified by Gomi et al. [7]. To determine the accuracy of CSA and pyrosequencing, we used primer sets which amplify fragments containing the nucleotide present at position 108838 (supplementary Tables 1 and 2). These fragments were cloned into the *Eco*RI site of a pUC based pCR2.1 vector using a TA Cloning Kit in accordance with the manufacturer's instructions (Invitrogen, UK) and transformed into One Shot competent TOP10 *Escherichia coli* (Invitrogen, UK). Clones containing the vector plus insert were isolated and the DNA was purified using a QIAprep Spin Miniprep Kit (Qiagen, UK) according to the manufacturer's instructions. The DNA concentration was measured on a Gene Spec I Spectrophotometer (Nalca Instruments Ltd., UK) and Tris–EDTA (10 mM) was used to normalise the concentrations (i.e. DNA from clones containing the wildtype allele and clones containing the vaccine allele were both diluted to a concentration of 200 ng/μl each). DNA from clones containing the wildtype SNP at 108838, and clones containing the vaccine SNP at 108838, were then mixed in ratios of 100:0, 90:10, 70:30, 50:50, 30:70, 10:90 and 5:95. The allele frequencies at position 108838 were analysed in triplicate by CSA and pyrosequencing using published methods [13,16]. For mixtures where the one allele was present at <10%, the experiment was repeated, giving six readings per SNP rather than just three. Relative SNP percentages were calculated automatically for the pyrosequencing, by measuring the area under the curve for loci with dual peaks. The relative percentages for CSA were calculated according to the method described by Mattocks et al. [16].

Table 1
Vaccines used in this study.

Company	Vaccine[a]	Year (country) of purchase	Number of SNPs analysed
Merck	Batch 1: Lot 1 (A)	2003 (U.K.)	35
	Batch 2: Lot 1 (B)	2004 (U.K.)	15
	Batch 2: Lot 2 (C)	2005 (U.K.)	15
	Batch 3: Lot 1 (D)	2005 (U.S.)	15
	Batch 3: Lot 2 (E)	2005 (U.S.)	15
GSK	Batch 1: Lot 1 (1)	2003 (U.K.)	35
	Batch 2: Lot 1 (2)	2008 (U.K.)	15
	Batch 2: Lot 2 (3)	2008 (U.K.)	15
	Batch 2: Lot 3 (4)	2008 (U.K.)	15
	Batch 3: Lot 1 (5)	2010 (U.K)	15

[a] Vaccine lot identifiers were anonymised for the purpose of this study. Numbers and letters in parenthesis are abbreviated identifiers for each vaccine.

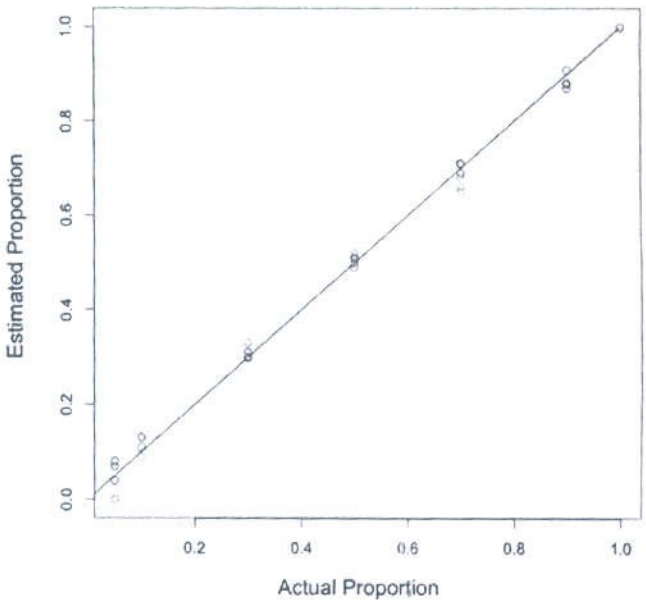


Fig. 2. Calibration of the two different methods for determining the frequency of alleles at polymorphic loci. The three estimates obtained by pyrosequencing (black symbols) and three obtained by CSA (grey symbols) are plotted for each mixture, along with a 1:1 line illustrating the known frequency.

2.5. Statistical methods

The significance of the genetic differences among the various vaccines was evaluated using generalized linear modelling of the arcsine transformed allele frequencies.

3. Results

3.1. Comparison of CSA and pyrosequencing for allelic quantification

The accuracy of CSA and pyrosequencing for allele mixtures were comparable (Fig. 2), but the pyrosequencing was significantly closer to the true proportions ($P=0.012$): the standard deviation around the known frequency being 0.016 (max. 0.03) compared to 0.027 (max. 0.05) for CSA. When the mixtures of allele frequencies were at their most different, the pyrosequencing still detected the lowest frequency allele, whereas CSA did not (Fig. 2). Because of this greater sensitivity and reproducibility, pyrosequencing was used for further analyses. When quantifying alleles in the vaccines, if the wildtype allele was detected at ≤10%, the PCR and relevant assay was repeated.

3.2. Variation in lots of Oka/GSK and Oka/Merck

The allele frequencies observed at the fifteen loci analysed in all of the GSK and Merck lots are given in Table 2. Three of the loci were fixed for the novel vaccine allele (560, 106262 and 107252). With the exception of positions 89734 which retained the ancestral allele in all Merck batches, and 105724 which retained the ancestral

62

Table 2
Variation in lots of Oka/GSK and Oka/Merck.

SNP[a]	ORF	P-Oka[b]	Oka/GSK lots[c,e]					Oka/Merck lots[d,e]				
			A	B	C	D	E	1	2	3	4	5
560	5' non-cod	T	0	0	0	0	0	0	0	0	0	0
19431	14	T	61	57	57	57	64	79	81	80	85	83
58595 (530)	31	A	71	67	67	68	78	45	46	48	47	49
87280	50	A	100	84	80	74	100	100	85	85	85	87
89734	51	A	24	25	25	25	19	100	100	100	100	100
97748 (585)	55	G	45	56	50	58	30	61	56	64	67	60
105169	61/62	A	50	21	21	21	61	56	50	53	53	51
105356 (1260)	62	T	13	6	0	0	0	34	36	31	33	31
105705	62	T	11	0	0	0	0	51	0	0	0	0
105724 (1137)	62	A	100	100	100	100	100	93	81	82	81	100
106262 (958)	62	T	0	0	0	0	0	0	0	0	0	0
107136	62	T	40	0	32	33	0	50	50	48	48	46
107252 (628)	62	T	0	0	0	0	0	0	0	0	0	0
107797 (446)	62	A	69	55	56	55	55	70	75	68	68	68
108838 (99)	62	A	100	60	60	63	60	100	76	75	77	75

[a] Numbers refer to the nucleotide position in Dumas; numbers in parenthesis refer to the affected amino acid residue within a particular ORF.
[b] P-Oka bases are identical to those in Dumas at every position; P-Oka sequence is from Gomi et al. [7].
[c] Oka/GSK-A was analysed by CSA, Oka/GSK-B, -C & -D were analysed by pyrosequencing.
[d] Oka/Merck-1 was analysed by CSA, Oka/Merck-2, -3, -4 & -5 were analysed by pyrosequencing.
[e] Numbers refer to the percentage wildtype allele.

allele in all GSK batches, the remaining loci were a mixture of the of the ancestral (wildtype) allele and the vaccine allele in varying proportions.

3.3. Comparison between and within Merck and GSK Oka vaccine preparations

The percentage wildtype alleles present in the vaccine preparations from Merck and GSK for 15 of the 42 loci known to differ between pOka and the Oka Biken vaccine preparation are shown in Fig. 3 (data in Table 2). As can be seen in Fig. 3, there is a strong correlation between the allele frequencies in the vaccines from the two companies ($r = 0.79$, $P = 0.0005$). The implications of this result are discussed further (see below). For each vaccine we compared genetic variation between different lots from the same batch, between different batches of the same vaccine and between the two vaccine preparations. There was a significant trend across most loci for the Merck vaccine preparations to have higher frequencies of the wildtype allele ($P = 3.422 \times 10^{-5}$), as illustrated in Fig. 3. There was significant batch to batch variation between the three Merck batches ($P = 7.181 \times 10^{-7}$) and between the three GSK batches ($P = 9.697 \times 10^{-10}$). Although the amount of variation between batches was not significantly different for the two vaccine companies ($P = 0.160$), there was significantly more variation in allele frequencies among lots from a single batch of GSK vaccine compared to lots from a single batch of Merck vaccine ($P = 0.006$). The implications of these between and within-vaccine variations are discussed.

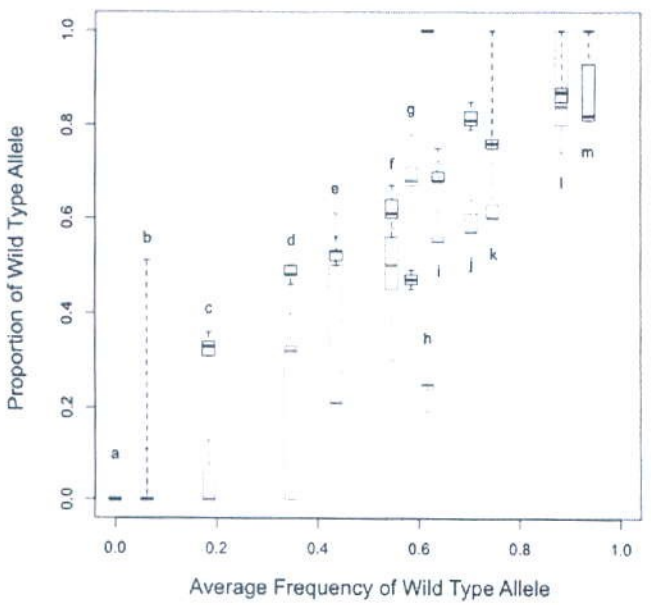


Fig. 3. Comparison of range and average allele frequencies at polymorphic sites in Oka/Merck (black) and Oka/GSK (grey) vaccines. The whiskers on the box plots represent the full range of estimates of the wildtype allele, from the three batches obtained from each company; the box illustrates the inter-quartile range. The band inside the box represents the median value. Letters indicate the SNP position as below: a–560, 106262, 107252; b–105705; c–105356; d–107136; e–105169; f–97748; g–58595; h–89734; i–107797; j–19431; k–108838; l–87280; m–105724.

4. Discussion

We and others [10,11,13] have confirmed that the Oka vaccine comprises multiple haplotypes, each of which contains different numbers of vaccine mutations. Our data show three important findings. First, we confirm previous reports of the loss of wildtype alleles in the GSK as compared to Merck at 4 loci (560, 105705, 106262 and 107252), particularly where the wildtype allele was rare (i.e. at low frequency). Additionally, we show that where loci are mixed for vaccine and wildtype SNPs, the frequency of the wildtype allele at these loci is on average lower in the GSK than in the Merck vaccine. These findings are likely to be explained by production differences. Prior to development of the commercial vaccine in the 1980s, Smith Kline Beecham attempted to produce a genetically uniform vaccine—as a part of this the GSK seed lot underwent serial terminal dilutions in WI38 cells before further passages in MRC5s to generate the GSK working seed lot and vaccine stocks (Fig. 1). At the very least, this would be expected to reduce the amount of variability present in the vaccine mixture, if not indeed succeeding in making the vaccine genetically uniform. In contrast, the Merck vaccines are derived directly from the seed stock without any attempted purification before further passages in MRC5 cells ([7], Merck Product information IPC-VRV3-I-032008—summarised in Fig. 1), and are therefore expected to be more of a mixture of multiple haplotypes, as in the original seed stock.

Our second observation is that despite the differences in production processes, the allele frequencies in the Merck and GSK vaccines are strongly correlated (Fig. 3). This is an unexpected observation. If the vaccine alleles were simply neutral in the *in vitro* environment of vaccine production one would not expect to see a correlation in allele frequencies between the two vaccines given the differences in the manufacturing process (Fig. 1). Taking into consideration the GSK terminal dilution procedures, there are two possible explanations. If we assume that the GSK process succeeded in producing a genetically uniform vaccine, then the vaccine alleles could have arisen by *de novo* mutation and spread in the GSK production line after purification had occurred. However, two questions then arise: why have the vaccine mutations appeared at the same loci and with approximately the same frequency, as the Merck vaccine, and what would explain the lower frequency of the ancestral alleles in the GSK vaccine? One possibility is that both the Merck and GSK production processes select for the same intermediate allele frequencies, but that the GSK values have had insufficient time to reach this stable "optimum" value through the accumulation of mutations following the loss of the ancestral allele during the process of serial terminal dilutions. An alternative explanation is that the GSK serial dilutions did not result in a genetically uniform population but rather one that remained polymorphic with approximately the same allele frequencies as the original seed mixture. Both explanations would account for the lower frequency of the ancestral allele in GSK batches at those loci where the ancestral allele was initially rare in the seed stock, since it is the rare alleles that would tend to be lost by serial dilution and be prone to ascertainment bias (whereby rare alleles would have been detected if they were slightly more common in the Merck population but not vice versa). The fact that the ancestral allele is rarer in GSK at all but two loci (Fig. 3, 58595 and 87280), suggests a third possibility: that some difference in the Merck production favours selection of the ancestral alleles at the majority of loci.

Finally, we have observed that the Merck vaccine has more similar allele frequencies between lots of the same batch, than does the GSK vaccine. If the variation between lots were due to chance (i.e. random genetic drift), then this observation would imply that the Merck protocols maintain larger sample sizes of virus at each generation than the GSK, as the effects of genetic drift are more pronounced in smaller populations than larger populations. Alternatively, if as suggested earlier, selection is occurring in the Merck production process, this could explain the more similar allele frequencies observed in the Merck vaccines than the GSK.

In summary, our data suggest that evolutionary processes do influence production of live attenuated vaccines and affect their composition. We have focused on variable loci that have previously been identified as being of potential biological importance for vaccine attenuation and as immune targets [13]. However, there is evidence to suggest other loci may also play a key role in attenuation [17]. More extensive sequencing of different batches and lots from each source would give a better idea of the allele frequencies present at all variable loci, allowing us to distinguish between the different hypotheses described here as they make different predictions. If the lower frequency of ancestral alleles in GSK batches were due to ascertainment bias, this trend would disappear once all loci were sequenced. If the trend were due to the loss of rare alleles in the GSK production line, more extensive sequencing would reveal a pattern in which the GSK allele frequencies were more extreme than those in Merck batches, i.e. closer to zero in GSK at loci where they were rare in Merck batches, and closer to one where they were common. Finally, if there were genome-wide selection against ancestral alleles in GSK, that trend should be apparent across most vaccine loci irrespective of their frequency. Our analyses of the differences in allele frequencies between the vaccines provide an insight into the various evolutionary processes that are clearly affecting the composition of live attenuated vaccines. The data suggest that both batch to batch variation and variation between vaccines manufactured by different companies is not insignificant. To date, there is little evidence that the differences between the GSK and Merck vaccines or the batch to batch variation, affect efficacy or safety. However, a recent paper reported more breakthrough infections in children immunized with one dose of the GSK vaccine as compared with the Merck preparation, although the differences were not significant [18]. A previous publication also reported lower antibody titres following vaccination with the GSK preparation as compared to the Merck, albeit in the context of co administration of MMR vaccine [1]. Whether these data reflects greater variation in batch to batch immunogenicity of the GSK vaccine remains to be established. Nonetheless, understanding the evolutionary processes influencing this vaccine is clearly an important consideration for continued quality assurance of production.

Acknowledgements

RKK was funded by the Medical Research Council (grant no. G0700814). JB receives funding from the UCL/UCLH Collaborative Biomedical Research Centre. We thank the MRC Centre for Molecular Virology (grant no. G0900950) for infrastructure support.

Appendix A. Supplementary data

Supplementary data associated with this article can be found, in the online version, at doi:10.1016/j.vaccine.2011.02.021.

References

[1] Lau YL, Vessey SJ, Chan IS, Lee TL, Huang LM, Lee CY, et al. A comparison of safety, tolerability and immunogenicity of Oka/Merck varicella vaccine and VARILRIX in healthy children. Vaccine 2002;20(23–24):2942–9.
[2] Sharrar RG, LaRussa P, Galea SA, Steinberg SP, Sweet AR, Keatley RM, et al. The postmarketing safety profile of varicella vaccine. Vaccine 2000;19(7–8):916–23.
[3] Galea SA, Sweet A, Beninger P, Steinberg SP, Larussa PS, Gershon AA, et al. The safety profile of varicella vaccine: a 10-year review. J Infect Dis 2008;197(Suppl. 2):S165–9. Review.
[4] Goulleret N, Mauvisseau E, Essevaz-Roulet M, Quinlivan M, Breuer J. Safety profile of live varicella virus vaccine (Oka/Merck): five-year results of the European Varicella Zoster Virus Identification Program (EU VZVIP). Vaccine 2010;28(36):5878–82.
[5] Quinlivan M, Breuer J. Molecular studies of Varicella zoster virus. Rev Med Virol 2006;16(July–August (4)):225–50. Review.
[6] Takahashi M, Otsuka T, Okuno Y, Asano Y, Yazaki T. Live vaccine used to prevent the spread of varicella in children in hospital. Lancet 1974;2(7892):1288–90.
[7] Gomi Y, Sunamachi H, Mori Y, Nagaike K, Takahashi M, Yamanishi K. Comparison of the complete DNA sequences of the Oka varicella vaccine and its parental virus. J Virol 2002;76(November (22)):11447–59.
[8] Gomi Y, Imagawa T, Takahashi M, Yamanishi K. Oka varicella vaccine is distinguishable from its parental virus in DNA sequence of open reading frame 62 and its transactivation activity. J Med Virol 2000;61(August (4)):497–503.
[9] Quinlivan MA, Gershon AA, Nichols RA, La Russa P, Steinberg SP, Breuer J. Vaccine Oka varicella-zoster virus genotypes are monomorphic in single vesicles and polymorphic in respiratory tract secretions. J Infect Dis 2006;193(7):927–30.
[10] Loparev VN, Rubtcova E, Seward JF, Levin MJ, Schmid DS. DNA sequence variability in isolates recovered from patients with postvaccination rash or herpes zoster caused by Oka varicella vaccine. J Infect Dis 2007;195(4):502–10.
[11] Tillieux SL, Halsey WS, Thomas ES, Voycik JJ, Sathe GM, Vassilev V. Complete DNA sequences of two oka strain varicella-zoster virus genomes. J Virol 2008;82(November (22)):11023–44.
[12] Quinlivan ML, Gershon AA, Steinberg SP, Breuer J. Rashes occurring after immunization with a mixture of viruses in the Oka vaccine are derived from single clones of virus. J Infect Dis 2004;190(4):793–6.
[13] Quinlivan ML, Gershon AA, Al Bassam MM, Steinberg SP, LaRussa P, Nichols RA, et al. Natural selection for rash-forming genotypes of the varicella-zoster vaccine virus detected within immunized human hosts. Proc Natl Acad Sci USA 2007;104(1):208–12.
[14] D'Hondt E, Berge E, Colinet G, Duchene M, Peetermans J. Production and quality control of the Oka-strain live varicella vaccine. Postgrad Med J 1985;61(Suppl. 4):53–6.
[15] Frey CR, Sharp MA, Min AS, Schmid DS, Loparev V, Arvin AM. Identification of CD8+ T cell epitopes in the immediate early 62 protein (IE62) of varicella-zoster

virus, and evaluation of frequency of CD8+ T cell response to IE62, by use of IE62 peptides after varicella vaccination. J Infect Dis 2003;188(1):40–52.
[16] Mattocks C, Tarpey P, Bobrow M, Whittaker. comparative sequence analysis (CSA): a new sequence-based method for the identification and characterization of mutations in DNA. J Hum Mutat 2000;16(November (5)):437–43.
[17] Zerboni L, Hinchliffe S, Sommer MH, Ito H, Besser J, Stamatis S, et al. Analysis of varicella zoster virus attenuation by evaluation of chimeric parent Oka/vaccine Oka recombinant viruses in skin xenografts in the SCIDhu mouse model. Virology 2005;332(1):337–46.
[18] Spackova M, Wiese-Posselt M, Dehnert M, Matysiak-Klose D, Heininger U, Siedler A. Comparative varicella vaccine effectiveness during outbreaks in day-care centres. Vaccine 2010;28(3):686–91. Erratum in: Vaccine. 2010 May 7;28(21):3754.

Areko 5

65

SUPPLEMENT ARTICLE

Molecular Analysis of the Oka Vaccine Strain of Varicella-Zoster Virus

Koichi Yamanishi

National Institute of Biomedical Innovation, Ibaraki, Osaka, Japan

Live attenuated Oka vaccine was subjected to molecular analysis, with the long-term goal of identifying genes in the vaccine strain responsible for its attenuation. Complete genomic sequences for both the Oka parent virus and the Oka vaccine virus were determined and compared. There were differences in only 42 bases between the 2 viruses. More than one-third (15/42) of the nucleotide substitutions in V-Oka were found in open reading frame (ORF) 62. These differences were also observed when sequences of Japanese low-passage clinical isolates of varicella-zoster virus (VZV) were compared with the Oka vaccine strain. The ORF62 gene encodes an immediate early (IE) protein, IE62, that is the major transactivator of VZV and, as such, is critical to initiating the VZV gene expression cascade. Several insertions and deletions were also observed in comparing the 2 sequences, largely in the internal tandem repeat units. Functional differences between the 2 types of Oka virus were also examined. Oka vaccine was found to consist of a mixture of different subpopulations, and the parental Oka virus replicates more efficiently than does the vaccine strain. Development of a bacterial artificial chromosome for VZV expression should lead to the discovery of additional differences in wild and vaccine types and, thus, enhance our understanding of the genetic basis for attenuation of the Oka vaccine strain.

Live attenuated varicella vaccines derived from the parent Oka (P-Oka) strain of varicella-zoster virus (VZV) are used routinely to prevent or modify the severity of varicella in children in Japan and many other countries [1–4]. The vaccine Oka strain (V-Oka) was developed by Takahashi and colleagues, using the empirical approach of passing P-Oka, which is a clinical isolate recovered from skin lesions of a child with varicella, in cultured human and guinea pig cells [5]. Attenuation of V-Oka was established clinically by inoculating susceptible children. These children had no signs of varicella, developed VZV IgG antibodies, and were protected from illness when they were exposed to wild-type VZV. Attenuation was also demonstrated by the reduced virulence of V-Oka in immunocompromised children with leukemia or other immunosuppressive conditions [5–9]. Finally, V-Oka exhibits a low secondary transmission rate in comparison with wild-type VZV, with secondary transmission occurring only when the vaccine recipient had cutaneous lesions, and cases of varicella resulting from secondary V-Oka transmission are characteristically mild [10, 11]. The development of live varicella vaccine was accomplished before methods were available to investigate the genetic basis for V-Oka attenuation. New tools can now be used to clarify what molecular changes were introduced that distinguish P-Oka and V-Oka and which of those changes are likely to be associated with the reduced pathogenicity of V-Oka. Conceivably, the results from such studies could drive the future development of a molecularly engineered immunogenic vaccine that lacks any functional VZV virulence genes. Here, we summarize our work related to understanding the molecular mechanisms of V-Oka attenuation.

COMPARISON OF THE DNA SEQUENCES OF V-OKA AND P-OKA VIRUSES

The first approach that we used to investigate V-Oka attenuation was to sequence the complete genomes of

Potential conflicts of interest: K.Y. has participated as a speaker at events sponsored by Research Foundation for Microbial Diseases of Osaka University.

Financial support: supplement sponsorship is detailed in the Acknowledgments.

Reprints or correspondence: Dr. Koichi Yamanishi, Dept. of Microbiology, Osaka University Medical School, 2-2 Yamada-oka, Suita, Osaka 565-0871, Japan (yamanishi@nibio.go.jp).

The Journal of Infectious Diseases 2008; 197:S45–8

© 2008 by the Infectious Diseases Society of America. All rights reserved.

0022-1899/2008/19705S2-0003$15.00

DOI: 10.1086/522122

V-Oka and P-Oka, on the basis of the hypothesis that correlations between DNA sequence and virulence could be identified. The full-length DNA sequences of V-Oka and P-Oka were determined by amplifying regions across the whole genome by polymerase chain reaction (PCR), followed by cloning and direct sequencing of the PCR products [12]. When the complete DNA sequences of V-Oka and P-Oka viruses were compared, only 42 bases were found to be different (figure 1). These differences did not include the substitutions in the terminal repeat segment (TRS), because these changes are duplicated in the internal repeat segment (IRS) of the VZV genome.

The DNA sequence information was used to predict amino acid sequences of predicted VZV gene products [12]. This analysis revealed that base substitutions at 20 nucleotide positions in V-Oka would result in amino acid conversions, and base substitutions at 17 nucleotide positions were silent mutations. The remaining 5 base substitutions occurred in noncoding regions. At 30 positions, alternative base substitutions appeared in V-Oka, indicating that V-Oka contained a mixture of genomes that differed with respect to the particular nucleotide (figure 1). Fifteen of these substitutions resulted in differences between the amino acid residues in the respective V-Oka gene products, so that V-Oka was predicted to contain viruses with variations in the amino acid at each of these positions. Surprisingly, more than one-third (15/42) of the nucleotide substitutions in V-Oka were found in open reading frame (ORF) 62 and therefore in the duplicated gene, ORF71, and its flanking regions. Approximately half (8/20) of the predicted amino acid substitutions resulted from nucleotide substitutions within ORF62. This observation of enhanced variability in the ORF62 region was of particular interest because ORF62 and ORF71 encode the immediate early (IE) 62 protein, which is the major viral transactivator of VZV and directs the transcription of all VZV genes required for its replication and for the production of progeny virions. In addition to the changes in IE62, 12 other amino acid substitutions were identified on the basis of differences in the V-Oka and P-Oka DNA sequences. These mutations occurred in ORFs 6, 9A, 10, 21, 31, 39, 50, 52, 55, 59, and 64. Among these, the gene products for which the characteristics, functions, or predicted functions are known include ORF6 (helicase primase complex), ORF10 (tegument/regulatory protein), ORF21 (nucleocapsid), ORF31 (glycoprotein B), ORF39 (integral membrane protein), ORF50 (glycoprotein M), ORF55 (helicase primase complex), and ORF59 (uracil DNA glycosylase).

In addition to the nucleotide substitutions, the V-Oka sequence had several deletions and insertions, compared with P-Oka in certain regions, including the tandem repeat regions and the origin of DNA replication. The VZV genome has 5 repeat regions, designated R1, R2, R3, R4, and R5, that appear

Position	ORF	Oka vaccine	Oka parent
560	5'/1	C (NCR)	T (NCR)
703	1	T/C(Gln)	T (Gln)
753	1	T/C(Pro)	T (Pro)
2515	3/4	T/C(NCR)	T (NCR)
5745	6	G (Pro)	A (Ser)
10900	9A	T/C(Trp/Arg)	T (Trp)
12779	10	T/C(Ala/Val)	T (Ala)
19431	14	T/C(Stop)	T(Stop)
26125	18	G (Asn)	A (Asn)
31732	21	T/C(Thr/Ile)	C (Thr)
38036	22	T/C(Thr)	T (Thr)
39227		T/G(Pro)	T (Pro)
58595	31	A/G(Ile/Val)	A (Ile)
59287		A/G(Pro)	A (Pro)
64067	35	A/G(Ala)	A (Ala)
71252	39	T/C(Met/Thr)	T (Met)
82225	45	A/G(Pro)	A (Pro)
84091	47	A/G(Glu)	G (Glu)
87280	50	A/G(Cys)	A (Cys)
87306		T/C(Ser/Gly)	T (Ser)
89734	51	A/G(Thr)	A (Thr)

Position	ORF	Oka vaccine	Oka parent
90535	52	A/G(Ile/Val)	A (Ile)
94167	54	C (Leu)	T (Leu)
97748	55	G/A(Ala/Thr)	G (Ala)
97796		T/C(Cys/Arg)	T (Cys)
101099	59	A/G(Leu/Pro)	A (Leu)
105169	61/62	A/G(NCR)	A (NCR)
105310	62	A/G(Leu/Ser)	A (Leu)
105356		C (Val)	T (Ile)
105544		G (Ala)	A (Val)
105705		C (Ala)	T (Ala)
106282		C (Gly)	A (Arg)
106710		A/G(Ala)	A (Ala)
107136		C (Ala)	T (Ala)
107252		C (Gly)	T (Ser)
107599		A/G(Val/Ala)	A (Val)
107797		A/G(Leu/Pro)	A (Leu)
108111		C (Pro)	T (Pro)
108838		A/G(Met/Thr)	A (Met)
109137	62/63	A/G(NCR)	A (NCR)
109200		A/G(NCR)	A (NCR)
111660	64	A/G(Gln/Arg)	A (Gln)

Figure 1. Mutations between the Oka vaccine virus (V-Oka) and the parent virus (P-Oka). NCR, noncoding region; ORF, open reading frame. Adapted from [12], with permission from the American Society for Microbiology.

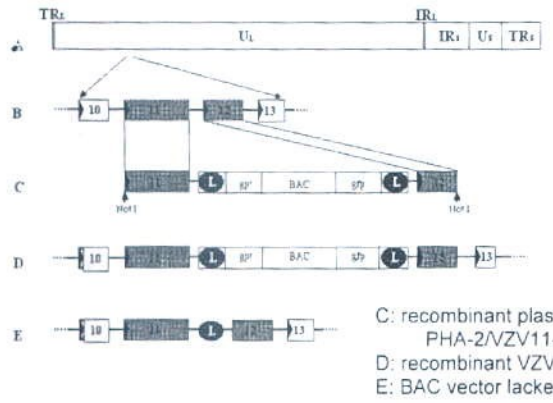


Figure 2. Construction of the varicella-zoster virus (VZV) genome bacterial artificial chromosome (BAC) in *Escherichia coli*. The VZV genome *(A)* is approximately 125 kbp long and consists of terminal repeat (TR), unique long (UL), internal repeat (IR), and unique short (US) DNA domains. The recombinant plasmid, PHA-2/VZV11-12 *(C)*, contained 2.0 kbp each of 2 sequences from VZV *(shaded boxes 11 and 12)*, as well as the BAC vector, the *gpt* gene, and the *gfp* gene, flanked by *lox*P sites. The open reading frame (ORF) 11 and ORF12 fragments of the genome of the VZV wild-type strain, P-Oka *(shaded boxes 11 and 12)* were generated by polymerase chain reaction amplification using the appropriate primers. The recombinant VZV rV01 *(D)* was generated by transfection of the VZV BAC plasmid into HEL cells. The recombinant VZV rV02, which lacked the BAC vector sequences *(E)*, was generated by superinfection of VZV rV01 and a recombinant adenovirus, AxCANCre. The VZV rV02 contains a single *lox*P site. The circle enclosing an L represents the *lox*P site. Adapted from [15].

in ORFs 11, 14, and 22 and in the intergenic regions between ORFs 62 and 63 (and the corresponding region between 70 and 71), and between ORFs 60 and 61, respectively. The length of the repeats in regions R1, R3, and R4 were variable in V-Oka. The VZV genome contains an origin of replication in the IRS, which is duplicated in the TRS; each origin region is ~270 bp in length. The P-Oka genome contained 269 bp in this region and was 8 bp longer than V-Oka. The average full-length genome of V-Oka was slightly longer than that of P-Oka because of these insertions and deletions.

BIOLOGICAL COMPARISON OF V-OKA AND P-OKA VIRUSES

When the sequencing of V-Oka revealed that it consisted of a mixture of subpopulations with some sequence differences, viruses were isolated from V-Oka by plaque purification [13, 14]. Thirteen V-Oka isolates were obtained. When ORF62 was amplified and sequenced from each isolate, one clone, designated S7-01, had all of the 8 predicted amino acid substitutions compared with P-Oka. In contrast, another clone, S7-13, had the minimum number of substitutions compared with P-Oka, with only 5 predicted changes in amino acid residues. Therefore, these 2 clones were chosen to determine whether the ORF62 mutations correlated with differences in the replication of S7-01 and S7-13. A comparison of the plaque sizes of S7-01, S7-13, V-Oka, and P-Oka showed that P-Oka produced the largest plaques. V-Oka and S7-13 showed relatively larger plaques than S7-01. In particular, S7-01 showed significantly smaller plaques compared with P-Oka ($P < .01$). When these V-Oka progeny viruses, V-Oka, and P-Oka were compared by infectious center assay using human embryonic lung fibroblasts, the number of cells infected by P-Oka was 2.1-fold, 4.2-fold, and 2.6-fold higher than the number infected by V-Oka, S7-01, and S7-13, respectively. These results suggested that the efficiency of viral replication differed slightly among the V-Oka clones and that P-Oka replication was relatively more efficient than V-Oka replication.

To further assess the biological significance of differences at ORF62 of the V-Oka clones and P-Oka, the capacity of each version of IE62 to transactivate the ORF28 (VZV polymerase) promoter was evaluated. IE62 has well-established transactivating effects on this promoter. A reporter plasmid, pLuc-Pol, that had the DNA polymerase promoter upstream of the luciferase ORF was constructed and used for transient luciferase assays. The mutant IE62s expressed by the V-Oka variants were predicted to have less transactivating activity than IE62 encoded by P-Oka. The results of the luciferase assays showed trends that were consistent with the differences observed between P-Oka and V-Oka variants in mean plaque size and in infectious center assays. These findings support the possibility that both viral replication and cell-cell spread may be diminished in V-Oka because of altered potency of IE62 for inducing VZV gene transcription.

ORF10 protein, which is a homologue of herpes simplex virus type 1 VP16, is a virion-associated transactivator that can stimulate transcription from the ORF62 promoter. The base substitution identified in ORF10 caused a predicted amino acid conversion. Given the importance of IE62 as the major VZV transactivating protein, this change had the potential to affect V-Oka replication. However, when the ORF10 proteins encoded by V-Oka and P-Oka were compared for their capacities to enhance transcription from the ORF62 promoter, the P-Oka ORF10 gene product was somewhat more potent, but this difference was not significant.

GENETIC DIFFERENTIATION OF V-OKA VIRUS FROM OTHER CLINICAL ISOLATES OF VZV

To demonstrate that the changes in ORF62 were associated with the process of P-Oka attenuation by passage in cultured cells to generate V-Oka, clinical isolates were evaluated to determine the nucleotide sequence of ORF62 [13, 14]. All of the low-passage clinical isolates of VZV differed from V-Oka at the same 15 bases that were found to be different between V-Oka and P-Oka. The differentiation of V-Oka from other clinical

isolates, including P-Oka, was also evident from changes that altered the cleavage sites for *Bss*HII and *Nae*I to a unique pattern in V-Oka. V-Oka was successfully identified using 7 of 8 enzymes, with the exception of *Mae*II. On the basis of PCR and restriction enzyme digestion, all 54 VZV clinical isolates were shown to have sequence differences from V-Oka. Thus, the empirical attenuation of V-Oka introduced genetic changes in V-Oka that resulted in a mixture of genetic variants that appear to differ consistently from wild-type VZV.

DEVELOPMENT OF A BACTERIAL ARTIFICIAL CHROMOSOME (BAC)

A more complete analysis of the mutations in V-Oka that lead to its attenuation may be accomplished by introducing the changes observed by PCR and sequencing as single mutations or combinations of mutations into the P-Oka genome. Toward this end, we have developed a BAC that contains the P-Oka genome (figure 2) [15]. After electroporation into *E. coli* strain DH10B, the VZV BAC was stably propagated over multiple generations of its host. Human embryonic lung cells transfected with VZV BAC DNA that was recovered from DH10B showed cytopathic effects, and spread of the virus to neighboring cells was observed. The BAC vector sequences are flanked by *lox*P sites, and coinfection of the reconstituted virus with a recombinant adenovirus expressing Cre recombinase removed the residual bacterial sequences. The resulting recombinant, designated rV02, replicated as well as the parental virus in cultured cells. This P-Oka BAC should facilitate the next phase of investigations of the molecular mechanisms of V-Oka attenuation.

Acknowledgments

Supplement sponsorship. This article was published as part of a supplement entitled "Varicella Vaccine in the United States: A Decade of Prevention and the Way Forward," sponsored by the Research Foundation for Microbial Diseases of Osaka University, GlaxoSmithKline Biologicals, the Sabin Vaccine Institute, the Centers for Disease Control and Prevention, and the March of Dimes.

References

1. National Advisory Committee on Immunization. An Advisory Committee Statement (ACS). National Advisory Committee on Immunization (NACI). NACI update to statement on varicella vaccine. Can Commun Dis Rep **2002**; 28(ACS-3):1–7.
2. División Epidemiología. Boletín Oficial 2001: coberturas vacunales. Montevideo, Uruguay: Ministerio de Salud Pública, **2001**.
3. National Health and Medical Research Council. The Australian immunisation handbook. 8th ed. Canberra: Australian Government Publishing Service, **2003**:240–52.
4. Pinot de Moira A, Nardone A. Varicella zoster virus vaccination policies and surveillance strategies in Europe. Euro Surveill **2005**; 10:43–5.
5. Takahashi M, Otsuka T, Okuno Y, et al. Live vaccine used to prevent the spread of varicella in children in hospital. Lancet **1974**; 2:1288–90.
6. Ueda K, Yamada I, Goto M, et al. Use of a live varicella vaccine to prevent the spread of varicella in handicapped or immunosuppressed children including MCLS (muco-cutaneous lymphnode syndrome) patients in hospitals. Biken J **1977**; 20:117–23.
7. Ozaki T, Nagayoshi S, Morishima T, et al. Use of a live varicella vaccine for acute leukemic children shortly after exposure in a children's ward. Biken J **1978**; 21:69–72.
8. Gershon AA, LaRussa P, Steinberg S. The varicella vaccine: clinical trials in immunocompromised individuals. Infect Dis Clin North Am **1996**; 10:583–94.
9. LaRussa P, Steinberg S, Gershon AA. Varicella vaccine for immunocompromised children: results of collaborative studies in the United States and Canada. J Infect Dis **1996**; 174(Suppl 3):S320–3.
10. Arvin AM, Gershon AA. Live attenuated varicella vaccine. Annu Rev Microbiol **1996**; 50:59–100.
11. Grossberg R, Harpaz R, Rubtcova E, Loparev V, Seward JF, Schmid DS. Secondary transmission of varicella vaccine virus in a chronic care facility for children. J Pediatr **2006**; 148:842–4.
12. Gomi Y, Sunamachi H, Mori Y, Nagaike K, Takahashi M, Yamanishi K. Comparison of the complete DNA sequences of the Oka varicella vaccine and its parental virus. J Virol **2002**; 76:11447–59.
13. Gomi Y, Imagawa T, Takahashi M, Yamanishi K. Comparison of DNA sequence and transactivation activity of open reading frame 62 of Oka varicella vaccine and its parental viruses. Arch Virol Suppl **2000**; (17): 49–56.
14. Gomi Y, Imagawa T, Takahashi M, et al. Oka varicella vaccine is distinguishable from its parental virus in DNA sequence of open reading frame 62 and its transactivation activity. J Med Virol **2000**; 61:497–503.
15. Nagaike K, Mori Y, Gomi Y, et al. Cloning of the varicella-zoster virus genome as an infectious bacterial artificial chromosome in *Escherichia coli*. Vaccine **2004**; 22:4069–74.

Anexo6 70 69

ADVANCES IN VIRUS RESEARCH, VOL. 39

PROBLEMS AND PROSPECTS FOR PREPARATION OF KILLED ANTIVIRAL VACCINES

E. I. Budowsky

N. D. Zelinsky Institute of Organic Chemistry
U.S.S.R. Academy of Sciences
Moscow 117913, U.S.S.R.

I. Introduction
II. Principal Requirements for Inactivation Step
III. Principal Requirements for Inactivating Agents
IV. Determination of Minimum Duration of Agent Action
V. Effects of Different Factors on the Kinetics of Infectivity Inactivation
  A. Biological Factors
  B. Chemical Factors
VI. Changes in Virion Immunogenicity Due to Action of Inactivating Agents
  A. Protective and Immunogenic Efficiency of Killed Vaccines
  B. Immunogenic Specificity
  C. Improvement of Killed Vaccines
VII. Conclusion
References

I. Introduction

Immunization is the most efficient way of preventing infectious diseases in humans and domestic animals. However, only about 20 medicinal vaccines have been prepared since the initial work by Jenner, and about a dozen of these have found wide application (Warren, 1986; Murphy and Chanock, 1986). As a conservative estimate, an additional 20 medicinal vaccines for presently known serious diseases need to be developed within the next few years (Warren, 1986). In addition, the WHO and UNICEF programs for protecting children against the gravest infectious diseases, as well as for substantially extending immunization of adults, require a manifold increase in the variety and production of medicinal vaccines. Although there are many more vaccines for veterinary purposes, the variety and production of these vaccines are still insufficient to significantly reduce the loss of cattle and poultry due to infectious diseases, particularly in developing countries.

To increase the availability of a variety of vaccines requires a rational approach and strategy for the production, control, and utilization of

English translation copyright © 1991 by Academic Press, Inc.

vaccines. This article deals with some of the problems and prospects regarding the production of whole-virion killed antiviral vaccines and considers the principles and approaches needed to reduce the time required in developing production techniques and to ensure the safety and efficiency of vaccines.

Because of advances in genetic engineering, much attention has centered on the development of techniques for the production of artificial (synthetic) subvirion vaccines. However, their applicability has remained problematic (Barry *et al.*, 1976; Bittle *et al.*, 1982; McKercher *et al.*, 1985), and only the vaccine against hepatitis B is actually in use at present. There is a lack of scientific principles for constructing artificial vaccines, and the empirical approach, which is expensive and laborious, can yield a satisfactory result only by chance. This is why the prevention of viral diseases in humans and domestic animals is presently based on whole-virion vaccines, either live (attenuated) or killed (inactivated).

An argument against the use of live vaccines, especially in medicine, is not so much the risk of the reversion of an attenuated virus to the original pathogenic type (e.g., Evans *et al.*, 1985), which can be prevented in many cases by the choice or construction of the attenuated virus, but rather the other postvaccinal complications caused by the reproduction of nonpathogenic viruses in the organism (Huppert and Wild, 1984, 1986; Brunell, 1985). Such a reproduction (an increase in the number of virions by many orders of magnitude) is a prerequisite for the induction of the immune response after inoculation with a live vaccine. In principle it is impossible to avoid completely postvaccinal complications caused by live vaccines.

Huppert and Wild (1986) have reviewed some primary events induced by virus reproduction in animal organisms that lead to complications such as damage to the host cell chromosomes (Clifton *et al.*, 1970) and suppression of some functions, including the immune response and the overproduction of interferons (Oldstone *et al.*, 1982). Obviously, the same results can also be induced by reproduction of contaminating virus(es) from the cells or tissues used for the propagation of the virus. Only the suspected contaminants can be detected with the required certainty; all other viruses may escape routine inspection procedures.

Pathological consequences of virus reproduction (e.g., malignancies, autoimmune diseases, neuropathologic disorders, and teratogenic malformations) can manifest themselves long after vaccination, even after the complete clearance of the virus from the organism ("hit and run" mechanism, Galloway and McDougall, 1983), or as a result of virus persistency (Wyatt, 1973; Chantler *et al.*, 1981; Haase *et al.*,

1985). We do not know which of the more recently discovered diseases were found because of improvements in diagnostic methods or were the result of virus reproduction due to immunization with live vaccines widely used over the last decades.

The character, frequency, and gravity of postvaccinal complications depend on the vaccinal strain and the immune status of the vaccine (Brunell, 1985) and therefore cannot be predicted. The safety of each viral strain can only be determined by assessing the consequences, including remote ones, of vaccination on a large population. Such large-scale experiments on humans are only practicable in exclusive cases and are hardly permissible for reasons of humaneness. Therefore, less hazardous, properly prepared, killed vaccines (Norrby, 1987; Willems and Sanders, 1981) must be used in place of living ones.

In the early 1950s, when it was not yet known which components of the virion were responsible for its infectivity and immunogenicity, the reagent (formaldehyde) and production conditions were determined on a purely empirical basis for the killed whole-virion vaccine against poliomyelitis (Salk *et al.*, 1953; Salk and Gori, 1960). The success of this vaccine, which practically eradicated poliomyelitis in the developed countries within a short period of time, was a convincing demonstration of the applicability of killed whole-virion vaccines for the prevention of virus diseases in humans and domestic animals. A number of studies were initiated on production procedures and the properties of killed antiviral vaccines (Salk and Gori, 1960; Schaffer, 1960; Gard, 1957, 1960; Lo Grippo, 1960; Potash, 1968; Hortmann, 1979; Kleczkowski, 1968; Ginoza, 1968).

However, the success of the killed poliomyelitis vaccine gave rise to an unfounded conviction that formaldehyde was the optimal, universal inactivating agent for the production of killed vaccines. This conviction slowed down the development of principles of inactivation of virus infectivity and created obstacles to the assessment of many published (see, e.g., Fulginity *et al.*, 1967; Salk and Salk, 1977; Brooksby, 1981; King *et al.*, 1981; Beck and Strohmaier, 1987) and unpublished data demonstrating the inadequate safety of killed antiviral vaccines prepared with the aid of formaldehyde. The presence of the infectious viruses in some batches of formol vaccines is usually ascribed to a faulty technique at the infectivity inactivation step in vaccine production (King *et al.*, 1981; Beck and Strohmaier, 1987). Such a possibility cannot be completely excluded; however, it is more likely, that the inevitable and uncontrollable restoration of infectivity of the inactivated virus during storage of the vaccine is a result of the reversibility of the reactions of formaldehyde with nucleic acid components (Gard, 1960; McGhee and von Hippel, 1975a,b; Beland *et al.*, 1984). In principle, the

use of formaldehyde cannot ensure the safety of killed antiviral vaccines. Therefore, the use of formaldehyde in the production of killed vaccines, as well as the importation of meat products from the countries using such vaccines in cattle breeding is prohibited in West Germany (Strohmaier, 1987). Attempts are still being made to improve the techniques for inactivation with formaldehyde and even to use this agent in the production of new killed vaccines (see, e.g., Hilleman, 1980; Relyveld and Ben-Efraim, 1983; Girard *et al.*, 1988; Newmark, 1988). The selectivity of formaldehyde with respect to the nucleic acids in the virion is not high. Attempts to improve the safety of vaccines by increasing the concentration or duration of action of formaldehyde led to a significant modification in the viral proteins and glycoproteins (Deng and Beutner, 1974) and hence to a reduction in the efficiency and a distortion in the specificity of the vaccines.

The inadequate safety and efficiency of formol vaccines led to a wide search for new inactivating agents (Gard, 1957, 1960; Lo Grippo, 1960; Potash, 1968; Kleczkowski, 1968; Ginoza, 1968). In the majority of cases, however, the new agents and ways of inactivation differed from those already known only in that they have never been used before and it is unlikely that they would ever be used for the production of killed vaccines. To date only a few agents or techniques have found application in the production of killed vaccines; these include ultraviolet radiation, β-propiolactone, ethyleneimines, etc. These agents are not always helpful in producing safe and efficient killed antiviral vaccines because both the choice of the agent and the determination of inactivation conditions are carried out empirically.

Data on the efficiency of killed vaccines can be contradictory and difficult to interpret, which leads to distorted ideas regarding the production of safe and efficient preparations and the use of killed vaccines. As will be shown below, the shortcomings of the presently used killed vaccines are avoidable: they are due to the absence of scientifically based and properly formulated requirements for the decisive step in the production of killed vaccines—inactivation of the infectivity of the virus-containing starting material.

The present state of virology, immunology, molecular biology, and bioorganic chemistry allows a rigorous statement of the problem and a reasonable choice of the optimal agents and conditions for the selective inactivation of the viral genome in the virion. The possibility of producing safe and highly efficient killed antiviral vaccines for the prevention of most viral diseases in humans and domestic animals is limited only by the availability of the purified virus in sufficient quantities for production of the killed vaccine.

It is not the purpose of this article to review the numerous works (including patents) devoted to the development of production procedures

and to the study of properties of killed antiviral vaccines. The random choice of agents, the empirical adjustment of inactivation conditions, and the use of inappropriate techniques for determining the safety and protective efficiency of preparations make it in most cases impossible to compare published data and assess their significance. Rather, this article refers only to works that recognize both the hopelessness of the empirical approach and the necessity and possibility of the development of methods to produce safe and efficient killed vaccines and appropriate techniques to control the efficiency of preparations.

II. Principal Requirements for Inactivation Step

The main objective of the inactivation step in the production of killed antiviral vaccines is to irreversibly reduce (inactivate) the infectivity of the original virus-containing material to such an extent as to ensure the safety of the vaccine and, at the same time, to retain maximum (possibly, the whole) immunogenicity of the virion, thus securing the protective efficiency of the vaccine.

Safety is the decisive requirement in any medicinal or veterinary preparation. At present, a preparation is considered a safe vaccine if infectivity has been "completely" inactivated, i.e., when any dose of the preparation has a zero probability of causing infection. However, the inactivation of viruses within a population is an aleatory process; therefore the term "complete inactivation" is meaningless. One can only speak of a sufficient inactivation which ensures the statistical (Koshland, 1985) safety of the vaccine, i.e., the maximum admissible probability of an infectious virus being present in annual production of the preparation. It should be emphasized that the strictest laboratory controls cannot guarantee the safety of millions of doses of vaccines which are used for immunization (Henderson, 1952; Gard, 1956). The degree of inactivation of the original virus-containing material necessary for a warranted safety of the vaccine can be estimated as follows. A preparation can be regarded as a safe medicinal vaccine if the probability of its causing infection is only once in 10 to 100 years, i.e., the probability of an infectious virus being present in any annual production of the vaccine does not exceed 10^{-1} to 10^{-2}. Assuming that 10^8 to 10^{10} virions are usually required to immunize an animal (see Mandel, 1985), the sufficient safety of the preparation produced at a rate of 10^6 to 10^8 doses a year will be achieved by a reduction in the infectivity of the original virus-containing material as great as 15 to 20 orders of magnitude. The degree of inactivation of the infectivity of the original

material to ensure the safety of the vaccine is determined by the dangerousness of the corresponding disease for each virus and must be established by medical or veterinary authorities.

The infectivity of a virus is due to its capability to reproduce. A necessary condition for reproduction is the replication of the viral genome, which can be prevented by chemical modification, caused by the action on the virion of various reagents and ionizing or ultraviolet radiation (Kleczkowski, 1968; Ginoza, 1968; Wang, 1976; Fraenkel-Conrat, 1980; Singer and Grunberger, 1986; Strauss *et al.*, 1986). Since these chemical agents modify nucleic acids, they can cause vaccine-cell mutations (see, e.g., Auerbach *et al.*, 1977; IARC Working Group, 1985). Therefore, the presence of inactivating agents in the final product is not acceptable and they should be neutralized or removed from the vaccine before its use.

The action of any agent on the virus evokes modification of not only the nucleic acid responsible for virus infectivity, but also of other virion components responsible for immunogeneity, leading to alteration of protective efficiency and immunogenic specificity of virion (Deng and Beutner, 1974; Onica *et al.*, 1980, 1982), and hence to the protective efficiency of the vaccine. Therefore, rational selection of a suitable agent that can give sufficient inactivation while preserving virus immunogenicity is most important.

III. Principal Requirements for Inactivating Agents

Agents used for the inactivation of infectivity in the production of killed antiviral vaccines should meet a number of requirements as discussed below.

1. *Irreversibility of agent-involving reactions that block replication:* It is evident that a reversible modification of the genome polynucleotide can result in the restoration of the infectivity of the inactivated virus during storage (Gard, 1960; Budowsky and Pashneva, 1971). For the production of killed vaccines, agents that reversibly modify nucleic acids, such as aldehydes, e.g., formaldehyde (McGhee and von Hippel, 1975a,b) and glyoxal (Broude and Budowsky, 1971), and nucleophilic agents, e.g., bisulfite (Hayatsu, 1976) and hydroxylamine (Budowsky *et al.*, 1972), cannot be used. It should be noted, however, that the action of the majority of chemical agents leads to an irreversible modification of nucleic bases (Kochetkov and Budowsky, 1972; Singer and Grunberger, 1986).

2. *Selectivity:* The action of the agent must preferentially lead to modification of the nucleic acid inside the virion. An increase in selectivity increases the reliability of the technology used to produce killed

vaccines. The data available concerning the chemistry of nucleic acids, proteins, lipids, and other virion components permit a reasonable choice of appropriate agents or the synthesis of new ones having an adequate degree of selectivity for the various viruses which differ in the type of genome polynucleotide, composition, and physical stability of the virion.

The most promising agents are those whose selectivity is due not so much to peculiarities in chemical reactivity but to the possibility of their concentration increase near the polynucleotide of the virion. This is possible in cases where the agent has an increased affinity to the polynucleotides by virtue of the formation of specific complexes, e.g., owing to intercalation (Berman and Young, 1981; Hearst and Thiry, 1977) or the positive charge of the reactant (Budowsky and Zalesskaya, 1985) (for more details, see section VI, C).

In addition to the above general requirements, there are also a number of specific ones, dependent on physical and biological factors. Physical factors include the stability of the virion during and after inactivation. Because the destruction of the virion leads to a dramatic reduction in immunogenicity, this factor should also be taken into consideration when choosing an appropriate inactivating agent and when determining the minimum and maximum duration of inactivation. In order to increase the physical stability of the virion, bifunctional agents, e.g., diepoxybutane, which induces formation of protein–protein (Baumert *et al.*, 1978) and polynucleotide–protein cross-links (Sköld, 1981), along with modification of the polynucleotide, should be used. Biological factors include the repair of lesions in the viral DNA inside the infected cell (Friedberg, 1984). The repair efficiency depends not only on the type and physiological state of the cell but also on the nature of the damage. For the inactivation of the infectivity of viruses containing double-stranded DNA, agents are preferred whose action results in the formation of DNA lesions that are difficult to repair, such as interchain cross-links in polynucleotides [caused by bifunctional alkylating agents, e.g., diepoxybutane (Ötvös and Elekes, 1975; Verly *et al.*, 1971), or by ultraviolet irradiation in the presence of psoralens (Hearst and Thiry, 1977)].

IV. Determination of Minimum Duration of Agent Action

The degree of modification of virion components and changes in the infectivity and immunogenic properties are affected by the length of time over which the agent acts. Therefore, after selection of an appropriate agent for a given virus, it is necessary to determine both the minimum duration of action of the agent that ensures the safety of the

vaccine (t_1 or t_1', Fig. 1) and the maximum duration at which the protective efficiency of the vaccine (immunogenicity of the virus) is still preserved in sufficiently full measure (t_2, Fig. 1).

Experimentally, one can control a reduction in the infectivity of the virus suspension by, at most, 10 orders, even if one increases the sample volume (within reasonable limits) and takes advantage of a series of successive passages. However, the production of safe killed antiviral vaccines requires that the infectivity of the original virus-containing material be reduced by at least 15 to 20 orders of magnitude. Therefore, the safety of killed antiviral vaccines cannot be determined experimentally (see Henderson, 1952) and "must be built into the production method itself" (Gard, 1956). The minimum duration of agent action (t_1 or t_1', Fig. 1), at which the necessary reduction in infectivity is achieved, can only be determined using a kinetic approach. This requires an accurate kinetic description of the inactivation process for the corresponding virus under the conditions and with the agent actually used for inactivation. Data can be obtained from the early (experimentally controlled) part of the survival curve, taking into consideration the effects of biological and chemical factors on the inactivation kinetics.

It should be emphasized that an accurate kinetic description should be based on a precise and reliable determination of the infectivity of the viral suspension during inactivation. Systematic errors in the in-

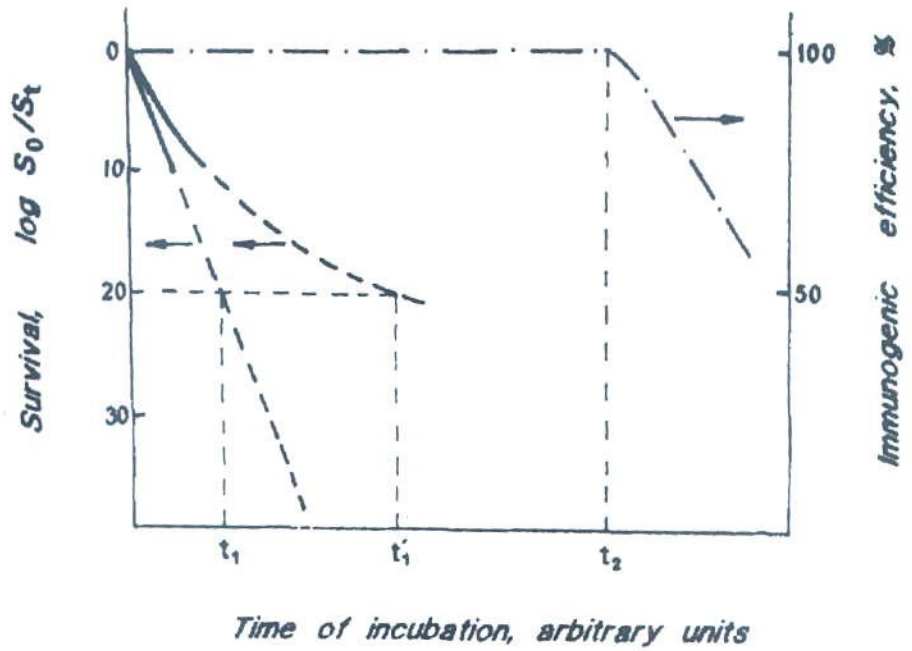


FIG. 1. Dependence of the infectivity and immunogenicity of the virus-containing material on the duration of action of the inactivating agent. t_1 or t_1', Minimum duration that ensures the safety of the vaccine; t_2, maximum duration that ensures the sufficient immunogenic (protective) efficiency of the vaccine.

fectivity (titer) determination can lead to erroneous values for the inactivation rate constant and the minimal duration of the agent action (t_1). Underestimation of infectivity is most hazardous because it leads to overestimation of the rate constant, underestimation of the t_1 value, and insufficient safety of the killed vaccine. Therefore, the adequacy of the infectivity determination method deserves special attention (Budowsky *et al.*, 1990). A reliable value of t_1 can be obtained using the kinetic approach when the survival curves provide a good kinetic description up to a specified degree of reduction in infectivity.

Some principles regarding the application of the kinetic approach to the determination of the minimum duration of treatment by an inactivating agent will be considered below.

If the correlation between the degree of inactivation of infectivity and the degree of modification of the genome are not distorted by biological factors, e.g., processes of genome repair and multiple reactivation by recombination (Friedberg, 1984; Agut *et al.*, 1984; Agol *et al.*, 1985) or reassortment of the segmented viral genome (Wenske *et al.*, 1985; Gombold and Raming, 1986; Stott *et al.*, 1987), the approaches and principles of chemical kinetics can be used to investigate and describe infectivity inactivation. On the assumption that the formation of the first inactivating lesion, regardless of its position in the viral nucleic acid, blocks the complete replication of the genome, the survival curves for the virus during the action of the inactivating agent obey Eq. (1):

$$S = S_0 \exp(-Akt) \tag{1}$$

where S_0 and S are the infection titers of the virus-containing material before and at time t after the start of the agent action, A is the concentration of chemical agent or radiation intensity, and k is the rate constant for inactivation, i.e., modification of a nucleotide residue per genome.

For Eq. (1) to be valid the formation of an inactivating damage should be a single-hit process. If a lesion appears as a result of the slow spontaneous transformation of a modified nucleotide residue, as in the case of N^7-methylation of guanine (see O'Connor *et al.*, 1988), the experimentally determined inactivation rate can be undervalued. Since it takes considerable time from the infectivity inactivation to the utilization of the vaccine, the duration of inactivation calculated by extrapolation of the early part of the survival curve can turn out not only greater than actually needed for vaccine safety (t_1), but even greater than t_2, i.e., the time of treatment admissible based on the efficiency of the final product.

If the values of A and k are constant during inactivation, the survival curves are exponential. In this case, the inactivation duration

required for a reduction of infectivity to a given extent can be calculated according to Eq. (2):

$$t_1 = [2.3/(Ak)]\log(S/S_0) \tag{2}$$

To calculate the minimum duration of agent action from Eq. (2) one must prove that the agent concentration and the inactivation rate constant are constant and must determine the k value from data on the inactivation rate within the experimentally controllable part of the survival curve. Note that the value of the constant depends not only on the nature of the agent and inactivation conditions (pH, temperature, and composition of the solution), but also on the species and strain of the virus.

V. Effects of Different Factors on the Kinetics of Infectivity Inactivation

The application of Eq. (2) is justified only when the inactivation kinetics are unaffected by biological and chemical factors. The lack of safety of killed vaccines is often due to a disregard of those factors in the development of techniques for inactivation of the viral suspension.

A. Biological Factors

The effects of biological factors can lead to a deviation from exponential survival curves as a result of a weakening in the dependence of the degree of inactivation of the infectious viral suspension on the number of virions having a damaged genome. Various repair systems can reduce by several orders of magnitude the number of modified residues in the viral DNA before its replication. The inactivation of viruses containing double-stranded genome DNA is a multihit process. When using an inactivating agent there is a lag period before the infectivity of the suspension starts to drop (Haynes, 1964). The duration of the lag period depends on the repair efficiency, i.e., on the nature and physiological state of the infected cell. In general, inactivation kinetics for DNA-containing viruses (if inactivating lesions form in a single step) can be described by Eq. (3) (Atwood and Norman, 1949):

$$\log(S/S_0) = \log(n) - Akt \tag{3}$$

where n is the extrapolation number (Alper *et al.*, 1960) equivalent to the number of lesions per genome at which virion reproduction is prevented. Experimental values of $\log(S/S_0) = f(t)$ after the lag time

allow the values of n and k to be computed and used for determining the value of t_1 according to Eq. (4), derived from Eq. (3):

$$t_1 = [1/(Ak)][\log(n) - \log(S/S_0)] \quad (4)$$

The multiple reactivation of DNA- and RNA-containing viruses may be due to recombination processes and reassortment of the segmented genome. These processes can bring about deviations in exponential survival curves in the form of a "tail," but manifest themselves only at a high multiplicity of infection and reflect the features characteristic of the procedure in determining the infectivity of the viral suspension in a cell culture or in chicken embryos. Because the influence of these processes on survival curves is negligible at a small multiplicity of infection (<1), the calculation of t_1 can be based on standard kinetic equations. In this case immunization should be based on those techniques for which the multiplicity of infection of cells is certainly much less than one, even in the site where the vaccine is introduced.

The influence of biological factors on the kinetics of inactivation of the infectivity of the viral suspension should be either taken into account in the description of survival curves or can be made negligible through the use of an appropriate immunization procedure.

B. Chemical Factors

The effect of virtually all chemical factors on the kinetics of infectivity inactivation is expressed by a reduction in the inactivation rate during the action of the agent. As a result, tailing of the survival curves occurs, i.e., a deviation from the exponential function takes place with an increase in the degree of inactivation. The deviation may not occur in the experimentally controllable part of the survival curve, but may prove most appreciable at such degrees of inactivation as are necessary for the vaccine to be safe. The principal chemical factors affecting the inactivation kinetics and some procedures helpful in preventing or taking into account the effect of those factors when determining the minimum duration of inactivation are considered below.

1. Heterogeneity of Viral Suspension

In a viral suspension with heterogeneously accessible virions, the proportion of the less accessible virions among those having survived grows with an increase in the degree of inactivation, resulting in a drop of the inactivation rate during the agent action (Salk and Gori, 1960). Survival curves will differ for inactivation of a homogeneous or a heterogeneous suspension. The difference grows as the degree of

inactivation, the amplitude of difference in accessibility among virions, and the contents of the less accessible virions in the population increase.

The accessibility of virions in a heterogeneous viral suspension may be affected by the presence in the original material of formations such as whole cells or their debris, aggregates of viruses, macromolecules, and salts. The virions within these formations are obviously less accessible to agents than those that are free. The number of shielded vs. free virions in a suspension cannot be determined with experimental accuracy. As a rule, the size of such shielded formations is many times greater than the size of a free virion, so that virions should be made equally accessible by purification of the virus-containing material before inactivation (see Salk and Gori, 1960).

2. Heterogeneity of Virus Population

In a heterogeneous virus population the inactivation kinetics can be affected by the accessibility of the genome inside the virion, due to differences in the composition, structure, and packing of virus particles (Rauth, 1965; Budowsky *et al.*, 1974, 1981a, 1990; Furuse *et al.*, 1979). Such differences arise in the course of reproduction or purification of the virus and can affect the accessibility of the genome, i.e., the inactivation rate, by several times, leading to a tailing of the survival curve. This heterogeneity can be reduced to a minimum and standardized at the various steps in the production of virus and the preparation of virus for inactivation.

Tailing of survival curves can also be caused by another type of population heterogeneity: the presence of virus particles containing more than one copy of the genome (Dahlberg and Simon, 1969). To prevent reproduction of such particles the number of inactivating damages per particle should be proportional to the number of genome copies. The inactivation kinetics for each subpopulation of particles containing n genome copies can be described by Eq. (3). The total survival curve for such a heterogeneous population can be described by the sum of the curves for all subpopulations, taking into account the percentage of each subpopulation that differs in the number of genome copies. It is impossible to obtain these data for every initial batch of virus-containing material. Therefore, the complications involving inactivation kinetics, caused by this kind of heterogeneity, should be prevented by using proper methods for preparation and purification of the initial material.

Because of the effect of a heterogeneous virus population on the kinetics of infectivity inactivation, certain qualifications for the development and technological standardization of the steps in the inac-

tivation (see Gard, 1956) and the production and purification of virus-containing material used for producing killed vaccines are necessary.

3. Nonuniformity of Agent Action within Inactivated Volumes

Ultraviolet radiation is a very convenient and highly selective inactivating agent (Kleczkowski, 1968; Murphy and Gordon, 1980; Day, 1980). Because of the difference in the absorption spectra between nucleic acids and other virion components, radiation in the range of 250 to 270 nm is chiefly absorbed by nucleic bases, photomodification of which blocks the replication of polynucleotides. The genome photomodification rate and hence the virus infectivity photoinactivation are proportional to the incident light intensity. When light passes through a solution, the radiation intensity decreases when the path length and optical density of the solution are increased. The accessibility of virions to light, i.e., the inactivation rate for each virion in the solution, will depend not only on the intensity of the incident light, but also on the position of the virion in the irradiated volume relative to the light source. In measuring the action of ultraviolet radiation on unstirred suspensions, the survival curves, which reflect the total inactivation rate, depart from the exponential (Fig. 2) and can be described by Eq. (5) (Morowitz, 1950; Budowsky *et al.*, 1981b).

$$\log(S/S_0) = \{\log[1/(2.3D_\lambda)]\}[\mathrm{Ei}(I_0Et\times 10^{-D_\lambda}) - \mathrm{Ei}(I_0Et)] \qquad (5)$$

where I_0 is the intensity of the incident radiation, E is the cross-section of infectivity inactivation for a given virus under the action of light of wavelength λ, D_λ is the optical density of the irradiated layer at that wavelength, and Ei is the exponential integral function.

If the irradiated solution is stirred vigorously, all the virions in the solution become equally accessible to the light, i.e., they absorb equal doses of radiation, and the survival curves become exponential at any optical density of the irradiated layer (Fig. 3) (Budowsky *et al.*, 1981b). The slope of the exponential curve depends on the optical density of the irradiated layer, as expressed by Eq. (6).

$$\log(S/S_0) = [I_0Et(1-10^{-D_\lambda})]/(2.3D_\lambda) \qquad (6)$$

The kinetics of the inactivation of virus infectivity due to the action of ultraviolet light on stirred or unstirred solutions with any optical density of the irradiated layer permit a sufficiently rigorous protocol as noted by Budowsky *et al.* (1981a,b).

Naturally, such a description is quite simple and is accurate only if a monochromatic radiation source is used. Sources emitting radiation at 254 nm (low-pressure mercury lamps) are inexpensive and readily

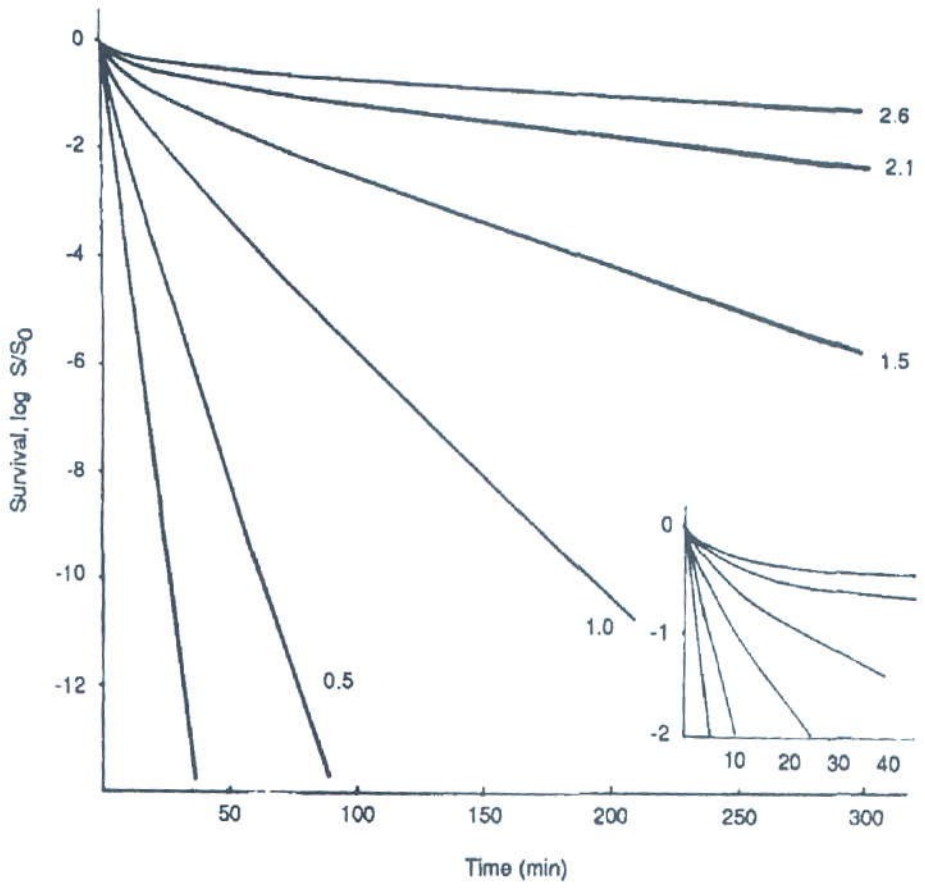


FIG. 2. Theoretical survival curves as calculated by Eq. (5) for the action of UV radiation on nonstirred viral suspensions with various optical densities of the irradiated layer (Budowsky *et al.*, 1981b). The optical density of the irradiated layer is shown for each curve. *Inset:* The twofold enlargement of the initial part of the picture.

available and can be used for inactivation of practically unlimited volumes of viral suspensions.

Photoinactivation of viruses is one of the most promising techniques for obtaining safe vaccines. Unfortunately, neglect of the factors affecting the kinetics of photoinactivation repeatedly lead to an insufficient inactivation of infectivity of the virus-containing material, which undeservedly discredits the photochemical method of inactivation.

It should be emphasized, however, that some viruses, e.g., the tick-borne encephalitis virus, are physically unstable and can be destroyed even at low doses of ultraviolet radiation (Effimova *et al.*, 1982), which results in a virtually complete loss of immunogenicity. In such cases, bifunctional agents (see Section III), such as diepoxybutane, should be used, thus preventing the virion from being destroyed and thereby

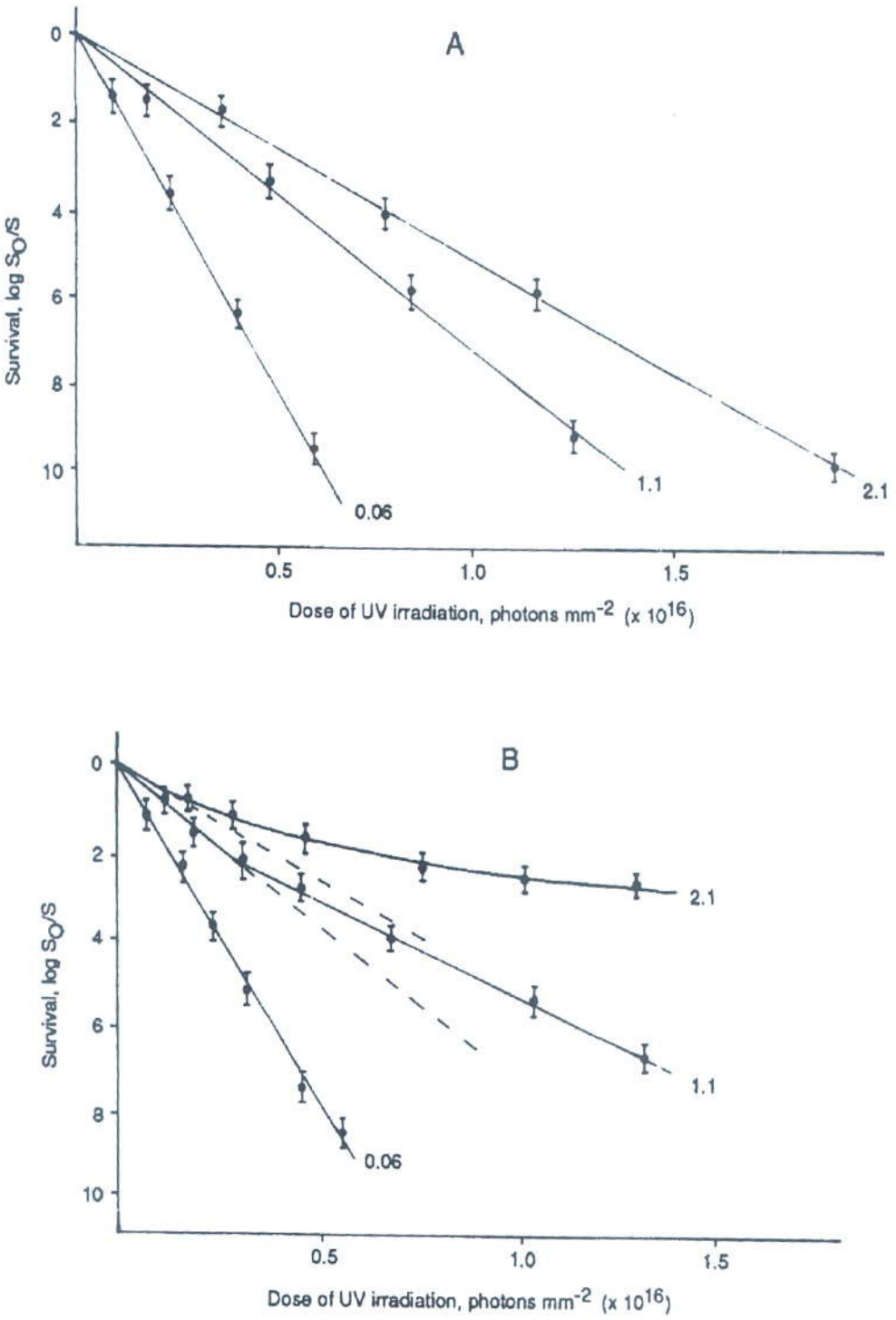


FIG. 3. Survival curves for bacteriophage MS2 by the action of UV (254 nm) radiation on stirred (A) and nonstirred (B) suspensions with various optical densities of the irradiated layer at 254 nm (shown by the numbers at each curve). Solid and dashed lines are theoretical curves calculated according to Eqs. (5) and (6), respectively. (From Budowsky *et al.*, 1981c.)

helping to preserve the protective efficiency of the vaccine. Photoinactivation kinetics provides a rather rigorous description only for purified viral suspensions, because the presence of sensitizers and quenchers of excited states in the original material may produce a marked effect on the course of photoinactivation. The use of chemical inactivating agents for the production of killed antiviral vaccines is more dependable and versatile.

4. Variation in Concentration of Agent during Inactivation

Many inactivating agents are very reactive and their concentration significantly decreases during inactivation due to hydrolysis and reactions with the components of the virus-containing medium. This is the main reason for tailing in the survival curves based on the action of these agents on a purified homogeneous virus suspension. Addition after partial inactivation of another agent or of another portion of the same agent is widely used in such cases for reaching "complete" inactivation (see, e.g., Fellowes, 1965). Such an empirical approach, however, cannot ensure safety of the killed vaccine and must be substituted by a kinetic one, as described below.

If, as a result of hydrolysis and/or reactions with the components of the medium, the agent concentration falls considerably during inactivation, then Eq. (7) (Budowsky and Zalesskaya, 1985, 1990; Budowsky *et al.*, 1990) can be used for the kinetic description of survival curves:

$$\ln(S/S_0) = [(\mathrm{kA}_0)/k_1][1 - \exp(-k_1 t)] \qquad (7)$$

where A_0 is the initial concentration of the agent and k and k_1 are the rate constants for the infectivity inactivation and consumption of the agent under experimental conditions.

It is evident that the calculation of the t_1 value from Eq. (7) requires that the values of k and k_1 be determined experimentally under the infectivity inactivation conditions. Changes in the agent concentration with time, and hence, the value of k_1, are determined by any suitable procedure. If the k_1 value is constant up to the expected instant when the infectivity is reduced to a given extent, then the k value can be obtained from Eq. (7) using the value obtained for k_1 and the initial rate of inactivation (Budowsky and Zalesskaya, 1985, 1990; Budowsky *et al.*, 1990). Alteration of experimental conditions significantly affects both the values of these constants and their proportion as well, leading to serious changes in the shape of the survival curves. Notwithstanding, experimental data on the inactivation of phage MS2 infectivity by β-propiolactone fit well, over a wide range, with the theoretical curves calculated from Eq. (7), using the values of k and k_1 under proper conditions (Fig. 4). This approach provides a rigorous

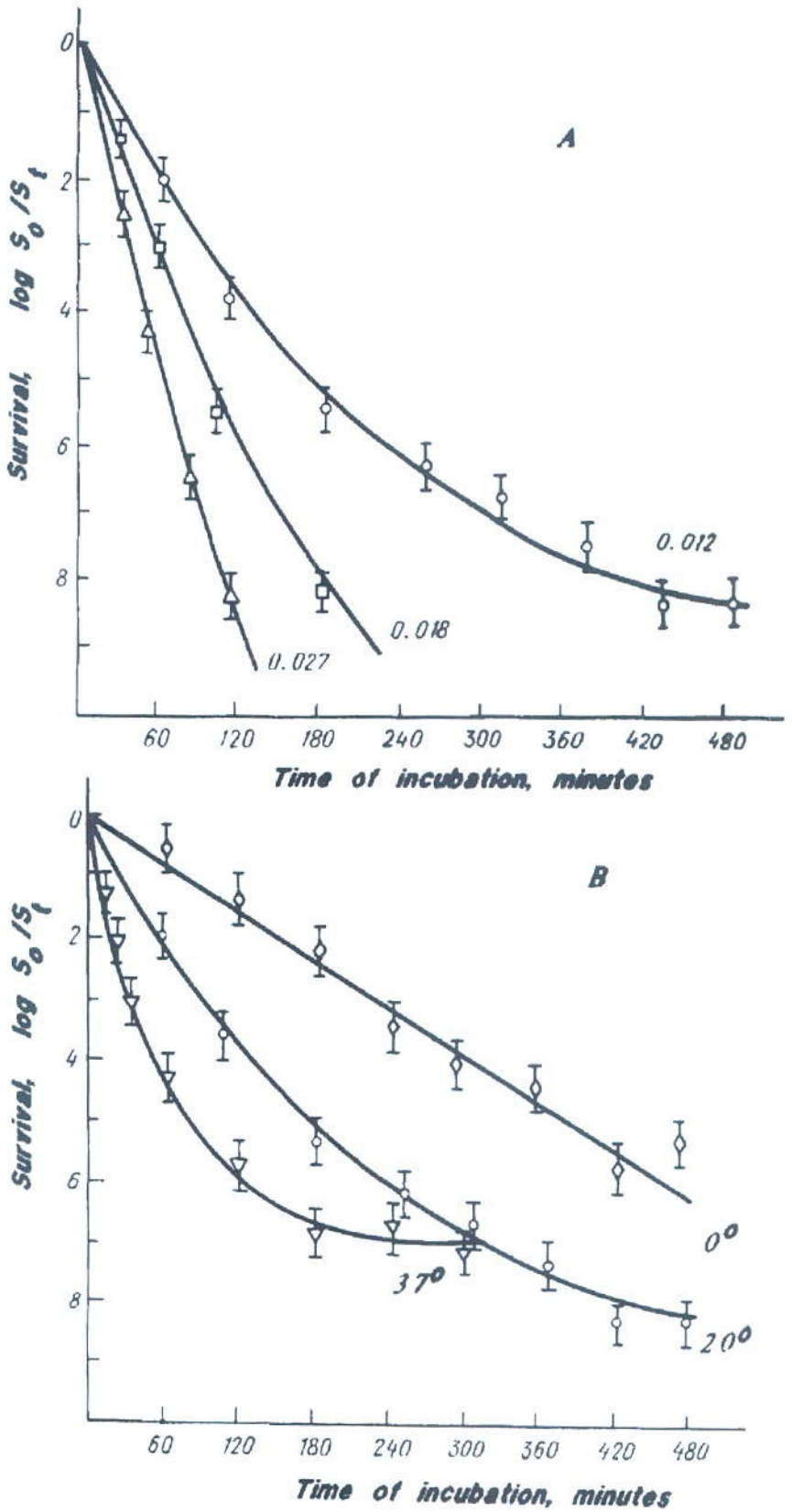


FIG. 4. Survival curves for bacteriophage MS2 after treatment with β-propiolactone. (A) Temperature is 20°C; concentrations of the agent are shown on the curves. (B) Concentration of the agent is 0.011 *M*; temperatures (°C) are shown on the curves. Solid lines are theoretical curves calculated according to Eq. (7) using the values of k and k_1 under relevant conditions. (From Budowsky and Zalesskaya, 1985.)

description of the kinetics of infectivity inactivation and can be used to determine the duration of action by the agent that is required for producing safe vaccines.

In the cases where the consumption of the agent by side reactions during inactivation affects the survival curve, another approach for determining t_1 can be used (Gard, 1960; Lo Grippo, 1960) in which the description of the inactivation kinetics also involves experimental data from the early part of the survival curve. Accordingly, empirical parameters are adjusted for an equation that satisfactorily describes the inactivation kinetics within the experimentally controllable portion of the survival curve, regardless of the actual values of the rate constants for the consumption of the agent and infectivity inactivation. This approach is not sufficiently accurate in the description of the inactivation kinetics and cannot be used at all in the case where the deviation of the survival curve from an exponential function is inappreciable or indiscernible within the experimentally controlled portion. For example, for the action of 0.0055 M β-propiolactone on an allantois suspension of the influenza virus, the experimentally controllable portion of the survival curve does not differ from the exponential. In the time t_1 calculated by extrapolation, i.e., neglecting the decrease in the agent concentration, the actual reduction in infectivity does not exceed 12 orders of magnitude, which is definitely too little to produce a safe killed vaccine (Budowsky *et al.*, 1990).

If the agent is consumed during inactivation, the survival curves, based on increasing the duration of incubation, reach a plateau (Fig. 4B), the height of which (residual infectivity) depends on both the initial concentration of the agent and the ratio k/k_1 (Budowsky and Zalesskaya, 1985, 1990). Any further incubation will obviously not add to the degree of inactivation in this case. Given the ratio k/k_1, the limiting degree of inactivation for any initial concentration of that agent can be determined from Eq. (8):

$$\ln(S_0/S) = A_0(k/k_1) \tag{8}$$

Equation (8) shows that at an initial concentration of 0.0055 M β-propiolactone, the survival curve for the influenza virus in the allantois reaches a plateau at an infectivity drop of 17 orders. A 20-order inactivation is never possible in this case (Budowsky *et al.*, 1990).

The above data show how to take into account or to avoid the influence of chemical factors on the kinetics of the virus infectivity inactivation. By taking into account factors such as pH, temperature, composition of the viral suspension, and initial concentration of the agent the action duration required for the production of safe killed vaccines for any virus and any inactivating agent can be determined.

VI. Changes in Virion Immunogenicity Due to Action of Inactivating Agents

Modification of the virion components responsible for virus immunogenicity inevitably leads to a decrease in the efficiency of the immune response to the virus. Changes in the immune response increase with increases in the modifications to the virion components, e.g., with increases in the time of action of any inactivating agent. After the necessary degree of infectivity inactivation is achieved, excessive action by the agent is not needed for vaccine safety and can actually reduce the vaccine efficiency. The production of an efficient killed vaccine requires that the inactivating action be stopped before time t_2 (Fig. 1), when the changes in protective efficiency do not surpass the acceptable extent.

Two additional problems should be considered in preparing killed vaccines. The first problem involves the inactivation agent: the instantaneous cessation of the agent action at the proper time, i.e., before time t_2. Using radiation (ultraviolet or ionizing) is most convenient, but the inactivating action of ionizing radiation is due to water radiolysis products, whose selectivity with respect of the virion components is low. As discussed below, even minute radiolytic damage to proteins dramatically increases their accessibility to proteinases. In the case of viruses, this could lead to a rapid degradation of viral proteins, including those containing protective antigens, as well as of the virion as a whole after inoculation of the vaccine. Most probably this is the reason for failure of many attempts to use ionizing radiation for the preparation of killed vaccines (Newmark, 1988).

For a cessation of the action of chemical agents, dilution or cooling of the reaction mixture is commonly used. This leads to a deceleration in the modification of the virion components and in some cases to a decrease in the selectivity of the agent action (Budowsky and Zalesskaya, 1990), resulting in a further, often inadmissible, decrease in the virus immunogenicity. Only removal or neutralization of the inactivating agent before time t_2 can provide sufficient efficiency for the killed vaccines.

The second, much more complicated and not yet resolved problem is the determination of t_2. As shown above, time t_1 can be reliably determined based on the rational formulation of the term "safety" and using the kinetic approach. This is possible because there are direct methods of determining infectivity for many viruses, and the correlation of the degree of infectivity inactivation with the type and extent of genome modification is known for many of inactivating agents. However, there are not clearly formulated criteria for the limits of

permissible changes in virus immunogenicity in the production of killed vaccines. At present, there are no adequate techniques for the determination of changes in virus immunogenicity during the action of inactivating agents and there are no simple and direct methods for at least semiquantitative determination of the efficiency of killed vaccines. It is not yet possible to evaluate the maximum permissible (with respect to the protective efficiency and specificity of the vaccine) degree, nature of modification of the viral components, or maximum allowable duration (t_2) of the inactivating action. Therefore, only general principles, regarding the estimation of time t_2, can be considered.

A. Protective and Immunogenic Efficiency of Killed Vaccines

Further discussion requires the definitions of these terms:

1. *Protective efficiency:* The strength of the organism's defense against challenge with an infectious pathogenic virus (calculated per standard dose of the vaccine).
2. *Immunogenic efficiency:* The extent of the immunity (immune response) with respect to viral antigen(s), irrespective of their protective potency (calculated per standard dose of the vaccine).
3. *Virion immunogenicity:* The potency of a virion that is part of a vaccine to induce the immune response with respect to some viral antigen(s).

The events leading to the development of antiviral immunity after a single inoculation are different for live and killed vaccines. The dependence of the protective efficiency of live and killed vaccines on the dose (the number of inoculated virions) are significantly different.

If the dose of a live vaccine exceeds the minimal one, i.e., if it is sufficient to overcome the nonspecific defense barriers of the organism, reproduction of the virus takes place after inoculation, leading to an increase in the number of virions containing a complete set of native antigens. The development of an efficient immune response requires that the number of virions reach some critical value (N_c); but the reproduction of the virus takes place even after N_c is reached, which promotes the maximal development of the immune response. A decrease in the number of virions occurs later, after the development of a sufficiently efficient protective immunity. On this basis, it is possible to assume that, in the case of live vaccines, if $N<N_m$, i.e., if the initial dose (N) contains less than the minimal number (N_m) of virions, the antiviral immunity does not develop at all; but if $N>N_m$, development of the maximum protective immunity takes place. However, it should be stressed that if the number of virions cannot reach

the N_c value due to some nonspecific defense system (e.g., Hirsh, 1982; Bukoski *et al.*, 1983), then the maximum protective efficiency cannot be obtained. In this case it is impossible to increase the vaccine efficiency by increasing the dose.

In the case of killed vaccines, the inoculated virus does not reproduce. Therefore, to develop the maximum immune response with these vaccines doses containing no less than N_c virions are required (Mandel, 1985). Increasing the dose should not lead to a significant increase in the immune response, whereas decreasing the dose (below N_c) should lead to a gradual decrease in the immune response.

Because the action of inactivating agents leads to direct or indirect damage of the viral antigens, the virions in the killed vaccines usually contain an incomplete set of active antigens, and therefore their immunogenicity may be less than that of the native virus. Using the same dose of killed vaccine as live vaccine, the decrease in the number of active copies of any antigen leads to a decrease in the immunogenic efficiency with respect to this antigen. In other words, the efficiency of the immune response against any viral antigen depends not only on the dose (N), but also on the number of active copies of this antigen per virion (n_i), i.e., on the virion immunogenicity with respect to this antigen. The total number of copies of each antigen in the initial virion ($n_{i,t}$), as well as the rate (extent) of their inactivation under the conditions for the killed vaccine production, are different. Because it is not known which antigen(s) of the virion determines the protective efficiency of the vaccine, only the influence of the inactivation of one of the viral antigens on the virus immunogenicity with respect to this antigen will be considered below.

1. Kinetics of Changes in Immunogenicity Directly Caused by Modification of Antigens

The type of chemical modifications caused by the action of inactivating agents and their location in the virion components are generally not known. Which of these modifications and to what extent these modifications can alter the immunogenic properties of every antigen, particularly those responsible for the protective efficiency of the vaccine are also not known. Generally the decrease in the number of intact antigens of a given type conforms to single-hit kinetics, at least to such an extent that modification does not distort the higher structure of the virion components and of the virion as a whole.

Each antigen is represented in the virion by a multitude of copies, the total number of which ($n_{i,t}$) by far surpasses that necessary for maximum immunogenicity with respect to the antigen in question. Therefore, the immunogenicity of the virion with respect to a given

antigen is preserved as long as inactivation of excessive copies ($n_{i,e}$) continues, i.e., until the mean number of immunologically intact antigens per virion decreases to a critical value ($n_{i,c}$). Even if inactivation of each antigen copy obeys single-hit kinetics, the decrease in the virion immunogenicity with respect to any given antigen under the action of an inactivating agent obeys multihit kinetics. In other words, in all cases a decrease in immunogenicity is observed only after a certain lag period. The duration of the lag period for each antigen depends not only on the rate of the inactivation of this antigen, i.e., of the proper modification of the respective antigen under the infectivity inactivation conditions, but also on the excessive number of copies of this antigen per virion. The kinetics of the changes in virion immunogenicity with respect to each antigen can be described for a first approximation by Eq. (9) (see Atwood and Norman, 1949):

$$\mathrm{Im}/\mathrm{Im}_0 = 1 - (1-]^{-k_i t A})^{n_{i,e}} \tag{9}$$

where Im_0 and Im are the virion immunogenicities for a given antigen before and after t minutes of the inactivating action; $n_{i,e}$ is the excessive number of copies of this antigen per virion; k_i is the rate constant for the inactivation of this antigen under the conditions of the virus infectivity inactivation; and A is the concentration of the inactivating agent.

Equation (9) can be rewritten as

$$t = [1/(k_i A)]\ln[1-(1-\mathrm{Im}/\mathrm{Im}_0)^{1/n_{i,e}}] \tag{10}$$

In principle, Eq. (10) can be used for calculation of the maximum duration of treatment, t_2, i.e., the duration of the lag period in the decrease of the virion immunogenicity with respect to this antigen under the conditions of the virus infectivity inactivation. This would require the availability of k_i and $n_{i,e}$ values for the corresponding antigen, as well as the existence of a method for determining Im with respect to this antigen. Unfortunately, such a method, as well as the aforementioned data, are presently unavailable. Nevertheless, Eq. (10) gives significant general information: it shows that t_2 for any antigen, under the conditions for preparation of killed vaccines, is inversely proportional to the concentration of the inactivating agent and is dependent on an excessive number of the corresponding antigen per virion in the virus-containing starting material. It should be stressed that some copies of different antigens can be lost either during purification or due to the action of enzymes, e.g., proteinases, during reproduction of the virus. Therefore the excessive number of copies of certain antigens, and, hence, the t_2 value, can vary from batch to batch and may be less than theoretically predicted. A decrease

in the copy number of some antigens below the critical value can take place during storage of the vaccine due to enzymatic degradation of viral proteins and/or glycoproteins. This can be prevented by the removal or complete inactivation of the respective enzymes immediately after preparation of the vaccine.

The excessive number, inactivation rate constant, and time t_2 are different for different antigens. Therefore the immunogenicity of the virion with respect to some antigens may diminish considerably, while remaining the same with respect to others. It should be emphasized that a significant inactivation of one of the antigens can evoke an appreciable decrease in the protective efficiency of the killed vaccine (Norrby *et al.*, 1975; Norrby and Penttinen, 1978; Kendall *et al.*, 1980). Although the dependence of the vaccine protective efficiency on the time of treatment should be similar to that of the virion immunogenicity, there is no simple correlation between the t_2 for protective efficiency and that for immunogenicity for antigens chosen by chance, even including some protective ones. Therefore the t_2 value for the vaccine protective efficiency can be obtained only by means of a direct, at least semiquantitative, method for determining protectivity. As discussed below, the methods used at present are, as a rule, inadequate and often misleading.

2. *Other Reasons for Changes in Vaccine Immunogenic (Protective) Efficiency during or after Infectivity Inactivation*

In many cases the modification of the virion components by inactivating agents reduces the physical stability of the virion. After a certain extent of modification, characteristic of the virus and the inactivating agent, a spontaneous destruction of the virion may occur during either inactivation or storage. The destruction of the virion results in an abrupt drop in immunogenic efficiency (see, e.g., Ceglowski, 1965; Barry *et al.*, 1977; Beale, 1982). An excessive duration of the inactivating action certainly leads to a drop in the immunogenic efficiency as a result of destruction of the virion, but the absence of a few macromolecules of the virion does not produce any appreciable effect on stability. The dependence of the virion stability on the duration of agent action is therefore represented by a multihit curve. In other words, the decrease in the virion stability during the agent action, determined by the drop in immunogenic efficiency, appears only after a lag. This lag time depends on a number of factors: the nature and number (per virion) of lesions, i.e., the nature and concentration of the agent, the influence of each lesion on intra- and intermolecular interactions, and the distribution of lesions among the virion components.

As noted above, virion destruction during inactivation or during the subsequent storage of the vaccine can be avoided or considerably reduced by using bifunctional inactivating chemical agents capable of linking the virion components together (see, e.g., Budowsky *et al.*, 1981c).

Factors other than those specified above also reduce the protective efficiency of killed vaccines. For example, even a slight radiation-induced modification in proteins is known to stimulate their rapid enzymatic degradation (Davies *et al.*, 1987; Davies, 1987, 1988). It can be assumed that a chemical modification in the proteins of the virion envelope will also accelerate their digestion by enzymes (Horiuchi *et al.*, 1985). This might clearly reduce the vaccine efficiency either on account of a reduction in the number of copies of the native antigen per virion or by virtue of the destabilization and consequent destruction of the virions. Such negative consequences will evidently be more expressed for the more heavily modified macromolecules responsible for the immunogenicity and stability of the virion. This is one more argument in favor of searching for the most selective agents and the stringent choice of conditions which would ensure genome modification to the extent necessary for vaccine safety and would reduce to a minimum the extent of modification of other virion components.

3. *Determination of Immunogenic (Protective) Efficiency of Killed Vaccines*

Estimation of the maximum allowable time for the action of the inactivating agent, as well as the control of the immunogenic (protective) efficiency of the final product immediately after infectivity inactivation and during storage of the vaccine plays a decisive role in preparing efficient killed vaccines. Adequate, semiquantitative, and reliable methods for the estimation of protective efficiency are needed. Accurate data can be obtained only by a direct, properly designed method *in vivo*. Because direct methods are expensive and time-consuming, indirect methods, which are faster and simpler, are generally used for testing the efficiency of live vaccines or for determining the number of intact virions in virus-containing materials. The validity of these methods for testing killed vaccines has not been rigorously determined and in most cases is questionable. The adequacy of these methods for killed vaccines will be considered below.

a. Direct Method. As already mentioned, a regular dependence of the immune response on the dose (N, number of inoculated virions per animal) in the case of killed vaccines exists only between minimal (N_m) and critical (N_c) doses. The influence of changes in virion immunogenicity, caused by inactivation of antigens or virion degradation,

on the immune response at the same dose (on the immunogenic efficiency) of killed vaccine can be observed only if $N_m < N < N_c$. Therefore the first step in testing protective efficiency changes should be the study of the dose–response curve, using noninfectious, native (with respect to the set of antigens and virion integrity) virus. This curve determines the N_m and N_c values and, hence, selection of the proper dose (N_p) for further experiments. The second step, investigation of the dependence of protective efficiency on the time of the inactivating agent action, should be performed at dose N_p. This is the only way to determine directly the maximum time of the inactivating agent treatment (t_2), as well as the protective efficiency changes during storage of the killed vaccine.

Such an approach requires a method for determining the true protective efficiency, which only by chance coincides with the immunogenic efficiency with respect to some individual antigens, even protective ones. Therefore the immunogenic efficiency (seroconversion), i.e., the appearance of antibodies against some viral antigens after vaccination, cannot be used as a measure of the protective efficiency of the vaccine. It should be stressed that this approach, if not substantiated rigorously, can give erroneous and even misleading results.

b. Indirect Methods. Many indirect methods are based on the determination of the amount (concentration) of some viral macromolecules in suspension. Specific antibodies (mono- and polyclonal) are widely used, as well as the measurement of the enzymatic activity of some virion macromolecules, such an neuraminidase. However, this approach, originally developed and quite appropriate for a quantitative determination of a native virus, is inapplicable for the determination of the protective efficiency of viruses whose components are modified by the action of inactivating agents, for the following reasons. First, it is not known how the changes in macromolecules detected with antibodies or by enzymatic activity are related (if at all) to the changes affecting the virion immunogenicity with respect to the corresponding protective antigens of those macromolecules. Second, even if such a correlation exists and is known, the data obtained reflect only the decrease in the amount of active antigen in solution. Virion destruction, leading to a dramatic reduction in the immunogenic efficiency, does not produce any effect in the sample on the amount of viral protein capable of binding to antibodies or possessing enzymatic activity. On the other hand, even if the integrity of the virion remains unchanged, the amount of intact antigens provides no information about the alteration in virion immunogenicity with respect to the antigen in question, unless the excessive number of copies of this antigen per virion is known.

For viruses capable of agglutinating erythrocytes, some idea about virion integrity can be obtained from the hemagglutination reaction, which is also used as a criterion for immunogenic efficiency of a killed vaccine. For the agglutination of erythrocytes, two active hemagglutinin molecules per virion are needed in principle, i.e., the critical number of active molecules of hemagglutinin for the hemagglutination reaction is two. The critical number of protective antigens of hemagglutinin or other virion components responsible for protection is obviously much more than two. Therefore, the hemagglutination reaction gives no information concerning either the protective efficiency of the vaccine or its changes due to the action of inactivating agents.

The indirect techniques presently known do not properly evaluate the changes in the protective efficiency of the virus-containing material during the course of inactivation of infectivity or during the storage of killed vaccines.

B. Immunogenic Specificity

The action of inactivating agents leads not only to the inactivation of natural antigens but also to the formation of new (artificial) antigens as a result of modification of viral proteins, glycoproteins, etc. (cf. Onica *et al.*, 1980, 1982). As a consequence, immunization with an inactivated virus might cause an immune response not only to the natural, but also to the artificial, antigens. The efficiency of the immune response to the new antigens will increase as their number increases, especially when the critical number of copies of the new antigen per virion is reached.

The immune specificity of the new antigens is determined not only by the structure of the corresponding fragment of the viral macromolecule, but also by the structure of the reaction product, i.e., by the inactivating agent. In other words, the modification of proteins of different viruses by the same agent may give rise to the formation of new antigens with a similar or even identical immune specificity. Clearly, the immune response against artificial antigens effected by inoculation of an inactivated virus can significantly reduce (to zero) the efficiency of a subsequent immunization of the same animal with a vaccine against another virus but produced with the help of the same agent (cf. Schutze *et al.*, 1985; Flexner *et al.*, 1988).

At present, killed antiviral vaccines are obtained with the aid of a few inactivating agents. The above effect of modification on the immunogenic specificity of viruses raises a new, very serious, problem. Several times in their life most humans and domestic animals undergo

vaccination against various virus diseases. It is necessary therefore that the artificial antigens appearing as a result of the action of inactivating agents be different for the different vaccines. In other words, one must have a set of inactivating agents that produce different artificial antigens, so as to inactivate each virus using only one agent that has not been used for the inactivation of any other virus. This problem can only be solved on a global scale with the involvement of the World Health Organization (WHO) and other international organizations.

C. Improvement of Killed Vaccines

The only way to overcome the above-mentioned disadvantages in the preparation of the killed vaccines is by the maximum possible increase in the selectivity of the action of the inactivating agent. The possibility of increasing the selectivity to such an extent to allow the consequences of antigen modification—alterations of immunogenic efficiency and/or specificity of the sufficiently inactivated virus—to be neglected is discussed below.

Most chemical agents do not display specific affinity for any virion component. Therefore, the concentration of these agents near each virion component is not different from the overall concentration of the agents in solution, and so selectivity, i.e., the proportion between the extents of modification for the genome and for other virion components, is dependent only on the number and accessibility of the reactive groups of these components. By adjusting common agents and inactivation conditions, the selectivity of action can be changed within a narrow range. For example, a reduction in pH from 8 to 6 does not actually affect the proportion of ionic forms of nucleic bases and, therefore, the rate of the reaction of nucleic acids with chemical agents (Borodavkin *et al.*, 1977); but such a reduction in pH brings about an increase in the degree of protonation of the most nucleophilic groups in proteins, the sulfhydryl and imidazole groups of cysteine and histidine residues, respectively. This will clearly result in a reduction in the relative rate of modification of proteins by electrophilic agents. Thus, a variation in pH within the limits tolerable for virion stability may raise the selectivity of action of electrophilic agents.

As mentioned above, a far more promising way to increase selectivity is the use of agents that have an increased affinity for polynucleotides. Such affinity causes an increase in the concentration of agent near the genome in the virion. It is well known that if a low-molecular-weight compound possesses specific affinity for a certain type of macromolecule, the concentration of that compound near such

macromolecules (local concentration) will be higher—in proportion to the extent of affinity (association constant)—than the overall concentration of the compound as calculated for the total volume of the reaction mixture (Gorshkova and Chimitova, 1983). The local concentration of the compound decreases with distance from the polymer, and does not differ from the overall concentration at a distance greater than 1 nm. The specific affinity of the inactivating agent for polynucleotides will increase the rate of genome modification (infectivity inactivation), causing no changes in the modification rate for the protective antigens on the surface of the virion and removed more than 1 nm from the genome.

Nucleic acid is the only polyanion in the virion. Therefore, the local concentration of agents which are oligocations will be considerably higher near the viral genome than near the antigenic determinants located on the surface of the virion. An increase in the total positive charge of the agent will increase its local concentration near the genome.

An example of a series of compounds exhibiting a difference in the total positive charge is ethyleneimine and its oligomers which contain the same reactive aziridine group. In going from a monomer to a tetramer, the positive charge at pH 7.5 in this series increases almost twofold and is accompanied by a hundredfold increase in the rate constant for infectivity inactivation of bacteriophage MS2 (as calculated from the overall concentration of agent) (Budowsky *et al.*, 1985) (Table I). These compounds become reactive only as a result of protonation of the aziridine nitrogen atom (Dermer and Ham, 1969). The pK values for the aziridine group drop by nearly five units when passing from a monomer to a tetramer. A corresponding decrease occurs in the concentration of the reactive form of agent in relation to its total concentration (Table I). An estimate made on the basis of these data indicates that the local concentration of agent near the phage RNA increases about 10^6 times when passing from monomeric ethyleneimine to the tetramer form. Because the total concentration of agents near the surface antigens remains practically unchanged when passing from the monomer to the tetramer, one can assert, taking into account the almost ten-thousandfold higher proportion of protonated monomer (in comparison with tetramer) at pH 7.5, that the selectivity of action of the tetramer is ca. 10 orders of magnitude higher than that of monomeric ethyleneimine (Table I). It should be emphasized that even the use of acetylethyleneimine can lead to killed vaccines with satisfactory protective efficiency (Fellowes, 1965). Obviously, an increase in the selectivity by many orders of magnitude in the transition to tetrameric ethyleneimine offers a simple way to prepare highly efficient killed vaccines.

TABLE I

ACTION OF ETHYLENEIMINES ON PHAGE MS2

Parameter	Ethyleneimines			
	Mono-	Di-	Tri-	Tetra-
pK values of aziridine group	8.1	5.15	4.10	3.3
Protonation of aziridine group at pH 7.5	7.9×10^{-1}	4.0×10^{-3}	4.0×10^{-4}	6.3×10^{-5}
Total positive charge of molecule at pH 7.5	0.80	1.00	1.42	1.52
Rate constants of phage MS2 infectivity inactivation at pH 7.5	1.5	13	47	150
Relative local concentration of agent in vicinity of RNA[a]	1	1.7×10^{3}	6.2×10^{4}	1.3×10^{6}
Relative selectivity index[b]	1	3.4×10^{5}	1.2×10^{8}	1.6×10^{10}

[a]Calculated from the rate constant values taking into account the extent of aziridine nitrogen protonation.

[b]Calculated from the relative concentration values taking into account the fraction of compound protonated at aziridine nitrogen.

This example illustrates the possibility of increasing the modification selectivity by means of a rational choice of inactivating agent. It is possible to practically completely preclude modification of the envelope components and surface antigenic determinants of the virus under conditions of infectivity inactivation sufficient for the safety of the vaccine.

VII. CONCLUSION

This article demonstrates the necessity and usefulness of chemical principles in the rational choice of agents for the selective inactivation of the viral genome—the decisive step in the production of killed antiviral vaccines. The kinetic approach takes into account chemical and biological factors, as well as techniques for the production and purification of the viral suspension and procedures of vaccination. The

minimum duration of agent action required for the production of a safety vaccine can be also determined reliably in every case.

Another aspect of the problem in production of killed vaccines is far less clear, that is, the determination of the maximum permissible duration of inactivation. It is evident that the modification of the virion components responsible for immunogenicity reduces the protective efficiency of the vaccine. The extent of this reduction depends on the nature and degree of modification of the components, i.e., on the nature of both the virus and agent, on the conditions and duration of inactivation. This article considered the general principles regarding the kinetics of the dependence of the reduction in the immunogenic efficiency on the duration of inactivation. However, these principles can be used only to determine the maximum permissible duration of inactivation if appropriate and accurate techniques are available for quantitative estimation of the protective efficiency of modified viruses. At present, the direct technique, which is time consuming and laborious, can provide such an estimation, only on the condition that the experiment has been carried out correctly, which may not the case. As a rule, indirect techniques, which are simpler and faster, are used. The commonest indirect techniques (hemagglutination reaction, immunological and enzymological determination of the amount of corresponding virion components in the preparation under investigation) show that the results obtained are as a rule misleading and subject to misinterpretation. It will be necessary in the future to state principles and to develop experimental procedures that will take a reasonable amount of time and effort, but will give sufficient accuracy in the evaluation of the protective efficiency of killed antiviral vaccines.

In conclusion, it is worthwhile emphasizing that the principles considered in this article can and must be used for the inactivation of viruses that contaminate labile macromolecular medicinal and veterinary preparations obtained from donor blood, animal organs, animal cell cultures, etc. This is of increasing importance in connection with studies on virus leucoses of cattle, hepatitis, and acquired immunodeficiency syndrome (AIDS). Even the most ingenious contemporary techniques of detection, including polymerase chain reaction (PCR), do not guarantee the complete absence of contamination in preparations of even those viruses for which these techniques were intended. Therefore, the only warrant of safety for such preparations is a sufficient degree of infectivity inactivation of all contaminating viruses, including those whose presence is only suspected. The physiological activity of macromolecular preparations can be solved only by the selective inactivation of virus infectivity in conformity with the principles considered in this article.

ACKNOWLEDGMENTS

I am indebted to G. A. Titova for valuable help in the preparation of the manuscript, and to Dr. V. Klishko for translation of this article.

REFERENCES

Agol, V. I., Drozdov, S. G., Grachev, V. P., Kolesnikova, M. S., Kozlov, V. G., Ralph, N. M., Romanova, L. I., Tolskaya, E. A., Tyufanov, A. V., and Victorova, E. G. (1985). Recombinants between attenuated and virulent strains of poliovirus type 1: Derivation and characterization of recombinants with centrally located crossover points. *Virology* **143**, 467–477.

Agut, H., Bellocq, C., van der Werf, S., and Girard, M. (1984). Recombination and rescue between temperature-sensitive mutants of poliovirus type 1. *Virology* **139**, 393–402.

Alper, T., Gillies, N. E., and Elkind, M. M. (1960). The sigmoid survival curve in radiobiology. *Nature (London)* **186**, 1062–1064.

Atwood, K. C., and Norman, A. (1949). On the interpretation of multihit survival viruses. *Proc. Natl. Acad. Sci. U.S.A.* **35**, 696.

Auerbach, C., Moutschen-Dahmen, M., and Moutschen, J. (1977). Genetic and cytogenetical effects of formaldehyde and related compounds. *Mutat. Res.* **39**, 317–362.

Barry, D. W., Meiner, R. E., Statton, E., Dunlop, R. C., Rastogi, C. R., Hannah, J. E., Blackburn, R. I., Nortman, D. F., and Graze, P. R. (1976). Comparative trial of influenza vaccines. I. Immunogenicity of whole virus and split product vaccines in man. *Am. J. Epidemiol.* **104**, 34–46.

Barry, D. W., Mayner, R. E., Meisler, J. M., and Seligmann, E. B. (1977). Evalution and control of vaccines for the national influenza immunization program. *J. Infect. Dis.* **136**, 407–412.

Baumert, H. G., Sköld, S.-E. and Kurland, C. G. (1978). RNA–protein neighbourhoods of the ribosome obtained by cross-linking. *Eur. J. Biochem.* **89**, 353–359.

Beale, J. (1982). Synthetic peptides as the basis for future vaccines. *Nature (London)* **298**, 14–15.

Beck, E., and Strohmaier, K. (1987). Subtyping of European foot-and-mouth disease virus strains by nucleotide sequence determination. *J. Virol.* **61**, 1621–1629.

Beland, F. A., Fullerton, N. F., and Heflich, R. H. (1984). Rapid isolation, hydrolysis and chromatography of formaldehyde-modified DNA. *J. Chromatogr.* **308**, 121–131.

Berman, H. M., and Young, P. R. (1981). The interaction of intercalating drugs with nucleic acids. *Annu. Rev. Biophys. Bioeng.* **10**, 87–114.

Bittle, J.-L., Houghten, R. A., Alexander, H., Shinnick, T. M., Sutcliffe, J. G., Lerner, R. A., Rowlands, D. J., and Brown, F. (1982). Protection against foot-and-mouth disease by immunisation with a chemically synthesized peptides predicted from the viral nucleotide sequence. *Nature (London)* **298**, 30–33.

Borodavkin, A. V., Budowsky, E. I., Morozov, Y. V., Savin, F. A., and Simukova, N. A. (1977). Electronic structure, UV absorption spectra and reactivity of nucleic acid components. *Itogi Nauki Tekh.: Mol. Biol.* **14**. (In Russ.)

Brooksby, J. B. (1981). Tracing outbreaks of foot-and-mouth disease. *Nature (London)* **293**, 431–432.

Broude, N. E., and Budowsky, E. I. (1971). The reaction of glyoxal with nucleic acid components. III. Kinetics of the reactions with monomers. *Biochim. Biophys. Acta* **254**, 380–388.

Brunell, P. A. (1985). Inactivated and live vaccines. *In* "Immunochemistry of Viruses. The Basis for Serodiagnosis and Vaccines" (M. H. V. van Regenmortel and A. R. Neurath, eds.) pp. 171–188. Elsevier, Amsterdam.

Budowsky, E. I., and Pashneva, N. N. (1971). Mechanism of the mutagenic action of hydroxylamine. V. Chemical reactivation of hydroxylamine inactivated MS2 phage. *Biochim. Biophys. Acta* **246**, 329–334.

Budowsky, E. I., and Zalesskaya, M. A. (1985). Principles of selective inactivation of the viral genome. III. Kinetics of bacteriophage MS2 infectivity inactivation by beta-propiolactone. *Mol. Biol. (Moscow)* **19**, 1139–1147.

Budowsky, E. I., and Zalesskaya, M. A. (1990). Principles of selective inactivation of the viral genome. V. Rational choice of inactivation conditions for decrease of infectivity to predetermined extent by the action of beta-propiolactone. *Vaccine* (in press).

Budowsky, E. I., Turchinsky, M. F., Domkin, V. D., Pogorelov, A. G., Pisarenko, V. N., and Kusova, K. S. (1972). Mechanism of the mutagenic action of hydroxylamine. VI. Reaction of hydroxylamine with the uracil nucleus. *Biochim. Biophys. Acta* **277**, 421–437.

Budowsky, E. I., Krivisky, A. S., Klebanova, L. M., Metlitskaya, A. Z., Turchinsky, M. F., and Savin, F. A. (1974). The action of mutagens on MS2 phage and on its infective RNA. Kinetics of the chemical and functional changes of the genome under hydroxylamine treatment. *Mutat. Res.* **24**, 245–258.

Budowsky, E. I., Bresler, S. E., Friedman, E. A., and Zeleznova, N. V. (1981a). Principles of selective inactivation of viral genome. I. Ultraviolet-induced inactivation of influenza virus. *Arch. Virol.* **68**, 239–247.

Budowsky, E. I., Kostjuk, G. V., and Kost, A. A. (1981b). Inactivation of MS2 phage by the action of diepoxybutane. *Dokl. Akad. Nauk SSSR* **258**, 1463–1465.

Budowsky, E. I., Kostyuk, G. V., Kost, A. A., and Savin, F. A. (1981c). Principles of selective inactivation of viral genome. II. Influence of stirring and optical density of the layer to be irradiated upon ultraviolet-induced inactivation of viruses. *Arch. Virol.* **68**, 249–256.

Budowsky, E. I., Zalesskaya, M. A., Leschinskaya, V. P., and Kostjanovsky, R. G. (1985). Inactivation of the phage MS2 infectivity by the action of ethyleneimines. *Bioorg. Khim.* **11**, 988–990.

Budowsky, E. I., Friedman, E. A., Zeleznova, N. V., and Noskov, F. S. (1990). Principles of selective inactivation of the viral genome. VI. Kinetics of influenza virus inactivation by the action of beta-propiolactone. *Vaccine* (in press).

Bukoski, J. F., Woda, B. A., Habu, S., Okamura, K., and Welsh, R. M. (1983). Natural killer cell depletion enhances virus synthesis and virus-induced hepatitis *in vivo*. *J. Immunol.* **131**, 1531–1542.

Ceglowski, W. C. (1965). Antibody response to the non-infectious 7 μm components of the virus of foot-and-mouth disease. *Virology* **25**, 1328.

Chantler, J. K., Ford, D. K., and Tingle, A. J. (1981). Rubella-associated arthritis: Rescue of rubella virus from peripheral blood lymphocytes two years postvaccination. *Infect. Immunol.* **32**, 1274–1280.

Clifton, C. E., Raffel, S., and Starr, M. P. (1970). Virus-induced chromosome abnormalities. *Annu. Rev. Microbiol.* **24**, 479–500.

Dahlberg, J. E., and Simon, E. H. (1969). Physical and genetic studies of Newcastle disease virus: Evidence for multiploid particles. *Virology* **38**, 666–678.

Davies, K. J. A. (1987). Protein damage and degradation by oxygen radicals. I. General aspects. *J. Biol. Chem.* **262**, 9895–9901.

Davies, K. J. A. (1988). Intracellular proteolytic systems may function as secondary antioxidant defences: An hypothesis. *J. Free Radicals Biol. Med.* **2**, 155–173.

Davies, K. J. A., Lin, S. W., and Pacifici, R. E. (1987). Protein damage and degradation by oxygen radicals. IV. Degradation of denatured proteins. *J. Biol. Chem.* **262**, 9914–9920.

Day, R. S. (1980). The photobiology of DNA viruses: λ, T4 and ϕX_{174}. *In* "Comprehensive

Virology" (H. Fraenkel-Conrat and R. R. Wagner, eds.), Vol. 17, pp. 353–449. Plenum, New York.

Deng, J.-S., and Beutner, E. H. (1974). Effect of formaldehyde, glutaraldehyde and sucrose on the tissue antigenicity. *Int. Arch. Allergy* **47,** 562–569.

Dermer, O. C., and Ham, G. E. (1969). "Ethyleneimine and Other Aziridines." Academic Press, New York.

Effimova, V. F., Elbert, L. B., Krutianskaya, G. L., Kost, A. A., and Budowsky, E. I. (1982). UV inactivation of the tick-borne encephalitis virus. *Vopr. Virusol.* **27,** 94–98.

Evans, D. M., Dunn, G., Minor, P. D., Schild, G. C., Cann, A. J., Stanway, G., Almond, J. W., Currey, K., and Maizel, J. V. (1985). Increased neurovirulence associated with a single nucleotide change in a non-coding region of the Savin type 3 poliovaccine genome. *Nature (London)* **314,** 548–550.

Fellowes, O. N. (1965). Comparison of the inactivation and antigenicity of foot-and-mouth disease virus by acetylethyleneimine and by combined effect of ultraviolet light and β-propiolactone. *J. Immunol.* **95,** 1100–1112.

Flexner, C., Murphy, B. R., Rooney, J. F., Wohlenberg, C., Yuferov, V., Notkins, A., and Moss, B. (1988). Successful vaccination with a polyvalent live vector despite existing immunity to an expressed antigen. *Nature (London)* **335,** 259–262.

Fraenkel-Conrat, H. (1980). Chemical modification of viruses. *In* "Comprehensive Virology" (H. Fraenkel-Conrat and R. R. Wagner, eds.), Vol. 17, pp. 245–283. Plenum, New York.

Friedberg, E. C. (1984). "DNA Repair." Freeman, San Francisco, California.

Fulginity, V. A., Eller, J. J., Downie, A. W., and Kempe, C. H. (1967). Atypical measles in children previously immunized with inactivated measles vaccine. Altered reactivity to measles virus. *JAMA, J. Am. Med. Assoc.* **202,** 1075–1080.

Furuse, K., Hirashima, H., Harigai, H., Ando, A., Watanabe, K., Kurosawa, K., Inokushi, Y., and Watanabe, I. (1979). Grouping of RNA coliphages based on the analysis of the sizes of their RNAs and proteins. *Virology* **97,** 328–341.

Galloway, D. A., and McDougall, J. K. (1983). The oncogenic potential of herpes simplex viruses: Evidence for a "hit-and-run" mechanism. *Nature (London)* **302,** 21–24.

Gard, S. (1956). Aspects on production and control of formalin-treated poliovirus vaccines. *Proc. Int. Congr. Standardizazione Immunomicrobiol., Rome.*

Gard, S. (1957). Chemical inactivation of viruses. *In* "The Nature of Viruses" (G. E. W. Wolstenholme and E. C. P. Millar, eds.), pp. 123–141. Ciba Found. Symp., Churchill, London.

Gard, S. (1960). Theoretical considerations in the inactivation of viruses by chemical means. *Ann. N.Y. Acad. Sci.* **83,** 638–648.

Ginoza, W. (1968). Inactivation of viruses by ionizing radiation and by heat. *Methods Virol.* **4,** 139–209.

Girard, M., Barre-Sinoussi, F., Rey, F., Yagello, M., Kieny, M. P., Chermann, J. C., Muchmore, E., Fultz, P., Lecocq, J. P., Gluckman, J. C., and Montonier, L. (1988). Immunization of chimpanzees against HIV using whole inactivated virions. *Int. Conf. AIDS, 4th Abstr. Book 2* Abstr. No. 6576, p. 290.

Gombold, J. L., and Raming, R. F. (1986). Analysis of reassortment in genome segments in mice mixedly infected with rotaviruses SA11 and RRV. *J. Virol.* **57,** 110–116.

Gorshkova, I. I., and Chimitova, T. A. (1983). Kinetic regularities of affinity modification. *In* "Affinity Modification of Biopolymers" (D. G. Knorre, ed.), pp. 56–85. Nauka, Novosibirsk. (In Russian).

Haase, A. T., Gantz, D., Eble, E., Walker, D., Stowring, L., Ventura, P., Blum, H., Wietgrefe, S., Zupanic, M., Tourtellotte, W., Gibbs, C. F., Norrby, E., and Rozenblatts, S. (1985). Natural history of restricted synthesis and expression of measles virus

genes in subacute sclerosing panencephalitis. *Proc. Natl. Acad. Sci. U.S.A.* **82,** 3020–3024.

Haynes, R. H. (1964). *In* "Physical Processes in Radiational Biology" (L. Augenstein, ed.), p. 51. Academic Press, New York.

Hayatsu, H. (1976). Bisulfite modification of nucleic acids and their constituents. *Prog. Nucleic Acid Res. Mol. Biol.* **16,** 75–124.

Hearst, J. H., and Thiry, L. (1977). The photoinactivation of an animal RNA virus (vesicular stomatitis virus) with the aid of newly synthesized psoralen derivatives. *Nucleic Acids Res.* **4,** 1339–1347.

Henderson, W. (1952). Significance of tests for non-infectivity of foot-and-mouth disease vaccines. *J. Hyg.* **50,** 195.

Hilleman, M. R. (1980). New developments with new vaccines. *In* "New Development With Human and Veterinary Vaccines" (A. Mizrahi, I. Hertman, M. Klingberg, and A. Kohn, eds.), pp. 21–49. Alan R. Liss, New York.

Hirsh, R. L. (1982). The complement system: Its importance in the host response to viral infection. *Microbiol. Rev.* **46,** 71–85.

Horiuchi, S., Takata, K., and Morino, Y. (1985). Purification of a receptor for formaldehyde-treated serum albumin from rat liver. *J. Biol. Chem.* **260,** 482–488.

Hortmann, D. M. (1979). Viral vaccines and their ways. *Rev. Infect. Dis.* **146,** 502–516.

Huppert, J., and Wild, T. F. (1984). Virus disease without virus. *Ann. Virol.* **135,** 327.

Huppert, J., and Wild, T. F. (1986). Virus-related pathology: Is the continued presence of the virus necessary? *Adv. Virus Res.* **31,** 357–385.

IARC Working Group on the Carcinogenic Risk to Humans: Allyl and Allylic Compounds, Aldehydes, Epoxides and Peroxides (1985). *IARC Sci. Publ.* **36.**

Kendall, A. P., Bozeman, F. M., and Ennis, F. A. (1980). Further studies of the neuraminidase content in inactivated influenza vaccines and the neuraminidase antibody responses after vaccination (mmunologically primed and unprimed populations. *Infect. Immunol.* **29,** 966–971.

King, A. M., Underwood, B. O., McCahon, D., Newman, J. W., and Brown, F. (1981). Biochemical identification of viruses causing the 1981 outbreaks of foot-and-mouth disease in the UK. *Nature (London)* **293,** 479–480.

Kleczkowski, A. (1968). Methods of inactivation by ultraviolet radiation. *Methods Virol.* **4,** 93–138.

Kochetkov, N. K., and Budowsky, E. I., eds. (1972). "Organic Chemistry of Nucleic Acids. Part B." Plenum, New York.

Koshland, D. E., Jr. (1985). Benefits, risks, vaccines, and the courts. *Science* **227,** 854.

Lo Grippo, G. A. (1960). Investigation of the use of beta-propiolactone in virus inactivation. *Ann. N.Y. Acad. Sci.* **83,** 578–594.

McGhee, J. D., and von Hippel, P. H. (1975a). Formaldehyde as a probe of DNA structure. I. Reaction with exocyclic amino groups of DNA bases. *Biochemistry* **14,** 1281–1296.

McGhee, J. D., and von Hippel, P. H. (1975b). Formaldehyde as a probe of DNA structure. II. Reaction with endocyclic imino groups of DNA bases. *Biochemistry* **14,** 1297–1303.

McKercher, P. D., Moore, D. M., Morgan, D. O., Robertson, B. H., Callis, J. J., Kleid, D. G., Shire, S. J., Yansura, D. G., Dowbenko, D. G., and Small, B. (1985). Dose–response evaluation of a genetically engineered foot-and-mouth disease virus polypeptide immunogen in cattle. *Am. J. Vet. Res.* **46,** 587–590.

Mandel, B. (1985). Virus neutralization. *In* "Immunochemistry of Viruses. The Basis for Serodiagnosis and Vaccines" (M. H. Van Regenmortel and A. R. Neurath, eds.), pp. 53–69. Elsevier, Amsterdam.

Morowitz, H. J. (1950). Absorption effects on volume UV irradiation of microorganisms. *Science* **111**, 229–230.

Murphy, B. K., and Chanock, R. M. (1986). Antiviral immunisation. *In* "Fundamental Virology" (B. N. Fields and D. M. Knipe, eds.), pp. 469–502. Raven, New York.

Murphy, T. M., and Gordon, M. P. (1980). Photobiology of RNA viruses. *In* "Comprehensive Virology" (H. Fraenkel-Conrat and R. R. Wagner, eds.), Vol. 17, pp. 285–391. Plenum, New York.

Newmark, P. (1988). Receding hopes of AIDS vaccines. *Nature (London)* **333**, 699.

Norrby, E. (1987). Toward new viral vaccines for man. *Adv. Virus Res.* **32**, 1–36.

Norrby, E., and Penttinen, K. (1978). Difference in antibodies to the surface components of mumps virus after immunization with formalin-treated and live virus vaccines. *J. Infect. Dis.* **138**, 672–676.

Norrby, E., Enders-Ruckle, G., and Ter Meulen, V. (1975). Differences in the appearance of antibodies to structural components of measles virus after immunization with inactivated and live virus. *J. Infect. Dis.* **132**, 262–269.

O'Connor, T. R., Boiteux, S., and Laval, J. (1988). Ring-opened 7-methylguanine residues in DNA are a block to *in vitro* DNA synthesis. *Nucleic Acids Res.* **16**, 5879–5894.

Ötvös, L., and Elekes, I. (1975). Stereochemistry of the reactions of biopolymers. IV. Explanation of stereospecific and asymmetric reactivity of DNA in cross-linking alkylation. *Tetrahedron Lett.* **29**, 2481.

Oldstone, M. B. A., Sinha, Y. N., Blount, P., Tishon, A., Rodriguez, M., von Wedel, R., and Lampert, P. W. (1982). Virus-induced alterations in homeostasis: Alterations in differentiated functions of infected cells *in vivo*. *Science* **218**, 1125–1127.

Onica, D., Margineanu, I., and Dobe, M. A. (1980). Antigenic specificity of glutaraldehyde-treated rabbit albumin. *Mol. Immunol.* **17**, 783–789.

Onica, D., Margineanu, J., Medesan, C., Calugaru, A., and Mancinela, M. (1982). Antibodies against glutaraldehyde-modified albumin in normal mouse sera. *Mol. Immunol.* **19**, 1021–1027.

Potash, L. (1968). Methods in human virus vaccine preparation. *Methods Virol.* **4**, 371–463.

Rauth, A. M. (1965). The physical state of viral nucleic acid and the sensitivity of viruses to ultraviolet light. *Biophys. J.* **5**, 257–273.

Relyveld, E. H., and Ben-Efraim, S. (1983). Preparation of vaccines by the action of glutaraldehyde on toxins, viruses, allergenes and cells. *Methods Enzymol.* **93**, 24–59.

Salk, J. E., and Gori, J. B. (1960). A review of theoretical, experimental and practical considerations in the use of formaldehyde for the inactivation of poliovirus. *Ann. N.Y. Acad. Sci.* **83**, 609–637.

Salk, J., and Salk, D. (1977). Control of influenza and poliomyelitis with killed virus vaccines. *Science* **195**, 834.

Salk, J. E., Bennett, B. L., Lewis, L. J., Ward, E. N., and Yongner, J. S. (1953). Studies on human subjects on active immunisation against poliomyelitis. I. A preliminary report of experiments in progress. *JAMA, J. Am. Med. Assoc.* **151**, 1081–1098.

Schaffer, F. L. (1960). Interaction of highly purified poliovirus with formaldehyde. *Ann. N.Y. Acad. Sci.* **83**, 564–577.

Schutze, M. P., Leclerc, C., Jolivet, M., Audibert, F., and Chedid, L. (1985). Carrier-induced epitopic suppression—a major issue for future synthetic vaccines. *J. Immunol.* **135**, 2319–2322.

Singer, B., and Grunberger, D. (1986). "Molecular Biology of Mutagens and Carcinogens." Plenum, New York.

Sköld, S. E. (1981). RNA–protein complexes identified by cross-linking of polysomes. *Biochimie* **63**, 53–60.

Stott, J. L., Oberst, R. D., Channell, M. B., and Osburn, B. I. (1987). Genome segment reassortment between two serotypes of bluetongue virus in a natural host. *J. Virol.* **61**, 2670–2674.

Strauss, B., Larson, K., Rabkin, S., Sagher, D., and Sahm, J. (1986). Termination of synthesis resulting from modified bases in DNA. *In* "The Role of Cyclic Nucleic Acid Adducts in Carcinogenesis and Mutagenesis" (B. Singer and H. Bartsch, eds.), *IARC Sci. Publ.* **70**, 387–392.

Strohmaier, K. (1987). Die Maul- und Klauenseuche. III. Erfahrungen und Folgerungen aus 20 Jaren Bekampfung der Maul-und Klauenseuche. *Tieraerztl. Umsch.* **42**, 417–422.

Verly, W. G., Branier, L., and Feit, P. W. (1971). Inactivation of the T7 coliphage by the diepoxybutane stereoisomers. *Biochim. Biophys. Acta* **228**, 400–411.

Wang, S. Y., ed. (1976). "Photochemistry and Photobiology of Nucleic Acids," Vols. 1 and 2. Academic Press, New York.

Warren, K. S. (1986). New scientific opportunities and old obstacles in vaccine development. *Proc. Natl. Acad. Sci. U.S.A.* **83**, 9275–9277.

Wenske, E. A., Chanock, S. J., Urata, L., and Fields, B. N. (1985). Genetic reassortment of mammalian reoviruses in mice. *J. Virol.* **56**, 613–616.

Willems, J. S., and Sanders, C. R. (1981). Cost effectiveness and cost benefit analysis of vaccines. *J. Infect. Dis.* **144**, 486–493.

Wyatt, H. V. (1973). Poliomyelitis in hypogammaglobulinemics. *J. Infect. Dis.* **128**, 802–806.

Aneko 7 106 105

INT. J. RADIAT. BIOL., 1987, VOL. 52, NO. 5, 795–804

Influencing of ionizing radiation on herpes simplex virus and its genome

A. RÖSEN†, D. M. TAYLOR‡ and G. DARAI†

† Institut für Medizinische Virologie der Universität Heidelberg, Im Neuenheimer Feld 324, 6900 Heidelberg, F.R. Germany
‡ Kernforschungszentrum Karlsruhe, Institut für Genetik und für Toxikologie von Spaltstoffen, Postfach 3640, D 7500 Karlsruhe 1, F.R. Germany und Lehrstuhl für Strahlentoxikologie der Universität Heidelberg, F.R. Germany

(*Received 30 April 1987; accepted 5 June 1987*)

The effects of cobalt-60 γ-rays, 10 MeV electrons and 52 MeV deutrons on the survival of plaque-forming ability has been studied in various strains of herpes simplex virus (HSV). The results show that the D_0 for the loss of plaque-forming ability in different HSV strains lies in the range 1–3 kGy. Irradiation of isolated HSV-1 DNA with cobalt-60 γ-rays resulted in damage, as indicated by electrophoresis of purified viral DNA and by restriction endonuclease analysis, at doses of 1 kGy, with complete loss of structure at doses above 4 kGy. The infectivity of the irradiated naked DNA was lost at doses above 4 kGy, but after irradiation of the intact virus some plaque-forming ability was retained after doses of 10 or even 40 kGy. Thus the organization within the viral capsid may play a protective role by modifying the severity of the radiation damage, and preserving at least some degree of infectivity.

Int J Radiat Biol Downloaded from informahealthcare.com by Prevention Research Center on 08/03/11
For personal use only.

1. Introduction

The investigation of the sensitivity of genetic elements to ionizing radiation is of special importance, particularly in view of environmental pollution by natural or man-made radioactive contaminants, since it focuses attention on the determination of mutation, or the complete eradication, of elements with coding capacity or of controlling mechanisms for specific gene functions. It is also important in view of structural analysis of viral components (Anderegg *et al.* 1961, Schmidt *et al.* 1983), the widespread use of radiation to sterilize medical products and the interest in possible uses of radiation to sterilize biological products (Ward 1980).

The goal of the present study was to investigate the influence of ionizing radiation on the infectivity of both intact pure herpes simplex virus (HSV) and its isolated highly purified genome. Studies of the influence of radiation and of the environment, and the size of the DNA, on the radiosensitivity of viruses have been reported by others (Cameron *et al.* 1979). However, we believe this to be one of the first studies in which classical virological methods have been combined with modern molecular biological methods to compare the radiosensitivity of an intact virus and its highly purified isolated DNA.

The choice of HSV as a model for this investigation was based on the following: firstly that out knowledge of the influence of ionizing radiation on this virus is limited (Braun 1978, Cameron *et al.* 1979), secondly that this human virus is spread worldwide and is a member of the family of human herpesviridae which includes three other very important viruses, varicella-zoster-virus, cytomegalo-virus and Epstein–Barr-virus; thirdly that the pathogenesis and molecular biology of this virus

RIGHTSLINK

are well documented (Rawls 1985, Roizman and Batterson 1985, Spear and Roizman 1980), and finally that HSV shares common biological properties and genomic structures with other members of the family of herpesviridae (Honess 1984).

2. Materials and methods

2.1. *Cells and media*

Monkey kidney cells (RC-37), baby hamster kidney cells (BHK-21), and human embryonic foreskin fibroblasts (HFF-3) were grown in Eagle's basal medium balanced with Earle's salt solution (BME) supplemented with 10 per cent foetal calf serum, twice the standard concentration of amino acids and vitamins, 100 iu penicillin/ml and 100 μg streptomycin/ml (BME-FCS-10) as described previously (Darai *et al.* 1978).

2.2. *Virus*

HSV-1 KOS (Smith 1964, Parris *et al.* 1980), HSV-1/17 (Brown *et al.* 1973, Preston *et al.* 1978), HSV-Thea (Darai *et al.* 1982 a), HSV-1 ANG (Darai and Munk 1976), HSV-2 Müller (Darai *et al.* 1982 a) and HSV-2 HG52 (Timbury 1971) were used in this study. Essentially the viruses were grown on the appropriate cell cultures using Eagle's basal medium balanced with Earle's salt solution supplemented with 10 per cent foetal calf serum. The viruses were purified so that the virions were not contaminated with any components of the infected cells. All these strains were propagated in HFF-3 cell cultures at a multiplicity of infectious virus (MOI) of 0·01 PFU/cell. The cultures were incubated for 48 h at 37°C. The cultures were then freeze-thawed three times to obtain suspensions of virus. These were clarified by centrifugation at 1200 ***g*** for 15 min at 4°C and stored at −70°C until use. The infectivity was titrated by plaque assay using RC-37 monkey cells as described previously (Darai *et al.* 1980 b).

2.3. *Radiation*

The pure virus samples were suspended in distilled water and exposed to ionizing radiation in 1 ml volumes frozen at −80°C in dry ice. Irradiation was carried out using ^{60}Co γ-rays (Gammacell 220, Atomic Energy of Canada, Ltd; dose rate about 6·2 kGy/h), 10 MeV electrons (linear accelerator, V-7703, Varian Associates, Palo Alto, California: dose rate about 10 kGy/h), and 52 MeV deuterons (from the Karlsruhe isochronous cyclotron). The viruses were irradiated in polyethylene tubes for the ^{60}Co studies and in special plexiglas chambers for the linear accelerator and isochronous cyclotron irradiations. The radiation dose was checked using small thermoluminescent dosimeters placed at the back and front of one of the plexiglas irradiator chambers. The DNA samples (100 μl) were irradiated in aqueous solution (DNA concentration 10 μg/100 μl) at 18°C in polypropylene tubes. The DNAs could not be irradiated at −80°C, as were the virus samples, since DNA of ca. 150 kbp undergoes molecular fragmentation at this temperature.

2.4. *Virus titration*

The titres of virus were determined using RC-37 cell cultures as described previously (Darai *et al.* 1978).

Int J Radiat Biol Downloaded from informahealthcare.com by Prevention Research Center on 08/03/11
For personal use only.

RIGHTSLINK

2.5 *Restriction enzyme analysis*

The following restriction endonucleases were used: BamHI, EcoRI, and HindIII. These enzymes were purchased from Boehringer (Mannheim, F.R. Germany). Incubations were carried out using 1 μg DNA according to a standard procedure for each enzyme, and the resulting DNA fragments were separated on 0·5, 0·8 or 1·0 per cent agarose slab gels (Seakem, Biomedical, Rockland, MD, U.S.A.). Electrophoresis was performed at 4°C in vertical gels (35 × 20 × 0·3 cm) at 75 V (constant voltage). The gels were stained with ethidium bromide (0·5 μg/ml) and photographed under UV light.

2.6. *DNA preparation*

Intact viral DNA was prepared from RC-37 cells infected at a MOI of 0·01 PFU with the individual HSV strains and grown at 34°C as described previously (Wilkie 1973, Darai *et al.* 1982 a).

The DNA which was purified extensively after isopycnic CsCl gradient centrifugation and the purity was found to be very high as reflected in the adsorbance A260/A280 ratio of 1·85–2·0, values fully in accordance with internationally accepted criteria of purity. The G + C contents were 67–69 per cent and the DNAs were found to be very stable at 18°C. The DNAs used in this study were double-stranded and highly purified. No single-stranded DNA or nicks were detected by S1 enzyme treatment which showed that 99 per cent of the viral DNA was intact. The purity of the isolated DNA used in these studies is clearly demonstrated in the restriction enzyme cleavage patterns illustrated in Lanes 1 of figure 2 (*a*), (*b*) or (*c*). For comparative analyses, DNA from *Tupaia* adenovirus (Darai *et al.* 1980 a, Matz *et al.* 1980), *Tupaia* herpesvirus strain 2 (Darai *et al.* 1981 a), Mycoplasma hyorhinis (Darai *et al.* 1982 b), and phage lambda c1857 S7 (Daniels *et al.* 1983) purchased from Biolabs, Beverly, MA, U.S.A. were used.

2.7. *Transfection assay*

The infectivity of the viral DNA in BHK-21 cell cultures was measured using the method described by Stow and Wilkie (1976).

3. Results

3.1. *Sensitivity of HSV to ionizing radiation*

The retention of plaque-forming ability was used to assess the sensitivity of intact viruses from several strains of HSV-1 and 2 to γ-rays, electrons or deuterons. The calculated survival curves and the values for D_0, the radiation dose at which 37 per cent of the initial plaque-forming ability remains, are listed in table 1. The survival curves for three strains of HSV after irradiation with ^{60}Co γ-rays are given in figure 1. The data shown for each virus strain represent single experiments in which single or duplicate samples of virus were irradiated at each dose level. Numerical data on the changes in plaque-forming ability for HSV-1 strain 17 after irradiation with ^{60}Co γ-rays are listed in table 2. This strain shows a monoexponential survival curve over the whole dose range tested, from 0 to 40 kGy.

The observed data for 10 MeV electrons show values for D_0 which are comparable with the range of values for γ-rays in all the strains tested. The single study with 52 MeV deuterons yielded a D_0 value similar to that found for most of the HSV strains after irradiation with gamma rays.

Int J Radiat Biol Downloaded from informahealthcare.com by Prevention Research Center on 08/03/11
For personal use only.

RIGHTSLINK

Table 1. Radiation effects on survival of plaque-forming ability after irradiation of herpes simplex virus.

Radiation	Virus	Survival curve	$D_0 \pm 1$ s.e. (kGy)
60 Co γ-rays	HSV-1-Thea	99 E—0·81 ± 0·04 D	1·2 ± 0·1
	HSV-1-ANG	108 E—0·67 ± 0·04 D	1·6 ± 0·1
	HSV-1-KOS	99 E—0·96 ± 0·04 D	1·0 ± 0·1
	HSV-2-Müller	105 E—0·67 ± 0·05 D	1·6 ± 0·1
10 MeV electrons	HSV-1-Thea	100 E—0·34 ± 0·01 D	2·9 ± 0·1
	HSV-1-Thea	100 E—0·63 ± 0·04 D	1·6 ± 0·1
	HSV-1-ANG	100 E—0·27 ± 0·01 D	3·6 ± 0·2
	HSV-2-Müller	100 E—0·41 ± 0·02 D	2·4 ± 0·1
	HSV-2-HG52	100 E—0·54 ± 0·02 D	1·8 ± 0·1
52 MeV deuterons	HSV-1-Thea	101 E—0·77 ± 0·02 D	1·3 ± 0·03

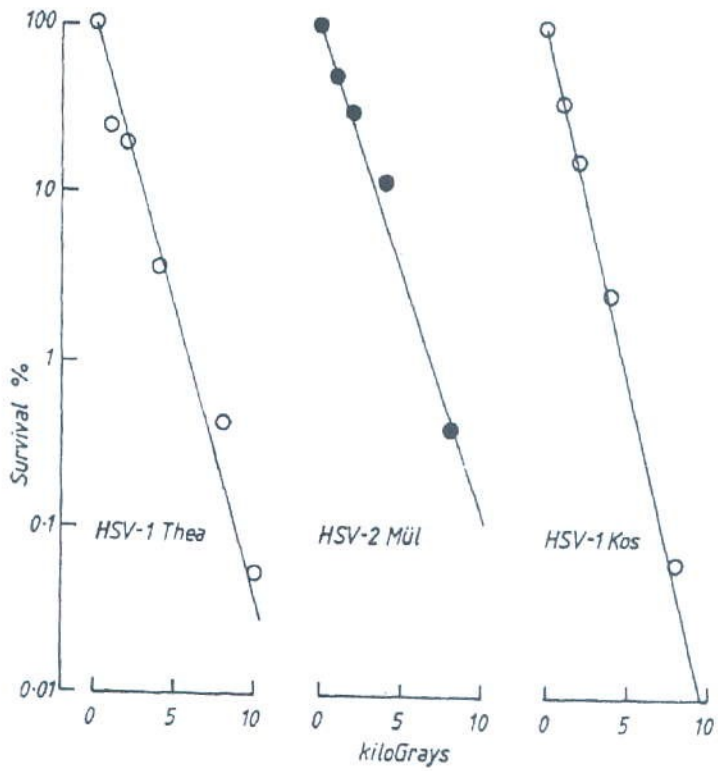


Figure 1. The effect of ^{60}Co γ-rays on the survival of plaque-forming ability in three strains of *herpes simplex virus*. The D_0 values are: HSV-1 Thea 1·2; HSV-2 Müller 1·6; and HSV-1 KOS 1·0 kGy.

Int J Radiat Biol Downloaded from informahealthcare.com by Prevention Research Center on 08/03/11
For personal use only.

RIGHTSLINK

110
109

Table 2. Protocol of a γ-irradiation experiment of HSV-1 strain 17 at a dose rate of 1 kGy/min.

Radiation doses (kGy)	Results of virus titration	
	PFU × ml^{-1}	Survival (per cent)
0†	$1{\cdot}9 \times 10^6$	100·00
1	$1{\cdot}3 \times 10^6$	76·1
2	$6{\cdot}5 \times 10^5$	34·2
4	$6{\cdot}1 \times 10^5$	31·7
8	$3{\cdot}2 \times 10^5$	16·7
10	$5{\cdot}7 \times 10^4$	3·0
20	$2{\cdot}5 \times 10^3$	0·13
40	2·5	0·0001
60	<1	

† Control experiment.

Int J Radiat Biol Downloaded from informahealthcare.com by Prevention Research Center on 08/03/11
For personal use only.

3.2. *Stability of the HSV-1 genome to ionizing radiation*

The stability of the HSV-1 genome after irradiation with ^{60}Co γ-rays was studied by electrophoresis of the viral DNA on agarose slab gels.

The results of this study for HSV-1 strains KOS and 17 are given in figure 2. The viral DNAs were irradiated with ^{60}Co γ-rays at doses 1, 2, 4, 8, 10 and 12 kGy. Aliquots of the individual samples were analysed directly on a 0·8 per cent agarose slab gel. The data in figure 2 (*a*) show that the viral DNA molecule began to disintegrate after 1 kGy (lane 2), but a broader DNA band was still detectable after 4 kGy (lane 4). In contrast no DNA band was observed at the position at which untreated viral DNA migrates when the irradiation doses were increased to 8 kGy or more (lanes 5, 6 and 7).

For further analysis the individual irradiated DNAs were analysed by a variety of restriction endonucleases. The results of this study for HSV-1 strains KOS and 17 are shown in figures 2 (*b*) and (*c*). The irradiated DNAs of HSV-1 strain KOS (figure 2 (*b*) and strain 17 (figure 2 (*c*)) were cleaved with the restriction endonuclease EcoRI and the resulting DNA fragments were separated electrophoretically. No significant differences between the cleavage patterns of the viral DNA irradiated with 2 kGy (lanes 3) and that of the untreated DNA (lanes 1) were detectable. Although the cleavage pattern of the DNA sample irradiated with 4 kGy (lanes 4) was still present, a smear through the lanes was observed indicating an increasing proportion of broken DNA molecules. Very severe damage of the DNA molecules was observed after irradiation with 8 kGy upwards (lanes 5 to 7 of figure 2 (*b*) and lane 5 of figure 2 (*c*)). The EcoRI DNA fragments K, L, M and N of HSV-1 (marked with letters in figure 2 (*b*)) appeared highly resistant to ionizing radiation. After 12 kGy (lane 7, figure 2 (*b*)) these DNA fragments were still present at the same migration position as the fragments obtained from untreated DNA (lane 1, figure 2 (*b*)). This may be largely a reflection of the known better stability of small restriction fragments in gels after any random fragmentation.

RIGHTSLINK

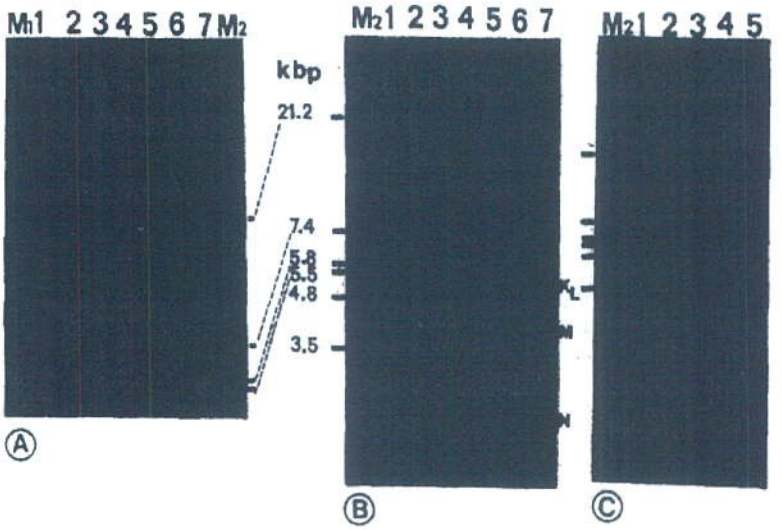


Figure 2. Analysis of DNA of herpes simplex virus type 1 strains KOS (*a* and *b*) and strain 17 syn (*c*) after irradiation with γ-rays using agarose slab gel electrophoresis and restriction enzyme digestion. Lanes of panel (a): DNA of HSV-1 KOS untreated (1) served as internal marker, after γ-ray irradiation with 1 kGy (2), 2 kGy (3), 4 kGy (4), 8 kGy (5), 10 kGy (6), 12 kGy (7). DNAs (1 μg of each sample) ran on agarose slab gel (0·8 per cent), 25 × 20 × 0·3 cm, and electrophoresis was performed at constant voltage (75 V), at 4°C for 18 h. Ethidium bromide staining and photographed under UV light. Phage lambda DNA undigested (M1) and digested with EcoRI (M2) served as molecular weight marker. Lanes of panel (*b*): 1 μg of each DNA sample corresponding to the lanes in the order of panel (*a*) was digested with restriction endonuclease Eco RI. The DNA fragments were separated on agarose slab gels (0·6 per cent), 35 × 20 × 0·3 cm) and electrophoresis was performed for 20 h under the same conditions described for panel (*a*). Lanes of panel (*c*): DNA of HSV-1 strain 17 syn untreated (1) served as internal marker, after γ-ray irradiation with 1 kGy (2), 2 kGy (3), 4 kGy (4) and 8 kGy (5). The DNA fragments were separated electrophoretically under the same conditions as described for panel (*b*).

3.3. *Study on the target size specificity*

In order to determine whether the effects of γ-rays were influenced by the target size of the HSV genome a comparative analysis was performed using other well-characterized pure DNAs from different viral species. The results of this study are shown in figure 3. The DNAs of tree shrew adenovirus DNA (TAV) of 35 kbp (Darai *et al.* 1980 a, Matz *et al.* 1980) (lanes 1), phage lambda c1857 S7 DNA of 48 kbp (Daniels *et al.* 1983) (lanes 2), HSV-1 strain KOS DNA of 150 kbp (Parris *et al.* 1980) (lanes 3), tree shrew herpesvirus DNA of 210 kbp (Darai *et al.* 1981 a) (lanes 4), and Mycoplama hyorhinis DNA of 750 kbp (Darai *et al.* 1982 b) (lanes 5) were irradiated with 1, 2, 4 and 8 kGy and subsequently analysed electrophoretically. Although the molecular size of TAV (35 kbp) DNA is about four times smaller than that of the HSV-1 genome (145 kbp), complete disintegration of the TAV-DNA was observed after a 2 kGy irradiation. The slightly larger phage lambda DNA (lane 2) had already disintegrated after a 1 kGy irradiation.

Int J Radiat Biol Downloaded from informahealthcare.com by Prevention Research Center on 08/03/11
For personal use only.

RIGHTSLINK

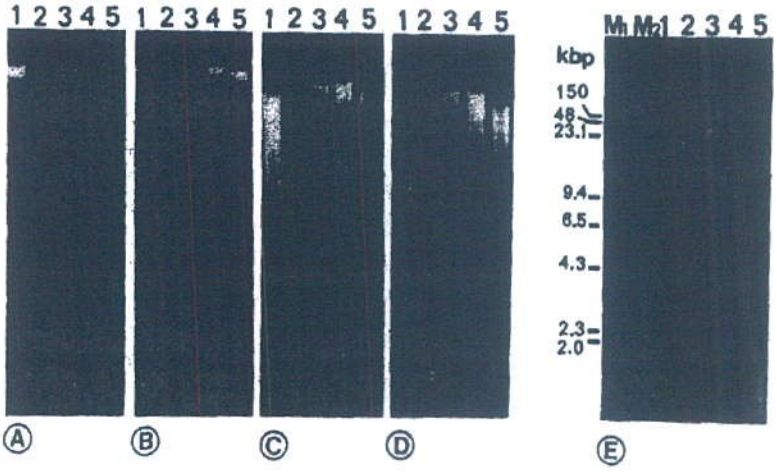


Figure 3. Analysis of different DNAs after γ-ray irradiation. Lanes: 1, DNA of tree shrew adenovirus (TAV); 2, DNA of phage lambda; 3, DNA of herpes simplex virus type 1 (HSV-1 KOS); 4, DNA of tree shrew herpesvirus strain 1 (THV-1); and 5, DNA of *Mycoplasma hyorhinis*. Panels: (*a*) untreated DNAs; (*b*) to (*e*) after γ-ray irradiation: (*b*) 1 kGy; (*c*) 2 kGy; (*d*) 4 kGy; and (*e*) 8 kGy. The electrophoresis was performed using 0·5 per cent agarose slab gel, 35 × 20 × 0·3 cm, at constant voltage (75 V), at 4°C, for 13 h. Ethidium bromide staining and photographed under UV light. Native herpes simplex virus DNA and phage lambda DNA (M1) and phage lambda DNA digested with restriction endonuclease Eco RI (M2) served as molecular weight marker.

3.4. *Infectivity of irradiated HSV genome*

The infectivity of the viral genome after ^{60}Co γ-irradiation was determined by transfection assays using BHK-21 cell cultures. One microgram of native and individually irradiated (1, 2, 4, 8, 10 and 12 kGy) DNAs of HSV-1 strains KOS and 17 were screened. The results of this study are summarized in table 3. It was found that the retention of plaque-forming ability was as follows: After transfection with unirradiated HSV-1 of strains KOS and 17 DNA, titres of 5·1 × 10 PFU/μg DNA respectively were determined. The percentages of the unirradiated DNA plaque-forming ability of irradiated HSV-1 KOS were found to be 37 per cent after 1 kGy, 12·2 per cent after 2 kGy, and 3·2 per cent after 4 kGy. Similar results were found for the retention of plaque-forming ability by the irradiated DNA of HSV-1 strain 17 (table 3). The infectivity of the viral DNAs was abolished (<1 PFU/μg DNA) when the viral genomes were irradiated with 8 kGy or more.

4. Discussion

The studies of the effects of ^{60}Co γ-rays or 10 MeV electrons on intact and highly purified HSV virions indicate that the radiation-induced loss of plaque-forming ability approximates to a monoexponential function for doses up to 10 or even 40 kGy, and even at the latter very high dose some plaque-forming ability was retained, 2·5 PFU/ml after 40 kGy to HSV-1-17 (table 2). The D_0 value for the inhibition of plaque-forming ability was found to lie between 1 and 3·6 kGy.

The D_0 values reported here are in general agreement with those reported for viruses by other workers, for example, Wollmann and Lacassagne (1940) found values of 0·5 and 4 kGy for the D_0 for the inactivation of the *E. coli* phages C. 16 and

Int J Radiat Biol Downloaded from informahealthcare.com by Prevention Research Center on 08/03/11
For personal use only.

RIGHTSLINK

Table 3. Infectivity of the DNAs of herpes simplex virus strains KOS and 17 after irradiation with ^{60}Co γ-rays.

	DNA†			
	HSV-1 KOS		HSV-1 17	
Radiation (kGy)	PFU/μg DNA	(per cent)	PFU/μg DNA	(per cent)
0 (native)	5107	(100)	3000	(100)
1	1936	(37·9)	1115	(37·1)
2	625	(12·2)	341	(11·3)
4	165	(3·2)	80	(2·6)
8				
10	<1	(0)	<1	(0)
12				

† 1 μg HSV-1 DNA = 10^{-3} pM (≅ 6×10^9 DNA molecules).

S. 13, respectively after irradiation with X-rays. More recently, Ward (1980) reported D_0 values of between 0·14 and 2·0 kGy for the inactivation of Poliovirus Type 1-CHAD by γ-rays; in this study the observed value of D_0 increased as the concentration of tryptose-phosphate broth in the medium in which the virions were irradiated increased. This indicates the protective effect on virus inactivation exerted by the components of the medium, presumably those which act as free-radical scavengers. In our study the pure virions were suspended in distilled water and irradiated in dry ice, thus the effects of both direct damage to the virion by adsorption of radiation energy and indirect damage from the radiolysis products of water were measured. It is therefore to be expected that the degree of damage we observed was considerably greater than would have arisen if the irradiations had been carried out in full culture medium.

The investigation of the effect of γ-rays on the isolated pure viral DNAs provided a number of interesting results. Electrophoretic analysis of the intact HSV-1 KOS DNA showed some evidence of an altered electrophoretic pattern even after a dose of 1 kGy and this increased in severity up to 8 kGy at which dose the characteristic DNA band had almost completely disappeared (figure 3, lanes 3). Similarly, the results of the electrophoretic analysis of the restriction endonuclease fragments showed some evidence of damage at a dose of 1 kGy but the basic cleavage pattern was lost only at doses of 8 kGy or above (figure 2 (*b*)). This very severe damage at doses above 4 kGy is reflected in the results of the transfection experiments (table 3) which showed virtually complete loss of infectivity of the HSV-1 KOS and HSV-1-17 DNAs at doses greater than 4 kGy. Analysis of the data shown in table 3 shows that up to 4 kGy the data for both strains can be fitted to a monoexponential function with a D_0 of about 1 kGy. For the DNA from HSV-1 KOS the D_0 is identical with that observed following γ-irradiation of the intact virus; for HSV-1-17 the D_0 for the isolated DNA was less than that for the intact virus (table 2). The complete loss of infectivity of the viral DNA after doses of more than 4 kGy contrasts with the retention of some degree of plaque-forming ability in the intact virus after much larger doses of radiation, even up to 40 kGy. This may indicate that in the intact virus the viral DNA is partially protected from radiation damage so that the degree of injury induced per Gy is less severe than when naked DNA is irradiated. This

Int J Radiat Biol Downloaded from informahealthcare.com by Prevention Research Center on 08/03/11
For personal use only.

RIGHTSLINK

113

protective role may be played by the proteins, polyamines or other components of the viral capsid and provides another indication of the potential for modification of the severity of the effect of a toxin, in this case ionizing radiation, by molecular organization.

The results shown in figures 2 and 3 and in table 3 also suggest that almost complete fragmentation of the viral DNA is needed to destroy its infectivity completely. This may be important in relation to the possible use of radiation to sterilize biological products for use in medicine, since the radiation doses needed to ensure the sterilization of any viruses present, > 500 kGy, would most likely severely damage protein and other components of the product.

Int J Radiat Biol Downloaded from informahealthcare.com by Prevention Research Center on 08/03/11
For personal use only.

Acknowledgment

This study was supported in part by the Deutsche Forschungsgemeinschaft. Schwerpunktprogramm 'Persistierende Virusinfektionen: Molekulare Mechanismen und Pathogenese' (Project II B 6-Da 142/1-3).

References

ANDEREGG, J. W., GEIL, P. H., BEEMAN, W. W., and KAESBERG, P., 1961, An x-ray scattering investigation of wild cucumber mosaic virus and a related protein. *Biophysical Journal*, **1**, 657–667.

BRAUN, R. W., 1978, Einfluß von Röntgenstrahlen auf die Transformationsrate embryonaler Rattenfibroblasten durch Herpes Simplex Virus Typ 1 und 2. Medical doctor thesis, University of Heidelberg.

BROWN, S. M., RITCHIE, D. A., and SUBAK-SHARPE, J. H., 1973, Genetic studies with herpes simplex virus type 1. The isolation of temperature-sensitive mutants, their arrangement into complementation groups and recombination analysis leading to a linkage map. *Journal of General Virology*, **18**, 329–346.

CAMERON, K. R., TOMKINS, L. M., EGLIN, R. P., ROSS, L. J. N., WILDY, P., and RUSSELL, W. C., 1979, The effects of ultraviolet and ionizing radiation on herpesviruses. SV40 and adenoviruses in relation to the small-plaque effect. *Archives of Virology*, **62**, 31–40.

DANIELS, D. L., SCHROEDER, J. L., BLATTNER, F. R., SZYBALSKI, W., and SANGER, F., 1983, *Lambda II: Appendix, Genbank 12.0*, edited by R. W. Hendrix, J. W. Robert, F. W. Stahl and R. A. Weisberg (Cold Spring Harbor, New York: Cold Spring Harbour Laboratory).

DARAI, G., FLÜGEL, R. M., MATZ, B., and DELIUS, H., 1981 a, DNA of tupaia herpesviruses. *Herpesvirus DNA, Developments in Molecular Virology*, edited by Y. Becker (The Hague, Boston, London: Martinus Nijhoff), pp. 345–361.

DARAI, G., FLÜGEL, R. M., ZÖLLER, L., MATZ, B., KRIEG, A., GELDERBLOM, H., DELIUS, H., and LEACH, R. H., 1981 b, The plaque-forming factor for mink lung cells present in cytomegalovirus and herpes-zoster virus stocks identified as mycoplasma hyorhinis. *Journal of General Virology*, **55**, 201–205.

DARAI, G., MATZ, B., FLÜGEL, R. M., GRAFE, A., GELDERBLOM, H., and DELIUS, H., 1980 a. An adenovirus from tupaia (tree shrew): growth of the virus, characterization of viral DNA, and transforming ability. *Virology*, **104**, 122–138.

DARAI, G., and MUNK, K., 1976, Neoplastic transformation of rat embryo cells with herpes simplex virus. *International Journal of Cancer*, **18**, 469–481.

DARAI, G., SCHOLZ, J., KURZ, W., and KOCH, H. G., 1982 a, Intertypic superinfection of herpes simplex virus *in vivo* leads to reisolation of latent viruses with newly acquired lymphotropic properties. *Developments in Biological Standardization*, edited by M. Bonneau (Basel, München: W. Hennessen and S. Karger), pp. 67–80.

DARAI, G., SCHWAIER, A., KOMITOWSKI, D., and MUNK, K., 1978, Experimental infection of *Tupaia belangeri* (tree shrews) with herpes simplex virus types 1 and 2. *Journal of Infectious Diseases*, **137**, 221–226.

RIGHTSLINK

DARAI, G., ZÖLLER, L., MATZ, B., DELIUS, H., SPECK, S. T., and FLÜGEL, R. M., 1982 b, Analysis of mycoplasma hyorhinis genome by use of restriction endonucleases and by electron microscopy. *Journal of Bacteriology*, **150**, 788–794.

DARAI, G., ZÖLLER, L. MATZ, B., SCHWAIER, A., FLÜGEL, R. M., and MUNK, K., 1980 b, Experimental infection and the state of viral latency of adult tupaia with herpes simplex virus type 1 and 2 and infection of juvenile tupaia with temperature-sensitive mutants of HSV type 2. *Archives of Virology*, **65**, 311–318.

HONESS, R. W., 1984, Herpes simplex and 'the herpes complex': diverse observations and a unifying hypothesis. *Journal of General Virology*, **65**, 2077–2107.

KIEFF, E. D., BACHENHEIMER, S. L., and ROIZMAN, B., 1971, Size, composition and structure of the DNA of subtypes 1 and 2 herpes simplex virus. *Journal of Virology*, **8**, 125.

MATZ, B., DELIUS, H., FLÜGEL, R. M., and DARAI, G., 1980, Physical map of the tupaia adenovirus DNA by cleavage with restriction endonucleases and partial denaturation. *Journal of General Virology*, **41**, 421–423.

PARRIS, D. S., DIXON, R. A. F., and SCHAFFER, P. A., 1980, Physical mapping of herpes simplex virus type 1 ts mutants by marker rescue; correlation of the physical and genetic maps. *Journal of Virology*, **100**, 275–287.

PRESTON, V. G., DAVISON, A. J., MARSDEN, H. S., TIMBURY, M. C., SUBAK-SHARPE, J. H., and WILKIE, N. M., 1978, Recombinants between herpes simplex virus types 1 and 2: analyses of genome structures and expression of immediate early polypeptides. *Journal of Virology*, **28**, 499–517.

RAWLS, W. E., 1985, Herpes simplex virus. *Virology*, edited by B. N. Fields (New York: Raven Press), pp. 527–562.

ROIZMAN, B., and BATTERSON, W., 1985, Herpesviruses and their replication. *Virology*, edited by B. N. Fields (New York: Raven Press), pp. 497–526.

SCHMIDT, T., JOHNSON, J. E., and PHILLIPS, W. E., 1983, The spherically averaged structures of cowpea mosiac virus components by X-ray solution scattering. *Virology*, **127**, 65–73.

SMITH, K. O., 1964, Relationship between the envelope and the infectivity of herpes simplex virus. *Proceedings of the Society for Experimental Biology and Medicine*, **115**, 814–816.

SPEAR, P. G., and ROIZMAN, B., 1980, Herpes simplex viruses. DNA tumour viruses. *Molecular biology of tumour viruses*, Part 2, edited by J. Tooze (Cold Spring Harbor, New York: Cold Spring Harbor Laboratory), pp. 615–745.

STOW, N. D., and WILKIE, N. M., 1976, An improved technique for obtaining enhanced infectivity with herpes simplex virus type 1 DNA. *Journal of General Virology*, **33**, 447–458.

TIMBURY, M. C., 1971, Temperature-sensitive mutants of herpes simplex virus type 2. *Journal of General Virology*, **13**, 373–517.

WILKIE, N. M., 1973, The synthesis and substructure of herpes virus DNA: The distribution of alkali-labile single strand interruptions in HSV-1 DNA. *Journal of General Virology*, **21**, 453–467.

WARD, R. L., 1980, Mechanisms of poliovirus inactivation by the direct and indirect effects of ionizing radiation. *Radiation Research*, **83**, 330–344.

WOLLMAN, E., and LACASSAGNE, A., 1940, Recherches sur le phénomène de twort-d'hérelle. Evaluation des dimensions des bactériophages au moyen des rayons X. *Annales de l'Institut Pasteur*, **64**, 5–39.

Int J Radiat Biol Downloaded from informahealthcare.com by Prevention Research Center on 08/03/11
For personal use only.

RIGHTSLINK

Anexo 8 40 115

Environmental Science & Technology

Article

pubs.acs.org/est

Virus Inactivation Mechanisms: Impact of Disinfectants on Virus Function and Structural Integrity

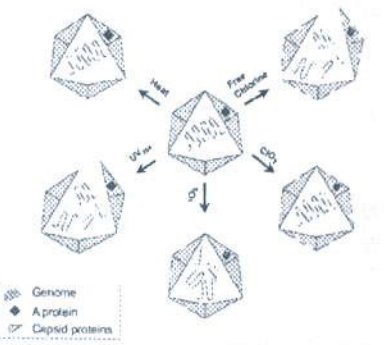
Krista Rule Wigginton,[†,‡,§] Brian M. Pecson,[†,∥] Thérese Sigstam,[†,∥] Franziska Bosshard,[†] and Tamar Kohn[†,*]

[†]Laboratory of Environmental Chemistry, School of Architecture, Civil and Environmental Engineering (ENAC), École Polytechnique Fédérale de Lausanne (EPFL), CH-1015 Lausanne, Switzerland

[‡]Department of Civil and Environmental Engineering, University of Maryland, College Park, Maryland 20742, United States

Supporting Information

ABSTRACT: Oxidative processes are often harnessed as tools for pathogen disinfection. Although the pathways responsible for bacterial inactivation with various biocides are fairly well understood, virus inactivation mechanisms are often contradictory or equivocal. In this study, we provide a quantitative analysis of the total damage incurred by a model virus (bacteriophage MS2) upon inactivation induced by five common virucidal agents (heat, UV, hypochlorous acid, singlet oxygen, and chlorine dioxide). Each treatment targets one or more virus functions to achieve inactivation: UV, singlet oxygen, and hypochlorous acid treatments generally render the genome nonreplicable, whereas chlorine dioxide and heat inhibit host-cell recognition/binding. Using a combination of quantitative analytical tools, we identified unique patterns of molecular level modifications in the virus proteins or genome that lead to the inhibition of these functions and eventually inactivation. UV and chlorine treatments, for example, cause site-specific capsid protein backbone cleavage that inhibits viral genome injection into the host cell. Combined, these results will aid in developing better methods for combating waterborne and foodborne viral pathogens and further our understanding of the adaptive changes viruses undergo in response to natural and anthropogenic stressors.



INTRODUCTION

Industrial processes take advantage of numerous treatment methods (e.g., UV irradiation, pasteurization, and chemical oxidation) to inactivate pathogenic bacteria and viruses for the sterilization of food and water supplies as well as vaccine production. While such treatments have been used for decades or even centuries, surprisingly little is known about what imparts their biocidal activity. Recent progress has been made toward unraveling how these treatments inactivate bacteria;[1] however, such detailed mechanistic understanding does not exist for viruses.

Virus inactivation is complicated by the fact that highly related viruses can exhibit different disinfection kinetics when treated with the same biocide.[2−5] For example, echovirus 1 is approximately 100× more susceptible to inactivation by monochloramine than echovirus 11 under the same conditions.[5] Similarly, Poliovirus 1 Bruhilde is twice as resistant to chlorine as the very similar Poliovirus 1 Mahoney.[2,3] These variable responses suggest that even minor variations in structural or genomic components can have a marked impact on viral resistance to inactivation. The type and extent of damage a virus can sustain before losing its ability to infect is largely unknown.

The specific mechanisms that lead to virus inactivation are also unclear. Previous studies demonstrated that exposure to inactivating oxidants and radiation results in modifications to viral proteins[2,6−10] and nucleic acids.[7,8,11,12] Based on detected damage in these biomolecules, researchers have proposed a number of virus inactivation mechanisms.[12−15] In many of these reports, however, inactivation is attributed to detected virus modifications without determining if these modifications were causal to or simply concurrent with inactivation and the loss of specific virus functions (e.g., host recognition, genome replication). Furthermore, many of the studies probe only a small portion of the virus particle or track bulk modifications (e.g., changes in spectroscopic properties, antibody recognition, etc.). Consequently, the proposed mechanisms are often contradictory. For example, poliovirus inactivation by FC has been independently attributed to both protein damage[8] and RNA damage.[12,16] In terms of specific function losses, FC inactivation of adenovirus was attributed to damage in viral proteins necessary for genome delivery,[15] whereas FC treatment of human picornaviruses and feline caliciviruses was attributed to a loss in host cell recognition.[8] A systematic understanding of virus inactivation based on linking specific modifications to losses in essential virus functionalities would potentially direct the development and optimization of

Received: July 20, 2012
Revised: October 3, 2012
Accepted: October 4, 2012
Published: October 26, 2012

 © 2012 American Chemical Society dx.doi.org/10.1021/es3029473 | Environ. Sci. Technol. 2012, 46, 12069−12078

116

treatments and strengthen our understanding of virus adaptation to environmental stressors.

In light of these points, we explored the effects of five common disinfectants (free chlorine (FC), singlet oxygen ($^1O_2$), chlorine dioxide (ClO_2), UV radiation, and heat) on bacteriophage MS2, a common surrogate for enteric viruses due to its similar shape and composition. MS2 is an icosahedral virus with a single stranded RNA genome (3690 nt) that encodes four proteins: a coat protein (CP; 13.7 kDa), a maturation, or assembly protein (AP; 44.0 kDa), a replicase and a lyticase.[17] The virus particle contains 180 copies of the CP and a single AP copy--the specific role of the AP is largely unknown. MS2 particles attach to receptors on the F-pili of *Escherichia coli* at which point the genome and portions of the AP are injected into the host cell. Once inside the host cell, MS2 proteins are translated by the host ribosome and MS2 RNA is transcribed by a complex of MS2 replicase and three host proteins.

The specific goals of this study were to (1) quantify how each of the vital viral functions is affected by exposure to inactivating treatments, (2) identify the affected protein and genome regions that cause the losses in function, and (3) seek generalities on the mode of action among different inactivating treatments. We developed methods to track the loss of the three essential virus functions—host binding, genome injection, and genome replication. Simultaneous with these assays, we located and tracked chemical modifications in the genome and virus proteins with quantitative reverse transcription polymerase chain reaction (qRT-PCR) and quantitative protein mass spectrometry (MALDI-TOF MS), respectively. This approach allowed us to monitor the distribution and quantify the extent of modifications across the virus genome and proteome rather than observe bulk chemical and structural changes. Furthermore, to make meaningful comparisons between different treatment methods, we measured damage at well-defined levels of inactivation.

EXPERIMENTAL SECTION

Chemicals and Microorganisms. All reagents and organisms used are described in the Supporting Information (SI).

General Experimental Approach. In brief, our work was divided into three sets of experiments: first, we determined the rate of infectivity loss of MS2 for five disinfecting agents (infectivity assays): free chlorine (FC), singlet oxygen ($^1O_2$), chlorine dioxide (ClO_2), UV at 254 nm, and heat at pasteurizing temperature (72 °C). Second, we determined the extent to which virus functions (host binding, genome injection, and genome replication) were affected during inactivation (functionality assays). Third, we quantified the degradation of the individual virus components during inactivation, namely the MS2 genome, capsid protein, and A protein (integrity assays).

Infectivity Assays. All experiments were conducted with constant stirring in dilution buffer at room temperature (DB, 5 mM PO_4^{2-}, 10 mM NaCl, pH 7.4), and reaction solutions contained between 1×10^{11} and 5×10^{11} plaque forming units of MS2 per milliliter (PFU/mL). Inactivation kinetics were established for each of the disinfecting treatments prior to the virus functionality and integrity studies. Kinetics were expressed in terms of first-order kinetics (ln C/C_0 versus disinfectant dose), with inactivation rate constants $k_{infectivity}$. ClO_2 is well-known to deviate from first-order kinetics at higher doses;[18,19] consequently, only the initial 2−3 logs were considered for which a first-order model was applied. MS2 samples were inactivated with heat, UV and $^1O_2$ as previously described[9,20] and the specifics of FC and ClO_2 inactivation experiments are described in detail in the SI.

Virus Functionality Assays. Virus functionality experiments were conducted to assess the rate at which the MS2 population loses its ability to bind to the host cell, and the rate at which the MS2 population loses its ability inject its genome. In these experiments, viruses with intact host binding (see Binding Assay below), and viruses with intact genome injection mechanisms (see Injection Assay below) were isolated after disinfection treatment. Their concentration was then determined by enumerating the number of genome copies in the sample by quantitative RT-PCR (qRT-PCR), targeting genome segment 3 (see SI Table S1 for location and corresponding primers).

Specifically, sacrificial reactors containing MS2 were treated to several inactivation levels between 0 and 3 $\log_{10}$ as discussed for the infectivity assays. These low levels of inactivation were chosen to avoid confounding effects of nonspecific host binding, as quantified in experiments with *E. coli* that lacked F-pili (DSMZ No. 13127). Small aliquots were enumerated by culturing to determine the exact inactivation level. Each sample was then divided into three subsamples: one subsample was assayed for its ability to bind to the host cell, one subsample was assayed for its ability to inject its genome into the host cell, and one subsample was used as the PCR control. This latter sample served to quantify the loss in PCR signal due to genome degradation by the disinfectant, rather than due to reduction in host binding or injection. The genomes of viruses in the PCR control samples were extracted and the number of genome copies was determined by qRT-PCR as previously described.[20] For each level of inactivation, the number of genome copies, n_t was determined, and compared to the number of genome copies in the untreated sample (n_0). The first-order rate constant of PCR signal decrease due to genome damage by the disinfectant, k_{damage}, was calculated by plotting $\ln(n_t/n_0)$ versus dose.

Binding Assay. The MS2 *E. coli* host was grown to log growth phase (optical density of 0.2). At this point, 10 mM $CaCl_2$ was added to the bacteria and 10 mL aliquots were transferred to media tubes and placed on ice. At 4 °C, bacterial growth is inhibited but the extracted F pili provide attachment sites for the viruses; the viral genomes, however, do not eject and eclipse at this temperature.[21] Bacterial suspensions were inoculated with equal volumes of untreated MS2 control samples or partly inactivated samples such that the multiplicity of infection (MOI) in the control samples equaled 0.01; this low MOI value increased the likelihood that no more than one virus adsorbed to a given bacterium. The samples were incubated on ice for 90 min and then centrifuged at 3000*g* for 15 min at 4 °C. The resulting bacterial pellet contained host-attached virus; viruses that failed to bind were removed with the supernatant. The pellet was washed with Tris buffer (TB, 50 mM Tris HCl, pH 8) four times and finally suspended in 200 μL of TB. Total RNA (viral and bacterial) was extracted from the pellet and the qRT-PCR assay[22] was used to quantify the number of viruses bound to the host cells. The first-order rate constant of genome loss measured with the binding assay, $k_{observed}$ was calculated from $\ln(n_t/n_0)$ values at several treatment doses. This measured rate constant was corrected

for the decrease in PCR signal due to genome damage, to obtain the true rate constant of binding loss, $k_{binding}$:

$$k_{binding} = k_{observed} - k_{damage}$$

Injection Assay. To determine the impact of inactivating treatments on the genome injection capacity of viruses, bacteriophage control samples and inactivated samples were first bound to host cells at 4 °C for 30 min as described above. Approximately 0.2 mM chloramphenicol was then added to the bacterial-viral suspensions and the samples were incubated at 4 °C for another 60 min. By inhibiting bacterial protein synthesis,[23] chloramphenicol prevented the translation of the viral replicase proteins that are essential for genome amplification, and thus prevented injected bacteriophage genomes from replicating. The sample temperatures were then raised to 37 °C for 30 min to initiate genome injection into the host cells. Samples were treated by vigorous pipetting with freshly prepared 0.1% SDS to detach bacterial F pili from the cells. As a result, genomes in viruses bound to host cell pili were separated from genomes inside the host. Sample suspensions were centrifuged and rinsed twice with 0.1% SDS and twice with TB to separate bacterial pellets from unbound virus and detached pili. RNA was extracted from the pellets and quantified with qRT-PCR. The first-order rate constant for genome loss measured from the injection assays, $k_{observed}$ was calculated from $\ln(n_t/n_0)$ values at several treatment doses. This measured rate constant was corrected for the decrease in PCR signal due to genome damage and due to the loss of binding to obtain the true rate constant for loss of genome injection, $k_{injection}$:

$$k_{injection} = k_{observed} - k_{binding} - k_{damage}$$

Replication. No experimental assay was available to directly measure the rate constant for the loss of the replication function, $k_{replication}$. It was therefore calculated based on the rate constants for infectivity, binding and injection loss:

$$k_{replication} = k_{infectivity} - k_{binding} - k_{injection}$$

Details for the rationale of this calculation is given in the Results section.

Virus Integrity Assays. In order to correlate the observed functionality losses to virus particle damage, we assessed the integrity of viral genomes and viral proteins using qRT-PCR and protein mass spectrometry techniques, respectively. Samples (10 mL) were disinfected as described in the Infectivity Assay section to obtain inactivation levels between 0 and 9 $\log_{10}$. Aliquots of 100 μL were removed and enumerated by culturing to determine the exact level of inactivation. A second set of 100 μL aliquots was collected, and their RNA was extracted for viral genome analysis as described previously.[20] The remaining volume was utilized to assess protein integrity.

Genome integrity. Six MS2 genome segments (SI Table S1) were measured separately by qRT-PCR; combined, these fragments covered approximately 50% of the translated genome region. We subsequently calculated the intact fraction of each segment, n_i/n_{i0}, where n_{i0} and n_i represent the number of intact genome segments, i, detected before and after a given level of disinfection, respectively. "Intact segment" therefore refers to a segment capable of amplification by qRT-PCR. Individual segment decay constants (k_{app}) were calculated from first-order fits of $\ln(n_i/n_{i0})$ versus dosage and $\log_{10}$ inactivation.

We estimated the intact proportion of the full MS2 genomes at different levels of disinfection, N/N_0, by first finding the product of the intact fractions of the individual segments, and then extrapolating this value to account for the genome portion not covered by the PCR assay:[22]

$$\frac{N}{N_0} = \left(\prod \frac{n_i}{n_{i0}}\right)^{\text{genome length/total length of all PCR segements}}$$

Only genome segments with a decay rate significantly different from zero (SI Table S2, $p < 0.05$) were used to determine N/N_0.

Protein Integrity. [^{15}N] bacteriophage internal standard stock was added to the control and treated samples for quantitative MALDI-MS analysis (the production of [^{15}N] bacteriophages is described in the SI). The labeled and native proteins were then digested into peptides with proteases. In silico digestions of the capsid protein (CP) and assembly protein (AP) and the corresponding [^{15}N]-labeled proteins were conducted with the ExPASy protein tool PeptideMass (SI Tables S3 and S4).[24] For the CP analysis, the spiked samples (~10 mL) were split into two equal volumes for trypsin and chymotrypsin protease treatments and concentrated with 100 kDa Microcon centrifugal filters (Millipore, Billerica, MA) to a final volume of 20 μL. For protease treatment, CP samples were first denatured at 95 °C for 10 min. Cysteines were acetylated with freshly prepared iodoacetamide (5 μL 25 mM in TB) at 37 °C for 1 h at which point the reactions were quenched with excess cysteine. Each sample was spiked with freshly prepared trypsin or chymotrypsin stocks at a 50:1 capsid protein to enzyme ratio and digested overnight at 37 °C. For the AP analysis, internal standard-spiked samples were separated with SDS PAGE to purify AP from the more abundant CP.[25] The separation was conducted with 12% polyacrylamide gels and Coomassie staining. The AP lane (42 kDa) was cut and immediately subjected to cysteine acetylation followed by in-gel digestion with trypsin and chymotrypsin.[26]

All MALDI measurements were performed with an ABI 4800 MALDI-TOF-TOF (Applied Biosystems, Rotkreuz, Switzerland). Sample deposition onto MALDI plates and instrument settings were described previously.[9]

Calibration curves with [^{15}N] MS2 peptide internal standards were prepared to track the fraction of unmodified peptides (i.e., no mass change: cp_i/cp_{i0} for capsid proteins and ap_i/ap_{i0} for A protein, respectively) at various doses of disinfecting treatments. Calibration curves were established by plotting the known ratio of native [^{14}N] peptides to labeled [^{15}N] peptides on the x-axis and the measured MALDI peak height ratios of native peptides to labeled peptides ([^{14}N] peptide peak height/[^{15}N] peptide peak height) on the y-axis (SI Figure S1). Peptide decay generally exhibited first-order kinetics for FC, $^1O_2$, and UV (SI Figure S2). First-order peptide decay rate constants (k_{app}) were calculated in terms of both dosage and $\log_{10}$ inactivation.

The fraction of unmodified MS2 capsid proteins (CP/CP_0) was approximated as the product of the intact peptide fractions:

$$\frac{CP}{CP_0} = \prod \frac{cp_i}{cp_{i0}}$$

An analogous analysis of was conducted for the A protein. However, since MALDI was unable to capture the entirety of

amino acids in the A protein (A protein coverage was 42–67%), AP/AP_0 was determined by extrapolation as follows:

$$\frac{AP}{AP_0} = \left(\prod \frac{ap_i}{ap_{i0}}\right)^{\text{number of amino acids in A protein / number of amino acids detected by MALDI}}$$

Only peptides with decay rates different from zero (SI Tables S5, and S6; $p < 0.05$) were considered in the protein decay analyses.

RESULTS

Virus Functionality Loss. For MS2 to be infective, it must (1) bind to its host cell, (2) inject its genome inside the host cell, and (3) replicate once its genome is within the host cell. Each of these functions can be viewed as an assembly of several steps needed to complete the function (e.g., the genome replication function encompasses both translation and transcription). All of these functions must be intact for MS2 to be infective. The probability that a given population of MS2 is infectious can thus be expressed as follows:

$$P_{\text{infectivity}} = P_{\text{binding}} \times P_{\text{injection}} \times P_{\text{replication}}$$

where $P_{\text{infectivity}}$, P_{binding}, $P_{\text{injection}}$, and $P_{\text{replication}}$ represent the probability that viruses are capable of infecting, binding, injecting and replicating at a particular level of treatment, respectively. Of these four probabilities, the former three were experimentally assessed with the infectivity, binding, and injection assays. The respective probabilities correspond to the fraction of viruses with intact functionality upon treatment (e.g., $P_{\text{infectivity}} = C/C_0$). Because we were unable to directly measure the genome replication function, $P_{\text{replication}}$ at a particular treatment dose was thus determined based on the following relationship:

$$P_{\text{replication}} = \frac{P_{\text{infectivity}}}{P_{\text{binding}} \times P_{\text{injection}}}$$

The decay of $P_{\text{infectivity}}$, P_{binding}, $P_{\text{injection}}$, and $P_{\text{replication}}$ followed first-order kinetics versus dose with FC, $^1O_2$, UV, and heat treatments (SI Figure S3). For ClO_2, binding and injection were only assessed over the initial 2–3 $\log_{10}$ of inactivation due to its deviation from first order kinetics at higher inactivation levels (SI Figure S4). From these data, we determined first-order rate constants for infectivity loss ($k_{\text{infectivity}}$), binding loss (k_{binding}), genome injection loss ($k_{\text{injection}}$), and replication loss ($k_{\text{replication}}$) (SI Table S7).

Our results demonstrate that replication was inhibited by FC, $^1O_2$, and UV ($k_{\text{replication}} > 0$, Figure 1 and SI Table S7), whereas this function remained mostly intact following ClO_2 and heat treatment ($k_{\text{replication}}$ not different from 0). Host binding was impacted by $^1O_2$, ClO_2, and heat treatments (i.e., $k_{\text{binding}} > 0$), but showed minimal effect from UV and FC. These two treatments did impair viral genome injection, as did $^1O_2$ to a minor extent, ($k_{\text{injection}} > 0$), whereas heat and ClO_2 treatment did not.

Virus Component Decay. MS2 virus proteins are largely responsible for interactions with the host cell and injection mechanisms; an intact genome, in contrast, is necessary for the formation of new virus particles within the host cell. We therefore assume that measured losses in binding and injection functions are primarily due to protein damage and calculated losses in replication functions are due to genome degradation. To test this assumption, we monitored the decay of all three

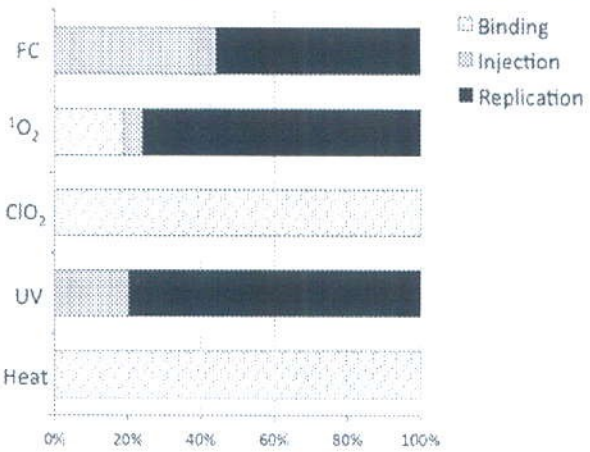


Figure 1. Relative contribution of binding, injection and replication loss to over all inactivation. The Figure is based on the rate constants k_{binding}, $k_{\text{injection}}$, $k_{\text{replication}}$, and $k_{\text{infectivity}}$ shown in SI Table S7.

MS2 components: the genome (N), the capsid protein (CP), and the assembly protein (AP).

Genome damage was negligible following heat and ClO_2 treatment, whereas UV, FC, and $^1O_2$ treatments resulted in extensive genome damage (Figure 2A). Protein damage followed a different trend than genome damage (Figure 2B and C): FC and ClO_2 caused extensive damage in the CP, with little or no detectable intact CPs remaining after 5 $\log_{10}$ inactivation (Figure 2B). The CP damage incurred by UV treatment was less pronounced, yet still extensive. For treatment by $^1O_2$, in contrast, most CP remained intact. Here, "intact protein" refers to unaltered protein mass. It is possible that physical and chemical modifications not resulting in mass changes could also impact vital virus functions; however, due to methodology limitations, we have considered only those protein modifications detectable with mass spectrometry. It should be emphasized that each capsid contains 180 copies of CP and that CP/CP_0 represents the intact fraction of individual CPs in a population rather than the intact fraction of the entire capsid. In other words, small quantities of measured CP damage in a sample population can have a large impact on the number of unmodified intact virus capsids.

Similar to the CP results, ClO_2 and FC had the most prominent effect on the integrity of the AP (Figure 2C). In contrast to the CP, however, $^1O_2$ caused more extensive damage in the AP than UV. MS2 only contains a single copy of AP; therefore, the reported intact fraction of AP (AP/AP_0) represents the fraction of virus particles with unmodified APs.

Location of Damage within Genome and Proteins. The qRT-PCR and quantitative MS analyses employed herein allowed us to observe the distribution of genome and protein damage, by separately analyzing the decay of different genome segments (n_i) or CP- and AP-derived peptides (cp_i or ap_i). Substantial nucleic acid damage occurred across most of the six measured genome segments as the virus was inactivated with FC, $^1O_2$, and UV (Figure 3A, SI Table S2); however, ClO_2 and heat treatment resulted in negligible degradation. Damage due to FC, $^1O_2$, and UV treatments was not consistent across the monitored regions of the viral RNA (Figure 3A, SI Table S2). The relative reactivities of each of the RNA segments with FC (segment $n_2 > n_3 \approx n_6 > n_5 > n_4 > n_1$) were similar to those with

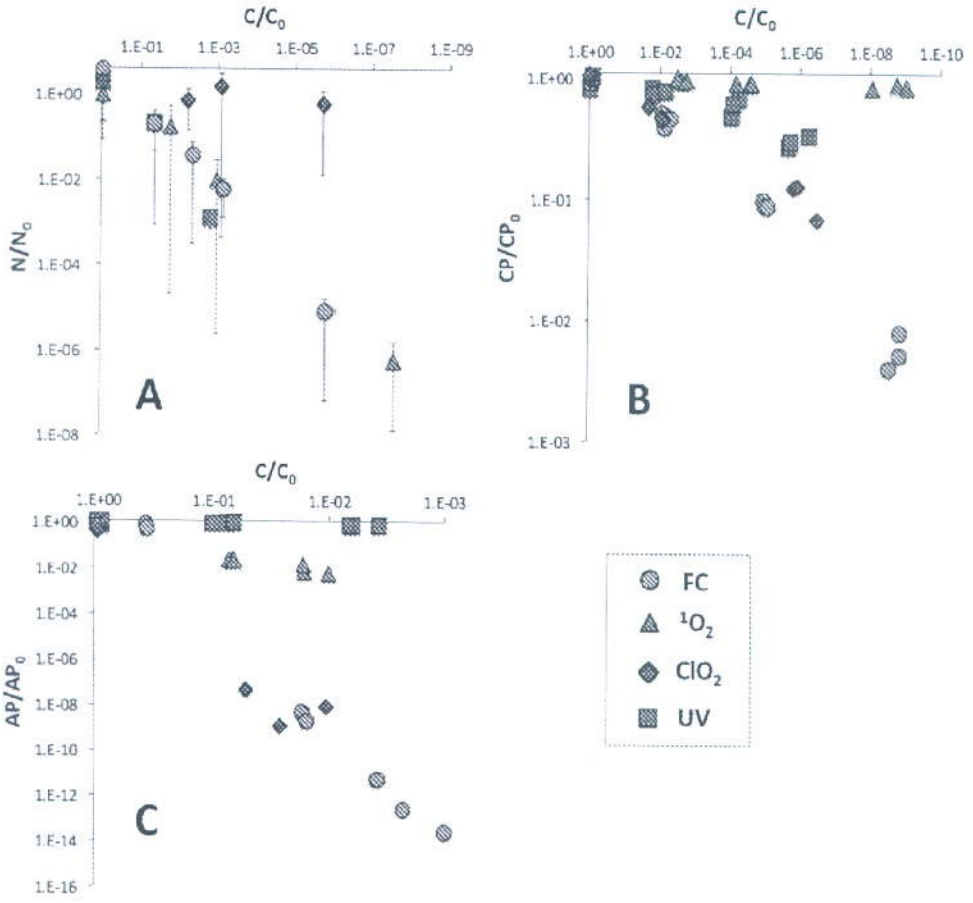


Figure 2. Decay of (A) genome (N/N_0), (B) capsid protein (CP/CP_0), and (C) assembly protein (AP/AP_0) as a function of infective viruses (C/C_0) following FC, $^1O_2$, ClO_2, and UV treatments. Error bars in genome plot (A) correspond to high and low measured values.

$^1O_2$ (segment $n_2 > n_3 > n_6 \approx n_5 > n_4 \approx n_1$); the reactivity trend differed significantly with UV (segment $n_2 = n_4 > n_1 = n_3 = n_5 > n_6$), illustrating that certain regions of the genome are more susceptible to FC and $^1O_2$ chemical attack and others to UV radiation.

Regression analysis conducted on CP and AP peptide concentrations ($\ln(cp_i/cp_{i0})$ or $\ln(ap_i/ap_{i0})$ versus disinfectant dose or $\log_{10}$ inactivation) identified a number of peptides that were modified during inactivating treatments (Figure 3B and C, SI Tables S5 and S6). FC treatment caused significant decay in every measured CP peptide when treated up to 8.5-$\log_{10}$ inactivation. ClO_2 and UV treatments were more selective, with decreases in cp_i/cp_{i0} observed in four and six of the 11 CP peptides, respectively, following 6-$\log_{10}$ inactivating treatment. Singlet oxygen treatment caused the most specific damage; only one CP peptide (Ser84-Lys106) decreased significantly following 8.3-$\log_{10}$ inactivating treatment.

The AP peptide MALDI-TOF MS signals measured in the virus digests were much weaker than the CP peptides due to the fact that there are 180 times fewer APs in the virus samples. As a result, poorer AP coverage (42–67%) was achieved compared to CP coverage (97%) (SI Table S8). Similar to the CP, FC, and ClO_2 treatments caused more extensive damage to the AP peptides at a particular level of inactivation than the $^1O_2$ and UV treatments (Figure 3C).

DISCUSSION

Disinfectants Exert Characteristic Impact on Vital Virus Functions. The importance of a given function to virus inactivation can be assessed by comparing the relative contributions of binding, injection, and replication to the overall rate of inactivation for the five disinfectant treatments (Figure 1, SI Table S7). A direct comparison of the disinfectants illustrates that each one has a characteristic mode of inactivation. Although it may not be surprising that the physical treatments (heat, UV) exhibit different inactivation patterns than the chemical oxidants ($^1O_2$, FC, ClO_2), there are also dramatic differences within the physical and chemical groups. This implies that not only the type of disinfectant (e.g., oxidant vs denaturing agent), but also their specific chemical reaction mechanism (e.g., ene reaction, chlorination, or one-electron transfer) dictates functional impairment.

The extent to which each disinfectant inhibited virus functions is in agreement with the level of genome and protein degradation (Figures 1 and 2). For example, substantial genome damage resulted from treatments that inhibited replication functions (UV, $^1O_2$, FC), but was not present after treatments that did not inhibit replication (ClO_2 and heat). Similarly, we observed extensive CP and AP degradation by treatments (FC, ClO_2) that resulted in significant loss in protein-mediated binding or injection functions. Modest protein damage occurred following treatments (UV, $^1O_2$) that

dx.doi.org/10.1021/es3029473 | Environ. Sci. Technol. 2012, 46, 12069–12078

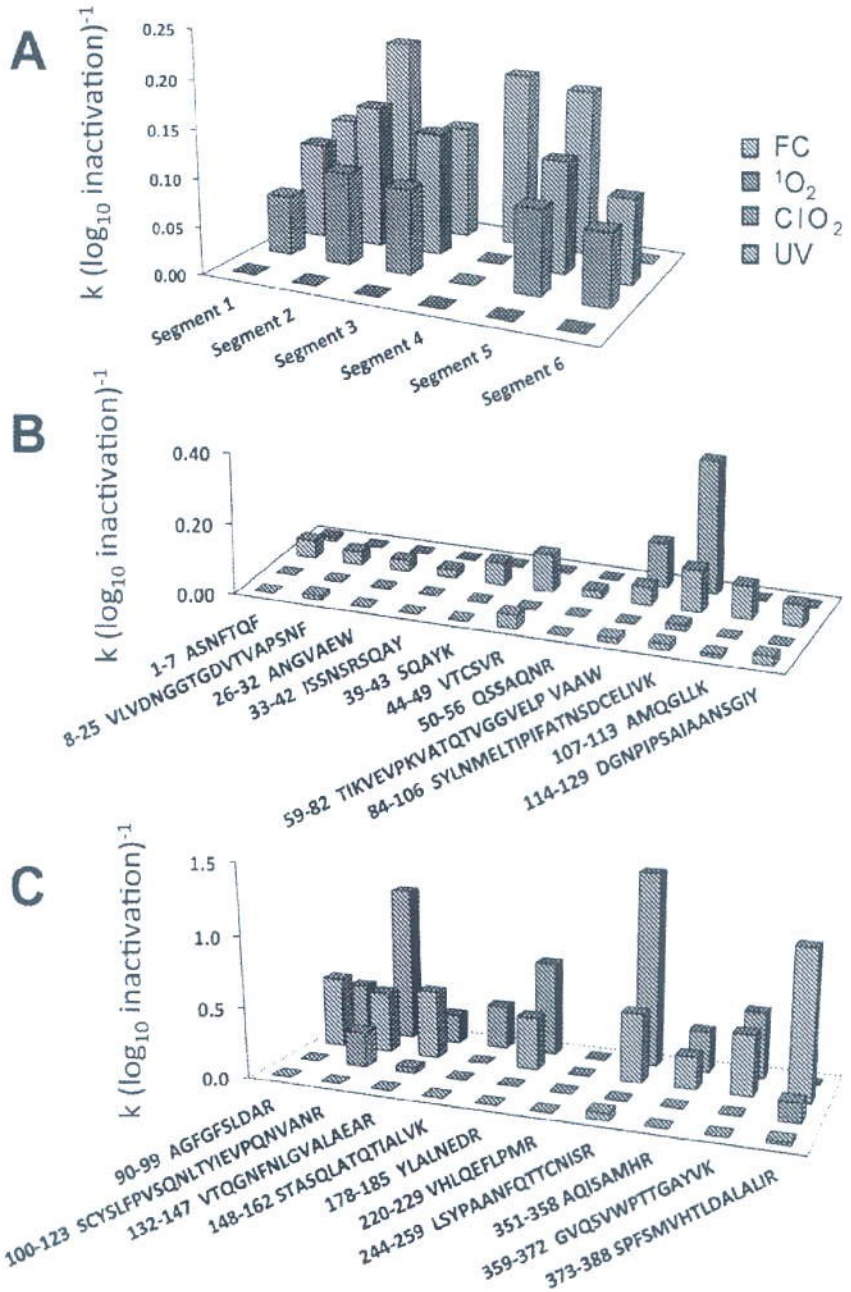


Figure 3. Decay rate constants of MS2 (A) genome segments, (B) CP peptides, and (C) a selection of AP peptides as a function of $\log_{10}$ inactivation. See SI Tables S2, S5, and S6 for a complete list of rates as a function of dose and the associated errors.

induced moderate protein-mediated function loss. Because $^1O_2$ and ClO_2 impaired binding, whereas FC and UV inhibited genome injection, it appears that MS2 does not have a critical "weakest link" that is susceptible to all of the virucidal treatments.

Reported reaction rate constants for the tested disinfectants with MS2 monomer components (i.e., amino acids and nucleotides) provide an opportunity to relate our findings with established chemical kinetics. For both FC and ClO_2, rate constants with amino acids are up to 3−4 orders of magnitude larger than rate constants with nucleotides.[27−29] This is in agreement with our finding that viral protein damage plays a major role in ClO_2; however, it fails to account for the large contribution of genome damage with FC inactivation. Reported reaction rate constants for $^1O_2$ and photochemical constants for UV are more similar among nucleotides and amino acids.[30−33] Yet, in both cases, genome damage dominates. This highlights the fact that qualitative predictions based on the relative magnitude of rate constants must take into account the structure of the virus particle.[34]

Molecular-Level Inactivation Mechanisms Are Unique for Individual Disinfectants. *UV Treatment.* Both viral genome and protein damage due to UV irradiation have been reported previously;[8,35−37] correspondingly, here we have detected damage in the MS2 genome and proteins (Figure 2). Our function assays demonstrate that UV causes MS2

inactivation primarily by inhibiting genome replication, but also by inhibiting genome injection (Figure 1). Replication inhibition is easily rationalized by the similarity of the rate of viral RNA decay and the rate of replication function loss (SI Tables S2 and S7); that is, for each UV-induced modification, the genome lost its ability to replicate. This is consistent with observations that UV irradiation transforms RNA itself (e.g, forming uracil cyclobutane dimers, uracil hydrate, and cytosine hydrate[38,39]) or cross-links it to other molecules (RNA−RNA and RNA−protein[40,41]) leading to products that the *E. coli* host cannot repair.[42] These nucleic acid photoproducts are known to block viral reverse transcriptase,[43] and therefore halt qRT-PCR amplification. Because UV modifications that inhibit MS2 genome replication thus also inhibit qRT-PCR amplification, the PCR signal loss is an appropriate proxy for biologically relevant genome damage by UV.

A number of chemical modifications in the CP with UV treatment (Figure 3B, SI Table S5) may explain why UV also impairs the genome injection function (Figure 1, SI Table S7). CP peptide decay rates with UV were comparable to the AP peptide decay rates (SI Tables S5 and S6); however, the fact that there are 180 copies of the CP per virion suggests that widespread damage occurs in the whole capsid shell concurrent with the loss of injection function. The CP peptide with the highest degradation rate was Val44-Arg49, this sequence undergoes a site-specific backbone cleavage between the Ser47 and Val48 residues.[9,44] If we assume that the measured Val44-Arg49 peptide degradation is due entirely to the protein backbone cleavage reaction (indeed, no other products were detected in our previous studies),[9] then the cleavage of approximately seven CPs occurs when 90% of the viruses have been inactivated ($cp_i/cp_{i0} = 0.96$ at 1 $\log_{10}$ inactivation, thus 4% 180 of CP damaged; Figure 3B, and SI Tables S5 and S7). The MS2 capsid is assembled under tension, and the virus transforms this stored energy to inject its genome into the host cell.[45] It is feasible that cleaving the CP backbone disrupts the scaffolding required to develop this tension, thereby reducing the energy available for genome injection.

Singlet Oxygen. $^1O_2$ caused inactivation primarily by impairing genome replication. Host binding was mildly affected, and a minor impairment in genome injection was found (Figure 1). Significant genome decay occurred with $^1O_2$ treatment, which corresponds to the observed replication function impairment. At least one major RNA product, 8-oxo-7,8-dihydroguanosine (8-oxoG), has been identified following exposure to $^1O_2$.[42] Although it is unknown if this product specifically affects the activity of the viral RNA-dependent RNA polymerase or the host cell's ribosomal machinery, it can lead to mutations during transcription by DNA-dependent RNA polymerases.[46] If RNA-dependent RNA polymerases undergo the same error, the presence of 8-oxoG in the genome may cause inactivation by producing mutations that render the viruses noninfective.

The loss in binding function is not likely the result of CP degradation by $^1O_2$. The one CP peptide (Ser84-Lys106) that decreased significantly with $^1O_2$ treatment experienced only moderate damage (Figure 3, SI Table S5). Based on the measured decay rate, only 3.6 modified peptides were present in an entire capsid following 1 log inactivation ($cp_i/cp_{i0} = 0.98$ at 90% inactivation; Figure 3B, and SI Tables S5 and S7). In contrast, several peptides in the AP were chemically modified during $^1O_2$ treatment (Figure 3, SI Table S6). One AP peptide, Ser78-Lys89, had a degradation rate constant (4.78×10^3 L $mg^{-1}s^{-1}$) similar to the binding function loss rate (3.5×10^3 L $mg^{-1}s^{-1}$; SI Table S7), suggesting that modification of this peptide by $^1O_2$ may be involved in the inhibition of host binding. This hypothesis aligns with observations that the AP plays a crucial role in MS2 binding to *E. coli* pili.[47,48]

Free Chlorine. FC has been shown to act on both genome[7,12,49] and proteins.[8,15] Here, FC treatment of MS2 caused losses in both genome- and protein-mediated functions, namely replication and injection (Figure 1, SI Table S7). The loss in genome replication coincided with extensive genome damage. The distribution of genome damage with FC was similar to that observed for $^1O_2$, but differed significantly from UV (Figure 3A). This is likely due to the fact that chemical oxidants are limited to solvent accessible areas of the virus particle, whereas UV penetration is not dictated by virus structure. Furthermore, FC induced genome damage at levels comparable to UV and $^1O_2$ treatments (Figure 2). Compared to UV and $^1O_2$, however, the replication function loss induced by FC accounted for a smaller proportion of overall inactivation (Figure 1). Thus, not all of the genome damage induced by FC contributed to inactivation. This suggests that it is not the location of genome modifications, but rather its type that determines the virucidal effect. Known products of RNA oxidation by FC include 5-chlorocytidine, 8-choloroguanosine, and to a lesser extent, 8-chloroadenosine.[42] The effects of these products on genome replication in the host, and hence their biological relevance for virus inactivation, is unknown. Certain types of genome damage may therefore be "read over" by the host machinery, such that multiple modification events are required to cause inactivation.

Contrary to $^1O_2$, the extensive degradation of the AP by FC did not lead to loss in binding. As observed for the genome, protein modifications induced by FC thus appear to be of less biological consequence compared to $^1O_2$. The extensive and widespread chemical modification of the CP (Figure 3) was unexpected given that $^1O_2$, also a chemical oxidant, did not appear to significantly attack any residues located at the interior of the CP. This suggests that FC altered the capsid structure in a manner that facilitated access to interior protein structures. FC can attack the protein backbone[28] and herein we detected a site-specific CP cleavage between capsid protein residues Glu50 and Ser51 (measured cleavage product mass = 5281 Da, theoretical mass of Asp1-Glu50 = 5281.7 Da; SI Figure S5) following FC treatment. Because both UV and FC treatments inhibited injection function and both treatments exhibited a site-specific CP cleavage, we propose that CP cleavage leads to the failure of MS2 to inject its genome.

Chlorine Dioxide. The most notable aspect of virus inactivation by ClO_2 is the absence of damage to the genome and lack of replication function inhibition (Figures 1 and 2). Instead, the inactivation action of ClO_2 is due primarily to the degradation of viral proteins. This is consistent with previous studies that demonstrated ClO_2 reacts more readily with amino acids than with nucleotides.[27,50,51]

On the protein level, ClO_2 is a selective oxidant, which reacts mainly with Cys, Trp and Tyr.[27] Similar to $^1O_2$, CP degradation was specific and affected mainly peptide Ser84-Lys106 (Figure 3, SI Table S5). The degradation of this peptide was more extensive with ClO_2 than for $^1O_2$, causing 67.5 out of 180 capsid proteins to be damaged at 90% inactivation (Figure 3B, SI Tables S5 and S7). However, the damage was not sufficient to disrupt the capsid protein's structure, as other susceptible residues remained protected. ClO_2 disinfection also resulted in

widespread AP degradation (Figure 3, SI Table S6). Several of the affected peptides exhibited degradation rates comparable to the observed binding inhibition rate, but poor coverage of the AP in these experiments did not allow for a conclusive statement about which AP region was most affected by ClO_2. In particular, AP peptide Ser78-Lys89, which was dominantly degraded by FC and $^1O_2$, was not detected in ClO_2 experiments. It is therefore not possible to assess if this peptide can be implicated in binding loss during ClO_2 treatment.

Heat. With heat treatment, the binding function decay rate was nearly equal to the inactivation rate and the injection and replication function rates were effectively zero (SI Table S7). This suggests that MS2 inactivation by heat (at 72 °C) is almost entirely due to MS2's loss in ability to bind with its host cell. The observed lack of replication function loss is in agreement with the lack of RNA degradation measured in the six regions of the MS2 genome (SI Table S2). Peptide modifications were not detected during heat treatment, suggesting that chemical modification of MS2 proteins did not occur. We previously demonstrated that heat treatment renders MS2 proteins more susceptible to protease attack,[20] which suggests that heat induces structural changes in the virus proteins. These transformations may cause inactivation by disrupting the specific structures needed to recognize and bind the host cells.

Rethinking Disinfectant Mode of Action and Design. Taken together, our results show that each treatment results in a unique MS2 inactivation pathway. Indeed, some of the inactivation mechanisms, particularly those that involve protein-mediated functions, rely on the modification of site-specific virus components. It is thus probable that different viruses, and even different serotypes, may have very different susceptibilities to inactivating treatments. For example, treatments (UV, FC) that cause protein backbone cleavage in MS2 in part inactivate the virus by inhibiting genome injection. However, the site-specific nature of the protein cleavages in MS2 suggests that protein backbone cleavage may not take place in viruses with different CP sequences. Indeed, CP cleavage was not observed following UV treatment of bacteriophage GA, a coliphage similar in morphology, composition, and life cycle to MS2; this was attributed to the absence of a cysteine residue in bacteriophage GA at the CP cleavage site.[44] Furthermore, this cleavage-based inactivation pathway can only be shared with viruses that exhibit the same tension-mediated injection function with MS2. Consequently, assigning general inactivation mechanisms based on the behavior of one virus strain may not be appropriate. Similar studies with other virus species will likely be required before general conclusions can be drawn about viral inactivation mechanisms by a particular disinfectant.

Nonetheless, these results have implications for our understanding of existing treatments and for the development and optimization of treatments. For example, oxidants like ClO_2 or heat treatments that target protein-mediated functions may be most effective for inactivating viruses with genome repair mechanisms (i.e., double-stranded DNA viruses). Likewise, UV treatment may be most effective for inactivating viruses without genome repair mechanisms (e.g., single-stranded RNA viruses), as it appears that nearly every detected modification in the MS2 proteins and genome contributed to a loss in virus infectivity. Treatments like UV and $^1O_2$ that inactivate viruses with little protein damage may be optimal for virus vaccine production, especially if an intact capsid is necessary to induce an immune response.[52] FC is a nondiscriminative treatment method, which causes high levels of nonspecific genome and protein damage; not all of this damage, however, necessarily inactivates the viruses. $^1O_2$ and UV on the other hand, are very efficient; selective protein damage resulted in binding or injection inhibition and the detected genome damage rendered the genome nonreplicable. Given the selective nature of UV and $^1O_2$ damage, a small number of mutations may be sufficient to defer MS2 inactivation by UV and $^1O_2$; consequently, viruses may easily evolve strategies to protect themselves from UV and $^1O_2$ than from FC.

This approach to virus inactivation mechanisms could also aid in understanding the fate of virus in natural systems. Invading viral pathogens, for example, are exposed to a barrage of host defense mechanisms including oxidative chemicals, including FC and reactive oxygen species. By elucidating inactivation mechanisms of an invading virus, we can better understand and predict the adaptations viruses may undergo to increase virulence and resistance. Similarly, the conditions that dictate the inactivation of marine viruses may depend on their ability to resist or adapt to stressors. For example, exposure to UV in the photic zone—where the majority of marine viruses are located[53]—can markedly decrease the abundance of certain virus strains.[54] Understanding the mechanisms of such phenomena is particularly important due to the fact that marine viruses influence global geochemical cycling[55] and ecosystem functioning.[56,57]

■ ASSOCIATED CONTENT

Supporting Information

A description of the reagents and organisms used; protocols for the disinfection by FC and ClO_2; the production of [^{15}N] metabolically labeled MS; and qRT-PCR protocols; tables containing degradation rate constants for viral infectivity and functions; degradation rate constants for individual genome segments, CP peptides and AP peptides; description of protein regions covered by MALDI; primer sequences and genome segments for qRT-PCR analysis; CP and AP peptides detected by MALDI; illustration of the decay of virus infectivity, binding function, injection function, and replication function with UV treatment; illustration of the disinfection kinetics by all five treatments; MALDI spectra showing CP cleavage upon disinfection by FC; example of calibration curve used to track C/C_0 for CP and AP peptides; example of the first-oder decay of a peptide. This material is available free of charge via the Internet at http://pubs.acs.org.

■ AUTHOR INFORMATION

Corresponding Author

*Phone: +41 (0)21 693 0891; e-mail: tamar.kohn@epfl.ch.

Present Address

[§]Department of Civil and Environmental Engineering, University of Maryland, College Park, Maryland 20742.

Author Contributions

[‖]B.M.P. and T.S. contributed equally to this work.

Notes

The authors declare no competing financial interest.

■ ACKNOWLEDGMENTS

This work was funded in part by a US-NSF international postdoctoral fellowship to K.R.W (IRFP No. 0905713), a Marie Curie Fellowship to B.M.P. (Grant No. 220706a), and a grant

from the Swiss National Science Foundation (Project No. 200021_118077). We thank Marc Moniatte, Nicholas Wigginton, and David Johnson for valuable discussions.

REFERENCES

(1) Winter, J.; Ilbert, M.; Graf, P. C. F.; Özcelik, D.; Jakob, U. Bleach activates a redox-regulated chaperone by oxidative protein unfolding. *Cell* **2008**, *135* (4), 691–701.

(2) Floyd, R.; Sharp, D.; Johnson, J. Inactivation by chlorine of single poliovirus particles in water. *Environ. Sci. Technol.* **1979**, *13* (4), 438–442.

(3) Sharp, D.; Leong, J. Inactivation of poliovirus-I (Brunhilde) single particles by chlorine in water. *Appl. Environ. Microbiol.* **1980**, *40* (2), 381–385.

(4) Baxter, C. S.; Hofmann, R.; Templeton, M. R.; Brown, M.; Andrews, R. C. Inactivation of adenovirus types 2, 5, and 41 in drinking water by UV light, free chlorine, and monochloramine. *J. Environ. Eng.* **2007**, *133* (1), 95–103.

(5) Cromeans, T. L.; Kahler, A. M.; Hill, V. R. Inactivation of adenoviruses, enteroviruses, and murine norovirus in water by free chlorine and monochloramine. *Appl. Environ. Microbiol.* **2010**, *76* (4), 1028–1033.

(6) Sano, D.; Pinto, R. M.; Omura, T.; Bosch, A. Detection of oxidative damages on viral capsid protein for evaluating structural integrity and infectivity of human norovirus. *Environ. Sci. Technol.* **2009**, *44* (2), 808–812.

(7) Dennis, W., Jr; Olivieri, V.; Kruse, C. Mechanism of disinfection: Incorporation of Cl-36 into f2 virus. *Water Res.* **1979**, *13*, 383–369.

(8) Nuanualsuwan, S.; Cliver, D. Capsid functions of inactivated human picornaviruses and feline calicivirus. *Appl. Environ. Microbiol.* **2003**, *69* (1), 350–357.

(9) Wigginton, K. R.; Menin, L.; Montoya, J. P.; Kohn, T. Oxidation of virus proteins during UV_{254} and singlet oxygen mediated inactivation. *Environ. Sci. Technol.* **2010**, *44* (14), 5437–5443.

(10) Hotze, E. M.; Badireddy, A. R.; Chellam, S.; Wiesner, M. R. Mechanisms of bacteriophage inactivation via singlet oxygen generation in UV illuminated fullerol suspensions. *Environ. Sci. Technol.* **2009**, *43* (17), 6639–6645.

(11) Li, J. W.; Xin, Z. T.; Wang, X. W.; Zheng, J. L.; Chao, F. H. Mechanisms of inactivation of hepatitis A virus in water by chlorine dioxide. *Water Res.* **2004**, *38* (6), 1514–1519.

(12) O'Brien, R.; Newman, J. Structural and compositional changes associated with chlorine inactivation of polioviruses. *Appl. Environ. Microbiol.* **1979**, *38* (6), 1034–1039.

(13) Kim, C. K.; Gentile, D. M.; Sproul, O. J. Mechanism of ozone inactivation of bacteriophage f2. *Appl. Environ. Microbiol.* **1980**, *39* (1), 210–218.

(14) Roy, D.; Wong, P.; Engelbrecht, R.; Chian, E. Mechanism of enteroviral inactivation by ozone. *Appl. Environ. Microbiol.* **1981**, *41* (3), 718–723.

(15) Page, M. A.; Shisler, J. L.; MariNas, B. J. Mechanistic aspects of adenovirus serotype 2 inactivation with free chlorine. *Appl. Environ. Microbiol.* **2010**, *76* (9), 2946–2954.

(16) Nuanualsuwan, S.; Cliver, D. Infectivity of RNA from inactivated poliovirus. *Appl. Environ. Microbiol.* **2003**, *69* (3), 1629–1632.

(17) Toropova, K.; Basnak, G.; Twarock, R.; Stockley, P. G.; Ranson, N. A. The Three-dimensional Structure of Genomic RNA in Bacteriophage MS2: Implications for Assembly. *J. Mol. Biol.* **2008**, *375* (3), 824–836.

(18) Thurston-Enriquez, J.; Haas, C.; Jacangelo, J.; Gerba, C. Inactivation of enteric adenovirus and feline calicivirus by chlorine dioxide. *Appl. Environ. Microbiol.* **2005**, *71* (6), 3100–3105.

(19) Lim, M. Y.; Kim, J.-M.; Ko, G. Disinfection kinetics of murine norovirus using chlorine and chlorine dioxide. *Water Res.* **2010**, *44* (10), 3243–3251.

(20) Pecson, B. M.; Martin, L. V.; Kohn, T. Quantitative PCR for determining the infectivity of bacteriophage MS2 upon inactivation by heat, UV-B radiation, and singlet oxygen: Advantages and limitations of an enzymatic treatment to reduce false-positive results. *Appl. Environ. Microbiol.* **2009**, *75* (17), 5544–5554.

(21) Paranchy, W.; Krahn, P.; Bradley, R. Stages in phage R17 infection. *Virology* **1970**, *41* (3), 465–473.

(22) Pecson, B. M.; Ackermann, M.; Kohn, T. Framework for using quantitative PCR as a nonculture based method to estimate virus infectivity. *Environ. Sci. Technol.* **2011**, *45* (6), 2257–2263.

(23) Brock, T. Chloramphenicol. *Bacteriol. Rev.* **1961**, *25* (1), 32–48.

(24) Gasteiger, E.; Gattiker, A.; Hoogland, C.; Ivanyi, I.; Appel, R. D.; Bairoch, A. ExPASy: The proteomics server for in-depth protein knowledge and analysis. *Nucleic Acids Res.* **2003**, *31* (13), 3784–3788.

(25) Laemmli, U. Cleavage of structural proteins during assembly of head of bacteriophage-T4. *Nature* **1970**, *227* (5259), 680–685.

(26) Shevchenko, A.; Wilm, M.; Vorm, O.; Mann, M. Mass spectrometric sequencing of proteins from silver stained polyacrylamide gels. *Anal. Chem.* **1996**, *68* (5), 850–858.

(27) Ison, A.; Odeh, I. N.; Margerum, D. W. Kinetics and mechanisms of chlorine dioxide and chlorite oxidations of cysteine and glutathione. *Inorg. Chem.* **2006**, *45* (21), 8768–8775.

(28) Pattison, D. I.; Davies, M. J. Absolute rate constants for the reaction of hypochlorous acid with protein side chains and peptide bonds. *Chem. Res. Toxicol.* **2001**, *14*, 1453–1454.

(29) Prutz, W. Hypochlorous acid interactions with thiols, nucleotides, DNA, and other biological substrates. *Arch. Biochem. Biophys.* **1996**, *332* (1), 110–120.

(30) Wilkinson, F.; Helman, W.; Ross, A. Rate constants for the decay and reactions of the lowest electronically excited singlet-state of molecular-oxygen in solution - an expanded and revised compilation. *J. Phys. Chem. Ref. Data* **1995**, *24* (2), 663–1021.

(31) Davies, M. Singlet oxygen-mediated damage to proteins and its consequences. *Biochem. Biophys. Res. Commun.* **2003**, *305* (3), 761–770.

(32) Gorner, H. Photochemistry of DNA and related biomolecules - quantum yields and consequences of photoionization. *J. Photochem. Photobiol. B* **1994**, *26* (2), 117–139.

(33) Khoroshilova, E. V.; Repeyev, Y. A.; Nikogosyan, D. N. UV protolysis of aromatic amino acids and related dipeptides and tripeptides. *J. Photochem. Photobiol. B* **1990**, *7* (2–4), 159–172.

(34) Wigginton, K. R.; Kohn, T. Virus disinfection mechanisms: The role of virus composition, structure, and function. *Curr. Opin. Virol.* **2012**, *2* (1), 84–89.

(35) Sirikanchana, K.; Shisler, J.; Marinas, B. J. Effect of exposure to UV-C irradiation and monochloramine on adenovirus serotype 2 eraly protein expression and DNA replication. *Appl. Environ. Microbiol.* **2008**, *74* (12), 3774–3782.

(36) Lytle, C.; Sagripanti, J. Predicted inactivation of viruses of relevance to biodefense by solar radiation. *J. Virol.* **2005**, *79* (22), 14244–14252.

(37) Eischeid, A. C.; Linden, K. G. Molecular Indications of Protein Damage in Adenoviruses after UV Disinfection. *Appl. Environ. Microbiol.* **2011**, *77* (3), 1145–1147.

(38) Miller, N.; Cerutti, P. Structure of the photohydration products of cytidine and uridine. *Proc. Natl. Acad. Sci. U. S. A.* **1968**, *59* (1), 34–38.

(39) Singer, B. Chemical modification of viral ribonucleic acid: 9. Effect of ultraviolet irradiation on TMV-RNA and other polynucleotides. *Virology* **1971**, *45* (1), 101–107.

(40) Wilms, C.; Noah, J.; Zhong, D.; Wollenzien, P. Exact determination of UV-induced crosslinks in 16S ribosomal RNA in 30S ribosomal subunits. *RNA* **1997**, *3* (6), 602–612.

(41) Zwieb, C.; Ross, A.; Rinke, J.; Meinke, M.; Brimacombe, R. Evidence for RNA-RNA cross-link formation in *Escherichia coli* ribosomes. *Nucleic Acids Res.* **1978**, *5* (8), 2705–2720.

(42) Wurtmann, E. J.; Wolin, S. L. RNA under attack: Cellular handling of RNA damage. *Crit. Rev. Biochem. Mol. Biol.* **2009**, *44* (1), 34–49.

(43) Smith, C.; Baeten, J.; Taylor, J. The ability of a variety of polymerases to synthesize past site-specific cis-syn, trans-syn-II, (6–4),

and Dewar photoproducts of thymidylyl-(3′- 5′)-thymidine. *J. Biol. Chem.* **1998**, *273* (34), 21933−21940.

(44) Wigginton, K. R.; Menin, L.; Sigstam, T.; Gannon, G.; Cascella, M.; Ben Hamidane, H.; Tsybin, Y. O.; Wahdel, P.; Kohn, T. UV radiation induces genome-mediated, site-specific cleavage in viral proteins. *ChemBioChem* **2012**, *13* (6), 837−845.

(45) Kuzmanovic, D.; Elashvili, I.; Wick, C.; Oconnell, C.; Krueger, S. The MS2 coat protein shell is likely assembled under tension: A novel role for the MS2 bacteriophage A protein as revealed by small-angle neutron scattering. *J. Mol. Biol.* **2006**, *355* (5), 1095−1111.

(46) Shibutani, S.; Takeshita, M.; Grollman, A. P. Insertion of specific bases during DNA synthesis past the oxidation-damaged base 8-oxodG. *Nature* **1991**, *349*, 431−434.

(47) Kozak, M.; Nathans, D. Fate of maturation protein during infection by coliphage MS2. *Nature* **1971**, *234* (50), 209−211.

(48) Krahn, P.; O'Callaghan, R.; Paranchych, W. Stages in phage R17 infection. VI. Injection of A protein and RNA into the host cell. *Virology* **1972**, *47* (3), 628−637.

(49) Li, J.; Xin, Z.; Wang, X.; Zheng, J.; Chao, F. Mechanisms of inactivation of hepatitis A virus by chlorine. *Appl. Environ. Microbiol.* **2002**, *68* (10), 4951−4955.

(50) Napolitano, M. J.; Stewart, D. J.; Margerum, D. W. Chlorine dioxide oxidation of guanosine 5′-monophosphate. *Chem. Res. Toxicol.* **2006**, *19* (11), 1451−1458.

(51) Stewart, D. J.; Napolitano, M. J.; Bakhmutova-Albert, E. V.; Margerum, D. W. Kinetics and mechanisms of chlorine dioxide oxidation of tryptophan. *Inorg. Chem.* **2008**, *47* (5), 1639−1647.

(52) Jurkiewicz, E.; Billasboas, M.; Silva, J.; Weber, G.; Hunsmann, G.; Clegg, R. Inactivation of simian immunodeficiency virus by hydrostatic-pressure. *Proc. Natl. Acad. Sci. U. S. A.* **1995**, *92* (15), 6935−6937.

(53) DeLong, E. F.; Preston, C. M.; Mincer, T.; Rich, V.; Hallam, S. J.; Frigaard, N. U.; Martinez, A.; Sullivan, M. B.; Edwards, R.; Brito, B. R. Community genomics among stratified microbial assemblages in the ocean's interior. *Science* **2006**, *311* (5760), 496−503.

(54) Noble, R.; Fuhrman, J. Virus decay and its causes in coastal waters. *Appl. Environ. Microbiol.* **1997**, *63* (1), 77−83.

(55) Lindell, D.; Sullivan, M.; Johnson, Z.; Tolonen, A.; Rohwer, F.; Chisholm, S. Transfer of photosynthesis genes to and from Prochlorococcus viruses. *Proc. Natl. Acad. Sci. U. S. A.* **2004**, *101* (30), 11013−11018.

(56) Waldor, M.; Mekalanos, J. Lysogenic conversion by a filamentous phage encoding cholera toxin. *Science* **1996**, *272* (5270), 1910−1914.

(57) Rohwer, F.; Thurber, R. V. Viruses manipulate the marine environment. *Nature* **2009**, *459* (7244), 207−212.

Anexo 9 126 125

Quarterly Reviews of Biophysics **26**, 1 (1993), pp. 27–48
Printed in Great Britain

Damage to proteins due to the direct action of ionizing radiation

E. S. KEMPNER

National Institute of Arthritis and Musculoskeletal and Skin Diseases, National Institutes of Health, Bethesda MD 20892, USA

1. INTRODUCTION 27

2. RADIATION DAMAGE AND THE PRIMARY STRUCTURE OF PROTEINS 29

3. RADIATION DAMAGE AND THE SECONDARY AND TERTIARY STRUCTURE OF PROTEINS 34

4. RADIATION DAMAGE AND THE QUATERNARY STRUCTURE OF PROTEINS 39
   - 4.1 *Creation of crosslinks by irradiation* 39
   - 4.2 *Retention of oligomeric structure* 40
   - 4.3 *Supermolecular structures* 40

5. LOSS OF BIOLOGICAL ACTIVITY AND IMPLICATIONS ABOUT SITE OF PRIMARY IONIZATION *VERSUS* SITES(S) AND NATURE OF DAMAGE 40

6. SUMMARY OF GENERALIZATIONS 43

7. REFERENCES 44

1. INTRODUCTION

Proteins exposed to ionizing radiation suffer both reversible and irreversible effects. Reversible effects are defined as those which disappear in a short period of time after the removal of the radiation field and without further treatment of the sample. Irreversible effects are those which cause a permanent alteration in the structure of a protein. It is the irreversible changes in irradiated proteins which will concern us here.

In general, the vast majority of radiation effects on macromolecules are due to the indirect action of the radiations. In these cases, radiation damage to some molecule results in the production of chemically reactive species which diffuse to and react with other molecules in the sample. Since radiation interactions occur randomly throughout the mass of any exposed material, and since most biological materials are principally (~ 80%) water, these reactive species are most often radiolytic products of water. Their ultimate reaction with macromolecules occurs at a specific chemical group defined by the nature of the particular radiolytic agent. Thus for every primary ionization, one or more reactants can be produced which are capable of diffusing to a macromolecule and reacting at a single locus (von

Sonntag, 1987). The nature of radiation damage in proteins due to these indirect effects is complex, since it is defined by the nature of the particular protein, the chemical environment in which it is irradiated, and the physical conditions which exist. Temperature is a critical physical factor since it directly affects diffusion rates; similarly, the time between radiation exposure and product analysis will also be an important factor. Physical barriers between the radiolytic product and the macromolecule obviously could have considerable influence on the final radiation damage.

The direct effects of radiation on macromolecules arise from interactions directly between the ionizing radiation and the macromolecules. By definition, the other molecules play no role in these effects. In comparison to indirect effects, the direct effects of ionizing radiation on macromolecules in liquid solution are quantitatively insignificant. Yet these direct effects are much more easily understood since they represent a much more limited set of mechanisms and considerably smaller range of products (Garrison, 1987).

At low temperature, diffusion rates are considerably reduced. In aqueous systems the major effect is the phase change from liquid to frozen state during which the diffusion constant changes by up to five orders of magnitude. The quantity of primary radiation products formed at low temperatures will be the same as that at room temperature, but their range of movement is grossly different. The reaction rate of these products is expected to decrease as the temperature is lowered, but the change in reaction rate is dwarfed by the change in diffusion rate. The experimental conditions which have been described for radiation exposure at low temperature (Harmon *et al.* 1985; Jung, 1984; Beauregard *et al.* 1987) effectively curtail the role of the indirect actions of radiation and the role of direct radiation damage on macromolecules becomes the predominant mechanism. Other procedures to minimize the indirect effects of radiation without affecting the direct mechanisms of molecular damage have been attempted, primarily the use of lyophilized samples. Lyophilized samples have ben successfully used in determining target sizes (see below) in several protein systems, but there have been notable failures, principally with membrane-bound proteins (Angelides *et al.* 1985).

Mathematical analysis of the probability of radiation damage to proteins has been developed for cases in which it is assumed that only the direct action of radiation is involved. Since primary ionizations from gamma rays and high-energy electrons occur at random in the mass of the sample, the probability of these interactions is described by the Poisson distribution. Furthermore, the energy transferred to the target molecule (average 65 eV) is so large that the molecule suffers irreversible changes, resulting in loss of structure and of function. Only molecules which have escaped primary ionizations will survive unaltered. 'Target theory' yields a relationship between the fraction of surviving protein molecules (N/N_0) and the amount of radiation absorbed (dose, D) which leads to an estimate of the mass (m) of the protein molecules:

$$N/N_0 = e^{-\Omega m D},$$

where Ω is a constant. The theory can be extended to cases where the protein

possesses some unique and measurable property such as biological activity or fluorescence. The surviving function can be measured in irradiated samples and the mass of the active structure can be calculated (Kempner & Fleischer, 1989). Since these target masses correspond to the known physical mass of a large number of proteins, the experimental conditions to limit molecular damage to the direct action of radiation are validated.

Using a variety of procedures, considerable data has accumulated about the nature of the direct damage in individual protein molecules. Some information arises from observed changes in protein structure; other analyses involve the loss of biological activity and the determination of target size. Each method of analysis yields a different kind of information. In reviewing these various results, emerging patterns will be sought which lead to general principles.

2. RADIATION DAMAGE AND THE PRIMARY STRUCTURE OF PROTEINS

Evidence concerning the types of covalent bond breakage can be seen in the radiation products from homopolymers of amino acids. Morishima & Hatano (1975) studied the EPR signals from homopolymers of glycine, alanine or glutamic acid which had been irradiated with ^{60}Co gamma rays *in vacuo* at 77 °K. They identified an unstable free radical (produced by the N–C_α bond scission) with the unpaired electron on the alpha carbon: ĊHR–CO–NH–. When warmed to room temperature, the spectra changed to that of a stable species, –NH–ĊR–CO–.

In carefully controlled studies, Hill *et al.* (1981), irradiated samples *in vacuo*, and analyzed the volatile radioproducts by EPR and by gas chromatography without exposure to oxygen. Homopolymers of alanine, glycine, valine, phenylalanine or tyrosine were irradiated in a ^{60}Co source at 25 °C or −196 °C. Low-molecular-weight products can be released from side groups with a single covalent bond break, while those from the peptide backbone require that two nearby bonds were broken. It was found that the products depended on the water content of the sample. Dried homopolymers contained 30 mol water per 100 mol peptide bonds unless special drying conditions were used (Hill *et al.* 1980). With traces of water present, carboxylic acids were released; thoroughly dried samples released no carboxylic acids. However, in both cases all homopolymers showed significant breakage between the α-carbon and the side chain. Acetamide was the principal volatile product released by radiation from polyglycine, poly-L-alanine and poly-L-valine. Therefore there were two main chain breaks at proximal C_α bonds (the peptide bond remained intact), and these were the primary products when no oxygen or water was present to cause subsequent reactions. In polyalanine, the yield of free radicals was about equal to the yield of acetamide and of methane, indicating that the bulk of the bond breakage had been accounted for.

Acetamide was not released from aromatic amino acids in polyphenylalanine and polytyrosine; the aromatic side groups protect against main-chain scission. However, they did yield the product toluene indicating the C_α–R group bond is still the most labile, just as with the aliphatic amino acids (see Fig. 1). Further EPR studies of metalloproteins (in aqueous solution) and non-metalloproteins [in $K_3Fe(CN)_6$ solutions] were reported by Symons & Taiwo (1992). Samples were

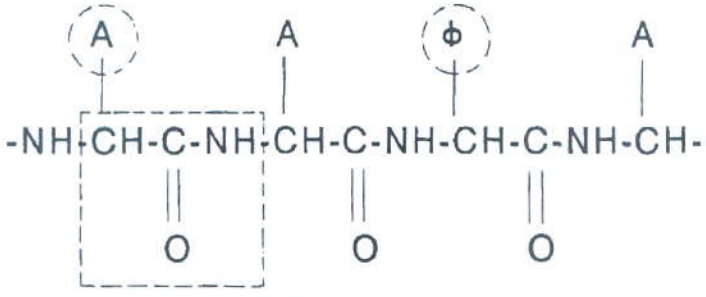


Fig. 1. Direct effects of radiation on proteins as revealed by EPR. A, aliphatic residues; ϕ, aromatic residues. Acetamide is a major product from aliphatic but not aromatic side chains. The dotted lines show chemcal groupings that are frequently released.

Table 1. *Per cent changes in amino acids in irradiated proteins*

	Lysozyme crystalline in air	Ribonuclease dry *in vacuo*	Chymotrypsin lyophilized *in vacuo*
Radiation dose (Mrad)	100	95	~ 20
Activity remaining	5 %	10 %	24 %
Alanine	+5	−4	−4
Arginine	−5·8	+2	−25
Aspartic acid	−6·5	0	+1
Cysteic acid	+6·5		−8
Cysteine	−16	−9	−6
Glutamic acid	−6	−1	+9
Glycine	−2·5	+14	−5
Histidine	−10	−8	−18
Isoleucine	−8	−3	−12
Leucine	−8	+9	−5
Lysine	−5	−7	−6
Methionine	−16	−4	−20
Phenylalanine	−13	−4	−6
Proline	−5		−8
Serine	−5	+5	+2
Threonine	−5·5	+1	0
Tryptophan	−20		
Tyrosine	−17	−7	−5
Valine	−7	+4	−12

frozen in air and irradiated with ^{60}Co gamma rays at 77 °K, then annealed to 135 °K for EPR measurements. They found electron-loss centres (holes) were confined to the polypeptide backbone amido groups (being trapped by proton transfer from nitrogen). However, ejected electrons could migrate to electron-capture centres 'well removed from the ionization sites'.

The EPR studies showed that the type and amount of radicals depend on water content of the sample, on gas phase, and on irradiation temperature.

Other evidence of damage in irradiated proteins comes from amino acid

analyses. Alexander & Hamilton (1960) examined some of the amino acids surviving in crystalline bovine serum albumin after irradiation *in vacuo*. Although there were only limited techniques available at that time, they found no major differences in radiation sensitivity among the amino acids. They estimated that the most sensitive amino acids differed from the least sensitive by less than a factor of three.

Lysozyme (Dose *et al.* 1966), ribonuclease (Jung & Schussler, 1968) and chymotrypsin (Kasche, 1971) were each irradiated until only low levels of activity remained. Their data (from crystalline, dry, or freeze-dried samples) are shown in Table 1. Each irradiated protein revealed no dramatic change in amino-acid composition, indicating that each amino-acid residue was as likely to be damaged as any other. The suggested higher radiation sensitivity of sulphydryl or aromatic amino acids is, at most, a secondary effect. Whether irradiated *in vacuo*, in oxygen, or at low temperature, the abundance of each amino acid was changed less than 20% compared to the others (Jung & Schussler, 1968).

In contrast to the EPR results, the amino-acid analyses of irradiated proteins do not appear to depend on radiation conditions. Another disparity is the prediction from EPR studies that removal of amino acid side chains due to scission at the C_α bond should result in a major increase in glycine content, but this is not seen in the amino acid analyses.

3. RADIATION DAMAGE AND THE SECONDARY AND TERTIARY STRUCTURE OF PROTEINS

The previous studies do not address the question of where in the polypeptide chain the damage occurs. In an irradiated protein, bond breakages of the polypeptide backbone lead to scission of the chain. These yield polypeptide fragments of much smaller molecular weight than the original protein which are easily separated by denaturing gel electrophoresis. Protein denaturation is accomplished by treatment with detergent, typically by heating in the presence of β-mercaptoethanol to break disulphide bonds. Denaturation involves the unfolding of individual polypeptides and the release of individual polypeptide subunits. These can be resolved by gel electrophoresis in which the relative movement of denatured protein subunits in an electrical field is inversely proportional to the size of the polypeptide. Polypeptides can be detected by a protein stain or (if a radiolabelled protein is used) radioactivity; specific proteins can be selectively detected by reaction with an antibody or even by biochemical activity if it survives these treatments. Intact polypeptides which survive irradiation and new radiolytic fragments can be quantitated by densitometric or radioactivity scanning of the gel. In many cases the amount of intact polypeptides remaining has been analyzed by target theory, giving a radiation-sensitive mass associated with subunit structure. This is the size of the unit in which radiation energy is absorbed, ultimately leading to breakage of covalent bonds in the polymer backbone. As shown in Table 2, most often these target sizes correspond to one or two subunits. A primary ionization occurs at a specific locus on one polypeptide, and the single exponential survival curve shows that a single hit is

Table 2. *Target size analysis of irradiated protein monomers*

	Monomer ($M_r \times 10^{-3}$)	Target (kDa)	Ref.
I. Membrane-bound proteins			
H^+-ATPase			
Neurospora	104	220	Bowman *et al.* (1985)
H^+, K^+-ATPase			
Pig gastric mucosa PM	100+38	92–143	Rabon *et al.* (1988)
Calcium pump protein (Ca^{2+}–ATPase)			
Rabbit SkM SR	115	277	McGrew *et al.* (1989)
Rabbit SkM SR	115	258	McGrew *et al.* (1987)
Rabbit SkM SR	115	213	Hymel *et al.* (1984)
Rabbit SkM SR reconst.	115	230	
Rabbit SkM SR	—	175	Anderson & Vilsen (1988)
Rabbit SR	—	150	le Maire *et al.* (1990)
Calcium pump protein (CPP)			
Dog cardiac SR	110	229	Chamberlain *et al.* (1983)
Calcium release channel			
Dog heart	340	1063	McGrew *et al.* (1989)
Rabbit skeletal	360	1069	
Calcium-binding protein			
Rabbit muscle	44	50	Hymel *et al.* (1984)
Na^+, K^+-ATPase α-subunit			
Guinea pig kidney usomes	—	128	Karlish & Kempner (1984)
Guinea pig kidney usomes	112	115	Jensen & Norby (1988)
Duck salt gland	—	115	Boldyrev *et al.* (1990)
D-β-Hydroxybutyrate dehydrogenase			
Beef heart mitochondrial vesicles, purified and reconstit.	31	104	McIntyre *et al.* (1983)
Glucose carrier-Na^+ symport			
Rabbit kidney BBM	165	298	Takahashi *et al.* (1985)
Rabbit Intestine BBM	73	66	Stevens *et al.* (1990)
Acetylcholinesterase			
Electric eel			
Type V	59	56	le Maire *et al.* (1990)
Type VI	59	48	
Band 3 (human RBC)	95	220	Cuppoletti *et al.* (1985)
Insulin receptor (human placenta)			
α-subunit	125+95	160	Fujita-Yamaguchi *et al.* (1989)
β-subunit	125+95	160	
HMG-CoA reductase			
Rat liver	97	100	Edwards *et al.* (1985)
A1 adenosine receptor			
Rat brain	35	35	Reddington *et al.* (1989)

Table 2. *cont.*

	Monomer ($M_r \times 10^{-3}$)	Target (kDa)	Ref.
α protein			
Rat kidney BBMV	345	355	Beliveau *et al.* (1988)
Bacterial rhodopsin	27	23	Jensen & Norby (1988)
II. Non-membrane proteins			
p21 *ras* protein	21	69	Santos *et al.* (1988)
Sulphite oxidase	55	92	Barber *et al.* (1987)
Tutin			
Rabbit psoas muscle	2800	5700	Horowits *et al.* (1986)
Nebulin			
Rabbit psoas muscle	900	1700	
Myosin			
Rabbit psoas muscle	200	190	
Bovine muscle		370	le Maire *et al.* (1990)
a-Actinin			
Rabbit psoas muscle	95	120	Horowits *et al.* (1986)
Actin			
Rabbit psoas muscle	42	49	
Vesicular Stomatitis Virus			
L protein	241	372	Bundo-Morita *et al.* (1988)
G protein	62	255	
N protein	47	87	
M protein	26	104	
CF1 ATPase (Spinach chloroplasts)			
α-subunit	58	67	Wang *et al.* (1988)
β-subunit	56	65	
γ-subunit	34	102	
δ-subunit	24	132	
ε-subunit	18	161	
Transferrin	80	75	Santos *et al.* (1988)
	—	62	le Maire *et al.* (1990)
Glutamate dehydrogenase			
Beef liver	56	73	Kempner & Miller (1983)
Glucose 6-phosphate	52	50	Jensen & Norby (1988)
dehydrogenase	—	62	le Maire *et al.* (1990)
Bovine serum albumin	67	70	Jensen & Norby (1988)
	—	62	le Maire *et al.* (1990)
	68	66	Suarez & Ferguson-Miller (1987)
β-galactosidase	116	117	Jensen & Norby (1988)
	—	142	le Maire *et al.* (1990)
β-lactoglobulin	18	20	
Trypsin inhibitor	20	20	
Carbonic anhydrase	29	37	
Aspartate transcarbamylase	34	30	
Ovalbumin	43	50	

Table 2. *cont.*

	Monomer ($M_r \times 10^{-3}$)	Target (kDa)	Ref.
Catalase	58	35	le Maire *et al.* (1990)
Ferritin	20	18	
Phosphoenolpyruvatecarboxylase			
Corn	160	170	
Alcohol dehydrogenase			
Horse liver	40	48	Suarez & Ferguson-Miller (1987)
Sendai virus			Gibson *et al.* (1988)
P protein			
wild type	74	182	
mutant	—	183	
HN protein, wild type	70	170	
NP protein			
wild type	60	114	
mutant	—	122	
M protein, mutant	40	85	
F protein			
wild type	63	68	
mutant	—	79	
Prostaglandin H synthase	72	66	Ruf *et al.* (1992)

responsible for the observed effect. Thus a target size equal to a dimer indicates that there must have been transfer of radiation energy from one subunit to another.

Further studies of energy transfer in a protein were presented in an elegant experiment (Jhun *et al.* 1991). The human erythrocyte glucose transporter is a 55000 M_r polypeptide which spans the membrane 12 times. Pepsin digestion cleaves the extra-membrane loops and reduces the mass by 50%, but the 12 transmembrane α-helices remain together in the membrane. After irradiation of this modified transporter, the ~ 3 kDa transmembrane peptides disappeared at a rate corresponding to a 34 kDa target size. This result requires that there was significant transfer of radiation energy across the noncovalent bonds between the helices. Heating the digested membrane to 100 °C before irradiation changed the inactivation curve to a much shallower slope, giving a target size < 5 kDa. Dissociation of the complex apparently prevented the energy transfer. In a parallel study, phospholamban (a 6 kDa protein with a single transmembrane-spanning α-helix) formed a pentameric assembly when purified. After irradiation the individual peptides disappeared with a target size of 5–6 kDa, indicating no energy transfer between members of this artificial assembly.

In general, breakage of covalent bonds in irradiated proteins will not appreciably alter their movement on SDS–PAGE (SDS–PAGE, sodium dodecyl sulphate polyacrylamide gel electrophoresis) unless the scission occurs in the 15% of the covalent bonds which are in the polymer backbone. These breaks will leave major fragments which will be seen on gels of irradiated samples as new bands

below the monomer band. They are not seen in unirradiated controls. If these are indeed radiation fragments, it is expected that at low radiation dosages they will appear and increase in amount, and then decrease after still higher exposures. Denaturing gels of irradiated proteins can show the appearance and nature of radiation fragments as small as 1–10 kDa. The absence of detectable protein stain at lower molecular weights could indicate that radiation yielded fragments so small that they migrated off the gel or that radiation damaged the groups reacting with the stain.

If the fragmentation is random throughout the peptide backbone, many different species of fragments will be produced and these will appear as a general smear of reactive material along the gel. However, if only a few specific bonds in the backbone are preferentially broken, unique bands will appear on the gel indicating specific fragments. Reports of both types have appeared.

The data shown in Table 3 summarize 25 independent reports in which random polypeptide fragments were observed on SDS–PAGE and 13 reports in which specific fragmentation was found. In several cases, independent studies of the same protein report opposite findings about production of specific radiation fragments. Detailed comparison of their radiation conditions or methods of assay reveal no correlation between detection of specific fragments and the buffer used or composition of the gas phase in the irradiated samples. Similarly, no correlations could be found between fragmentation and the conditions of SDS–PAGE, nor the reducing agent used nor heating conditions. In the table, proteins are grouped into 'Membrane-bound' and 'Non-membrane' proteins. Monomers from membrane-bound proteins predominantly do not show large specific fragments. There seems to be a correlation between specific fragmentation and non-membrane proteins. Published gel photos which do show specific bands produced by irradiation all show weakly-staining bands compared to the staining intensity in the monomer band of the unirradiated sample. Even where the radiation dose was sufficient to affect 50–80 % of the monomers, the fragments were no more than 10–20 % of the *decrease* in monomer band intensity. Norby & Jensen (1989) proposed that the 112 kDa α-subunit of Na,K-ATPase was composed of two independently radiation-sensitive regions of 70 and 42 kDa; a primary ionization in either domain leads to scission of covalent bonds in the polypeptide backbone of only that domain, but not the other region. A spectrum of fragments would be released from each damaged molecule: if the primary ionization were in the 70 kDa domain, the fragments would be (42 + 0–70) kDa. Analogously, primary ionizations in the 42 kDa domain would generate fragments of (70 + 0–42) kDa. Norby & Jensen (1991) calculated that a maximum of 18 % of the *original* peptides would be observed as a fragment because a second hit would split them even further.

Of the reports in which non-random (specific) fragments were observed, two were especially well-documented (Solomonson *et al.* 1987; le Maire *et al.* 1990). It should be noted that both used special conditions during irradiation. Solomonson *et al.* (1987) only observed these specific fragments when the protein was irradiated in the presence of free radical scavengers; in the absence of the

Table 3. *SDS–PAGE analysis of irradiated proteins. Observed degradation products*[a]

	Irradiation conditions		Fragments		
	Buffer	Gas phase	Random	Specific	Ref.
I. Membrane-bound proteins					
α-protein (kidney					
BBMV	Tris HEPES/KCl glycerol/sorbitol	Air	n	n	Beliveau *et al.* (1988)
Band 3 (human RBC)					
Inside-out vesicles	Tris/$MgSO_4$/Na_2SO_4	N_2	y	n	Cuppoletti *et al.* (1985)
β-protein (kidney)					
BBMV	Tris HEPES/KCl/glycerol/ sorbitol	Air	n	n	Beliveau *et al.* (1988)
Calcium-binding protein (skeletal muscle)					
SR	HEPES/KCl/sucrose	N_2	y	n	Hymel *et al.* (1984)
Calcium pump protein (cardiac)					
SR	Imidazole/sucrose/KCl	N_2	y	n	Chamberlain *et al.* (1983)
Calcium pump protein (skeletal muscle) (Ca^{2+}-ATPase)					
SR	HEPES/KCl/sucrose	N_2	y	n	Hymel *et al.* (1984)
Reconstituted in deoxycholate	HEPES/KCl/sucrose	N_2	y	n	Hymel *et al.* (1984)
Membranes & solubilized in $C_{12}E_8$	TES/NaCl/sucrose/Ca	N_2	y	y	Andersen & Vilsen (1988)
Glucose carrier-Na^+ symport					
BBMV	HEPES/sorbitol/glycerol /KCl	Air	y	n	Stevens *et al.* (1990)
	HEPES-Tris/sorbitol /glycerol/KCl	N_2	?	n	Takahashi *et al.* (1985)

H^+, K^+-ATPase	PIPES/Tris	Air	y	n	Rabon *et al.* (1988)
	Tris	N_2	?	n	Saccomani *et al.* (1981)
HMG-CoA reductase					
Hepatocytes	Eagles medium/BSA /Tricine	Air	n	n	Edwards *et al.* (1985)
Membranes	Sucrose ± DTT	Air	y	n	Ness *et al.* (1985)
D-β-Hydroxybutyrate dehydrogenase vesicles or phospholipids	HEPES/sucrose/EDTA /DTT	N_2	y	n	McIntyre *et al.* (1983)
Na^+, K^+-ATPase α-subunit					
Membranes	Histidine/sucrose/EDTA	Air	y	n	Karlish & Kempner (1984)
SDS-extracted membranes	Imidazole/sucrose/EDTA	N_2	y	n	Jensen & Norby (1988)
Na^+-dependent amino-acid transporter in plasma membrane	Tris/KCl/$CaCl_2$/$MgCl_2$ /glycerol/sorbitol	Air	n	n	McCormick *et al.* (1991)
II. Non-membrane proteins					
Alchol dehydrogenase (horse liver)	H_2O + SA	N_2	n?	y	Suarez & Ferguson-Miller (1987)
Aspartate transcarbamylase	HEPES/imidazole/acetate	Argon	n	y	le Maire *et al.* (1990)
Bovine serum albumin	H_2O + Alc. DH	N_2	?	y	Suarez & Ferguson-Miller (1987)
	HEPES/PO_4/DTT/EDTA /mannitol/benzoic	Vacuum	n	y	Solomonson *et al.* (1987)
Carbonic anhydrase	HEPES/imidazole/acetate	Argon	n	y	le Maire *et al.* (1990)
Catalse	HEPES/imidazole/acetate	Argon	n	y	le Maire *et al.* (1990)
Collagen α-chain (rat skin)	Lyophilized	Air	y	n	Cheung *et al.* (1990)
β-Galactosidase	Tris (lyophilized)	N_2	?	y	Potier *et al.* (1991)
	Tris (frozen)	Air	?	y	Potier *et al.* (1991)
Glutamate dehydrogenase	PO_4	Air	y	n	Kempner & Miller (1983)

Table 3—*cont.*

	Irradiation conditions		Fragments		
	Buffer	Gas phase	Random	Specific	Ref.
IgE	Borate/NaCl + cytochrome *c*	Air	y	y	Fewtrell *et al.* (1981)
Muscle proteins	K propionate/PO_4/Mg Acetate/EGTA/ATP/sucrose	Air	y	n	Horowits *et al.* (1986)
Nitrate reductase	HEPES/PO_4/DTT/EDTA	Vacuum	n	n	Solomonson & McCreery (1986)
	HEPES/PO_4/DTT/EDTA /mannitol/benzoate	Vacuum	n	n	Solomonson *et al.* (1987)
Ovalbumin	HEPES/imidazole/acetate	Argon	n	y	le Maire *et al.* (1990)
Prostaglandin H synthase	Tris (frozen)	Air	y	n	Ruf *et al.* (1992)
p21 *ras* protein	Tris/$MgCl_2$/ ± DTT	Air	y	n	Santos *et al.* (1988)
Sulphite oxidase	HEPES/PO_4/DTT/EDTA	Vacuum	n?	n	Barber *et al.* (1987)
Transferrin	Tris/$MgCl_2$/ ± DTT	Air	y	n	Santos *et al.* (1988)
Tyrosinase	H_2O	Air	n	n	Kempner & Miller (1989)

[a] From either explicit statements or examination of published gel photographs or scan traces. SR, sarcoplasmic reticulum; BBMV, brush-border membrane vesicles; RBC, red blood cells; DOC, deoxycholate.

scavengers, no specific fragments were seen (Solomonson & McCreery, 1986). Specific polypeptide fragments were seen on denaturing gels of proteins (carbonic anhydrase and aspartate transcarbamylase) irradiated in an argon atmosphere (le Maire *et al.* 1990); no specific fragments were seen if irradiation was performed in air (Potier, pers. comm.). A possible interpretation is that free radicals are responsible for random fragmentation: in the absence of scavengers the random breaks overwhelm the specific breaks and swamp out the feeble staining intensity of the specific breaks. Alternatively, free radical scavengers could cause healing of random covalent bond breaks in the polymer backbone, but not specific breaks; this hypothesis would require chemical differences between random and specific covalent bond breaks.

In aspartate transcarbamylase, the specific fragments were quite large (60–80 % of the original polypeptide size), implying that only relatively small segments were released. Microsequencing of five electrophoretic bands of aspartate transcarbamylase fragments revealed that all were from the amino terminus of the protein. The chain scissions were towards the carboxy terminus in loops and turns between α and β regions. Presumably there was a chain break at a specific backbone bond, or at least a cluster of sensitive bonds.

The concept of a single radiation-sensitive bond or cluster implies that for every amino-terminal fragment, there will be a corresponding carboxy-terminal fragment and the sum of the two fragments would be close to the original monomeric size. In the aspartate transcarbamylase data, the alleged sensitive region is near the carboxy terminus, thus any putative carboxy-terminal fragment would have a small molecular weight (4–12 kDa) and might not be seen on the gel. The model of two independently radiation-sensitive regions of the Na, K-ATPase α-subunit (Norby & Jensen, 1989, 1991) suggests that radiation energy may spread in a linear fashion along the backbone of the polypeptide. Other evidence for this mechanism of energy movement has been given (Kempner & Verkman, 1988).

4. RADIATION DAMAGE AND THE QUATERNARY STRUCTURE OF PROTEINS

4.1 *Creation of crosslinks by irradiation*

Denaturing gel electrophoresis can reveal the several polypeptide subunits of oligomeric proteins. If cross-links between subunits were created by irradiation, new bands would appear on SDS–PAGE above the position of individual subunits. In only a few cases (Fewtrell *et al.* 1981; Solomonson & McCreery, 1986) have these been noted, but the stain intensity of the crosslinked material indicated only a very small fraction of molecules were crosslinked. There are no new covalent associations between intact subunits and other radiation fragments (Potier *et al.* 1991). Since a radiation crosslinked protein would greatly increase the mass of the covalent structure, it would increase the probability of a second radiation interaction which would lead to destruction of the new structure. Therefore the amount of crosslinked protein which is present may not be very great.

4.2 *Retention of oligomeric structure*

Gel filtration HPLC analysis of β-galactosidase, a tetrameric homo-oligomer, revealed that the native form of the enzyme remained intact after irradiation. Denaturation of the enzyme showed that the individual polymers had been scissioned, but the fragments apparently stayed together and retained the characteristic movement of the native enzyme on HPLC (Potier *et al.* 1991). If this observation is true in general, it would explain the lack of subunit interchange in irradiated oligomers. Attempts to identify subunit interchange in irradiated samples were unsuccessful (Boyer & Kempner, 1992). It had been predicted by Simon *et al.* (1982) and especially by Verkman *et al.* (1984) that the nature of the radiation inactivation curve would be modified by the exchange process to give a target size of a monomer.

4.3 *Supermolecular structures*

Irradiation of frozen muscle fibres resulted in destruction of large protein molecules which are involved in organizing myosin filaments. However, irradiated myofibrils appeared normal in the electron microscope unless they were stressed by contraction or by passive stretch. Irradiated fibres which were stressed showed misalignment of the thick filaments (Horowits *et al.* 1986). These results are consistent with those from oligomeric proteins, suggesting that elements of complex structures can maintain their conformational relationships after irradiation until chemical or physical stress is presented to the system.

5. LOSS OF ACTIVITY AND IMPLICATIONS ABOUT THE SITE OF PRIMARY IONIZATION *VERSUS* SITE(S) AND NATURE OF DAMAGE

Target size analysis of thrombin activity in irradiated samples of prothrombin yielded important findings. Prothrombin is composed of a single polypeptide chain which has no thrombin activity unless the molecule is first treated to cleave the polypeptide. Two major products are produced, only one of which (thrombin) has activity. Irradiated prothrombin samples were cleaved and assayed for surviving thrombin activity. Analysis of these data gave a target size equal to the entire 582-residue prothrombin molecule, even though thrombin activity was restricted to the carboxy-terminal 307-residue region of the molecule. Thus even if the primary radiation interaction occurred in the non-thrombin portion of the molecule, damage appeared in the active region (Aronson & Preiss, 1962).

Another study involved the *arom* complex from *Neurospora*. This is a single protein which catalyzes five sequential reactions in the shikimic acid pathway (Fig. 2). Each reaction can be assayed independently. Radiation target analysis of each reaction gave a target size equal to the entire structure (Kempner *et al.* 1982), even though proteolysis experiments had shown that the individual reactions occurred at different regions of the polypeptide chain (Coggins *et al.* 1985). Therefore, no matter where in the polypeptide chain the primary ionization had occurred, damage appeared throughout the entire molecule.

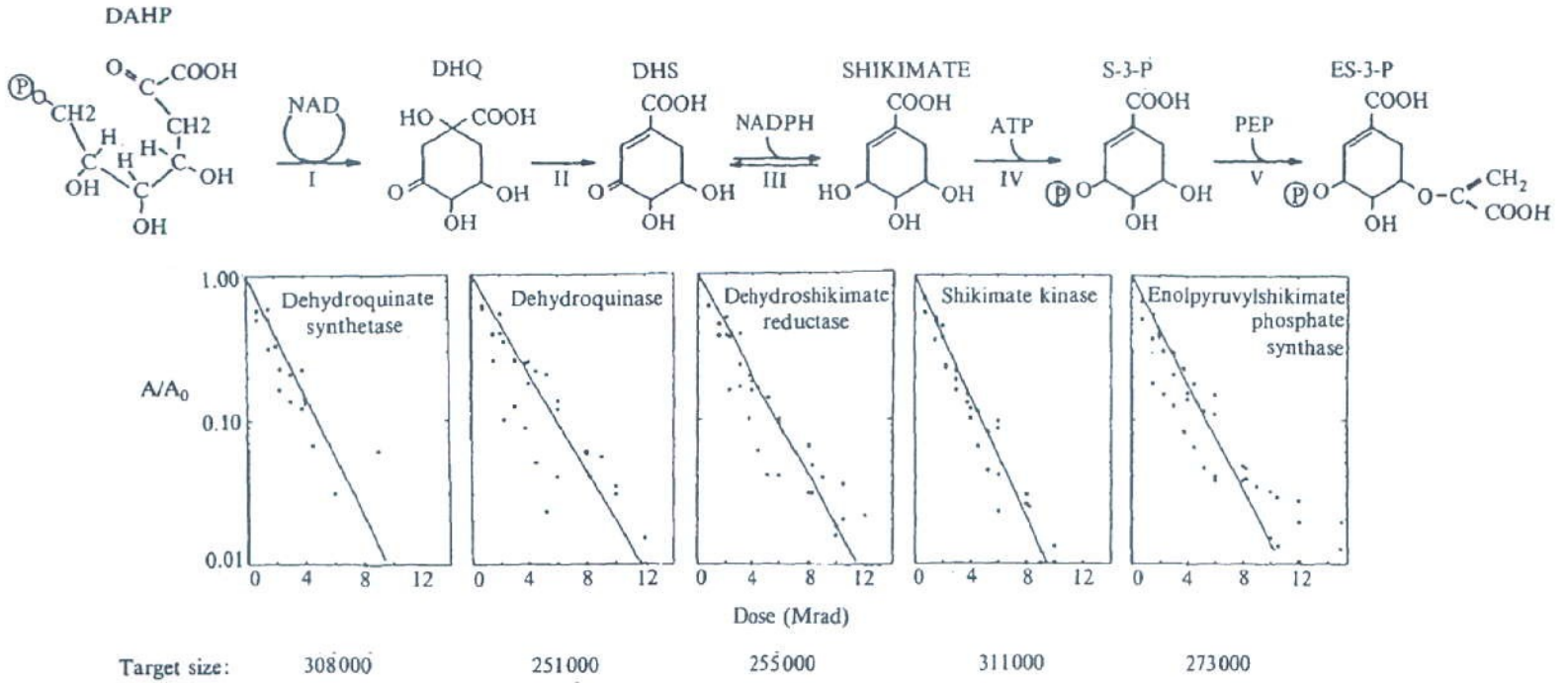


Fig. 2. Direct effects of radiation on the *arom* complex from *Neurospora*. Each of the five sequential reactions catalyzed by this protein were independently assayed. The radiation inactivation curve of each is shown. The target size was calculated from the slope of each curve. From Kempner *et al.* (1982).

Angiotensin-converting enzyme (ACE) is found in lung and in testicular tissues, but in different forms. Both enzymes are products of a single gene, utilizing two different transcription initiation sites. The larger enzyme from lung was believed to be composed of 'two independent, relatively stable domains loosely connected by a continuous polypeptide chain'. Target analysis of this activity in each tissue yielded target sizes of 140 and 74 kDa respectively, corresponding to the mass of entire polypeptide in each case (Sakaguchi *et al.* 1992).

Radiation fragments which retained enzymatic activity have been sought but were not detected (Solomonson & McCreery, 1986; Kempner & Miller, 1989). Contrasting results come from other studies which indicated radiation damage in a limited region of a polypeptide. This conclusion was deduced from target sizes for biological activity which were smaller than the mass of a polypeptide. These include both enzymatic activity and binding assays. The target sizes for sucrase and aminopeptidase N activities were less than the accepted molecular weight (Stevens *et al.* 1986). Solomonson *et al.* (1987) reported target sizes for 'partial reactions' of nitrate reductase were smaller than the mass of the polypeptide, although the target size for the complete reaction was equal to the full peptide mass. Binding assays are the most frequent source of these aberrantly-small target sizes. These include the binding of irradiated IgE to its receptor (Fewtrell *et al.* 1981), antibody binding to irradiated lipoprotein lipase (Olivecrona *et al.* 1985), stilbene and mercurial binding to irradiated band 3 protein (Verkman *et al.* 1986) and nucleotide and thallium binding to irradiated Na,K-ATPase (Norby & Jensen, 1989). All of these studies, save one, also reported that other functions of the protein (determined in the same samples) yielded target sizes equal to the entire polypeptide. Target sizes very much smaller than the original polypeptide may indicate that radiation fragments still retain function, especially with antibody-binding assays. Further, irradiation may have altered either the enzymatic rate constants or ligand dissociation constants – as shown convincingly by Norby & Jensen (1989). In such cases, target analysis must be extended to account for these additional effects (Bolger *et al.* 1989). Thus these scattered reports of unusually small target sizes need to be reinvestigated.

Several target analysis studies concerned the transfer of radiation energy through known polypeptide structures.

(*a*) In one study, an oligomeric protein (the nicotinic acetylcholine receptor) was crosslinked prior to radiation exposure (Lummis *et al.* 1988). Crosslinking doubled the target size for activity implying that radiation energy spread through the new covalent linkages.

(*b*) If two polypeptides are linked by a single disulphide bridge (as in ricin), then a primary ionization in one chain leads to damage in the other chain. If the disulphide bond is broken before radiation exposure, then there is no radiation energy transfer from one chain to another (Haigler *et al.* 1985). Presumably, intrachain disulphide bridges also could permit transfer of radiation energy.

(*c*) The only restriction of energy transfer within a covalent protein polymer has been observed in glycoproteins. Primary ionizations in the carbohydrate portions of glycoproteins (containing either *o*-linked or *n*-linked oligosaccharides) do not

lead to damage in the protein portion of the molecule (Kempner *et al.* 1986). The lack of energy transfer from carbohydrates into protein is due to limited radical migration from the site of glycosidic scission only to adjacent residues and not beyond (Nakamura *et al.* 1985).

(*d*) Non-covalent interactions between a protein and other molecules do not support the transfer of radiation energy. The presence of a lipid environment in a membrane does not contribute to direct radiation damage to membrane-bound proteins (Beauregard *et al.* 1987). A more direct test of radiation energy transfer by noncovalent interactions was reported by Kempner & Miller (1990). The association of avidin (a tetrameric protein of 4×16000 Da) with biotin (244 Da) occurs via multiple hydrogen bonds and hydrophobic interactions, resulting in a dissociation constant of $\sim 10^{-15}$ M. Radiation inactivation of biotinylated enzymes and of avidin- or streptavidin-linked ligands was the same whether these compounds were irradiated separately or together in the avidin–biotin complex. Thus even these apparently strong noncovalent interactions could not permit the transfer of radiation energy from one protein to another.

6. SUMMARY OF GENERALIZATIONS

Since all sweeping generalizations are false, the following observations are each subject to exceptions.

Very low temperatures and vacuum eliminate the indirect actions of ionizing radiation on proteins. Under these experimental conditions, high energy electrons or gamma rays result in covalent bond ruptures, principally at the C_α bond. The presence of water molecules or higher temperatures can modify the stable products which are observed. However, the amino-acid composition does not change appreciably in proteins irradiated under a variety of conditions. Thus, each amino acid is as likely to be damaged as any other. The bonds of a polypeptide backbone are broken at random, leading to a wide spectrum of fragment sizes. Under special irradiation conditions, random scissions are suppressed and specific fragments are seen. Primary ionizations in the oligosaccharide portion of glycoproteins do not lead to radiation damage in the polypeptide portion of the molecule. Oligomeric proteins remain intact after irradiation; therefore, radiation fragmentation of polypeptide subunits does not result in dissociation of the complex and exchange of subunits does not occur. Even supermolecular structures can maintain their organization after irradiation until they are stressed. Loss of activity occurs throughout the molecule no matter where in the polypeptide the primary ionization occurred. This loss of function could result from a conformational change due directly to the primary ionization, or it could require the transfer of radiation-deposited energy from the primary ionization site to other portions of the molecule where there may be rupture of covalent bonds and/or conformational changes.

Quo vadis? There are several areas of direct radiation effects on proteins where more information is needed. In all of the studies reviewed here, the effects observed result from an average energy deposition of 60 eV, although in fact there is a wide range of primary ionization energies. Thus at the most basic level, the

nature of molecular damage as a function of the energy deposited in the primary ionization deserves further investigation. Irradiation with low energy electrons (< 1 keV) would permit analysis of damage when the average primary ionization is < 60 eV; these new data also could be compared with those obtained by mass spectroscopy where ionizations normally are due to 70 eV electrons. There is a paradox between the EPR studies which suggest that there should be a net increase in glycine content after irradiation and the amino-acid analyses where this was not observed. Knowledge of the mechanism(s) of radiation-deposited energy transfer through and between polypeptides is needed. Some physical and chemical alterations in the microenvironment of proteins effect their radiation response; perhaps these effects are reflections of the energy transfer question.

These new data, together with the knowledge summarized here, should permit a reasonable outline of the mechanisms and effects of ionizing radiation directly on proteins to be derived.

7. REFERENCES

ALEXANDER, P. & HAMILTON, L. D. G. (1960). Irradiation of proteins in the solid state. II. chemical changes produced in bovine serum albumin. *Radiation Res.* **13**, 214–233.

ANDERSEN, J. P. & VILSEN, B. (1988). Radiation inactivation analysis of sarcoplasmic reticulum Ca–ATPase in membrane-bound form and in detergent-solubilized monomeric states. *FEBS Lett.* **234**, 120–126.

ANGELIDES, K. J., NUTTER, T. J., ELMER, L. W. & KEMPNER, E. S. (1985). Functional unit size of the neurotoxin receptors on the voltage-dependent sodium channel. *J. biol. Chem.* **260**, 3431–3439.

ARONSON, D. L. & PREISS, J. W. (1962). Molecular weights of human prothrombin and thrombin by electron irradiation. *Radiation Res.* **16**, 138–143.

BARBER, M. J., SOLOMONSON, L. P. & MCCREERY, M. J. (1987). Radiation inactivation of hepatic sulfite oxidase. *Arch. Biochem. Biophys.* **256**, 260–267.

BEAUREGARD, G., MARET, A., SALVAYRE, R. & POTIER, M. (1987). The radiation inactivation method as a tool to study structure-function relationships in proteins. *Methods in biochem. Analysis* **32**, 313–343.

BELIVEAU, R., DEMEULE, M., IBNOUL-KHATIB, H., BERGERON, M., BEAUREGARD, G. & POTIER, M. (1988). Radiation-inactivation studies on brush-border-membrane vesicles. *Biochem. J.* **252**, 807–813.

BOLDYREV, A. A., LOPINA, O. D. & FEDOSOVA, N. U. (1990). Na,K-ATPase: radiation inactivation studies. *Biochem. International* **21**, 45–52.

BOLGER, G. T., SKOLNICK, P. & KEMPNER, E. S. (1989). Radiation inactivation reveals discrete cation binding sites that modulate dihydropyridine binding sites. *Molec. Pharmacol.* **36**, 327–332.

BOWMAN, B. J., BERENSKI, C. J. & JUNG, C. Y. (1985). Size of the plasma membrane H^+–ATPase from *Neurospora crassa* determined by radiation inactivation and comparison with the sarcoplasmic reticulum Ca^{2+}–ATPase from skeletal muscle. *J. biol. Chem.* **260**, 8726–8730.

BOYER, T. D. & KEMPNER, E. S. (1992). Effect of subunit interactions on enzymatic activity of glutathione S-transferases: a radiation inactivation study. *Anal. Biochem.* **207**, 51–57.

BUNDO-MORITA, K., GIBSON, S. & LENARD, J. (1988). Radiation inactivation analysis of fusion and hemolysis by vesicular stomatitis virus. *Virology* **163**, 622–624.

CHAMBERLAIN, B. K., BERENSKI, C. J., JUNG, C. Y. & FLEISCHER, S. (1983). Determination of the oligomeric structure of the Ca^{2+} pump protein in canine cardiac sarcoplasmic reticulum membranes using radiation inactivation analysis. *J. biol. Chem.* **258**, 11997–12001.

CHEUNG, D. T., PERELMAN, N., TONG, D. & NIMNI, M. E. (1990). The effect of gamma-irradiation on collagen molecules, isolated α-chains, and crosslinked native fibers. *J. Biomed. mat. Res.* **24**, 581–589.

COGGINS, J. R., BOOCOCK, M. R., CAMPBELL, M. S., CHAUDHURI, S., LAMBERT, J. M., LEWENDON, A., MOUSDALE, D. M. & SMITH, D. D. S. (1985). Functional domains involved in aromatic amino acid biosynthesis. *Biochem. Soc. Trans.* **13**, 299–303.

CUPPOLETTI, J., GOLDINGER, J., KANG, B., JO, I., BERENSKI, C. & JUNG, C. Y. (1985). Anion carrier in the human erythrocyte exists as a dimer. *J. biol. Chem.* **260**, 15714–15717.

DOSE, K., RISI, S. & RAUCHFUSS, H. (1966). Veranderung von aminosauren und aktivitat bei rontgenbestrahlung von krystallisiertem lysozym. *Biophysik* **3**, 202–206.

EDWARDS, P. A., KEMPNER, E. S., LAN, S.-F. & ERICKSON, S. K. (1985). Functional size of rat hepatic 3-hydroxy-3-methylglutaryl coenzyme A reductase as determined by radiation inactivation. *J. biol. Chem.* **260**, 10278–10282.

FEWTRELL, C., KEMPNER, E., POY, G. & METZGER, H. (1981). Unexpected findings from target analysis of immunoglobin E and its receptor. *Biochemistry* **20**, 6589–6594.

FUJITA-YAMAGUCHI, Y., HARMON, J. T. & KATHURIA, S. (1989). Radiation inactivation experiments predict that a large aggregate form of the insulin receptor is a highly active tyrosine-specific kinase. *Biochemistry* **28**, 4556–4563.

GARRISON, W. M. (1987). Reaction mechanisms in the radiolysis of peptides, polypeptides, and proteins. *Chem. Revs.* **87**, 381–398.

GIBSON, S., BUNDO-MORITA, K., PORTNER, A. & LENARD, J. (1988). Fusion of a sendai mutant deficient in HN protein (ts271) with cardiolipin liposomes. *Virology* **163**, 226–229.

HAIGLER, H. T., WOODBURY, D. J. & KEMPNER, E. S. (1985). Radiation inactivation of ricin occurs with transfer of destructive energy across a disulfide bridge. *Proc. natl Acad. Sci. USA* **62**, 5357–5359.

HARMON, J. T., NIELSEN, T. B. & KEMPNER, E. S. (1985). Molecular weight determinations from radiation inactivation. *Methods in Enzymol.* **117**, 65–94.

HILL, D. J. T., GARRETT, R. W., HO, S. Y., O'DONNELL, J. H., O'SULLIVAN, P. W. & POMERY, P. J. (1981). Radiolysis of model polypeptides in the solid state: radiation sensitivity and side chain structure. *Rad. Chem. Phys.* **17**, 163–171.

HILL, D. J. T., HO, S. Y., O'DONNELL, J. H., O'SULLIVAN, P. W. & POMERY, P. J. (1980–1). The mechanism of radiation degradation of polypeptides. *Polymer Degradation and Stability* **3**, 83–86.

HOROWITS, R., KEMPNER, E. S., BISHER, M. E. & PODOLSKY, R. J. (1986). A physiological role for titin and nebulin in skeletal muscle. *Nature* **323**, 160–164.

HYMEL, L., MAURER, A., BERENSKI, C., JUNG, C. Y. & FLEISCHER, S. (1984). Target size of calcium pump protein from skeletal muscle sarcoplasmic reticulum. *J. biol. Chem.* **259**, 4890–4895.

JENSEN, J. & NORBY, J. G. (1988). Membrane-bound Na,K-ATPase: target size and radiation inactivation size of some of its enzymatic reactions. *J. biol. Chem.* **263**, 18063–18070.

JHUN, E., JHUN, B. H., JONES, L. R. & JUNG, C. Y. (1991). Direct effects of ionizing radiation on integral membrane proteins. *J. biol. Chem.* **266**, 9403–9407.

JUNG, C. Y. (1984). Molecular weight determination by radiation inactivation. In *Receptor Biochemistry and Methodology*, vol. 3 (ed. J. C. Venter & L. C. Harrison), pp. 193–208. New York: A. R. Liss.

JUNG, H. & SCHUSSLER, H. (1968). Zur Strahleninaktivierung von Ribonuclease. III. Aminosauren-Veranderungennach Bestrahlung in Trockenen. *Z. Naturforsch.* **23b**, 934–943.

KARLISH, S. J. D. & KEMPNER, E. S. (1984). Minimal functional unit for transport and enzyme activities of $(Na^+ + K^+)$-ATPase as determined by radiation inactivation. *Biochim. biophys. Acta* **776**, 288–298.

KASCHE, V. (1971). Specific protein–protein interaction and its application in studies on radiation-induced protein modification. Uppsala dissertations from the Faculty of Science, vol. 2. *Acta Universitatis Upsaliensis.*

KEMPNER, E. S. & FLEISCHER, S. (1989). Radiation inactivation of membrane components and molecular mass determination by target analysis. *Methods in Enzymol.* **172**, 410–439.

KEMPNER, E. S. & MILLER, J. H. (1983). Radiation inactivation of glutamate dehydrogenase hexamer: lack of energy transfer between subunits. *Science* **222**, 586–589.

KEMPNER, E. S. & MILLER, J. H. (1989). Radiation-damaged tyrosinase molecules are inactive. *Biophys. J.* **55**, 159–162.

KEMPNER, E. S. & MILLER, J. H. (1990). Direct effects of radiation on the avidin–biotin system. *J. biol. Chem.* **265**, 15776–15781.

KEMPNER, E. S. & VERKMAN, A. S. (1988). Direct effects of ionizing radiation unique to macromolecules. *Radiat. Phys. Chem.* **32**, 341–347.

KEMPNER, E. S., COLE, K. W. & GAERTNER, F. H. (1982). The functional unit of the arom conjugate in *Neurospora*. *J. biol. Chem.* **257**, 8919–8921.

KEMPNER, E. S., MILLER, J. H. & MCCREERY, M. J. (1986). Radiation target analysis of glycoproteins. *Anal. Biochem.* **156**, 140–146.

LE MAIRE, M., THAUVETTE, L., DE FORESTA, B., VIEL, A., BEAUREGARD, G. & POTIER, M. (1990). Effects of ionizing radiations on proteins. *Biochem. J.* **267**, 431–439.

LUMMIS, S. C. R., ELLORY, J. C. & SATTELLE, D. B. (1988). The cross-linking reagent dimethyl suberimidate modifies the target size of an insect nervous system nicotinic acetylcholine receptor. *Neuroscience Letters* **87**, 145–150.

MCCORMICK, J. I., JETTE, M., POTIER, M., BELIVEAU, R. & JOHNSTONE, R. M. (1991). Molecular size of a Na^+-dependent amino acid transporter in Ehrlich ascites cell plasma membranes estimated by radiation inactivation. *Biochemistry* **30**, 3704–3709.

MCGREW, S. G., BOUCEK, R. J. JR., MCINTYRE, J. O., JUNG, C. Y. & FLEISCHER, S. (1987). Target size of the ryanodine receptor from junctional terminal cisternae of sarcoplasmic reticulum. *Biochemistry* **26**, 3183–3187.

MCGREW, S. G., INUI, M., CHADWICK, C. C., BOUCEK, R. J. JR., JUNG, C. Y. & FLEISCHER, S. (1989). Comparison of the calcium release channel of cardiac and skeletal muscle sarcoplasmic reticulum by target inactivation analysis. *Biochemistry* **28**, 1319–1323.

MCINTYRE, J. O., CHURCHILL, P., MAURER, A., BERENSKI, C. J., JUNG, C. Y. & FLEISCHER, S. (1983). Target size of D-β-hydroxybutyrate dehydrogenase. *J. biol. Chem.* **258**, 953–959.

MORISHIMA, H. & HATANO, H. (1975). Electron paramagnetic resonance of several polyamino acids gamma-irradiated at 77 K. *Bull. Inst. Chem. Res. Kyoto* **53**, 15–22.

NAKAMURA, Y., OGIWARA, Y. & PHILLIPS, G. O. (1985). Free radical formation and degradation of cellulose by ionizing radiations. *Polym. Photochem.* **6**, 135–159.

NESS, G. C., MCCREERY, M. J., SAMPLE, C. E., SMITH, M. & PENDLETON, L. C. (1985). Sulfhydryl/disulfide forms of rat liver 3-hydroxy-3-methylglutaryl coenzyme A reductase. *J. biol. Chem.* **260**, 16395–16399.

NORBY, J. G. & JENSEN, J. (1989). A model for the step-wise radiation inactivation of the α_2-dimer of Na, K-ATPase. *J. biol. Chem.* **264**, 19548–19558.

NORBY, J. G. & JENSEN, J. (1991). Functional significance of the oligomeric structure of the Na, K pump from radiation inactivation and ligand binding. In *The Sodium Pump : Structure, Mechanism and Regulation* (ed. J. H. Kaplan & P. De Weer), pp. 173–188. New York: Rockefeller Univ. Press.

OLIVECRONA, T., BENGTSSON-OLIVECRONA, G., OSBORNE, J. C. JR. & KEMPNER, E. S. (1985). Molecular size of bovine lipoprotein lipase as determined by radiation inactivation. *J. biol. Chem.* **260**, 6888–6891.

POTIER, M., THAUVETTE, L., MICHAUD, L., GIROUX, S. & BEAUREGARD, G. (1991). Inactivation mechanism of tetrameric β-galactosidase by γ-rays involves both fragmentation and temperature-dependent denaturation of protomers. *Biochemistry* **30**, 8151–8157.

RABON, E. C., GUNTHER, R. D., BASSILIAN, S. & KEMPNER, E. S. (1988). Radiation inactivation analysis of oligomeric structure of the H,K-ATPase. *J. biol. Chem.* **263**, 16189–16194.

REDDINGTON, M., KLOTZ, K.-N., LOHSE, M. J. & HIETEL, B. (1989). Radiation inactivation analysis of the A_1 adenosine receptor of rat brain. *FEBS Letters* **252**, 125–128.

RUF, H. H., SCHUHN, D., DIETZ, R., NASTAINCZYK, W. & NIELSEN, M. (1992). Target size analysis of prostaglandin endoperoxide synthase. *Eur J. Biochem.* **204**, 1069–1073.

SACCOMANI, G., SACHS, G., CUPPOLETTI, J. & JUNG, C. Y. (1981). Target molecular weight of the gastric (H^+-K^+)-ATPase functional and structural molecular size. *J. biol. Chem.* **256**, 7727–7729.

SAKAGUCHI, H., HIROSE, S., KUME, T. & HAGIWARA, H. (1992). Minimal functional size or porcine lung and testicular angiotensin-converting enzymes deduced from radiation inactivation analysis. *FEBS Letters* **305**, 144–146.

SANTOS, E., NEBREDA, A. R., BRYAN, T. & KEMPNER, E. S. (1988). Oligomeric structure of p21 ras proteins as determined by radiation inactivation. *J. biol. Chem.* **263**, 9853–9858.

SIMON, P., SWILLENS, S. & DUMONT, J. E. (1982). Size determination of an equilibrium enzymic system by radiation inactivation. *Biochem. J.* **205**, 477–483.

SOLOMONSON, L. P. & MCCREERY, M. J. (1986). Radiation inactivation of assimilatory NADH:nitrate reductase from *Chlorella*. *J. biol. Chem.* **261**, 806–810.

SOLOMONSON, L. P., MCCREERY, M. J., KAY, C. J. & BARBER, M. J. (1987). Radiation inactivation analysis of assimilatory NADH:nitrate reductase. *J. biol. Chem.* **262**, 8934–8939.

STEVENS, B. R., FERNANDEZ, A., HIRAYAMA, B., WRIGHT, E. M. & KEMPNER, E. S. (1990). Intestinal brush border membrane Na^+/glucose cotransporter functions *in situ* as a homotetramer. *Proc. natl Acad. Sci. USA* **87**, 1456–1460.

STEVENS, B. R., KEMPNER, E. S. & WRIGHT, E. M. (1986). Radiation inactivation probe of membrane-bound enzymes: γ-glutamyltranspeptidase, aminopeptidase N, and sucrase. *Anal. Biochem.* **158**, 278–282.

SUAREZ, M. D. & FERGUSON-MILLER, S. (1987). Yeast and horse liver alcohol dehydrogenases: potential problems in target size analysis and evidence for a monomer active unit. *Biochemistry* **26**, 3340–3347.

SYMONS, M. C. R. & TAIWO, F. A. (1992). Radiation damage to proteins: an electron paramagnetic resonance study. *J. Chem. Soc. Perkin Trans.* **2**, 1413–1415.

TAKAHASHI, M., MALATHI, P., PREISER, H. & JUNG, C. Y. (1985). Radiation inactivation studies on the rabbit kidney sodium-dependent glucose transporter. *J. biol. Chem.* **260**, 10551–10556.

WANG, M. Y., CHIEN, L. F. & PAN, R. L. (1988). Radiation inactivation analysis of chloroplast CF_0-CF_1, ATPase. *J. biol. Chem.* **263**, 8838–8843.

VERKMAN, A. S., SKORECKI, K. & AUSIELLO, D. A. (1984). Radiation inactivation of oligomeric enzyme systems: Theoretical considerations. *Proc. natl Acad. Sci. USA* **81**, 150–154.

VERKMAN, A. S., SKORECKI, K. L., JUNG, C. Y. & AUSIELLO, D. A. (1986). Target molecular weights for red blood cell band 3 stilbene and mercurial binding sites. *Am. J. Physiol.* **251**, C541–C548.

VON SONNTAG, C. (1987). *The Chemical Basis of Radiation Biology*. London: Taylor & Francis.

Anexo 10 146 147

ARCHIVES OF BIOCHEMISTRY AND BIOPHYSICS
Vol. 352, No. 2, April 15, pp. 281–287, 1998
Article No. BB980604

Radiation Effects on the Native Structure of Proteins: Fragmentation without Dissociation

J. H. Miller, D. A. Fedoronko,[1] B. D. Hass,[2] M. Myint,[3] and E. S. Kempner[4]
Laboratory of Physical Biology, National Institute of Arthritis and Musculoskeletal and Skin Diseases, National Institutes of Health, Bethesda, Maryland 20892

Received September 29, 1997, and in revised form January 8, 1998

Several proteins (avidin, carboxypeptidase B, glucose-6-phosphate dehydrogenase, glutamate dehydrogenase, maltase, and peroxidase) composed of one to six subunits were irradiated in the frozen state. Each irradiated protein was examined by size-exclusion chromatography (SEC) and by denaturing gel electrophoresis (SDS–PAGE). All these proteins eluted from SEC as a single peak even though SDS–PAGE showed cleavage of the polypeptide backbone of the monomers. Thus, fragmentation of the subunits did not result in dissociation of the oligomeric structure.

Key Words: **radiation fragmentation; proteins; dissociation.**

The absorption of ionizing radiation results in breakage of chemical bonds. In proteins, this structural damage abolishes biological activity. The loss of activity in irradiated samples can be used to calculate the size of the structure which is associated with that activity. In this way, the direct action of γ rays or high-energy electrons has been utilized to determine the molecular mass (target size) of many proteins (1).

Saccomani *et al.* (2) showed that radiation target analysis also could be applied equally well to surviving protein subunit polypeptides detected on denaturing gel electrophoresis (SDS–PAGE). Target analyses of these data yielded a new dimension to the radiation studies—the ability to determine directly the mass of those structures which were severely damaged by a single radiation primary ionization, a size which is independent of any biological activity. This approach has been used successfully in many radiation studies. These target size measurements of both activity and structure depend only on the undamaged molecules which escaped radiation interactions.

Structural damage in irradiated proteins is extensive. Even when the biologically active region is localized to only a portion of the molecule, the loss of biochemical function yielded target sizes corresponding to the entire polypeptide (3, 4). From these studies, it was concluded that structural damage must have occurred throughout each molecule "hit" by radiation, no matter where this primary ionization had occurred. Radiation damage to protein structure has been reviewed (5). Many of these studies involved SDS–PAGE analysis of irradiated proteins which showed that the amount of monomers decreased exponentially with radiation dose. There must have been breakage of covalent bonds in the polypeptide backbone, generating fragments with different electrophoretic mobilities. These studies reported only faint Coomassie or silver staining as a smear at lower molecular weights, indicating "polypeptide fragmentation with production of a distribution of lower molecular weight peptides" (6). This conclusion appears to be general for a wide variety of proteins (5).

These studies revealed chain scissions in individual polypeptide subunits. However, nothing was known about the overall structure of irradiated proteins until a report of size-exclusion chromatography (SEC)[5] analysis of an irradiated oligomeric protein, β-galactosidase (7). The oligomeric structure survived even though individual polypeptides had been severely damaged. If the behavior of irradiated β-galactosidase were

[1] Present address: University of Michigan Medical School.
[2] Present address: University of North Dakota Medical School.
[3] Present address: Jefferson Medical School.
[4] To whom correspondence should be addressed at Bldg. 6, Room 140, NIH, Bethesda, MD 20892. Fax: (301) 402-0009.

[5] Abbreviations used: SEC, size-exclusion chromatography; LC, liquid chromatography; BCA, bicinchoninate; G6PDH, glucose-6-phosphate dehydrogenase.

0003-9861/98

true in general, such an important observation could yield new insight into macromolecular radiation damage. A radiation study was undertaken to test the generality of the observations of β-galactosidase. Several different proteins containing one or more subunits were examined by SEC and by denaturing gel electrophoresis. The behavior of each oligomeric protein was similar to that reported for β-galactosidase. More importantly, irradiated monomeric proteins also retained their original hydrodynamic character, indicating no dissociation of radiolytic fragments.

MATERIALS AND METHODS

The enzymes studied were bovine glutamate dehydrogenase (Sigma Chemical Co., G-7882; U.S. Biochemical, 16250), yeast glucose-6-phosphate dehydrogenase (Sigma Chemical Co., G-4134), carboxypeptidase B from porcine pancreas (Worthington), yeast maltase (α-glucosidase; Worthington), and two glycoproteins: horseradish peroxidase (Boehringer Mannheim, 814-407) and avidin (Sigma Chemical Co., A-9275) from egg white.

Samples of each protein were prepared at 2 mg protein/ml in buffer containing 20 mM cysteamine as follows: glutamate dehydrogenase was dissolved in 20 mM Tris buffer, pH 7.8; glucose-6-phosphate dehydrogenase was dissolved in 55 mM Tris buffer, pH 7.8, with 4.3 mM $MgCl_2$; peroxidase and avidin were dissolved in 50 mM Tris buffer, pH 7.0; carboxypeptidase B was dissolved in 25 mM Tris buffer, pH 7.8; and maltase was dissolved in 50 mM Hepes buffer, pH 7.2.

Aliquots of 250 μl of each enzyme solution were frozen in 2-ml glass ampoules and sealed with an oxygen/gas flame. Irradiations were conducted at −135°C with 10-MeV electrons from a linear accelerator at the Armed Forces Radiobiology Research Institute, Bethesda, Maryland, as previously described (8).

Irradiated samples were kept at −80°C until assay. Frozen samples were opened and allowed to equilibrate with air before thawing. The protein solutions were then thawed and the aliquots removed for assay. Solutions were filtered through 0.45-μm pore filters and applied to a LC size-exclusion column (Pharmacia Superdex 200) that had a lower molecular weight cutoff at about 10,000 M_r. Proteins were eluted with 0.05 M potassium phosphate containing 0.35 M KCl (pH 6.5). The eluate was monitored for UV absorption (280 nm). Column fractions (0.25 ml) were assayed for protein concentration by the BCA (bicinchoninate) reaction and for enzymatic activity. The cysteamine in each protein sample eluted at the lower molecular weight limit and gave a strong reaction with BCA.

Enzymatic assays were as follows: glutamate dehydrogenase was assayed as described (9), except that the α-ketoglutarate was reduced to 2 mM and neutralized with NaOH; glucose-6-phosphate dehydrogenase was assayed as described (10); peroxidase was assayed as described (11); carboxypeptidase B was assayed by hydrolysis of hippuryl-L-arginine as described in the Worthington manual, except that the absorbance was measured at 260 nm; and maltase activity was determined by hydrolysis of *p*-nitrophenyl-D-glucopyranoside as described in the Worthington manual.

Fractions from the main SEC peak containing enzymatic activity were pooled and aliquots taken for SDS–PAGE. SDS–PAGE was performed using the procedure of Schagger and von Jagow (12). Coomassie-stained gels were scanned with a Shimadzu CS-9000U scanning spectrophotometer.

Radiation target analysis of measured properties was performed as described previously (8) by fitting the surviving property as a simple exponential function of radiation dose. At least three independent radiation experiments were performed for each enzyme.

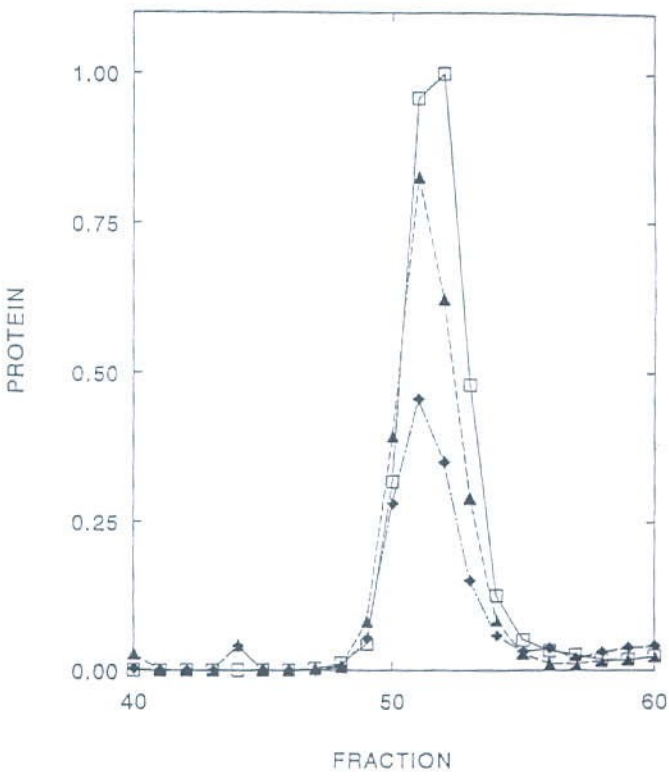


FIG. 1. Effect of radiation on carboxypeptidase B. Size-exclusion chromatography of a typical series of irradiated carboxypeptidase B. The BCA–protein reaction in eluted fractions (normalized to peak fraction in the control) is shown for unirradiated samples (□) and for samples that had received 26 (▲) or 86 (◆) Mrads.

RESULTS

Monomeric Proteins: Carboxypeptidase B, Peroxidase, and Maltase

Carboxypeptidase B is a monomeric protein of 34.5 kDa. SEC of carboxypeptidase B revealed a single protein peak as detected by the BCA protein reaction (Fig. 1). All enzymatic activity and ultraviolet light absorption coeluted with the protein peak (data not shown). In irradiated samples, no new protein peaks (Fig. 1) and no new enzymatic activity peaks were detected in lower molecular weight fractions. Thus, neither active nor inactive fragments of carboxypeptidase B were released by radiation exposure. In each fraction from the peak, the concentration of protein—detected both by UV absorption and by the BCA reaction—was progressively reduced by irradiation. Enzymatic activity in the peak also decreased. Although the areas of the peaks for protein and for enzymatic activity were reduced, the shapes of the peaks did not change with radiation dose. In each irradiated sample, the peak SEC fractions were pooled and subjected to SDS–PAGE. Denaturing gel electrophoresis of carboxypeptidase B always revealed a doublet of approximately 34,000 and 32,000

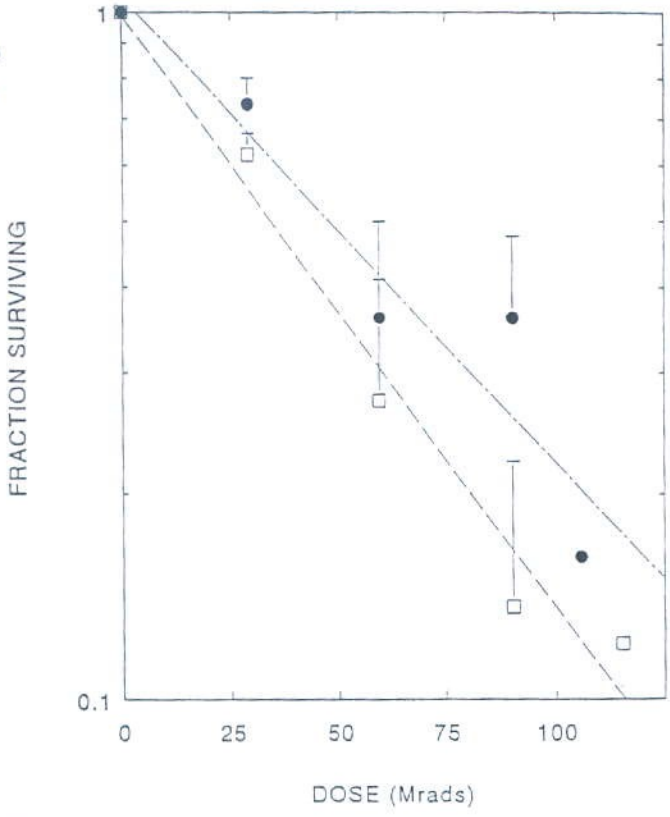


FIG. 2. Radiation inactivation of carboxypeptidase B. Surviving BCA–protein detected in the SEC peak (●) and surviving monomers detected by Coomassie stain on SDS–PAGE (□) decrease as simple exponential functions of radiation dose. Data from three independent experiments.

M_r, which might be isomeric forms of the enzyme. The number of surviving monomers on the gel was quantitated by spectrophotometric scan of the Coomassie stain. Radiation target analysis was performed for the protein detected in the SEC peak fractions and for the surviving monomers on SDS–PAGE (Fig. 2). Both properties decreased similarly with radiation dose, leading to target sizes comparable to that of the known 34.5-kDa size of carboxypeptidase B (Table I). Measurements of stain intensity on SDS–PAGE and integrated area of BCA-reactive protein peaks from SEC fractions are subject to greater experimental variability than most enzyme activity assays. This is reflected in greater scatter among these data, leading to much larger standard deviations in target size values.

Peroxidase, a monomeric glycoprotein, was studied in the same fashion. The SEC elution pattern yielded a single peak containing all the protein and all the activity. Irradiation resulted in decreased peak size of protein and even further reduction of enzymatic activity, but no shift of peak position or shape. No new peaks were observed. The quantitative survival as a function of radiation dose was used to calculate the target sizes shown in Table I. As expected (10), the monomer is destroyed by a single radiation hit anywhere in the protein portion of the molecule. The target size determined from the BCA-reactive protein in the SEC peak was unexpectedly smaller than the monomer size.

Maltase is a monomeric protein of 68.5 kDa. Size-exclusion chromatography of maltase (data not shown) revealed a single major protein peak as detected by ultraviolet light absorption and by the BCA–protein reaction. All enzymatic activity coeluted with the protein peak. In irradiated samples, no new protein peaks and no new enzymatic activity peaks were detected in lower molecular weight fractions. Irradiation reduced the size of the peaks, but did not alter the shape. The surviving protein detected on SEC peak fractions in the irradiated samples and the surviving monomers on SDS–PAGE were fit with simple, but different, exponential functions of radiation dose (Fig. 3). The target sizes for the two parameters of maltase are given in Table I; a single maltase monomer is destroyed by one primary ionization.

TABLE I

Target Analyses of Irradiated Proteins

	Native form	Subunit	Target size from SEC peak	Target size of monomer peak on SDS–PAGE
Glutamate dehydrogenase	Hexamer	56	75 ± 28	141 ± 41
β-Galactosidase[a]	Tetramer	116	ND	120
Avidin	Tetramer	15.6[b]	5.7 ± 2.4	17.6 ± 4.6
Glucose-6-phosphate dehydrogenase	Dimer	55	40 ± 23	91 ± 19
Peroxidase	Monomer	34[b]	6.5 ± 7.5	24 ± 8
Carboxypeptidase B	Monomer	34.5	29 ± 3	36 ± 6
Maltase	Monomer	68.5	53 ± 5	74 ± 12

[a] From (5).
[b] Protein portion.

A Dimeric Protein: Glucose-6-phosphate Dehydrogenase

The dimeric G6PDH molecules eluted on SEC as a single peak which contained all the enzymatic activity, UV absorption, and BCA-reactive protein. In irradiated samples elution occurred in the same fractions (Fig. 4); the peak sizes were smaller but not skewed. No new peaks of protein (or enzymatic activity) were observed in lower molecular weight fractions. The pooled peak material was examined by SDS–PAGE, revealing a monomer band of M_r ~50,000 as expected for this yeast enzyme. The surviving protein in the SEC peak and the amount of surviving monomers were fit as an exponential function of radiation dose, leading to the target sizes given in Table I. The present results indicate that a single radiation interaction leads to the destruction (polymer scission) of two G6PDH subunits, confirming the results of an independent study of the same yeast enzyme (13). A previous study of the bacterial form of G6PDH reported that subunits were destroyed individually by radiation (14).

A Tetrameric Protein: Avidin

Avidin, a nonenzymatic glycoprotein, was irradiated and analyzed by column chromatography. The tetramer eluted in one major peak in both normal and irradiated samples. The elution pattern was unaltered in irradiated samples; no distortion of the shape of the peak was seen (data not shown). Little or no tailing to lower molecular weights was observed and no protein peaks were observed at smaller molecular weights. Monomers revealed by denaturing electrophoresis of the pooled SEC peak were quantitatively assayed. The surviving tetramers (on SEC) and surviving 16-kDa subunits (on SDS–PAGE) each were fit with simple (but different) exponential functions of radiation dose. The target size for the loss of the monomer (from SDS–PAGE) agrees with the known size of the subunit (Table I) as reported previously (11). The target size obtained from the SEC protein peak is unexpectedly small.

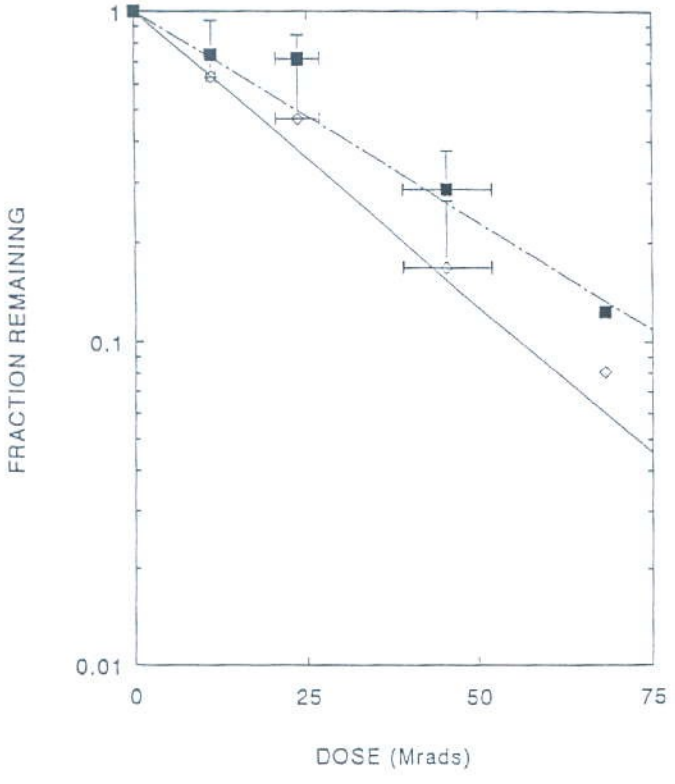


FIG. 3. Radiation inactivation of maltase. Surviving BCA–protein detected in the SEC peak (■) and surviving monomers detected by Coomassie stain on SDS–PAGE (◇) decrease as simple (but different) exponential functions of radiation dose. Data from three independent experiments.

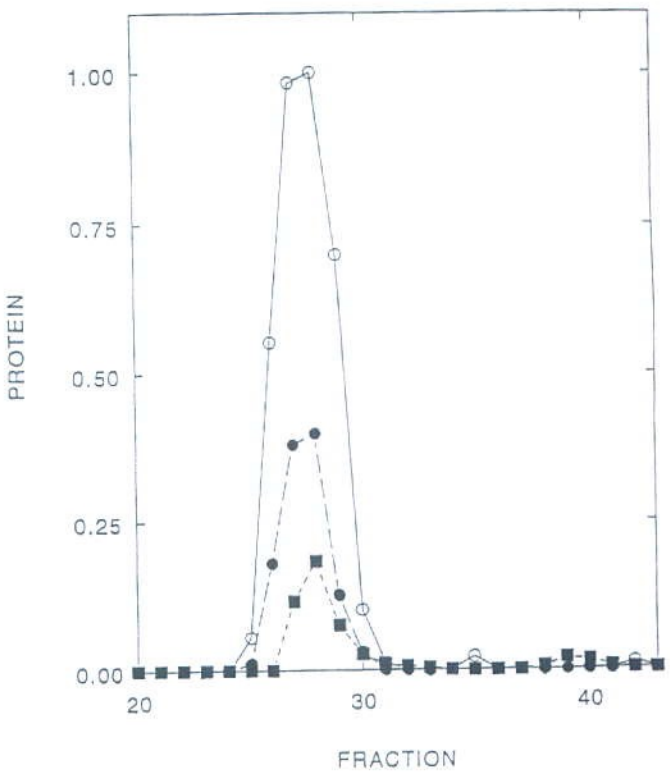


FIG. 4. Effect of radiation on glucose-6-phosphate dehydrogenase. Size-exclusion chromatography of a typical series of irradiated glucose-6-phosphate dehydrogenase. The BCA–protein reaction in eluted fractions (normalized to the peak fraction in the control) is shown for unirradiated (○) samples and for samples that had received 24 (●) or 49 (■) Mrads.

A Hexameric Protein: Glutamate Dehydrogenase

SEC of glutamate dehydrogenase revealed a single major protein peak as detected by the BCA–protein reaction and enzymatic activity (Fig. 5). Ultraviolet light absorption (data not shown) coeluted with the protein peak. In irradiated samples, no new protein

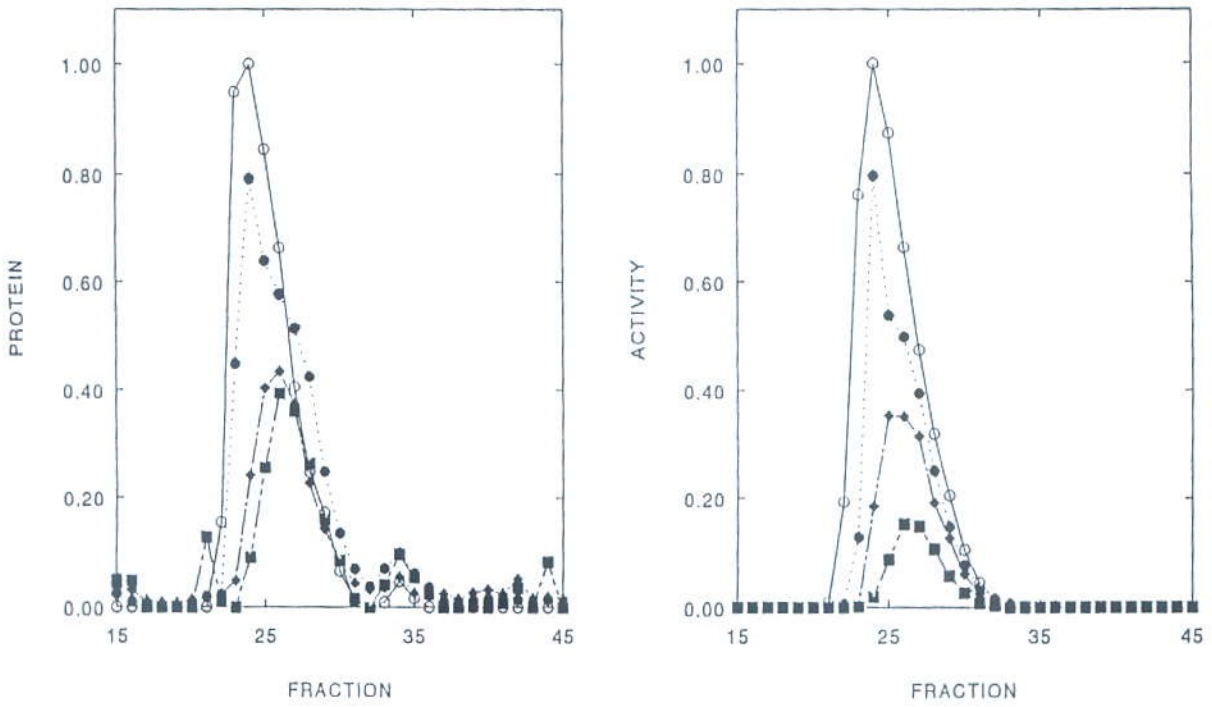


FIG. 5. Effect of irradiation on glutamate dehydrogenase. Size-exclusion chromatography of a typical series of irradiated enzyme. The panels show the BCA protein reaction (left) and the enzymatic activity (right) in eluted fractions (normalized to the peak fraction in the control) from unirradiated (○) samples and from samples which had received 12 (●), 18 (◆), or 30 (■) Mrads.

peaks and no new enzymatic activity peaks were detected in lower molecular weight fractions. Thus, neither active nor inactive fragments of glutamate dehydrogenase were released by radiation exposure. The concentration of protein in each fraction was progressively reduced by irradiation; enzymatic activity in the peak was reduced by radiation even further than the protein. Although the shape of the eluted peak was unchanged, the peak position shifted toward lower molecular weights but was still within the envelope of the unirradiated enzyme. (The apparent shift of protein in the 12-Mrad sample beyond the envelope seen in the figure was not observed in three other independent experiments.) The shift in peak position would correspond to a change of 200,000 in relative molecular weight. This apparent decrease in molecular size on SEC after irradiation is unique to glutamate dehydrogenase.

The shift in peak position of irradiated samples on SEC could be due to the production of lower molecular weight species which are still active. An alternative explanation is the presence of a spectrum of oligomeric sizes in the original preparation wherein the larger oligomers were selectively lost due to their greater radiation sensitivity. To distinguish between these possibilities, unirradiated samples of glutamate dehydrogenase were eluted from the size-exclusion column and the single peak was collected in four sequential fractions. Each fraction was then independently rechromatographed on the same column (data not shown). These elution patterns did not duplicate the peak envelope of the original preparation. Rather, each fraction ran true, showing the same relative retention time as that fraction did originally. Thus, the original sample must have contained a mixture of different-sized oligomers of glutamate dehydrogenase. The progressive shift of peak position in irradiated samples therefore was due to the selective loss of the larger oligomers.

SEC fractions containing the eluted enzyme were pooled. The hexameric glutamate dehydrogenase molecules were denatured. The monomers were resolved on SDS–PAGE and quantitatively detected by Coomassie stain. The number of surviving monomers decreased with radiation dose more rapidly than the total protein in the SEC peak (Fig. 6). Target analyses of these data (Table I) revealed a target size for the hexamer protein peak of 75 kDa, while the monomer band yielded a target size of 141 kDa. This value is considerably larger than that observed previously with samples in phosphate buffer (9), a buffer which can yield unusual target sizes (15).

DISCUSSION

Several different proteins from monomers to hexamers have been irradiated in the frozen state. Thawed samples were subjected to column chromatography;

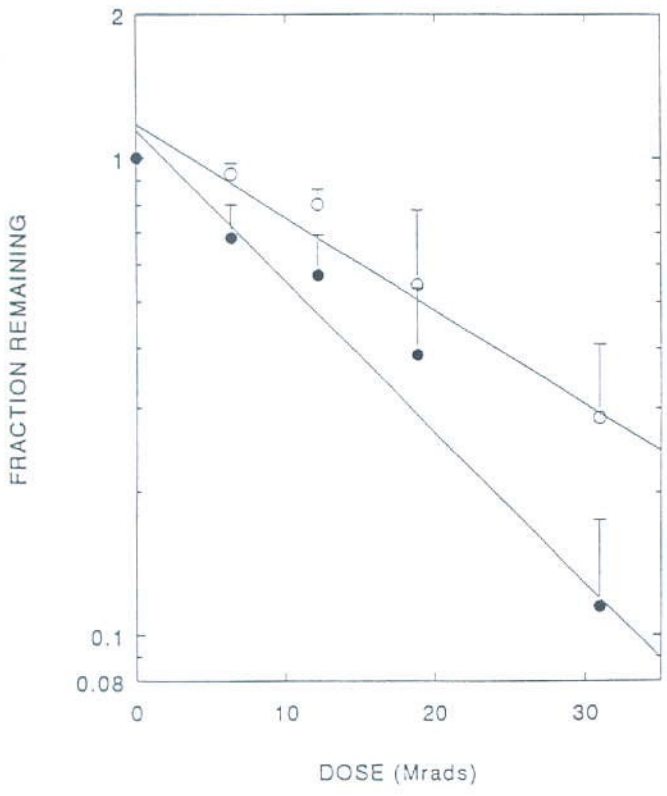


FIG. 6. Radiation inactivation of glutamate dehydrogenase. The surviving protein eluting in the hexameric peak on SEC (○) and the amount of remaining M_r 56,000 monomers (●) obtained from this peak both decrease exponentially with radiation dose. Data from three independent experiments.

each of these proteins eluted as a single major peak containing all enzymatic activity. The elution times corresponded to those expected for these proteins. After radiation exposure, relatively small changes are seen. The protein peak area slowly decreases; there is no appreciable tailing nor is there production of new peaks at lower molecular weight. This indicates that no appreciable dissociation occurs; if any fragments are released in these experiments, their size must be smaller than 10,000 M_r. Potier *et al.* (7) found fragments of irradiated β-galactosidase on gel filtration only if the sample was first denatured with guanidine. Maintenance of oligomeric structure in irradiated proteins indicates that subunit monomers are not released. This explains why no subunit exchanges could be observed in irradiated oligomers (16), even though they were predicted theoretically (17).

Only in the case of glutamate dehydrogenase did the position of the SEC peak shift in irradiated samples. Control experiments revealed that the enzyme preparation contained a spectrum of molecular sizes, all of which were enzymatically active. Since the larger species would be more sensitive to radiation, they are more readily destroyed than the smaller molecules. This is reflected by a shift in SEC peak position to lower molecular weights.

SEC analysis of each enzyme showed a slow decrease in protein peak area of irradiated samples while the enzymatic activity decreased much more rapidly. Either every irradiated enzyme molecule has reduced activity or there is a mixed population of active and inactive protein molecules. The first explanation requires a change in K_m while the second precludes any change. However, since irradiated enzymes have unchanged K_m (1), it is concluded that the SEC peak of irradiated enzymes contains a mixture of fully active surviving molecules and radiation-damaged molecules with no activity, consistent with the principles of radiation target theory.

For each protein, the peak fractions were pooled and examined by SDS–PAGE. The mobility of the denatured monomer was appropriate for the known subunit size. When exposed to large doses of ionizing radiation, each subunit was damaged so that it no longer moved with the monomer band on electrophoresis. The surviving monomer data were fit as simple exponential functions of radiation dose. Previous studies (reviewed in 5) established that radiation-damaged monomers suffered cleavages of the polypeptide backbone, yielding fragments with increased electrophoretic mobilities.

Technical problems (such as measurement of integrated stain intensity on SDS–PAGE) make the present determinations more variable than enzymatic assays in the same samples. Furthermore, small target sizes are a reflection of the very limited decrease of the measured property; thus, even after massive radiation exposure there is only a small decrease and determination of rate of loss (the slope of the inactivation curve) is problematic. These difficulties ultimately are reflected in the much larger errors associated with target size determinations of these properties.

After radiation exposures in which SDS–PAGE reveals damage to a considerable number of polypeptide subunits, the protein peak on SEC is relatively unaffected. Thus, even though individual subunits have suffered covalent bond breaks in the backbone of the polypeptide chain, the fragments do not separate nor does the oligomeric structure decompose. These conclusions are in agreement with the observations of β-galactosidase (7).

Analyses of the area of the SEC peak and of the SDS–PAGE band reveal independence of the two target sizes. The SDS–PAGE monomer band target sizes correspond to one or multiple monomers. However, interpretation of the radiation target sizes associated with the native oligomeric structure on SEC is more complex. In several of the cases reported here, the SEC target size was smaller than the known subunit mass. Target size based on the disappearance of protein in the SEC peak does not have a simple physical interpretation; it is dependent not only

on the mass of the protein, but also on the interactions among the fragments which retain the overall hydrodynamic properties of the protein. The oligomeric structure might depend on small regions of the polypeptide which survive primary ionizations occurring elsewhere in the polymer.

A surprising result obtained in this study comes from observations of three different monomeric proteins. Here there is no oligomeric structure. SEC shows that in solution these proteins elute as monomers. The target size based on the SEC protein peak is smaller than the known subunit. Despite the massive energy deposited in each primary ionization, the native form of the enzyme is not destroyed. Since the SDS–PAGE results show that there was polymer chain scission by each hit, there must be fragmentation without dissociation. Whereas the subunits of an oligomeric protein can be imagined as cooperative in maintaining the overall size of the complex, the monomeric proteins must differ. The present results for peroxidase, for carboxypeptidase B, and for maltase indicate that even severely damaged single polypeptides can preserve an overall structure similar to the native form. There must be some surviving affinity between the radiation fragments to account for this phenomenon.

Collectively, the various proteins examined here show that irradiated protein molecules, regardless of their number of subunits, maintain an oligomeric size close to that of the native protein. Even after radiation exposures which have fragmented a large proportion of the subunits, there is little dissociation of the structure of protein. Radiation target analysis has already revealed much about the role of the oligomeric state in the function of proteins (18). It also may divulge other aspects of the structural state of complex proteins.

REFERENCES

1. Kempner, E. S. (1988) *Adv. Enzymol.* **61,** 107–147.
2. Saccomani, G., Sachs, G., Cuppoletti, J., and Jung, C. Y. (1981) *J. Biol. Chem.* **256,** 7727–7729.
3. Aronson, D. L., and Preiss, J. W. (1962) *Radiat. Res.* **16,** 138–143.
4. Kempner, E. S., Cole, K. W., and Gaertner, F. H. (1982) *J. Biol. Chem.* **257,** 8919–8921.
5. Kempner, E. S. (1993) *Q. Rev. Biophys.* **26,** 27–48.
6. McIntyre, J. O., Churchill, P., Maurer, A., Berenski, C. J., Jung, C. Y., and Fleischer, S. (1983) *J. Biol. Chem.* **258,** 953–959.
7. Potier, M., Thauvette, L., Michaud, L., Giroux, S., and Beauregard, G. (1991) *Biochemistry* **30,** 8151–8157.
8. Harmon, J. T., Nielsen, T. B., and Kempner, E. S. (1985) *Methods Enzymol.* **117,** 65–94.
9. Kempner, E. S., and Miller, J. H. (1983) *Science* **222,** 586–589.
10. Kempner, E. S., Miller, J. H., and McCreery, M. J. (1986) *Anal. Biochem.* **156,** 140–146.
11. Kempner, E. S., and Miller, J. H. (1990) *J. Biol. Chem.* **265,** 15776–15781.
12. Schagger, H., and von Jagow, G. (1987) *Anal. Biochem.* **166,** 368–379.
13. Stitt, B. L., and Kempner, E. S. (1996) *Arch. Biochem. Biophys.* **334,** 268–276.
14. Jensen, J., and Norby, J. G. (1988) *J. Biol. Chem.* **263,** 18063–18070.
15. Kempner, E. S., and Miller, J. H. (1994) *Anal. Biochem.* **216,** 451–455.
16. Boyer, T. D., and Kempner, E. S. (1992) *Anal. Biochem.* **207,** 51–57.
17. Simon, P., Swillens, S., and Dumont, J. E. (1982) *Biochem. J.* **205,** 477–483.
18. Rodbell, M. (1994) *in* Les Prix Nobel 1994, pp. 188–205, Les Prix Nobel, Stockholm.